

# THE GAS

46<sup>th</sup>

Conference of the  
European Group on  
Atomic Systems



Université  
Lille1  
Sciences et Technologies



# LILLE - FRANCE

July 1-4, 2014

# BOOK OF ABSTRACTS

## Volume Editors

Daniel Hennequin (Chairman)

Radu Chicireanu

Jean François Clément

Jean Claude Garreau

Andre Severo Pereira Gomes

Florent Réal

Valérie Vallet

Philippe Verkerk

Véronique Zehnlé

Volume number: 38 D

N° ISBN: 2-914771-88-6

Published by European Physical Society

Managing Editor: P. Helfenstein, Mulhouse

# Institutional support

---



Recognize as an  
Europhysics Conference



Université  
Lille1  
Sciences et Technologies

UFR de  
Physique



**CEMPI** CENTRE EUROPÉEN  
POUR LES MATHÉMATIQUES, LA PHYSIQUE ET  
LEURS INTERACTIONS



Fédération  
Physique et Interfaces  
Lille Nord de France



# Exhibitors

---



---

*Book of Abstracts*

ITTEGAS

46<sup>th</sup> Conference of the  
European Group on  
Atomic Systems



---

LILLE - FRANCE

July 1-4, 2014

**Volume Editors**

Daniel Hennequin (Chairman)

Radu Chicireanu

Jean François Clément

Jean Claude Garreau

Andre Severo Pereira Gomes

Florent Réal

Valérie Vallet

Philippe Verkerk

Véronique Zehnlé

Volume number: 38 D

N° ISBN: 2-914771-88-6

Published by European Physical Society

Managing Editor: P. Helfenstein, Mulhouse



# CONTACT FOR THE EGAS 46 CONFERENCE

---

Daniel Hennequin  
Laboratoire PhLAM  
CNRS  
University Lille1 (Sciences and Technologies)  
F-59655 Villeneuve d'Ascq  
France  
daniel.hennequin@univ-lille1.fr

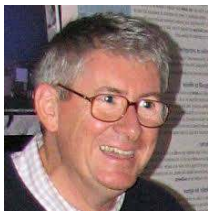
Copyright and cataloging information  
© 2014, European Physical Society.  
Reproduction rights reserved.

Europhysics Conference Abstracts are published by the European Physical Society. This volume is published under the copyright of the European Physical Society. We wish to inform the authors that the transfer of the copyright to the EPS should not prevent an author to publish an article in a journal quoting the original first publication or to use the same abstract for another conference. The copyright is just to protect the EPS against using the same material in similar publications. This book is not a formal publication. The summaries of talks contained in it have been submitted by the authors for the convenience of participants in the meeting and of other interested persons. The summaries should not be quoted in the literature, nor may they be reproduced in abstracting journals or similar publications, since they do not necessarily relate to work intended for publication. Data contained in the summaries may be quoted only with the permission of the authors.

# LOCAL ORGANIZING COMMITTEE

---

Members of the PhLAM institute  
CNRS - University Lille1 (Sciences and Technologies)  
F-59655 Villeneuve d'Ascq, France



Dr. Daniel Hennequin

[daniel.hennequin@univ-lille1.fr](mailto:daniel.hennequin@univ-lille1.fr)



Dr. Radu Chicireanu

[radu.chicireanu@univ-lille1.fr](mailto:radu.chicireanu@univ-lille1.fr)



Dr. Jean François Clément

[jean-francois.clement@univ-lille1.fr](mailto:jean-francois.clement@univ-lille1.fr)



Dr. Jean Claude Garreau

[jean-claude.garreau@univ-lille1.fr](mailto:jean-claude.garreau@univ-lille1.fr)



Dr. Andre Severo Pereira Gomes

[andre.gomes@univ-lille1.fr](mailto:andre.gomes@univ-lille1.fr)



Dr. Florent Réal

[florent.real@univ-lille1.fr](mailto:florent.real@univ-lille1.fr)



Dr. Valérie Vallet

[valerie.vallet@univ-lille1.fr](mailto:valerie.vallet@univ-lille1.fr)



Dr. Philippe Verkerk

[philippe.verkerk@univ-lille1.fr](mailto:philippe.verkerk@univ-lille1.fr)



Pr. Véronique Zehnle

[veronique.zehnle@univ-lille1.fr](mailto:veronique.zehnle@univ-lille1.fr)



Dr. Malgorzata Olejniczak

[gosia.olejniczak@univ-lille1.fr](mailto:gosia.olejniczak@univ-lille1.fr)

# EGAS BOARD MEMBERS

---

EGAS stands for European Group on Atomic Systems, formerly known as European Group on Atomic Spectroscopy (name changed in 2004). EGAS is a section of the AMOPD (Atomic, Molecular and Optical Physics Division) of the EPS (European Physical Society). The board consists of the following 14 members.

Check the EGAS website for more information: <http://www.eps-egas.org>



**Chair**

Pr. G. M. L. Tino

Università di Firenze and LENS



Pr. M. Auzinsh

University of Latvia



Pr. H. Bachau

Université de Bordeaux



**Secretary**

Pr. Peter Barker

University College, London



Dr. G. Gribakin

Queen's University, Belfast



Dr. W. Vassen

Vrije Universiteit, Amsterdam



Pr. C. Koch

University of Kassel



PD Dr. J. R. Crespo  
Lopez-Urrutia

MPI für Kernphysik, Heidelberg



Pr. T. Pfau

Universität Stuttgart



Pr. L. Pruvost

Université de Paris-Sud



Pr. X. Urbain

Université Catholique de Louvain



**Webmaster**

Pr. A. Weis

University of Fribourg



Pr. R. Wester

Universität Innsbruck



Pr. P. Törmä

Aalto University

This book contains all abstracts accepted as of June 1, 2014. The contributions are identified by

**PL** for Plenary Lecture

**IT** for Invited Talk

**CT** for Contributed Talk

**P** for posters, sorted by topics.

Odd numbered posters are presented on Tuesday, whereas even numbered posters are presented on Thursday.

# LIST OF ABSTRACTS

---

## Plenary lectures

1 [PL-1](#)

Wim Ubachs

Precision measurements on molecules for tests of fundamental physics

2 [PL-2](#)

W. van der Zande

FELIX Facility Nijmegen: molecular physics with intense radiation from 0.2 to 100 THz

3 [PL-3](#)

D.J. Wineland

Superposition, Entanglement, and Raising Schrödinger's Cat

4 [PL-4](#)

S. Haroche

Juggling photons in a box to explore the quantum world

5 [PL-5](#)

G. O'Sullivan

Current status of source development for extreme ultraviolet lithography (EUVL)

6 [PL-6](#)

A. Nicolas, L. Veissier, L. Giner, D. Maxein, J. Laurat and E. Giacobino

Quantum Storage in Cold Atomic Ensembles

7 [PL-7](#)

G. Rempe

Cold Polyatomic Molecules: The New Frontier

8 [PL-8](#)

O. Pedatzur, H. Soifer, D. Shafir, G. Orenstein, A.J. Uzan, M. Dagan, B. Bruner, N. Dudovich, V. Serbinenko, O. Smirnova and M. Ivanov

Resolving and manipulating attosecond processes via strong-field light-matter interactions

---

## Invited talks

- 9 IT-1  
G. Sansone  
Ultrafast electronic dynamics initiated by attosecond and intense XUV pulses
- 10 IT-2  
M Weidemüller  
Ultracold Rydberg Gases – Dipole Blockade, Interacting Polaritons and Energy Transport
- 11 IT-3  
G. Morigi  
Quantum crystals of photons and atoms
- 12 IT-4  
N. Radwell, T.W. Clark and S. Franke-Arnold  
Spatially dependent EIT from structured light
- 13 IT-5  
A. Antognini  
Muonic atoms: from atomic to nuclear and particle physics
- 14 IT-6  
M. Kunitzki, J. Voigtsberger, S. Zeller, L. Schmidt, R. Grisenti, M. Schöffler, F. Trinter, H. Kim, F. Trinter, W. Schöllkopf, D. Bressanini, T. Jahnke and R. Dörner  
Imaging the wavefunction of He<sub>2</sub>, He<sub>3</sub> and the Efimov state of He<sub>3</sub>
- 15 IT-7  
J.-M. Pirkkalainen, S.U. Cho, F. Massel, J. Tuorila, X. Song, P.J. Hakonen, T.T. Heikkilä and M.A. Sillanpää  
Optomechanics at microwave frequencies: mechanical resonators coupled to microwave cavities and superconducting qubits
- 16 IT-8  
D.B. Cassidy  
Some recent developments in experimental positronium physics
- 17 IT-9  
Rosario González Férrez  
Non-adiabatic effects in laser orientation and alignment of molecules

18 IT-10

*A.K. Hansen, O.O. Versolato, Ł. Kłosowski, S.B. Kristensen, A. Gingell, M. Schwarz, A. Windberger, J. Ullrich, J.R. Crespo López-Urrutia and M. Drewsen*

Rotational Cooling of Coulomb-Crystallized Molecular Ions by a Helium Buffer Gas

---

## Mini Symposium

19 PL-9

*J. Dalibard*

Bose-Einstein condensates and antiferromagnetic interactions: An illustration of symmetry breaking

20 IT-11

*F. Malet Giralt, A. Mirschink, J. Bjerlin, C. Mendl, S. Reimann and P. Gori-Giorgi*

Density Functional Theory for strongly-correlated ultracold atom gases

21 PL-10

*T. Fleig*

Rigorous Relativistic Many-Body Methods for Exploring Fundamental Physics in Atoms and Molecules

22 IT-12

*A. N. Wenz*

Experiments with finite Fermi systems in the crossover from few to many-body physics

---

## Contributed talks

23 CT-1

*G. Karras, E. Hertz, M. Ndong, F. Billard, D. Sugny, B. Lavorel and O. Faucher*

Controlling the orientation of the molecular angular momentum by shaping the polarization of a fs laser pulse

- 24 [CT-2](#)  
*S. Galtier, H. Fleurbaey, F. Nez, L. Julien and F. Biraben*  
High resolution spectroscopy of 1S-3S transition in hydrogen
- 25 [CT-3](#)  
*D. Guénot, E.P. Mansson, C.L. Arnold, D. Kroon, S.L. Sorensen, M. Gisselbrecht, A. L'Huillier, J.M. Dahlström and A.S. Kheifets*  
Probing double ionisation at the attosecond timescale
- 26 [CT-4](#)  
*A. Knie, A. Hans, M. Förstel, U. Hergenhahn, T. Jahnke, R. Dörner, A.I. Kuleff, L.S. Cederbaum, Ph.V. Demekhin and A. Ehresmann*  
Detecting ultrafast interatomic electronic processes in media by fluorescence
- 27 [CT-5](#)  
*E. Moufaretj, P. Ballin, I. Maurin, A. Laliotis and D. Bloch*  
Sub-Doppler linear spectroscopy in a vapour confined in an opal
- 28 [CT-6](#)  
*S. Knoop, P.S. Żuchowski, D. Kędziera, Ł. Mentel, M. Puchalski, H.P. Mishra, A.S. Flores and W. Vassen*  
Ultracold mixtures of metastable triplet He and Rb: scattering lengths from *ab initio* calculations and thermalization measurements
- 29 [CT-7](#)  
*M. Jacquey, V. Carrat, C. Cabrera-Gutiérrez, J.W. Tabosa, B. Viaris de Lesegno and L. Pruvost*  
Long-distance channeling of cold atoms exiting a 2D magneto-optical trap by a Laguerre-Gaussian laser beam
- 30 [CT-8](#)  
*C. Lovecchio, S. Cherukattil, M. Alì-Khan, F. Caruso and F.S. Cataliotti*  
Control of Quantum Dynamics on an Atom-Chip
- 31 [CT-9](#)  
*S. Ravets, D. Barredo, H. Labuhn, L. Beguin, A. Vernier, F. Nogrette, T. Lahaye and A. Browaeys*  
Rydberg blockade in arrays of optical tweezers
- 32 [CT-10](#)  
*N. Behbood, F. Martin Ciurana, G. Colangelo, M. Napolitano, G. Tóth, R.J. Sewell and M.W. Mitchell*  
Generation of a macroscopic spin singlet

- 33 [CT-11](#)  
*G. Labeyrie, E. Tesio, P. Gomes, G.-L. Oppo, W.J. Firth, G.R.M. Robb, A.S. Arnold, R. Kaiser and T. Ackemann*  
Optomechanical self-structuring in cold atoms
- 34 [CT-12](#)  
*A. Kosior and K. Sacha*  
Condensate Phase Microscopy
- 35 [CT-13](#)  
*V. Bolpasi, N.K. Efremidis, M.J. Morrissey, P.C. Condylis, D. Sahagun, M. Baker and W. von Klitzing*  
Ultra-high flux atom-lasers
- 36 [CT-14](#)  
*A. de Paz, A. Sharma, A. Chotia, E. Maréchal, P. Pedri, L. Vernac, B. Laburthe-Tolra and O. Gorceix*  
Quantum magnetism with a Bose-Einstein Condensate
- 37 [CT-15](#)  
*C.C. Kwong, T. Yang, D. Delande, R. Pierrat and D. Wilkowski*  
Coherent superflash effect in cold atoms: Revealing forward scattering field in optically dense medium
- 38 [CT-16](#)  
*F. Köhler, S. Sturm, A. Wagner, G. Werth, W. Quint and K. Blaum*  
A 13-fold improved value for the electron mass
- 39 [CT-17](#)  
*H. Ulbricht*  
Experimental Tests of Macroscopic Quantum Superposition
- 40 [CT-18](#)  
*Y.R.P. Sortais, J. Pellegrino, R. Bourgain, S. Jennewein, A. Browaeys, S.D. Jenkins and J. Ruostekoski*  
Collective suppression of light scattering in a cold atomic ensemble
- 41 [CT-19](#)  
*C. Blondel, M. Vandevraye, Ph. Babilotte and C. Drag*  
A new method to measure photoabsorption cross-sections questions the value of the photodetachment cross-section of  $H^-$

- 42 [CT-20](#)  
*C. Shah, P. Amaro, R. Steinbrügge, S. Bernitt, Z. Harman, S. Fritzsche, A. Surzhykov, J.R. Crespo López-Urrutia and S. Tashenov*  
Measurement of the X-ray emission anisotropies in the resonant photorecombination into highly charged ions
- 43 [CT-21](#)  
*M. Génévriez, X. Urbain, M. Brouri, K. Dunseath and M. Terao-Dunseath*  
Experimental and theoretical study of 3-photon ionization  $\text{He}(1s2s^3S)$  and  $\text{He}(1s2p^3P)$
- 44 [CT-22](#)  
*T.E. Wall, D.B. Cassidy and S.D. Hogan*  
Non-resonant two-photon excitation to high Rydberg states
- 45 [CT-23](#)  
*M. Trassinelli, A. Salehzadeh, T. Kirchner, C. Prigent, E. Lamour, J.-P. Rozet, S. Steydli and D. Vernhet*  
Contribution of multiple capture processes in slow collisions of highly charged ions with a many-electron target
- 46 [CT-24](#)  
*G. Rosi, F. Sorrentino, G.M. Tino, L. Cacciapuoti and M. Prevedelli*  
Measurement of the gravitational constant  $G$  by atom interferometry
- 47 [CT-25](#)  
*F. Lépine, S. Cohen, M.J.J. Vrakking and C. Bordas*  
Wavefunction Microscopy: Simple Atoms under Magnification
- 48 [CT-26](#)  
*P. Geyer, N. Dörre, P. Haslinger, J. Rodewald, S. Nimmrichter and M. Arndt*  
Quantum interferometry in the time-domain with massive particles
- 49 [CT-27](#)  
*K. Dulitz, A. Tauschinsky, M. Motsch, N. Vanhaecke and T.P. Softley*  
Transverse Focusing Effects in the Zeeman Deceleration of Hydrogen Atoms
- 50 [CT-28](#)  
*R. Geiger, W. Chaibi, B. Canuel, A. Bertoldi, A. Landragin, L. Amand, S. Gaffet, E. Cormier and P. Bouyer*  
Hybrid Atom-Optical Interferometry for Gravitational Wave Detection and Geophysics

- 51 [CT-29](#)  
*S. Kokkelmans, Z. Shotan, O. Machtey and L. Khaykovich*  
Three-body recombination for vanishing scattering lengths
- 52 [CT-30](#)  
*A. Mauracher, M. Daxner, J. Postler, S.E. Huber, S. Denifl, P. Scheier and J.P. Toennies*  
Detection of Negative Charge Carriers in Superfluid Helium Droplets: The Metastable Anions  $He^{-*}$  and  $He_2^{-*}$
- 53 [CT-31](#)  
*A. Cygan, P. Wcisło, S. Wójtewicz, P. Mastowski, R.S. Trawiński, R. Ciuryło and D. Lisak*  
Three different approaches to cavity-enhanced spectroscopy
- 54 [CT-32](#)  
*S.C. Mathavan, C. Meinema, J.E. van den Berg, H.L. Bethlem and S. Hoekstra*  
Deceleration, cooling and trapping of SrF molecules for precision spectroscopy
- 55 [CT-33](#)  
*M.R. Kamsap, J. Pedregosa-Gutierrez, C. Champenois, D. Guyomarc'h, M. Houssin and M. Knoop*  
Ion clouds in radio-frequency linear traps: transport and phase transitions
- 56 [CT-34](#)  
*S.H.W. Wouters, G. ten Haaf, J.F.M. van Rens, S.B. van der Geer, O.J. Luiten, P.H.A. Mutsaers and E.J.D. Vredenburg*  
High-resolution Focussed Ion Beam by laser cooling and compression of a thermal atomic beam
- 57 [CT-35](#)  
*E. Jordan, G. Cerchiari and A. Kellerbauer*  
Towards Laser Cooling of Negative Ions
- 58 [CT-36](#)  
*O.Yu. Andreev, E.A. Mistonova and A.B. Voitkiv*  
Transfer ionization in collisions of bare nuclei with light atoms
-

## Posters

---

### *Fundamental physics with atoms/molecules*

59 P-1

*A. Kozlov, V.V. Flambaum and V.A. Dzuba*  
Polarizabilities of Actinides and Lanthanides

60 P-2

*Ph.V. Demekhin*

On the breakdown of the electric dipole approximation for hard X-ray photoionization cross sections

61 P-3

*I. Temelkov, H. Knöckel, A. Pashov and E. Tiemann*

Finding pathways for creation of cold molecules by laser spectroscopy

62 P-4

*P. Stefańska and R. Szmytkowski*

The M1-to-E2 and E1-to-M2 cross-susceptibilities of the Dirac one-electron atom

63 P-5

*D. Solov'yev, V. Dubrovich, L. Labzowsky and G. Plunien*

Influence of external fields on the hydrogen atom in some problems of astrophysics

64 P-6

*S.M.K. Law and S.F.C. Shearer*

Above-threshold detachment of  $\text{Si}^-$  by few-cycle femtosecond laser pulses

65 P-7

*P. Wcisło, F. Thibault, H. Cybulski and R. Ciuryło*

Strong competition between velocity-changing and phase/state changing collisions in  $\text{H}_2$  spectra perturbed by Ar

66 P-8

*A.E. Bonert, D.V. Brazhnikov, A.N. Goncharov, A.M. Shilov, A.V. Taichenachev and V.I. Yudin*

Laser cooling of magnesium atoms with increased ultracold fraction

67 P-9

*K.N. Lyaschenko and O.Yu. Andreev*

Differential cross section of dielectronic recombination with H-like uranium

- 68 P-10  
*B.M. Lagutin, I.D. Petrov, V.L. Sukhorukov, A. Ehresmann, K.-H. Schartner and H. Schmoranzer*  
4d<sup>9</sup>np resonant Auger effect in Xe: interchannel interaction as a dominant effect in the population of high angular momentum final ionic states
- 69 P-11  
*I.D. Petrov, B.M. Lagutin, V.L. Sukhorukov, A. Ehresmann and H. Schmoranzer*  
Manifestation of the 4d-εf giant resonance in the N<sub>4,5</sub>OO Auger effect in Xe
- 70 P-12  
*A.T. Kozakov, A.V. Nikolsky, K.A. Googlev, I.D. Petrov, B.M. Lagutin, V.L. Sukhorukov, H. Huckfeldt, D. Holzinger, A. Gaul and A. Ehresmann*  
Nature of photoemission in the range of the 5s-photoelectron spectrum of iridium
- 71 P-13  
*H. Agueny, A. Makhoute and A. Dubois*  
Resonant electron-capture in ion-atom collisions: Fraunhofer diffraction pattern
- 72 P-14  
*J.C. Berengut, V.A. Dzuba, V.V. Flambaum and A. Ong*  
Using highly charged ions to probe possible variations in the fine-structure constant
- 73 P-15  
*J.C. Berengut, V.V. Flambaum, A. Ong, J.K. Webb, J.D. Barrow, M.A. Barstow, S.P. Preval and J.B. Holberg*  
Limits on the dependence of the fine-structure constant on gravitational potential from white-dwarf spectra
- 74 P-16  
*Gö. Başar, Gü. Başar, I.K. Öztürk, F. Güzelçimen, A. Er, S. Kröger and L. Windholz*  
Confirmation of New Even-parity Energy Levels of La I by Laser-Induced Fluorescence Spectroscopy
- 75 P-17  
*B. Decamps, J. Gillot, A. Gauguet, J. Vigué and M. Büchner*  
Production and detection of phase modulation of matter waves
- 76 P-18  
*J. Gillot, S. Lepoutre, A. Gauguet, J. Vigué and M. Büchner*  
Atom interferometry measurements of the He-McKellar-Wilkens and the Aharonov-Casher geometric phases

- 77 [P-19](#)  
*O. Kovtun, S. Tashenov, V. Tioukine, A. Surzhykov, V.A. Yerokhin and B. Cederwall*  
Strong correlation between the electron spin orientation and bremsstrahlung linear polarization observed in the relativistic regime
- 78 [P-20](#)  
*S. Werbowy, H. Hühnermann, J. Kwela and L. Windholz*  
Zeeman effect investigations in  $^{142}\text{Nd}$  II using Collinear Ion Beam Laser Spectroscopy
- 79 [P-21](#)  
*L. Windholz, B. Gamper, T. Binder and J. Dembczynski*  
New energy levels of the La Atom found by a combination of several spectroscopic techniques
- 80 [P-22](#)  
*Z. Uddin, L. Windholz, G.H. Guthöhrlein, S. Zehra and S. Jilani*  
New Energy Levels of the Pr Atom found by Analyzing a Fourier Transform Spectrum
- 81 [P-23](#)  
*A. Er, Gö. Başar, I.K. Öztürk, F. Güzelçimen, M. Tamanis, R. Ferber and S. Kröger*  
Investigation of Fourier Transform Spectrum of Niobium in Argon Discharge in the near-infrared
- 82 [P-24](#)  
*F. Güzelçimen, N. Al-Labady, Gö. Başar, I.K. Öztürk, A. Er, S. Kröger, M. Tamanis and R. Ferber*  
Investigation of the hyperfine structure of atomic vanadium for energetically high-lying levels up to  $45\,000\text{ cm}^{-1}$
- 83 [P-25](#)  
*I.K. Öztürk, B. Atalay, G. Çelik, F. Güzelçimen, A. Er, Gö. Başar and S. Kröger*  
Theoretical oscillator strengths for the Sc I
- 84 [P-26](#)  
*A. Tonoyan, A. Sargsyan, H. Hakhumyan, Y. Pashayan-Leroy, C. Leroy and D. Sarkisyan*  
Behaviour of atomic transitions of Rb  $D_2$  line in strong magnetic fields

- 85 [P-27](#)  
*E. Efremova, M. Gordeev and Yu. Rozhdestvensky*  
Localization of Atomic Populations due to Field of Running Waves
- 86 [P-28](#)  
*A. Laliotis, T. Passerat de Silans, I. Maurin, M. Ducloy and D. Bloch*  
Probing near field thermal emission with atoms
- 87 [P-29](#)  
*J. Singh and K.L. Baluja*  
Electron-impact study of O<sub>2</sub> molecule: *R*-matrix method
- 88 [P-30](#)  
*F. Tommasi, E. Ignesti, L. Fini and S. Cavaliere*  
Vanishing the delay of a light pulse induced by propagation in matter
- 89 [P-31](#)  
*Et. Es-sebbar, M. Deli and A. Farooq*  
Line intensities and pressure broadening coefficients in the  $\nu_1$  band of N<sub>2</sub>O molecule using IR spectroscopy : N<sub>2</sub>, O<sub>2</sub> and Ar bath gas effect
- 90 [P-32](#)  
*S. Kanda*  
Precision measurement of muonium hyperfine splitting at J-PARC
- 91 [P-33](#)  
*G.F. Gribakin and A.R. Swann*  
Positron binding to polar molecules
- 92 [P-34](#)  
*E. Fasci, N. Collucelli, A. Gambetta, M. Cassinerio, M. Marangoni, P. Laporta, L. Gianfrani, A. Castrillo and G. Galzerano*  
Quantum cascade laser emission width narrowing at the kHz level by means of optical feedback
- 93 [P-35](#)  
*V.V. Meshkov and A.V. Stolyarov*  
An efficient calculation of the scattering wavefunction and phase shift
- 94 [P-36](#)  
*D.A. Glazov, A.V. Volotka, V.A. Agababaeu, M.M. Sokolov, A.A. Shchepetnov, V.M. Shabaev, I.I. Tupitsyn and G. Plunien*  
Zeeman splitting in lithium-like and boron-like ions

- 95 P-37  
*J. Šmydke and P.R. Kaprálová-Žánská*  
Basis Set Optimization Method for Rydberg States – GTO Basis Sets for He and Be
- 96 P-38  
*S.K. Tokunaga, A. Shelkownikov, P.L.T. Sow, S. Mejri, O. Lopez, A. Goncharov, B. Argence, C. Daussy, A. Amy-Klein, C. Chardonnet and B. Darquié*  
Search for a parity violation effect in chiral molecules: old dream and new perspectives
- 97 P-39  
*A. Mohanty, E.A. Dijck, M. Nuñez Portela, A. Valappol, A.T. Grier, O. Böll, S. Hoekstra, K. Jungmann, C.J.G. Onderwater, R.G.E. Timmermans, L. Willmann and H.W. Wilschut*  
Atomic Parity Violation in a single trapped Ra<sup>+</sup> ion.
- 98 P-40  
*R.P.M.J.W. Notermans, R.J. Rengelink and W. Vassen*  
Measurement of the forbidden  $2^3S_1 \rightarrow 2^1P_1$  transition in quantum degenerate helium
- 99 P-41  
*V. Fivet, P. Quinet and M. Bautista*  
Radiative data of lowly-ionized iron-peak elements for transitions of astrophysical interest
- 100 P-42  
*J.R. Crespo López-Urrutia, S. Bernitt, J.K. Rudolph, R. Steinbrügge, S.W. Epp and J. Ullrich*  
QED tests of heliumlike systems with X-ray laser spectroscopy
- 101 P-43  
*J. Kaushal, H. Rey, O. Smirnova and H. van der Hart*  
Correlation Channels in Sequential Double Ionisation
- 102 P-44  
*J. Hinney, E. Haller, J. Hudson, A. Kelly, D. Cotta, G. Bruce and S. Kuhr*  
Towards single-atom-resolved detection of strongly correlated fermions in an optical lattice
- 103 P-45  
*D. Baye, L. Filippin and M. Godefroid*  
Accurate relativistic properties of hydrogenic atoms with the Lagrange-mesh method

104 P-46

*M. Auzinsh, A. Berzins, R. Ferber, F. Gahbauer, L. Kalvans, A. Mozers and A. Spiss*

Alignment to orientation conversion of rubidium atoms under D<sub>2</sub> excitation in an external magnetic field: experiment and theory

105 P-47

*M. Auzinsh, A. Berzins, R. Ferber, F. Gahbauer, U. Kalninsh, L. Kalvans, A. Papoyan, R. Rundans and D. Sarkisyan*

Experimental measurements and an improved theoretical description of magneto-optical signals of the cesium D<sub>1</sub> transition in an extremely thin cell

106 P-48

*M. Auzinsh, L. Kalvans, R. Lazda, J. Smits and L. Busaite*

The identification of stable dark states of a single nitrogen vacancy (NV) center surrounded by several <sup>13</sup>C atoms in a diamond lattice

107 P-49

*F. Köhler, J. Hou, S. Sturm, A. Wagner, G. Werth, W. Quint and K. Blaum*

The g-factors of lithiumlike <sup>40,48</sup>Ca<sup>17+</sup> and their isotopic effect

108 P-50

*J. Zamastil and V. Patkóš*

The self-energy of bound electron

109 P-51

*S.Y. Yousif Al-Mulla*

Modification of The Atomic Scattering Factor in Electric Field

110 P-52

*S. Scotto, R. Battesti, M. Fouché, E. Arimondo, D. Ciampini and C. Rizzo*

Rubidium spectroscopy in high magnetic fields

111 P-53

*M. Tajima, N. Kuroda, S. Ulmer, D.J. Murtagh, S. Van Gorp, Y. Nagata, M. Diermaier, S. Federmann, M. Leali, C. Malbrunot, V. Mascagna, O. Massiczek, K. Michishio, T. Mizutani, A. Mohri, H. Nagahama, M. Ohtsuka, B. Radics, S. Sakurai, C. Sauerzopf, K. Suzuki, H.A. Torii, L. Venturelli, B. Wünschek, J. Zmeskal, N. Zurlo, H. Higaki, Y. Kanai, E. Lodi Rizzini, Y. Nagashima, Y. Matsuda, E. Widmann and Y. Yamazaki*

Towards the hyperfine spectroscopy of ground-state antihydrogen atoms

- 112 P-54  
*A. Touat, M. Nemouchi, T. Carette and M.R. Godefroid*  
Calculations of the hyperfine constants of  $^{35}\text{Cl } 3p^4 4s^4 P$  and  $3p^4 4p^4 D$
- 113 P-55  
*M. Piwiński, Ł. Kłosowski, D. Dziczek and S. Chwirot*  
Coincidence studies of electron impact excitation of Zn atoms
- 114 P-56  
*H. Hartman, L. Engström, H. Lundberg and H. Nilsson*  
Two-photon Excitation of high-lying 4d levels in FeII and oscillator strengths for non-LTE stellar atmosphere models
- 115 P-57  
*L. Engström, H. Lundberg, H. Nilsson, H. Hartman and E. Bäckström*  
The FERRUM project: Experimental Transition Probabilities from Highly Excited Even 5s Levels in Cr II
- 116 P-58  
*R. Drozdowski, J. Kwela and L. Windholz*  
Computer modelling of intensities of helium Stark lines in regions of levels anticrossings.
- 117 P-59  
*P.L.T Sow, S. Mejri, S.K Tokunaga, O. Lopez, A. Goncharov, A. Argence, C. Chardonnet, A. Amy-Klein, B. Darquié and C. Daussy*  
A Widely Tunable 10  $\mu\text{m}$  QCL Locked to a Metrological Mid-IR Reference for Precision Molecular Spectroscopy
- 118 P-60  
*S. Carlström, J. Mauritsson and K.J. Schafer*  
Quantum State Preparation and Holography
- 119 P-61  
*R. Drozdowski, E. Baszanowska, P. Kamiński and G. von Oppen*  
Excitation of singlet and triplet He states by neutral He - He collisions at intermediate energy range
- 120 P-62  
*P. Lancuba and S.D. Hogan*  
A transmission-line decelerator for atoms in high Rydberg states

- 121 [P-63](#)  
*O.M. Hole, E. Bäckström, M. Kaminska, R. Nascimento, J.D. Alexander, M. Björkhage, M. Blom, L. Brännholmä, M. Gatchell, P. Halldén, F. Hellberg, G. Källersjö, A. Källberg, S. Leontein, L. Liljeby, P. Löfgren, A. Paál, P. Reinhed, S. Rosén, A. Simonsson, R.D. Thomas, D. Hanstorp, S. Mannervik, H.T. Schmidt and H. Cederquist*  
Measurements of anion lifetimes in the Double Electrostatic Ion Ring Experiment DESIREE: Preliminary results
- 122 [P-64](#)  
*J.S. Bumby, J.A. Almond, S. Skoff, N. Fitch, B.E. Sauer, M.R. Tarbutt and E.A. Hinds*  
Slow beams of cold molecular radicals for precision spectroscopy
- 123 [P-65](#)  
*K. Makles, I. Krasnokutska, C. Caer, S. Deleglise, T. Briant, P-F Cohadon, A. Heidmann and M. Makles*  
Cavity optomechanics with photonic crystal nanomembrane
- 

### ***Cold atoms and quantum gases***

- 124 [P-66](#)  
*V.S. Melezhik*  
Ultracold collisional processes in atomic traps
- 125 [P-67](#)  
*O. Machtey, Z. Shotan, S. Kokkelmans and L. Khaykovich*  
Three-body recombination at the scattering length's zero-crossings
- 126 [P-68](#)  
*M. Lepers, J.-F. Wyart and O. Dulieu*  
Anisotropic optical trapping of ultracold erbium atoms
- 127 [P-69](#)  
*E.A. Koval, O.A. Koval and V.S. Melezhik*  
Anisotropic quantum scattering in plane
- 128 [P-70](#)  
*P. Cheinet, R. Faoro, B. Pelle, E. Arimondo and P. Pillet*  
Control of few body resonant-transfer interactions in a cold Rydberg gas
- 129 [P-71](#)  
*A.A. Korobitsin and E.A. Kolganova*  
Theoretical study of the rare gases dimers

- 130 [P-72](#)  
O.A. Koval and E.A. Koval  
Modeling of bound states of quantum systems in a two-dimensional geometry of atomic traps
- 131 [P-73](#)  
T. Vanderbruggen, S. Palacios, S. Coop, N. Martinez and M.W. Mitchell  
A continuous source of spin-polarized cold atoms
- 132 [P-74](#)  
M. Robert-de-Saint-Vincent, R.J. Fletcher, J. Man, N. Navon, R.P. Smith and Z. Hadzibabic  
Superfluid transition in a 2D Bose gas with tunable interactions
- 133 [P-75](#)  
U. Eismann, C. Shi, J.-L. Robyr, R. Le Targat and J. Lodewyck  
Cavity-enhanced non-destructive detection of atomic populations in Optical Lattice Clocks
- 134 [P-76](#)  
C.E. Creffield and F. Sols  
Generating synthetic gauge potentials by split driving of an optical lattice
- 135 [P-77](#)  
M.R. Henriksen, S.A. Schäffer, B.T.R. Christensen, P.G. Westergaard, J. Ye and J.W. Thomsen  
Observing collective effects of Strontium in an optical cavity
- 136 [P-78](#)  
J.J. Kinnunen  
Spectroscopies of dilute Fermi liquids
- 137 [P-79](#)  
M. Witkowski, S. Bilicki, B. Nagórny, B. Przewięźlikowski, R. Munoz-Rodriguez, P.S. Żuchowski, R. Ciuryło and M. Zawada  
A Double Magneto-Optical Trap for Hg and Rb
- 138 [P-80](#)  
J.P. McGilligan, P.F. Griffin, E. Riis and A.S. Arnold  
Grating chips for quantum technologies.
- 139 [P-81](#)  
C.H. Carson, Yueyang Zhai, P.F. Griffin, E. Riis and A.S. Arnold  
Maximum Contrast Condensate Interference

- 140 [P-82](#)  
*C. Leboutteiller, S. Garcia, F. Ferri, J. Reichel and R. Long*  
Single atoms register in a micro-cavity for multi-particle entanglement
- 141 [P-83](#)  
*R. Romain, P. Verkerk and D. Hennequin*  
Observation of spatio-temporal instabilities in a Magneto-Optical Trap
- 142 [P-84](#)  
*S. Palacios, S. Coop, T. Vanderbruggen, N. Martinez and M.W. Mitchell*  
Tuning effective magnetic dipolar interactions in Rb spinor condensates
- 143 [P-85](#)  
*Y.N. Martinez de Escobar, S. Palacios, S. Coop, T. Vanderburggen and M.W. Mitchell*  
Modulation Transfer and Double-Resonance Optical Pumping with optical transitions in  $^{87}\text{Rb}$
- 144 [P-86](#)  
*C. Yuce*  
Quantum Tunneling in a Quasi-periodically Driven Optical Lattice
- 145 [P-87](#)  
*O. Vainio, L. Lehtonen, J. Järvinen, J. Ahokas, S. Sheludiyakov, D. Zvezdov, K.-A. Suominen and S. Vasiliev*  
Spontaneous coherence of magnons in spin-polarized atomic hydrogen gas
- 146 [P-88](#)  
*B. Vemersch and J.C. Garreau*  
Emergence of nonlinearity in bosonic ultracold gases
- 147 [P-89](#)  
*S. Coop, S. Palacios, N. Martinez, T. Vanderbruggen and M.W. Mitchell*  
Light-Shift Tomography of an Optical Dipole Trap
- 148 [P-90](#)  
*M. Plodzien, J. Zakrzewski and J. Major*  
Localization in disordered time-dependent lattices
- 149 [P-91](#)  
*C. Hainaut, I. Manai, J.F. Clément, R. Chicireanu, P. Szriftgiser and J.C. Garreau*  
Studying Anderson transitions with atomic matter waves

---

**Quantum optics/information/cold ions**

150 P-92

*J. Fiedler and S. Scheel*

Tomographic reconstruction of molecular properties from interference measurements

151 P-93

*B. Szymanski, J.-P. Likforman, S. Guibal, C. Manquest, L. Guidoni and M. Woytasik*

Heating-rate measurements in micro-fabricated surface traps containing Sr<sup>+</sup> ions

152 P-94

*G. ten Haaf, S.H.W. Wouters, S.B. van der Geer, O.J. Luiten, P.H.A. Mutsaers and E.J.D. Vredenbregt*

Focused ion beam based on laser cooling: towards sub-nm ion beam milling

153 P-95

*L. Schmöger, O.O. Versolato, M. Schwarz, M. Kohnen, T. Leopold, A. Windberger, J. Ullrich, P.O. Schmidt and J.R. Crespo López-Urrutia*

Towards precision laser spectroscopy with cold highly charged ions

154 P-96

*M. Schwarz, O.O. Versolato, L. Schmöger, M. Kohnen, T. Leopold, P. Micke, J. Ullrich, P.O. Schmidt and J.R. Crespo López-Urrutia*

A novel cryogenic Paul Trap for Quantum Logic Spectroscopy of Highly Charged Ions

155 P-97

*J.-Ph. Karr, A. Douillet, N. Sillitoe and L. Hilico*

Cold hydrogen molecular ion spectroscopy for proton to electron mass ratio measurement

156 P-98

*R.A. Nyman and J. Marelic*

Photon BEC in a dye-microcavity system and the effects of interactions

---

**Molecular physics, cold molecules and molecular ions**

157 P-99

*A. Grochola, J. Szczepkowski, W. Jastrzebski and P. Kowalczyk*

Investigation of the excited electronic KCs states studied by polarization labeling spectroscopy

- 158 [P-100](#)  
*J. Szczepkowski, P. Jasik, A. Grochola, W. Jastrzebski, J.E. Sienkiewicz and P. Kowalczyk*  
Spectroscopic study of the  $4^1\Sigma^+$  state of LiCs and comparison with theory
- 159 [P-101](#)  
*O. Ryazanova, V. Zozulya, I. Voloshin, V. Karachevtsev, L. Dubey and I. Dubey*  
Spectroscopic studies on binding of novel pheophorbide - phenazine conjugate to synthetic polynucleotides
- 160 [P-102](#)  
*S. Wójtewicz, A. Cygan, P. Masłowski, J. Domysławska, P. Wcisło, M. Zaborowski, M. Piwiński, D. Lisak, R.S. Trawiński and R. Ciuryło*  
Precise line-shape measurements of oxygen B-band transitions with absolute frequency reference
- 161 [P-103](#)  
*P.R. Kaprálová-Žánková and J. Šmydke*  
Towards ab initio dynamical simulations of atoms, molecules, and clusters in femtosecond XUV pulses
- 162 [P-104](#)  
*R. Hakalla, M. Zachwieja, W. Szajna, I. Piotrowska, M. Ostrowska-Kopeć, P. Kolek and R. Kępa*  
First analysis of the Herzberg ( $C^1\Sigma^+ \rightarrow A^1\Pi$ ) band system in the lesser-abundant  $^{13}\text{C}^{17}\text{O}$  isotopologue
- 163 [P-105](#)  
*M. Ivanova, A. Pashov, H. Knöckel, A. Stein and E. Tiemann*  
High resolution spectroscopy on alkali-alkaline earth molecules
- 164 [P-106](#)  
*T. Urbanczyk and J. Koperski*  
Separation of overlapped profiles originated from different complexes excited in a supersonic expansion beam experiment
- 165 [P-107](#)  
*D.A. Holland, R.J. Hendricks, S. Truppe, B.E. Sauer and M.R. Tarbutt*  
Direct laser cooling of the BH molecule
- 166 [P-108](#)  
*I. Ricciardi, S. Mosca, M. Parisi, P. Maddaloni, L. Santamaria, M. De Rosa, G. Giusfredi and P. De Natale*  
Ultra-narrow-linewidth Mid-infrared Optical Parametric Oscillator

- 167 P-109  
*R. Glöckner, A. Prehn, M. Krottenmüller, M. Zeppenfeld and G. Rempe*  
Rotational state manipulation of trapped polyatomic molecules
- 168 P-110  
*S Bouazza, R.A. Holt, D.S. Rosner and N.M.R. Armstrong*  
Fine Structure Analysis of the Configuration System of V II
- 169 P-111  
*J. Lovric, S. Briquez, D. Duflot, M. Monnerville, B. Pouilly and C. Toubin*  
Molecular dynamics simulations of palmitic acid adsorbed on NaCl surface.
- 170 P-112  
*A.S.P. Gomes, F. Réal, V. Vallet, Ch.R. Jacob, S. Höfener and L. Visscher*  
WFT-in-DFT Embedding with Coupled-Cluster Wavefunctions
- 171 P-113  
*M. Olejniczak, F. Réal, A.S.P. Gomes, F. Viot and V. Vallet*  
Theoretical modeling of thermodynamical properties of actinide complexes

---

***Applications of AMO Physics: Astrophysics, sensors, plasma physics,...***

- 172 P-114  
*G. Dobrev, A. Pashov, P. Crozet and A. Ross*  
Spectropolarimetry of the FeH molecule in the near-IR
- 173 P-115  
*C.H. Chang, C.H. Liu, K.F. Lee, K.Y. Lin, R.S. Chen and M.H. Chen*  
Low Temperature Plasma Jet for Application in Dental Bleaching
- 174 P-116  
*F. Bouchelaghem and M. Bouledroua*  
Transport properties drawn from ion-atom collisions. Case of  ${}^6\text{Li}-{}^6\text{Li}^+$  and  ${}^6\text{Li}-{}^7\text{Li}^+$
- 175 P-117  
*E. Träbert and P. Beiersdorfer*  
Laboratory astrophysics: EBIT spectra around the EUV bands of the SDO/AIA instrument
- 176 P-118  
*F. Rohart, S. Mejri, P.L.T. Sow, S.K. Tokunaga, B. Darquié, C. Daussy, A. Castrillo, H. Dinesan, E. Fasci and L. Gianfrani*  
Absorption line shape analysis beyond the bandwidth detection limit: application to the Boltzmann constant determination

---

## *Ultrafast processes*

177 P-119

F.L. Constantin

Frequency conversion with a photomixer for high-resolution broadband spectroscopy

---

## *Photophysics and collisions, AMO physics at large facilities*

178 P-120

G. Labaigt and A. Dubois

Close-coupling CI-approach of atomic and molecular collisions: new perspectives on inner-shell processes in  $H^+ - Li$

179 P-121

C. Prigent, M. Trassinelli, E. Lamour, A. Lévy, S. Macé, J.-P. Rozet, S. Steydli and D. Vernhet

Collisions dynamics of electrons, photons, and highly-charged ions with clusters to probe the aggregation in a pulsed supersonic jet

180 P-122

M. Ya. Agre

Multipole expansions in the theory of light radiation by atomic systems

181 P-123

N.B. Tyndall and C.A. Ramsbottom

Photoionization cross sections of  $Ar^+$  ions

182 P-124

P. Palmeri, P. Quinet, Z.W. Dai, Q. Wang, L.Y. Jiang, X. Shang, Y.S. Tian and W. Zhang

Determination of Radiative Parameters for the V I and V II Spectra: TR-LIF Measurements and HFR+CPOL Calculations

183 P-125

I.I. Fabrikant and G.F. Gribakin

Similarity between Ps-atom and electron-atom scattering

184 P-126

P.M. Mishra, J. Rajput, C.P. Safvan, S. Vig and U. Kadhane

Energetics of intermediate velocity proton collision with naphthalene

185 P-127

*P.M. Mishra, L. Avaldi, P. Bolognesi, K.C. Prince, R. Richter and U. Kadhane*

Valence shell photoelectron spectroscopy for PAHs and its significance

186 P-128

*E.V. Gryzlova, A.N. Grum-Grzhimailo, S.I. Strakhova and E.I. Kuzmina*

Two-photon sequential double ionization of noble gases by circular polarized XUV radiation

---

### *Mesoscopic quantum systems*

187 P-129

*P. Asenbaum, S. Kuhn, U. Sezer, S. Nimmrichter and M. Arndt*

Cavity cooling of silicon nanoparticles

---

### *Post-deadline papers*

188 P-130

*T. Ohyama-Yamaguchi and A. Ichimura*

Screening effect on multiple ionization of Ar<sub>2</sub> by highly charged ions

189 **List of Authors** (cross-referenced to abstract page)



**The EPS poster prize** will be awarded to the best student poster presented at the conference. The poster must be produced and presented by a student. The prize jury consists of members of the EGAS board. The winner of the prize, which consists of a diploma and €250, will be announced during the conference dinner.



## Precision measurements on molecules for tests of fundamental physics

Wim Ubachs<sup>1</sup>

<sup>1</sup>*Department of Physics and Astronomy, LaserLab, VU University, de Boelelaan 1081, 1081HV, Amsterdam, The Netherlands*

Presenting Author: w.m.g.ubachs@vu.nl

Due to the increased precision in frequency measurements, the development of ultra-stable lasers, extremely accurate atomic and molecular clocks, and techniques to produce and control ultracold samples of molecules, spectroscopic methods are now being employed to test our physical understanding of the universe as laid out in General Relativity and the Standard Model. Molecules, and molecular spectroscopy, is currently shifting to the forefront, because some phenomena and effects searched for are specifically enhanced in some of the nearly infinite variety of molecular species. Molecules and molecular spectroscopy is a testground to effectively probe variation of the proton-electron mass ratio, on a cosmological time scale; examples from optical spectroscopy and radio astronomy are presented setting bounds on drifting constants. Highly accurate laboratory measurements on the hydrogen molecule can be interpreted as test of QED in chemically bound systems, as well as probes to detect fifth forces.

## FELIX Facility Nijmegen: molecular physics with intense radiation from 0.2 to 100 THz

W.J. van der Zande<sup>1</sup>

<sup>1</sup>*Radboud University Nijmegen, Institute for Molecules and Materials, FELIX Facility, Nijmegen, The Netherlands*

Presenting Author: w.vanderzande@science.ru.nl

The FELIX facility Nijmegen is the result of two initiatives. An investment in semi-large research infrastructures, complementing a High Field Magnet Laboratory (HFML) with an intense THz light source and the move of staff and instrumentation of the successful FELIX facility from a FOM-Institute elsewhere to the Radboud University Nijmegen. In September 2011, the THz FEL, called FLARE, showed first lasing, in 2012, the first of three Free Electron Lasers in the IR to FIR region moved to Nijmegen was commissioned. While two remaining FEL beamlines are still constructed, user operation has resumed as of July 2013, delivering photons from 200 GHz (1500  $\mu\text{m}$ ) to 80 THz (4  $\mu\text{m}$ ) in intense picosecond pulses. In my talk, I will present the rationale behind the funding and operation of our FEL facility and their potential place in the field of atomic and molecular physics. I will report on the operation of the THz FEL. The ambition of the FELIX facility is to use the far infrared or THz part of the spectrum to unravel the dynamics of molecules at low frequencies in which large parts of molecules exhibit coherent motion. A significant part of the molecular research at our FELIX facility is aimed at determining molecular structures of ions or molecules using so-called action spectroscopy. One of the ambitions is to use these structural identifications to determine how nature has been able to develop molecular machinery that under isothermal conditions can employ the metastability of ATP to build new complex molecules and make molecular motors possible.

# Superposition, Entanglement, and Raising Schrödinger’s Cat

D.J. Wineland<sup>1</sup>

<sup>1</sup>*National Institute of Standards and Technology, Boulder, Colorado*

Presenting Author: david.wineland@nist.gov

Research on precise control of quantum systems occurs in many laboratories throughout the world, for fundamental research, new measurement techniques, and more recently for quantum information processing. I will briefly describe experiments on quantum state manipulation of atomic ions at the National Institute of Standards and Technology (NIST), which serve as examples of similar work being performed with many other atomic, molecular, optical (AMO) and condensed matter systems around the world. This talk is in part the “story” of my involvement that I presented at the 2012 Nobel Prize ceremonies.

# Juggling photons in a box to explore the quantum world

S. Haroche<sup>1</sup>

<sup>1</sup>*Laboratoire Kastler Brossel, École Normale Supérieure, Paris, France*

<sup>1</sup>*Collège de France, Paris, France*

Presenting Author: Serge.Haroche@lkb.ens.fr

I will recall the history of the Cavity QED experiments at ENS and will briefly describe the latest development of our work.

# Current status of source development for extreme ultraviolet lithography (EUVL)

G. O'Sullivan<sup>1</sup>

<sup>1</sup>*School of Physics, University College Dublin, Belfield, Dublin 4, Ireland*

Presenting Author: gerry.osullivan@ucd.ie

Extreme ultraviolet lithography requires the development of highly efficient sources as industry has placed a requirement for 250 W of EUV radiation emitted within a 2% bandwidth at 13.5 nm for efficient matching to Mo/Si multilayer mirrors. Ideally, the emission intensity at other wavelengths should be as low as possible to minimise the heat load on the multilayer optics and debris should not be an issue. For the past two decades, research has focussed on identifying the best target material and optimum plasma conditions. Initial research concentrated on laser produced or discharge plasmas of xenon as the 4d-5p array of Xe XI emits at 13.5 nm but the maximum conversion efficiency (CE) obtained, for laser pulse energy into in-band EUV emission, was only  $\sim 1\%$  [1]. Switching to tin, where 4d-4f and Sn IX- Sn XIV overlap to yield an intense unresolved transition array (UTA) at 13.5 nm gave a CE of 2% with Nd:YAG laser produced plasmas of pure Sn, while if the concentration was reduced to  $<5\%$ , a CE of 3% was obtained as a result of the reduction in plasma opacity at low Sn density [2, 3]. Since the plasma density scales as  $\lambda_L^{-2}$ , where  $\lambda_L$  is the laser wavelength, use of a CO<sub>2</sub> rather than Nd:YAG laser greatly reduces opacity and with slab targets of pure Sn, gives a CE of 2-5% [4].

Earlier work had shown that reheating of plasmas formed by a laser pre-pulse led to a further increase in CE. As a result, modern sources for high volume manufacturing are based on first vapourising Sn droplets of 30  $\mu\text{m}$  diameter with a low energy Nd:YAG pre-pulse and reheating the resulting lower density plasma with a CO<sub>2</sub> pulse [5]. CEs up to 6% have been demonstrated in the laboratory using this method while for industrial sources, operating at 100 kHz, a CE of  $\sim 4\%$  has been obtained giving 50 W of in-band EUV [6]. Research is still ongoing to further improve this figure largely centred on optimising laser pulse profiles and duration. Recent results indicate that the maximum CE obtainable should be of the order of  $\sim 9\%$  under optimum irradiation conditions.

**Acknowledgment:** This work was supported by Science Foundation Ireland under Principal Investigator research Grant No. 07/IN.1/I1771.

## References

- [1] S. S. Churilov *et al.* J. Opt. Lett. **28** 1478 (2003)
- [2] S. S. Churilov and A. N. Ryabtsev Phys. Scr. **73** 614 (2006)
- [3] P. Hayden *et al.* J. Appl. Phys. **99** 093302 (2006)
- [4] S. Harilal *et al.* Appl. Phys. Lett. **96** 111503 (2010)
- [5] K. Nishihara *et al.* Physics of Plasmas **15** 056708 (2008)
- [6] H. Mizogiuchi *et al.* Proc. 2013 International Workshop on EUV and Soft X-ray Sources, (Dublin Nov 5th -7th S21)

## Quantum Storage in Cold Atomic Ensembles

A. Nicolas<sup>1</sup>, L. Veissier<sup>1</sup>, L. Giner<sup>1</sup>, D. Maxein<sup>1</sup>, J. Laurat<sup>1</sup>, and E. Giacobino<sup>1</sup>

<sup>1</sup>Laboratoire Kastler Brossel, UPMC, ENS, CNRS, 4 place Jussieu, 75252 Paris Cedex05, France

Presenting Author: elg@lkb.upmc.fr

Cold and ultra-cold atomic ensembles are promising resources for quantum information (QI), since they allow generation and manipulation of quantum states of light. More specifically, in this paper, we show the realization of quantum memory registers that are essential devices for QI. Actually, a quantum optical memory, able to store quantum variables, must involve a direct and efficient coupling between light and matter, providing reversible mapping of quantum photonic information into and out of the material system, without reading the information.

Our quantum memory is based on an ensemble of three-level atoms in a Lambda configuration interacting with a signal field, which is the weak quantum light pulse to be stored, and with an additional control field, generating Electromagnetically Induced Transparency (EIT) for the signal field. When the control field is turned off, the quantum signal field pulse is converted into ground state spin coherence. For read-out, the control field is turned on again. Then the medium emits a weak pulse, similar to the original signal pulse. In principle this protocol allows direct mapping of the quantum state of light into long lived coherences in the atomic ground state of Caesium atoms without excess noise.

Cold atoms offer several advantages for quantum storage, in particular low decoherence and consequently long storage times. Here Caesium atoms are trapped in a magneto-optical trap (MOT) which is turned off during the memory operation period, in order for the atomic ensemble to be used in a field-free environment. The optical depth in the MOT can reach values of 40. Signal pulses containing 1/10 photon on the average have been stored with an efficiency of 20%. This set-up has been used for efficient storage of single photons carrying orbital angular momentum (OAM) [1]. Laguerre-Gauss LG+1 and LG-1 modes are imprinted on the signal pulse, using a spatial light modulator. After storage in the cold atom memory, the retrieved modes are analyzed. Coherent superpositions of LG modes, i.e. Hermite Gaussian modes were stored and retrieved [2]. A full memory characterization (process tomography) over the whole Bloch sphere was performed and a fidelity in the quantum domain was demonstrated.

Single photons carrying OAM are promising carriers for the implementation of qubits and qudits since OAM constitutes a quantized and infinite space. Interfacing them with quantum memories opens the way to their use in full-scale quantum networks.

### References

- [1] L. Veissier *et al.*, Opt. Lett. **38**, 712 (2013)
- [2] A. Nicolas *et al.* et al, Nature Photonics **8**, 234 (2014)

## Cold Polyatomic Molecules: The New Frontier

G. Rempe<sup>1</sup>

<sup>1</sup>*Max Planck Institute of Quantum Optics, D-85748 Garching, Germany*

Presenting Author: gerhard.rempe@mpq.mpg.de

Polyatomic molecules with their many degrees of freedom and their permanent electric dipole moment offer new perspectives for the exploration of fundamental physics and chemistry as well as for the implementation of novel ideas, e.g., in quantum information science. Reaching such goals requires the development of generally applicable and sufficiently simple molecular control techniques including slowing, trapping and cooling, as well as accumulation. The talk will highlight some recent achievements in this direction including the deceleration of molecules with a spinning centrifuge [1], their accumulation and trapping in tailor-made electrostatic fields [2], and their cooling via a Sisyphus effect which employs radio-frequency and microwave transitions between rotational states to decrease energy and spontaneous transitions between vibrational states to remove entropy [3].

### References

- [1] S. Chervenkov, X. Wu, J. Bayerl, A. Rohlfes, T. Gantner, M. Zeppenfeld, and G. Rempe, *Phys. Rev. Lett.* **112**, 013001 (2014).
- [2] B.G.U. Englert, M. Mielenz, C. Sommer, J. Bayerl, M. Motsch, P.W.H. Pinkse, G. Rempe, and M. Zeppenfeld, *Phys. Rev. Lett.* **107**, 263003 (2011).
- [3] M. Zeppenfeld, B.G.U. Englert, R. Glöckner, A. Prehn, M. Mielenz, C. Sommer, L.D. van Buuren, M. Motsch, and G. Rempe, *Nature* **491**, 570-573 (2012).

## Resolving and manipulating attosecond processes via strong-field light-matter interactions

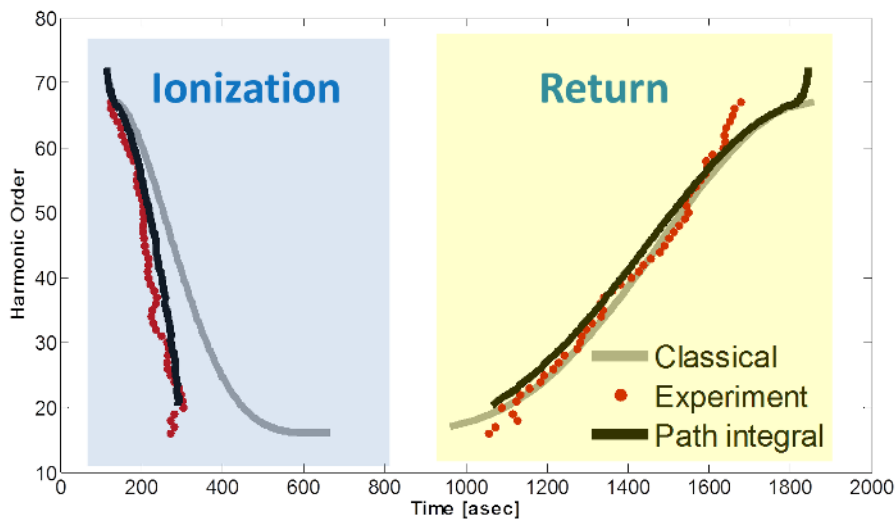
O. Pedatzur<sup>1</sup>, H. Soifer<sup>1</sup>, D. Shafir<sup>1</sup>, G. Orenstein<sup>1</sup>, A.J. Uzan<sup>1</sup>, M. Dagan<sup>1</sup>, B. Bruner<sup>1</sup>, N. Dudovich<sup>1</sup>, V. Serbinenko<sup>2</sup>, O. Smirnova<sup>2</sup>, and M. Ivanov<sup>2</sup>

<sup>1</sup>*Department of Complex Systems, Weizmann institute of science, 76100, Rehovot, Israel*

<sup>2</sup>*Max Born Institute, Max-Born-Str 2A, D-12489, Berlin, Germany*

Presenting Author: Nirit.Dudovich@weizmann.ac.il

The interaction of intense light with atoms or molecules can lead to the generation of extreme ultraviolet (XUV) pulses and energetic electron pulses of attosecond (10-18) duration. The advent of attosecond technology opens up new fields of time-resolved studies in which transient electronic dynamics can be studied with a temporal resolution that was previously unattainable. I will review the main challenges and goals in the field of attosecond science. As an example, I will focus on recent experiments where the dynamics of tunnel ionization, one of the most fundamental strong-field phenomena, were studied. Specifically, we were able to measure the times when different electron trajectories exit from under the tunneling barrier created by a laser field and the atomic binding potential. In the following stage, subtle delays in ionization times from two orbitals in a molecular system were resolved. These experiments provide an additional, important step towards achieving the ability to resolve multielectron phenomena – a long-term goal of attosecond studies.



# Ultrafast electronic dynamics initiated by attosecond and intense XUV pulses

G. Sansone<sup>1,2</sup>

<sup>1</sup>*Dipartimento di Fisica Politecnico Milano, Italy*

<sup>2</sup>*Institute of Photonics and Nanotechnology, CNR Politecnico Milano, Italy*

Presenting Author: giuseppe.sansone@polimi.it

The generation and characterization of trains and isolated attosecond ( $1\text{as} = 10^{-18}\text{ s}$ ) pulses have been achieved thanks to the continuous development of ultrafast intense laser sources over the last 20 years [1] and through theoretical advances in the description of their interaction with atomic and molecular systems [2]. Attosecond pulses are the shortest reproducible events produced so far and their duration is rapidly approaching the atomic unit of time ( $1\text{ a.u.} = 24\text{ as}$ ) [3, 4], which represents the natural timescale of the electronic motion inside the atom in the Bohr model. In quantum mechanics, this timescale is determined by the inverse of the spacing between energy levels and it ranges between a few femtoseconds and tens of attoseconds for valence and core shell electrons. The first applications of attosecond pulses were mainly focused on simple atoms or molecules to validate new experimental approaches and to gain time-resolved information on processes driven by electron-electron or electron-nuclear correlation. Experimental and theoretical results on the ultrafast dynamics initiated by isolated attosecond pulses in small molecules such as  $\text{N}_2$  will be presented. In these systems, several states of the neutral molecule (autoionizing states) or of the molecular ion can be accessed due to the large bandwidth of the attosecond pulses. The few-femtosecond and attosecond electron dynamics can be probed and controlled using a synchronized infrared few-cycle pulse [5]. New directions for the investigation of attosecond dynamics in more complex molecules will be discussed.

## References

- [1] T. Brabec and F. Krausz, *Rev. Mod. Phys.* **72**, 545 (2000).
- [2] M. B. Gaarde, J. L. Tate and K. J. Schafer, *J. Phys. B: At. Mol. Opt. Phys.* **41**, 132001 (2008).
- [3] K. Zhao et al., *Opt. Lett.* **37**, 3891 (2012).
- [4] E. Goulielmakis et al. *Science* **320**, 1614 (2008).
- [5] G. Sansone et al., *Nature* **465**, 763 (2010).

# Ultracold Rydberg Gases – Dipole Blockade, Interacting Polaritons and Energy Transport

M Weidemüller<sup>1,2</sup>

<sup>1</sup>*Physics Institute, University of Heidelberg, Germany*

<sup>2</sup>*Hefei National Laboratory for the Physical Sciences at the Microscale, University of Science and Technology of China*

Presenting Author: weidemueller@uni-heidelberg.de

Interfacing light and matter at the quantum level is at the heart of modern atomic and optical physics and enables new quantum technologies involving the manipulation of single photons and atoms. A prototypical atom-light interface is electromagnetically induced transparency, in which quantum interference gives rise to hybrid states of photons and atoms called dark-state polaritons.

Rydberg gases represent an ideal system to explore the interplay between coherent light excitation and dipolar interatomic interactions [1,2]. We have observed individual dark-state polaritons as they propagate through an ultracold atomic gas involving Rydberg states [3]. To further explore the dynamics of the dark-state polaritons, we have implemented a new all-optical method to in-situ image Rydberg atoms embedded in dense atomic gases [4]. Using this novel technique we show single shot images of small numbers of Rydberg atoms, allowing one to study the dynamics of strongly correlated many-body states as well as transport phenomena in Rydberg aggregates. We observe the migration of Rydberg electronic excitations, driven by quantum-state changing interactions similar to Forster processes found in complex molecules and light-harvesting complexes. The many-body dynamics of the energy transport can be influenced by a dissipative environment consisting of atoms in different Rydberg states [5].

Acknowledgment: Work done in collaboration with Vladislav Gavryusev, Georg Günter, Stephan Helmrich, Christoph S. Hofmann, Martin Robert-de-Saint-Vincent, Hanna Schempp, Shannon Whitlock (Physics Institute, University of Heidelberg), Martin Gärtner, Jörg Evers (MPI für Kernphysik, Heidelberg).

## References

- [1] M. Robert-de-Saint-Vincent *et al.*, Phys. Rev. Lett. **110**, 045004 (2013).
- [2] H. Schempp *et al.*, Phys. Rev. Lett. **112**, 013002 (2014).
- [3] C. S. Hofmann *et al.*, Phys. Rev. Lett. **110**, 203601 (2013).
- [4] G. Günter *et al.*, Phys. Rev. Lett. **108**, 013002 (2012).
- [5] G. Günter *et al.*, Science **342**, 954 (2013).

## Quantum crystals of photons and atoms

G. Morigi<sup>1</sup>

<sup>1</sup>*Universität des Saarlandes Theoretische Physik Campus E26 D-66041 Saarbrücken, Germany*

Presenting Author: giovanna.morigi@physik.uni-saarland.de

In this talk I will discuss several examples of selforganization of atoms inside a single-mode resonator. When a laser transversally pumps the atom, photon scattering into the resonator depends on the atoms density distribution within the cavity, and in turn determines the strength of the mechanical forces of light on the atoms, hence the atomic density. The dynamics is thus nonlinear and can lead to ordered atomic structures when the laser intensity exceeds a threshold determined, amongst other, by the rate of cavity losses. I will first discuss the dynamics of selforganization in the semiclassical regime, in which the atomic motion is cooled by the photon scattering processes which pump the cavity. I will then consider the quantum regime, where the atoms are ultracold bosons. The atoms are confined by an external optical lattice, whose period is incommensurate with the cavity mode wave length, and are driven by a transverse laser, which is resonant with the cavity mode. While for pointlike atoms photon scattering into the cavity is suppressed, for sufficiently strong lasers quantum fluctuations can support the build-up of an intracavity field, which in turn amplifies quantum fluctuations. In this parameter regime the atoms form clusters which are phase locked, thereby maximizing the intracavity photon number. I will argue that this system constitutes a novel setting where quantum fluctuations give rise to effects usually associated with disorder.

# Spatially dependent EIT from structured light

N. Radwell<sup>1</sup>, T.W. Clark<sup>1</sup>, and S. Franke-Arnold<sup>1</sup>

<sup>1</sup>SUPA, Optics Group, Physics and Astronomy, University of Glasgow, UK

Presenting Author: sonja.franke-arnold@glasgow.ac.uk

Recent years have seen vast progress in the generation and detection of structured light, with potential applications for high capacity optical data storage and quantum technologies in high dimensions. Interaction with atomic systems offers the possibility to process and store the information contained in such light beams. We are investigating the transmission of structured light through cold rubidium atoms trapped in our dark SPOT MOT [1].

Scattering and absorption of light by atoms is usually sensitive only to the intensity profile of a light beam, essentially producing a “shadow” of the atoms in the light beam. By simultaneously driving multiple atomic transitions it is possible to modify the absorption profile of a signal laser due to the presence of a second control beam, an effect known as EIT (electro-magnetically induced transparency). Here we report our first observations of EIT with holographically shaped signal and probe light, rendering the atoms transparent to light only at certain areas, see Fig. 1. Using liquid crystal devices with spatially varying directionality, so-called qplates [2], we produce light modes that are entangled in their polarisation and spatial phase profile, proportional to  $\sigma_+ e^{-i2q\varphi} + \sigma_- e^{i2q\varphi}$ , where  $\varphi$  denotes the azimuthal angle of the light beam,  $\sigma_{\pm}$  the polarisation and  $q$  the index of the qplate. This allows us to drive a Raman transition between the  $m_F = \pm 1$  ground states which satisfies EIT conditions only at discrete angles  $\varphi$ . The spatially varying atomic dark states result in a self-modulation of the incident light beams, effectively converting optical phase information into intensity information.

Potential extensions of this work include the generalisation to arbitrary phase structures, and the storage and read-out of spatial light from the atomic sample.

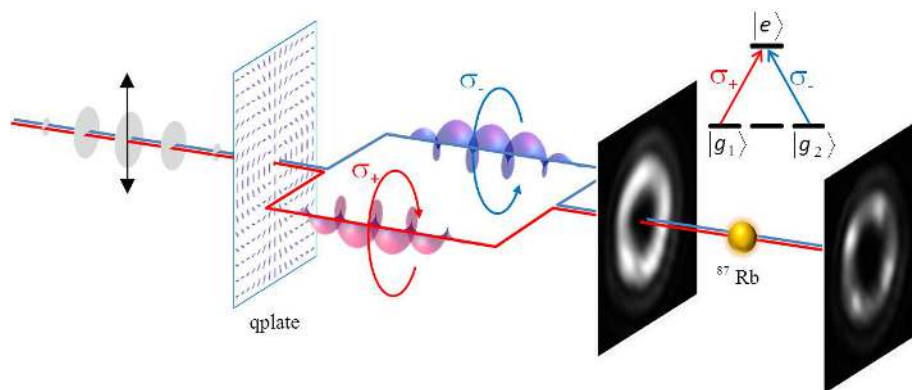


**Figure 1:** Schematic of experiment: linearly polarised probe light is converted via a qplate into light entangled in polarisation and phase structure before being transmitted through cold Rb atoms. The intensity profiles before and after interaction with the atoms are shown as insets.

## References

- [1] N. Radwell, G. Walker and S. Franke-Arnold, Phys. Rev. A. **88** 043409 (2013)
- [2] L. Marrucci *et al.*, J. Opt. **13** 064001 (2011)

# Muonic atoms: from atomic to nuclear and particle physics

A. Antognini<sup>1</sup>

<sup>1</sup>*Institute for Particle Physics, ETHZ, 8093 Zurich, Switzerland*

Presenting Author: aldo@phys.ethz.ch

Muonic atoms are atomic bound states of a negative muon and a nucleus. The muon, which is the 200 times heavier cousin of the electron, orbits the nucleus with a 200 times smaller Bohr radius. This enhances the sensitivity of the atomic energy levels to the nucleus finite size tremendously.

By performing laser spectroscopy of the  $2S - 2P$  transitions in muonic hydrogen we have determined the proton root mean square charge radius  $r_p = 0.84087(39)$  fm [1,2], 20 times more precisely than previously obtained. However, this value disagrees by 4 standard deviations from the value extracted from “regular “ hydrogen spectroscopy and also by 6 standard deviations from electron-proton scattering data. The variance of the various proton radius values has led to a very lively discussion [3] in various fields of physics: particle and nuclear physics (proton structure, new physics, scattering analysis), in atomic physics (hydrogen energy level theory, fundamental constants) and fundamental theories (bound-state problems, QED, effective field theories). The origin of this discrepancy is not yet known and the various (im)possibilities will be presented here.

An important piece of information regarding the “proton radius puzzle” is provided by spectroscopy of muonic deuterium and muonic helium [4]. In December 2013 we have succeeded for the first time to measure the  $2S_{1/2} - 2P_{3/2}$  transition in the  $\mu^4\text{He}^+$  ion at the Paul Scherrer Institute (Switzerland). As next we will measure transitions also in  $\mu^3\text{He}^+$ . Here we present preliminary results of muonic deuterium and helium spectroscopy, which beside helping to disentangle the origin of the observed “proton radius puzzle” also provide values of the corresponding nuclear charge radii with relative accuracies of few  $10^{-4}$ . These radii are interesting benchmarks for few-nucleon theories and can be combined with already measured isotope shifts in He and H.

## References

- [1] R. Pohl *et al.* Nature **466**, 213 (2010)
- [2] A. Antognini *et al.* Science **339**, 417 (2013)
- [3] R. Pohl, R. Gilman, G.A. Miller, K. Pachucki, Annu. Rev. Nucl. Part. Sci **63**, 165 (2013)
- [4] A. Antognini *et al.* Can. J. Phys. **89**, 47 (2011)

## Imaging the wavefunction of He<sub>2</sub>, He<sub>3</sub> and the Efimov state of He<sub>3</sub>

M. Kunitzki<sup>1</sup>, J. Voigtsberger<sup>1</sup>, S. Zeller<sup>1</sup>, L. Schmidt<sup>1</sup>, R. Grisenti<sup>1</sup>, M. Schöffler<sup>1</sup>, F. Trinter<sup>1</sup>, H. Kim<sup>1</sup>,  
F. Trinter<sup>1</sup>, W. Schöllkopf<sup>2</sup>, D. Bressanini<sup>3</sup>, T. Jahnke<sup>1</sup>, and R. Dörner<sup>1</sup>

<sup>1</sup>*University Frankfurt, Max von Laue Str. 1, 60483 Frankfurt, Germany*

<sup>1</sup>*Fritz-Haber-Institut der Max-Planck-Gesellschaft, Dept. of Mol. Phys., Berlin, Germany*

<sup>1</sup>*University of Insubria, Dipartimento di Scienza e Alta Tecnologia, Como, Italy*

Presenting Author: doerner@atom.uni-frankfurt.de

We report on the observation of the Efimov state of He<sub>3</sub> and show experimental images the wavefunctions of He<sub>2</sub> and He<sub>3</sub>. The experiments are performed by coulomb explosion imaging of mass selected He clusters using the COLTRIMS technique.

# Optomechanics at microwave frequencies: mechanical resonators coupled to microwave cavities and superconducting qubits

J.-M. Pirkkalainen<sup>1,2</sup>, S.U. Cho<sup>2</sup>, F. Massel<sup>3</sup>, J. Tuorila<sup>4</sup>, X. Song<sup>2</sup>, P.J. Hakonen<sup>2</sup>, T.T. Heikkilä<sup>3</sup>, and M.A. Sillanpää<sup>1,2</sup>

<sup>1</sup>Department of Applied Physics, Aalto University, P.O. Box 11100, FI-00076 Aalto, Finland

<sup>2</sup>O. V. Lounasmaa Laboratory, Aalto University, P.O. Box 15100, FI-00076 Aalto, Finland.

<sup>3</sup>Department of Physics, University of Jyväskylä, P.O. Box 35 (YFL) FI-40014 Jyväskylä, Finland

<sup>4</sup>Department of Physics, University of Oulu, FI-90014, Finland

Presenting Author: Mika.Sillanpaa@aalto.fi

Micromechanical resonators affected by radiation pressure forces allow to address fundamental questions on quantum properties of mechanical objects, or, to explore quantum limits in measurement and amplification. A new setup for the purpose is an on-chip microwave cavity coupled to a mechanical resonator (Fig. 1a). Under blue sideband irradiation, we demonstrate the possibility of building a mechanical microwave amplifier [1], with noise properties approaching the quantum regime. On the red sideband side, we show how one can couple mechanical resonators via the cavity bus, while simultaneously cooling the mechanical modes very close to the ground state of motion [2]. A recent development in linear optomechanics is the coupling of graphene membranes to microwave-frequency cavities. Here, we observe radiation pressure back-action on the motion of graphene.

One can add intriguing features to the basic optomechanics setup by including a superconducting qubit made with Josephson junctions. The nonlinearity of the two-level system allows for much more rich physics than is possible with linear cavities. We have realized a superconducting transmon qubit interacting with a micromechanical resonator [3]. We operate the qubit in the circuit cavity quantum electrodynamics (circuit QED) architecture, where the qubit is coupled also to a microwave cavity. Hence, the combined setup represents an artificial atom coupled to two different cavities (Fig. 1b). We measure the phonon Stark shift, splitting of the qubit spectral line into motional sidebands, and coherent sideband Rabi oscillations. Another motivation the tripartite system owes from the challenges to increase the single-quantum coupling strength to exceed the cavity dissipation rate. Motivated by this goal, we present a new design of the circuit optomechanical experiment, where the on-chip microwave cavity includes a Josephson charge qubit [4]. The cavity is coupled to a micromechanical resonator whose motion is visible as charge, and hence affects the cavity frequency. This way we were able to boost the coupling in the setup by six orders of magnitude up to the MHz regime.

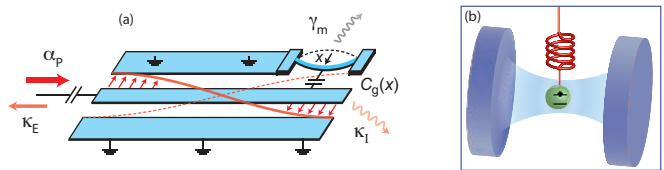


**Figure 1:** (a) A microwave resonator can be coupled capacitively to an arbitrary number of mechanical resonators. (b) Idea of introducing nonlinearity in optomechanics. Inside the cavity (blue) there is a quantum two-level system (green) which is mechanically compliant (red).

## References

- [1] F. Massel *et al.* Nature **480**, 351 (2011)
- [2] F. Massel *et al.* Nature Communications **3**, 987 (2012)
- [3] J.M. Pirkkalainen *et al.* Nature **494**, 211 (2013)
- [4] T.T. Heikkilä *et al.* Phys. Rev. Lett. **112**, 203603 (2014)

## Some recent developments in experimental positronium physics

D.B. Cassidy<sup>1</sup>

<sup>1</sup>*Department, of Physics and Astronomy, University College London, Gower Street, WC1E 6BT, London UK*

Presenting Author: d.cassidy@ucl.ac.uk

The use of a Surko-type buffer gas trap [1] has made it possible to turn ordinary neon-moderated d.c. positron beams [2] into devices that can deliver pulses containing millions of particles in a few ns burst [3]. These can be used to make a “gas” of positronium which, despite its 142 ns annihilation lifetime, can be probed with pulsed lasers in much the same way as any other atomic species [4]. The ability to create such a Ps gas makes feasible an array of hitherto impractical or impossible experiments, such as the production of molecular positronium [5]. In this talk I will discuss some experiments that can be carried out in this way that are related to the production of long-lived Rydberg positronium states, and their possible manipulation with inhomogeneous electric fields [6]. This work has many possible applications, including precision spectroscopy, scattering and even matter-antimatter gravity measurements [7].

### References

- [1] C. M. Surko, M. Leventhal, and A. Passner, *Phys. Rev. Lett.* **62**, 901 (1989)
- [2] *Positron Beams and Their Applications*, edited by P. G. Coleman (World Scientific, Singapore, 2000)
- [3] D. B. Cassidy, S. H. M. Deng, R. G. Greaves, and A. P. Mills Jr. *Rev. Sci. Instrum.* **77**, 073106 (2006)
- [4] D. B. Cassidy, T. H. Hisakado, H. W. K. Tom, and A. P. Mills, Jr. *Phys. Rev. Lett.* **109**, 073401(2012).
- [5] D. B. Cassidy, T. H. Hisakado, H. W. K. Tom, and A. P. Mills, Jr. *Phys. Rev. Lett.* **108**, 133402 (2012)
- [6] S. D. Hogan and F. Merkt *Phys. Rev. Lett.* **100**, 043001 (2008)
- [7] A. P. Mills, Jr. and M. Leventhal, *Nucl. Instrum.Methods in Phys. Res.* **B192**, 102-106 (2002).

## Non-adiabatic effects in laser orientation and alignment of molecules

Rosario González Férrez<sup>1</sup>

<sup>1</sup>*Dpto de Física Atómica, Molecular y Nuclear, Instituto Carlos I de Física Teórica y Computacional, Facultad de Ciencias, Universidad de Granada, 18071 Granada, Spain*

Presenting Author: rogonzal@ugr.es

We present a theoretical study of the laser-alignment and mixed-field-orientation of polar molecules. In these experiments, pendular states were created by means of linearly polarized strong laser pulses combined with tilted weak electric fields. The time dependent Schrödinger equation is solved into account the time profile of the experimental laser pulse and the theoretical results compared to the experimental observations. For perpendicular fields one obtains pure alignment, we demonstrate and analyze a strongly driven quantum pendulum in the angular motion of state-selected and laser-aligned OCS molecules. For tilted fields, we show that a fully adiabatic description of the process does not reproduce the experimentally observed orientation, and that it is mandatory to perform a time-dependent study taking into account the time profile of the laser pulse. Our results show that the adiabaticity of the mixed-field orientation depends at weak ac fields on the energy splitting of the states in a J-manifold, as well as on the formation of the quasi-degenerate doublets at stronger ac fields. These pendular doublets result in the transfer of population from a single occupied field-free rotational state into two strongly oriented and anti-oriented pendular states, reducing the overall orientation. Hence, we demonstrate that under ns laser pulses the weak dc field orientation is, in general, not adiabatic, so that a time-dependent description of the orientation process becomes mandatory. A revised condition for achieving adiabatic mixed-field orientation is provided.

# Rotational Cooling of Coulomb-Crystallized Molecular Ions by a Helium Buffer Gas

A.K. Hansen<sup>1</sup>, O.O. Versolato<sup>2</sup>, Ł. Kłosowski<sup>3</sup>, S.B. Kristensen<sup>1</sup>, A. Gingell<sup>1</sup>, M. Schwarz<sup>2</sup>,  
A. Windberger<sup>2</sup>, J. Ullrich<sup>2,4</sup>, J.R. Crespo López-Urrutia<sup>2</sup>, and M. Drewsen<sup>1</sup>

<sup>1</sup>QUANTOP – The Danish National Research Foundation Center for Quantum Optics, Department of Physics and Astronomy, Aarhus University, DK-8000 Aarhus C, Denmark

<sup>2</sup>Max-Planck-Institut für Kernphysik, Saupfercheckweg 1, D-69117 Heidelberg, Germany

<sup>3</sup>Institute of Physics, Faculty of Physics, Astronomy and Informatics, Nicolaus Copernicus University, Grudziadzka 5, 87-100 Torun, Poland

<sup>4</sup>Physikalisch-Technische Bundesanstalt, Bundesallee 100, D-38116, Braunschweig, Germany

Presenting Author: drewsen@phys.au.dk

In this talk, I will discuss recent experimental results on helium buffer-gas cooling of the rotational degrees of freedom of  $\text{MgH}^+$  molecular ions, which are trapped and sympathetically crystallized in a linear radio-frequency quadrupole trap [1]. With helium collision rates of only  $\sim 10 \text{ s}^{-1}$ , i.e. four to five orders of magnitude lower than in usual buffer gas cooling settings, we have cooled a single molecular ion to an unprecedented measured low rotational temperature of  $7.5_{-0.7}^{+0.9} \text{ K}$ . In addition, by only varying the shape and/or the number of atomic and molecular ions in larger Coulomb crystals, we have tuned the effective rotational temperature from  $\sim 7 \text{ K}$  up to  $\sim 60 \text{ K}$  by changing the micromotion energy. The very low helium collision rate may potentially even allow for sympathetic sideband cooling of single molecular ions, and eventually make quantum-logic spectroscopy of buffer gas cooled molecular ions feasible. Furthermore, application of the presented cooling scheme to complex molecular ions should have the potential of single or few-state manipulations of individual molecules of biochemical interest. This latter perspective can hopefully be exploited to disentangle various processes happening in complex molecules, like light harvesting complexes.

## References

[1] A. K. Hansen *et al.* Nature (2014) doi:10.1038/nature12996

# Bose-Einstein condensates and antiferromagnetic interactions: An illustration of symmetry breaking

J. Dalibard<sup>1</sup>

<sup>1</sup>*Collège de France and Laboratoire Kastler Brossel, CNRS - ENS - UPMC, 11 Place Marcelin Berthelot, 75005, Paris*

Presenting Author: jean.dalibard@lkb.ens.fr

In a spinor Bose gas, contact interactions can induce effective spin-spin interactions [1]. In the case of sodium atoms ( $^{23}\text{Na}$ , spin 1), these effective interactions are antiferromagnetic, which leads to a series of interesting phenomena. Here I will focus on recent experimental investigations that we have performed at ENS on a sodium condensate in the so-called Single Mode Approximation [2]: in this low temperature regime, all atoms occupy the same orbital wave function and only the spin degree of freedom is relevant. In the absence of external field, the exact ground state is expected to be the (massively entangled) singlet state, with a zero total spin [3]. However one can also use an approximate symmetry-breaking approach, in which all atoms condense a single spin state  $S_z = 0$  along an arbitrary  $z$  direction. I will discuss both approaches and connect them with the notion of a fragmented condensate [4], i.e., a situation where several states of a many-body system are simultaneously macroscopically populated [5].

This research has been performed in collaboration with Fabrice Gerbier, Tilman Zibold, Luigi De Sarlo, Emmanuel Mimoun, David Jacob, Lingxuan Shao, Vincent Corre and Camille Frapolli. It is supported by the ERC Synergy program (UQUAM project).

## References

- [1] D.M. Stamper-Kurn and M. Ueda, *Rev. Mod. Phys.* **85**, 1191 (2013)
- [2] see e.e.g. David Jacob, Lingxuan Shao, Vincent Corre, Tilman Zibold, Luigi De Sarlo, Emmanuel Mimoun, Jean Dalibard and Fabrice Gerbier, *Phys. Rev. A* **86**, 061601(R) (2012)
- [3] C.K. Law, H. Pu and N. Bigelow, *Phys. Rev. Lett.* **81**, 5257 (1998) ; T.L. Ho and S.K. Yip, *Phys. Rev. Lett.* **84**, 4031 (2000) ; Y. Castin and C. Herzog, *C. R. Acad. Sci.* **2** 419 43 (2001) ; S. Ashhab and A. J. Leggett, *Phys. Rev. A* **65**, 023604 (2002)
- [4] E.J. Mueller, T.L. Ho, M. Ueda and G. Baym, *Phys. Rev. A* **74**, 033612 (2006)
- [5] Luigi De Sarlo, Lingxuan Shao, Vincent Corre, Tilman Zibold, David Jacob, Jean Dalibard, Fabrice Gerbier, *New Journal of Physics* **15**, 113039 (2013).

# Density Functional Theory for strongly-correlated ultracold atom gases

F. Malet Giralt<sup>1,2</sup>, A. Mirtschink<sup>1</sup>, J. Bjerlin<sup>2</sup>, C. Mendl<sup>3</sup>, S. Reimann<sup>2</sup>, and P. Gori-Giorgi<sup>1</sup>

<sup>1</sup>*Theoretical Chemistry, Vrije University Amsterdam, the Netherlands*

<sup>2</sup>*Mathematical Physics, Lund University, Sweden*

<sup>3</sup>*Zentrum Mathematik, Technical University of Munich, Germany*

Presenting Author: f.maletgiralt@vu.nl

Density functional theory (DFT), extremely successful in electronic structure calculations [1,2], has received relatively little attention for the study of ultracold atomic systems. We show that a recently proposed DFT methodology [3,4], aimed at the study of strongly-correlated electronic systems, can be generalized for its application to their ultracold-gases counterparts.

## References

- [1] W. Kohn, *Rev. Mod. Phys.* **71**, 1253 (1999).
- [2] A. J. Cohen, Paula Mori-Sánchez and Weitao Yang, *Chem. Rev.* **112**, 289 (2012).
- [3] F. Malet *et al.* *Phys. Rev. B* **87**, 115146 (2013).
- [4] C. B. Mendl, F. Malet, and P. Gori-Giorgi, *Phys. Rev. B* **89**, 125106 (2014).

# Rigorous Relativistic Many-Body Methods for Exploring Fundamental Physics in Atoms and Molecules

T. Fleig<sup>1</sup>

<sup>1</sup>Laboratoire de Chimie et Physique Quantique, I.R.S.A.M.C., Université Paul Sabatier, F-31062, Toulouse

Presenting Author: timo.fleig@irsamc.ups-tlse.fr

Problems requiring an accurate knowledge of the electronic structure of small heavy-element molecules can nowadays be addressed with uncompromising electron correlation methods in the framework of the Dirac-Coulomb equation [1]. These methods owe their rigor to the relativistic four-component all-electron approach and their efficiency to creator-string driven algorithms. The first part of the presentation covers general principles of relativistic configuration interaction [2] and relativistic coupled cluster [3,4] and their current domains of applicability. Among these are, despite the design based on molecular double group symmetry, also purely atomic problems.

In the second part of the talk recent applications with an emphasis on research in fundamental physics will be discussed, in particular the search for the electric dipole moment of the electron. The relativistic four-component configuration interaction approach has been used to study  $\mathcal{P}$ - and  $\mathcal{T}$ -odd interaction constants in the  $\text{HfF}^+$  molecular ion [5,6] and the ThO molecule [7]. For ThO  $\Omega = 1$  we obtain a value of  $E_{\text{eff}} = 75.2 \left[ \frac{\text{GV}}{\text{cm}} \right]$  with

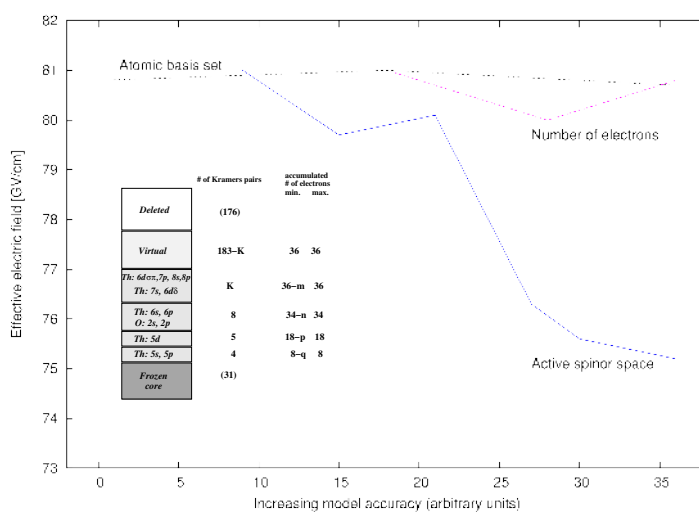


Figure 1: Model dependency of the electron EDM effective electric field in ThO.

an estimated error bar of 3% and 10% smaller than a previously reported result [*J. Chem. Phys.*, 139:221103, 2013]. The smaller effective electric field increases the previously determined upper bound [*Science*, 343:269, 2014] on the electron electric dipole moment to  $|d_e| < 9.7 \times 10^{-29} e \text{ cm}$  and thus mitigates constraints to possible extensions of the Standard Model of particle physics.

## References

- [1] T. Fleig, *Chem. Phys.* **395**, 2–15 (2012)
- [2] S. Knecht, H. J. Å. Jensen, T. Fleig, *J. Chem. Phys.* **132** 014108 (2010)
- [3] M. Hubert, L. K. Sørensen, J. Olsen, T. Fleig, *Phys. Rev. A* **86** 012503 (2012)
- [4] L. K. Sørensen, J. Olsen, T. Fleig, *J. Chem. Phys.* **134** 214102 (2011)
- [5] T. Fleig, M. K. Nayak, *Phys. Rev. A* **88** 032514 (2013)
- [6] K. C. Cossel *et al.*, *Chem. Phys. Lett.* **546** 1–11 (2012)
- [7] T. Fleig, M. K. Nayak, *J. Mol. Spectrosc.*, in press. (2014)

# Experiments with finite Fermi systems in the crossover from few to many-body physics

A. N. Wenz<sup>1,2</sup>

<sup>1</sup>*Physikalisches Institut, Ruprecht-Karls-Universität Heidelberg, 69120 Heidelberg, Germany*

<sup>2</sup>*Max-Planck-Institut für Kernphysik, Saupfercheckweg 1, 69117 Heidelberg, Germany*

Presenting Author: wenz@physi.uni-heidelberg.de

We study the crossover from few- to many-body physics by investigating an ultracold atom system that consists of one single impurity atom and an increasing number of majority atoms in a different spin state.

The experiments are performed with a system of fermionic  ${}^6\text{Li}$  atoms in two different spin states. Due to the elongated shape of our optical dipole trap the system is well described by the one-dimensional framework. Starting from the two-particle system where the single impurity atom interacts with only one majority atom, we measure the interaction energy as a function of the number of majority atoms by means of radio-frequency spectroscopy. In the two-particle case the experimentally determined interaction energies are in good agreement with the analytical prediction from T. Busch *et al.* [1]. For systems with more majority atoms, the interaction energy shows good agreement with numerical few-body calculations. Already for more than three majority atoms, the normalized interaction energies converge quickly towards a many body-limit. This limit coincides with the analytic prediction for an infinite number of majority atoms which we obtain by adapting the homogeneous solution of J. McGuire [2] to a trapped system.

## References

- [1] T. Busch *et al.*, Found. of Phys. **28**, 549 (1998).
- [2] J. McGuire, JMP 6, 432 (1965).

# Controlling the orientation of the molecular angular momentum by shaping the polarization of a fs laser pulse

G. Karras<sup>1</sup>, E. Hertz<sup>1</sup>, M. Ndong<sup>1</sup>, F. Billard<sup>1</sup>, D. Sugny<sup>1</sup>, B. Lavorel<sup>1</sup>, and O. Faucher<sup>1</sup>

<sup>1</sup>Laboratoire Interdisciplinaire Carnot de Bourgogne (ICB), UMR 6303 CNRS-Université de Bourgogne, 9 Av. A. Savary, BP 47 870, F-21078 DIJON Cedex, France

Presenting Author: gabriel.karras@u-bourgogne.fr

Over the last twenty years, lasers have been offer great potentials for controlling the rotational dynamics of molecules. The wealth of the information accessed and the number of potential applications is far richer as a molecular ensemble loses its isotropic behavior. Laser induced field-free molecular alignment is a representative example for the above [1]. In this case, the molecules are aligned along and perpendicular to the laser polarization axis at well spaced fractions of the molecular rotational period even after the pulse has been switched off. In the current work, we present an original way for enriching the aforementioned control of molecular rotation by orienting the angular momentum or equivalently by inducing unidirectional molecular rotation. The investigation is conducted in N<sub>2</sub> at atmospheric pressure. The desired unidirectional rotation was embedded to the molecular targets after they were irradiated with a pulse of rotating linear polarization. The effect is quantified using the rotational Doppler effect [2]. In translational Doppler effect, a photon with momentum  $p=h/\lambda$  reflected by a moving object with momentum  $p=mu$  is frequency shifted by  $\Delta v=2u/\lambda$ . The fact that electromagnetic waves posses also spin angular momentum gives rise to the angular analog of the aforementioned effect. Thus, when a circularly polarized photon with spin angular momentum  $\hbar$  interacts with a rotating body with angular velocity  $\Omega$ , its frequency is shifted by  $\Delta\omega=2\Omega$ . The experimental results are reproduced quite well by numerical simulations and comparison between the different schemes proposed for inducing angular momentum orientation is discussed. The dependence of the rotational frequency shift on different experimental parameters, such as laser intensity, polarization state, and pulse duration is also presented and compared with theoretical findings.

## References

- [1] H. Stapelfeldt, T. Seideman Rev. Mod. Phys. **75**, 543–557 (2003)
- [2] O. korech,U. Steinitz,R. J. Gordon, I. S. Averbukh. Y. Prior, Nat. Photonics **7**, 711–714 (2013)

# High resolution spectroscopy of 1S-3S transition in hydrogen

S. Galtier<sup>1</sup>, H. Fleurbaey<sup>1</sup>, F. Nez<sup>1</sup>, L. Julien<sup>1</sup>, and F. Biraben<sup>1</sup>

<sup>1</sup>Laboratoire Kastler Brossel, UPMC, ENS, CNRS, 4 place Jussieu, 75005 Paris, France

Presenting Author: sandrine.galtier@lkb.upmc.fr

The aim of our experiment is a new determination of the proton charge radius  $R_p$  from high resolution spectroscopy on hydrogen. The proton is the simplest stable hadronic system and a precise knowledge of its properties has fundamental interests. Today the proton charge radius is determined by three different methods:

*Low energy electron scattering.* A thorough analysis of all the scattering data has been made by I. Sick. The result is  $R_p = 0.895$  (18) fm. A new determination has also been done at Mainz university [1].

*Hydrogen spectroscopy.* Thanks to the optical frequency measurements and the Doppler free techniques, the energy shift due to the finite size of the proton can be now observed on the spectroscopy of hydrogen. The value of the proton radius extracted from the comparison between the experiment and the theory in hydrogen is  $R_p = 0.8760$  (78) fm.

*Spectroscopy of muonic hydrogen.* The principle of the experiment is to measure the 2S Lamb shift in muonic hydrogen (an atom formed with a proton and a muon,  $\mu$ -p). In July 2009, this experiment has been successful. The result is  $R_p = 0.8409$  (4) fm [2]. The figure below summarizes these different determinations of  $R_p$ .

The figure 1 shows clearly a discrepancy between the new value deduced from the muonic hydrogen spectroscopy and the previous ones. We aim to contribute to the "proton charge radius puzzle" by measuring the optical frequencies of two transitions in hydrogen, firstly the 1S-3S two photon transition and, secondly, the 1S-4S two photon transition. We realized a new cw-laser source at 205 nm to perform the two-photon spectroscopy of the 1S-3S transition. Light at 894 nm from a titanium-saphir laser is mixed with the fourth harmonic of a ND:YO<sub>4</sub> laser in a BBO crystal (at 266 nm). We obtained up to 15 mW of continuous narrow-band laser source à 205 nm [3]. We observed the 1S-3S transition and deduced its center frequency with an uncertainty 4 times better than previous results [4]. I will present this very preliminary result and the development of a liquid nitrogen cooled hydrogen beam.

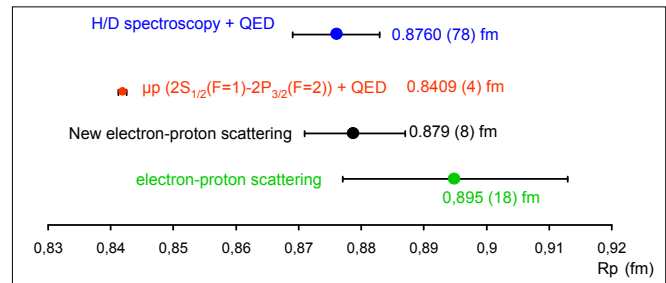


Figure 1: The different determinations of the proton charge radius.

## References

- [1] J. C. Bernauer *et al.*, Phys. Rev. Lett., **105**, 24 (2010)
- [2] A. Antognini *et al.*, Science, **339**, 417-420 (2013)
- [3] S. Galtier, F. Nez, L. Julien and F. Biraben, to be published in Opt. Comm.
- [4] O. Arnoult, F. Nez, L. Julien and F. Biraben, Eur. Phys. J. D., **61**, 243 (2010)

## Probing double ionisation at the attosecond timescale

D. Guénot<sup>1</sup>, E.P. Mansson<sup>1</sup>, C.L. Arnold<sup>1</sup>, D. Kroon<sup>1</sup>, S.L. Sorensen<sup>1</sup>, M. Gisselbrecht<sup>1</sup>, A. L’Huillier<sup>1</sup>, J.M. Dahlström<sup>2</sup>, and A.S. Kheifets<sup>3</sup>

<sup>1</sup>Department of Physics, Lund University, SE-221 00 Lund, Sweden

<sup>2</sup>Department of Physics, Stockholm University, Sweden

<sup>3</sup>Research School of Physical Sciences, The Australian National University, Canberra ACT 0200, Australia

Presenting Author: diego.guenot@fysik.lu.se

The development of ultrashort light pulses in the attosecond range allows scientists to explore the dynamics of electron correlation. The single ionization delay has been measured in various atoms using either the streaking technique or an interferometric technique ([1],[2]). Those studies triggered a lot of theoretical activities showing that the IR used to probe the ionized electrons changes their phase and therefore add an additional delay [3].

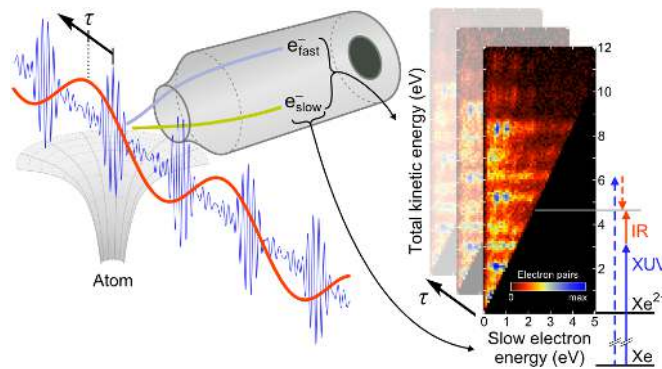


Figure 1: Principle of the experiment.

Recently the first time-resolved measurement of double ionization was performed in xenon using an interferometric technique combined with coincidence measurement (see fig.1). We measured a delay between double and single ionization of  $55 \pm 60$  as [4] in excellent agreement with our theoretical calculations. Those calculations aimed at understanding the influence of the IR-field in the case of double ionization in order to extract the one-photon delay. Unfortunately the exact shape of the two electron wave packet in the continuum is not known. In this work we report the calculation of the IR-induced delay in double photo ionization using three different models for the wave function; the two screened coulomb wave function, the Wentzel–Kramers–Brillouin (WKB) wave function and the three coulomb wave function [5]:

$$\Psi_{k_1, k_2}^{2C}(r_1, r_2) = F_1(Z_{eff}, k_1) \times F_1(Z_{eff}, k_2), \quad (1)$$

$$\Psi_{k_1, k_2}^{WKB}(r_1, r_2) = P e^{-i \frac{S}{\hbar}}, \quad (2)$$

$$\Psi_{k_1, k_2}^{3C}(r_1, r_2) = F_1(-1, k_1) \times F_1(-1, k_2) \times F_1(+1, k_{12}). \quad (3)$$

With  $k_1, k_2$  the wave vectors of the two electrons,  $Z_{eff}$  the effective screening between the electrons,  $F_1$  the coulomb wave function,  $P$  the amplitude probability and  $S$  the two-electrons action. The results obtained for the three different models are compared and discussed.

### References

- [1] M. Schultze *et al.*, Science 328, 1658 (2010)
- [2] K.Klünder *et al.*, Phys. Rev. Lett. **106**, 143002 (2011)
- [3] J. M. Dahlström *et al.*, Phys. Chem. Chem. Phys. **414**, 53 (2013)
- [4] E. Mansson *et al.*, Nature physic **292**, 1689 (2013)
- [5] D. Guénot *et al.*, in preparation

# Detecting ultrafast interatomic electronic processes in media by fluorescence

A. Knie<sup>1</sup>, A. Hans<sup>1</sup>, M. Förstel<sup>2</sup>, U. Hergenhahn<sup>2</sup>, T. Jahnke<sup>3</sup>, R. Dörner<sup>3</sup>, A.I. Kuleff<sup>4</sup>, L.S. Cederbaum<sup>4</sup>, Ph.V. Demekhin<sup>1</sup>, and A. Ehresmann<sup>1</sup>

<sup>1</sup>Institute of Physics, University of Kassel, 34132 Kassel, Germany

<sup>2</sup>Max-Planck-Institut für Plasmaphysik, EURATOM Association, 17491 Greifswald, Germany

<sup>3</sup>Institut für Kernphysik, J. W. Goethe Universität, 60438 Frankfurt, Germany

<sup>4</sup>Physikalisch-Chemisches Institut, Universität Heidelberg, 69120 Heidelberg, Germany

Presenting Author: knie@physik.uni-kassel.de

*Interatomic Coulombic Decay (ICD), a radiationless transition in weakly bonded systems, such as solutes or van-der-Waals bound aggregates, is an effective source for electrons of low kinetic energy. So far, the ICD processes could only be probed in ultra-high vacuum by using electron and/or ion spectroscopy. Here we show that resonant ICD processes can also be detected by measuring the subsequently emitted characteristic fluorescence radiation, which makes their study in dense media possible.*

ICD is an energy transfer mechanism that occurs inside a chemical environment between excited atoms and their atomic neighbors [1]. As a result of the energy transfer, electrons of low kinetic energy are created [2]. As these electrons are known to be genotoxic, it was suggested that ICD might contribute to radiation damage [3] and could be employed in novel cancer treatment scenarios [4,5]. So far, the emitted charged particles were used to detect ICD [2]. This is, however, not possible in dense – especially biological - media [6]. Here we employ the detection of fluorescence light to verify the occurrence of ICD in a model system. This novel approach is the only known method for tracing ICD in dense matter. Thus, it holds great promise for exploring the role of this efficient energy transfer mechanism in biological systems.

The present experiments were performed for the prototype Ne-clusters, for which it is known that resonant excitation of an inner valence electron triggers ICD [7]. The process is sketched in Fig. 1. An incoming photon resonantly excites an inner-valence (2s) electron of atom A (a). This electronic excitation is known to relax via two competing pathways: (i) by autoionization of the same atom A leading to the emission of fast electrons (kinetic energy between 23 and 27 eV); and, alternatively, (ii) via the resonant ICD which gives rise to the emission of slow electrons (kinetic energy between 0 and 10 eV) from Atom B (b). Both processes are ultrafast and completely suppress the resonant fluorescence of the initially excited state. If the first pathway takes place, the relaxation process ends. This is not the case in the second pathway which is described in Fig. 1. Importantly, ICD becomes the dominant relaxation pathway when the cluster size grows [8]. In ICD, a valence electron of atom A fills the hole in the inner-valence shell. The energy gained is ultrafast transferred to a valence electron of a neighboring atom B, leading to its release (b). As can be seen in Fig. 1, due to the presence of the excited electron, a part of the excess energy is still stored in atom A where one electron remains excited. This excess energy is not sufficient to further ionize the system and is released by the emission of a photon (c), which is used here to identify the preceding ICD.

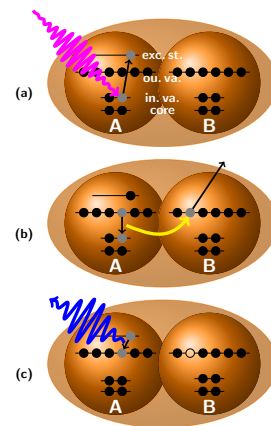


**Figure 1:** Schematic of fluorescence following ICD after resonant excitation in Ne-clusters.

## References

- [1] L. S. Cederbaum, J. Zobeley, F. Tarantelli Phys. Rev. Lett. **79** 4778 (1997).
- [2] U. Hergenhahn J. Elec. Spec. Rel. Phen. **184** 78 (2011).
- [3] P. H. P. Harbach *et al.* J. Phys. Chem. Lett. **4** 943 (2013).
- [4] K. Gokhberg *et al.* Nature **505** 661 (2014).
- [5] F. Trinter *et al.* Nature **505** 664 (2014).
- [6] N. Ottosson *et al.* J. Elec. Spec. Rel. Phen. **177** 60 (2010).
- [7] S. Barth *et al.* J. Chem. Phys. **122** 241102 (2005).
- [8] M. Öhrwall *et al.* Phys. Rev. Lett. **93** 173401 (2004).

# Sub-Doppler linear spectroscopy in a vapour confined in an opal

E. Moufarej<sup>1</sup>, P. Ballin<sup>1</sup>, I. Maurin<sup>1</sup>, A. Laliotis<sup>1</sup>, and D. Bloch<sup>1</sup>

<sup>1</sup>Laboratoire de Physique des Lasers, CNRS, UMR7538, Université Paris 13, Sorbonne-Paris-Cité, 99 avenue Jean-Baptiste Clément, 93 430 Villetaneuse, France

Presenting Author: athanasios.laliotis@univ-paris13.fr

There is a growing technological need to fabricate compact optical clocks [1]. Inspired by this need and the elimination of the Doppler broadening allowed by a sub-wavelength confinement of the atomic motion in the r.f. domain [2], we have analyzed, with high resolution laser spectroscopy, the optical spectrum of a gas confined in the sub-micron interstitial regions of an opal .

An opal consists of a crystalline arrangement of glass nanospheres, usually considered as a "soft preparation" for a photonic crystal. To avoid destructive chemical interactions between the bulk opal and the (heated) alkali-metal vapour; we have turned to a Langmuir-Blodgett (LB) preparation of a few layers opal [3,4] deposited on a window, around which the vapour cell is constructed (Fig. 1). In spite of the increasing structural defects in the successive layers of a LB opal defects, the essence of a deposited opal is a combination of a periodical layered structure -compact arrangement- with an empty gap between the flat window and the first layer of opals, promptly touching the window. With such a cell technology, the presence of a specular reflection beam is partly unexpected because the opal/window and opal/vacuum interfaces are strongly non planar (at a microscopic/wavelength scale). We show that this gap is responsible of this specular reflection and have a strong influence on it. The size of the "gap" region, relatively to the wavelength, is an essential parameter.

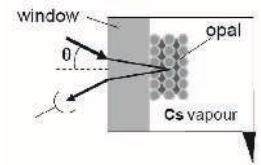


**Figure 1:** Schematic of the reflection spectroscopy on an opal (magnified in the caption) infiltrated by a cesium vapour.

On opals with 10 or 20 layers of 1  $\mu\text{m}$  spheres, sub-Doppler spectra are observed under near normal incidence evoking thin cell spectroscopy, with vapour confined in the gap region. The spectra are getting broader with the incidence angle. The original finding is that for large incidence angles ( $\theta = 40\text{-}50$  degrees), there is a narrow sub-Doppler structure superimposed to a broad spectrum [3,4]. The shape of this narrow structure, observed in purely linear spectroscopy, quickly evolves with the incidence angle. Its contrast is the highest for an incident beam TM-polarised. Recent experiments have confirmed these findings with 400 nm and 750 nm spheres, or for  $\lambda = 455$  nm Cs line. Our results are in agreement with a calculation taking into account the phase matching between the atomic contributions located in various layers of interstices, and the geometry of the periodical distribution of opals. From this, we deduce that the narrow structures observed for a large range of oblique incidences are associated to a genuine 3-D confinement. Our results allow envisioning very compact sub-Doppler references, applicable to weak (hardly saturable) molecular lines with a probed volume conceptually as small as several spheres. The detection of scattered light may also provide lineshapes more uniform with the incidence.

## References

- [1] S. Knappe et al., App. Phys. Lett., 85, 1460-1462 (2004)
- [2] R. H. Dicke, Phys. Rev., 89, 472-473 (1953)
- [3] P. Ballin et al., App. Phys. Lett., 102, 231115 - 231115-5 (2013)
- [4] P. Ballin et al., Proc. of SPIE., 8770, 87700J-1 - 87700J-6 (2013)

# Ultracold mixtures of metastable triplet He and Rb: scattering lengths from *ab initio* calculations and thermalization measurements

S. Knoop<sup>1</sup>, P.S. Żuchowski<sup>2</sup>, D. Kędziera<sup>3</sup>, Ł. Mentel<sup>4</sup>, M. Puchalski<sup>5</sup>, H.P. Mishra<sup>1</sup>, A.S. Flores<sup>1</sup>, and W. Vassen<sup>1</sup>

<sup>1</sup>LaserLaB, Department of Physics and Astronomy, VU University, Amsterdam, The Netherlands

<sup>2</sup>Institute of Physics, Faculty of Physics, Astronomy and Informatics, Nicolaus Copernicus University, Torun, Poland

<sup>3</sup>Department of Chemistry, Nicolaus Copernicus University, Torun, Poland

<sup>4</sup>Section of Theoretical Chemistry, VU University, Amsterdam, The Netherlands

<sup>5</sup>Faculty of Chemistry, Adam Mickiewicz University, Poznań, Poland

Presenting Author: s.knoop@vu.nl

We have investigated the ultracold interspecies scattering properties of metastable triplet He and Rb. We have performed state-of-the-art *ab initio* calculations of the relevant interaction potential, from which the scattering lengths are obtained for all four isotope combination [1]. Experimentally, we have studied thermalization of an ultracold mixture in a quadrupole magnetic trap, containing  $6 \times 10^6$  metastable triplet  $^4\text{He}$  atoms in the  $m_S = 1$  state and  $3 \times 10^8$   $^{87}\text{Rb}$  atoms in the  $F=2$ ,  $m_F=2$  Zeeman substate, from which we obtain tight bounds on the scattering length [2], in excellent agreement with the *ab initio* calculation. Our combined theoretical and experimental work provides a necessary step towards quantum degenerate  $\text{He}^* + \text{Rb}$  mixtures, which is interesting for few-body physics that require a large mass ratio. More general, our work shows the possibility of quantitative determination of scattering lengths for a system containing a heavy, many-electron atom using *ab initio* calculations.

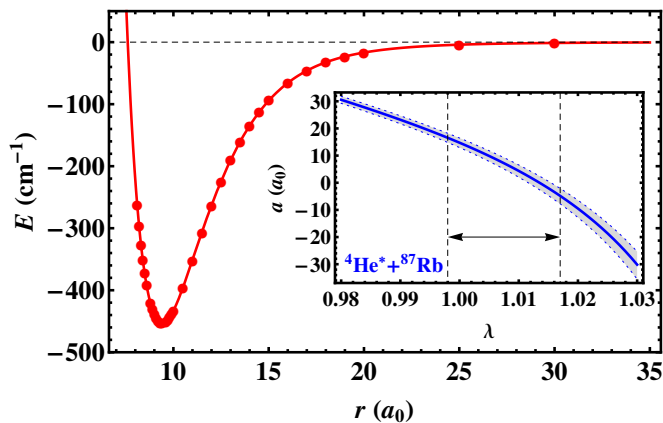


**Figure 1:** Results of the *ab initio* calculation on the  $^4\Sigma^+$  potential of  $\text{He}^*\text{Rb}$ . The inset shows the quartet scattering length for  $^4\text{He}^* + ^{87}\text{Rb}$  as function of the scaling parameter of the potential well depth  $\lambda$ , where the shaded area (bounded by the blue dotted lines) represents the uncertainties in the long-range coefficients  $C_6$  and  $C_8$ . The dashed vertical lines and the arrow represent the uncertainty in the *ab initio* potential.

## References

- [1] S. Knoop, P.S. Żuchowski, D. Kędziera, Ł. Mentel, M. Puchalski, H.P. Mishra, A.S. Flores, W. Vassen, in preparation  
 [2] H.P. Mishra, A.S. Flores, W. Vassen, S. Knoop, in preparation

## Long-distance channeling of cold atoms exiting a 2D magneto-optical trap by a Laguerre-Gaussian laser beam

M. Jacquey<sup>1</sup>, V. Carrat<sup>1</sup>, C. Cabrera-Gutiérrez<sup>1</sup>, J.W. Tabosa<sup>2</sup>, B. Viaris de Lesegno<sup>1</sup>, and L. Pruvost<sup>1</sup>

<sup>1</sup>Laboratoire Aimé-Cotton. CNRS, Univ. Paris-Sud, ENS-Cachan F-91405, Orsay, France  
<sup>2</sup>Departamento de Física, Universidade Federal de Pernambuco, 50.670-901 Recife, PE, Brazil

Presenting Author: marion.jacquey@u-psud.fr

Using a blue-detuned laser, shaped into a Laguerre-Gaussian (LG) donut mode we channel atoms exiting a 2-dimensional magneto-optical trap (2D-MOT) over a 30 cm distance. Compared to a freely-propagating beam, the atomic flux (about  $10^{10}$ at/s) is conserved whereas the divergence is reduced from 40 to 3 mrad. So, 30 cm far the 2D-MOT exit, the atomic beam has a 1 mm diameter and the atomic density is increased by a factor of 200 [1].

Such a LG-channeled-2D-MOT with a high density flux is a promising device to efficiently load a 3D-MOT reducing the capture volume and thus the required dimensions of the 3D-MOT trapping beams. The LG-channeled-2D-MOT is suitable for experiments on chips or for collision experiments.

The LG-channeled-2D-MOT has been studied versus the order of the LG mode (from 2 to 10) and versus the laser-atom frequency detuning (from 2 to 120 GHz). A clever version in which the LG mode frequency is locked to the repumping transition allows us to run the setup with two lasers instead of three.

### References

[1] V. Carrat, C. Cabrera-Gutiérrez, M. Jacquey, J. W. Tabosa, B. Viaris de Lesegno, and L. Pruvost Opt. Lett., **39**, 719-722 (2014)

# Control of Quantum Dynamics on an Atom-Chip

C. Lovecchio<sup>1</sup>, S. Cherukattil<sup>1</sup>, M. Alì-Khan<sup>1</sup>, F. Caruso<sup>1</sup>, and F.S. Cataliotti<sup>1,2</sup>

<sup>1</sup>LENS and Dipartimento di Fisica e Astronomia, Università di Firenze, Via Sansone 1, 50019, Sesto Fiorentino (FI), Italy  
<sup>2</sup>QSTAR, Largo Enrico Fermi 2, 50125 Firenze, Italy

Presenting Author: fsc@lens.unifi.it

We work with a novel multi-state cold-atom interferometer that is easy-to-use and fully merged with an Atom-Chip. We do not rely on external variables i.e. on spatially separated paths, but use internal atomic states. The multi-state functionality is achieved by coherent manipulation of BECs in different Zeeman states of the same hyperfine level by means of radio-frequency (RF) and static magnetic fields. The interferometric fringes are sharpened due to the higher-harmonic phase contributions of the multiple energetically Zeeman states. The complete coherence of the atom transfer between the condensates guarantees the full fringe visibility. The increase in sensitivity is paid by a reduction in the interferometer sensing range and an undesirable cross-sensitivity to magnetic fields. While the former is an intrinsic property of multi-path interferometers, we suggest how the effects of the latter can be reduced by using a differential measurement configuration. In addition, our interferometer does not require neither alignment nor high resolution imaging [1].

Driving the complex dynamics of physical systems to perform a specific task is extremely useful but challenging in several fields of science, and especially for fragile quantum mechanical systems. Even harder, and often unfeasible, is to invert the time arrow of the dynamics, undoing some physical process. We theoretically and experimentally drive forth and back through several paths in the five-level Hilbert space of a Rubidium atom in the ground state (see Figure 1). We achieve such an objective applying optimal control strategies to a Bose-Einstein condensate on an Atom-chip via a frequency modulated RF field. We apply also this technique to control the sensitivity of the multi state atom interferometer.

We further prove that backward dynamical evolution does not correspond to simply inverting the time arrow of the driving field neglecting the only-system part of the dynamics. Apart from the relevance for the foundations of quantum mechanics, these results are important steps forward in the manipulation of quantum dynamics that is crucial for several physical implementations and very promisingly powerful quantum technologies.

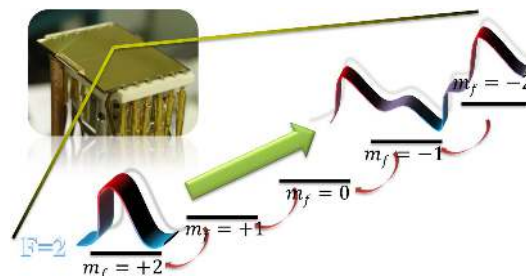


**Figure 1:** A condensate of  $^{87}\text{Rb}$  is created on an Atom-Chip in the  $|F =, m_F = +2\rangle$  state. The dynamics of the system is driven by coupling the different spin orientations with a radio-frequency electromagnetic field

## References

- [1] J. Petrovic *et al.* New Journal of Physics **15** (4), 043002 (2013)

## Rydberg blockade in arrays of optical tweezers

S. Ravets<sup>1</sup>, D. Barredo<sup>1</sup>, H. Labuhn<sup>1</sup>, L. Beguin<sup>1</sup>, A. Vernier<sup>1</sup>, F. Nogrette<sup>1</sup>, T. Lahaye<sup>1</sup>, and A. Browaeys<sup>1</sup>

<sup>1</sup>Laboratoire Charles Fabry, Institut d'Optique, CNRS, , Univ Paris Sud, 2 avenue Augustin Fresnel, 91127 Palaiseau cedex, France

Presenting Author: sylvain.ravets@institutoptique.fr

Controlling individual neutral atoms in arrays of optical tweezers is a promising avenue for quantum science and technology [1–2]. Using a spatial light modulator (SLM), we demonstrate our ability to trap single atoms in arrays of up to 100 traps separated by a few microns with controllable geometry. Using a two-photon excitation scheme, we coherently excite systems of two or three atoms to Rydberg states. The interaction between Rydberg atoms results in the observation of a characteristic Rydberg blockade effect. When the single-atom Rabi frequency for excitation to the Rydberg state is comparable to the interaction, we observe a partial Rydberg blockade where the populations vary in time with different frequency components. Comparing the experimental measurements with a model based on the optical Bloch equations, we are able to extract the van der Waals energy [3]. We measure the evolution of the C6 coefficient for different quantum numbers, distances and angles between the atoms. Despite the anisotropy of the interaction measured between two atoms in a D state, we are able to demonstrate a perfect blockade in arrays of three atoms with linear and triangular configuration. This work extends the potentialities of our system to 2D geometries, ideal for quantum simulation of frustrated quantum magnetism with Rydberg atoms.

### References

- [1] E. Urban *et al.* Nat. Phys. **5** 110 (2009)
- [2] A. Gaetan *et al.* Nat. Phys. **5** 115 (2009)
- [3] L. Beguin *et al.* Phys. Rev. Lett. **110** 263201 (2013)

# Generation of a macroscopic spin singlet

N. Behbood<sup>1</sup>, F. Martin Ciurana<sup>2</sup>, G. Colangelo<sup>2</sup>, M. Napolitano<sup>2</sup>, G. Tóth<sup>2,3,4</sup>, R.J. Sewell<sup>1</sup>, and M.W. Mitchell<sup>1,5</sup>

<sup>1</sup>ICFO-Institut de Ciències Fotoniques, Mediterranean Technology Park, 08860 Castelldefels, Spain.

<sup>2</sup>IKERBASQUE, Basque Foundation for Science, E-48011 Bilbao, Spain.

<sup>3</sup>Department of Theoretical Physics, UPV/EHU, P.O. Box 644, E-48080 Bilbao, Spain.

<sup>4</sup>Wigner Research Centre for Physics, Hungarian Academy of Sciences, P.O. Box 49, H-1525 Budapest.

<sup>5</sup>ICREA-Institució Catalana de Recerca i Estudis Avançats, 08015 Barcelona, Spain.

Presenting Author: naeimeh.behbood@icfo.es

Generating and detecting highly entangled macroscopic singlet states is of enormous interest. Such states are the ground states of many fundamental spin models (e.g. the anti-ferromagnetic Heisenberg model) [1], and may be useful for quantum information [2] and quantum metrology [3] applications. An ideal singlet has total angular momentum with zero mean and zero variance, a truly zero angular momentum. Approximate singlets can be identified with a generalized spin squeezing inequality (SSI) for unpolarized states [4], which show that total spin variance below a standard quantum limit (SQL) implies entanglement among the spins. We generate approximate singlet states using the tools of measurement-induced spin squeezing: quantum non-demolition measurement [5] and coherent magnetic rotations [6]. By squeezing all three spin components, we approach the zero of total spin. Using a cold rubidium atomic ensemble and near-resonant Faraday rotation probing, we have observed up to 3 dB of squeezing relative to the SQL, and a violation of the SSI by more than 5 standard deviations [7].

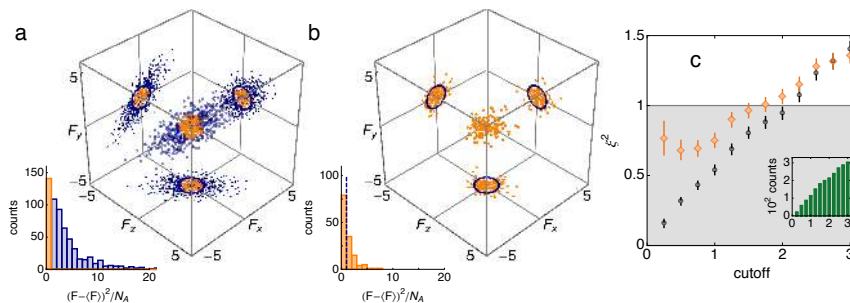


**Figure 1:** From the initial spin distribution (blue data in figure (a)), we select data with  $|\mathbf{F}^{(1)} - \langle \mathbf{F}^{(1)} \rangle|^2 / N_A < C$  (orange data in figure (a)), where  $C$  is a chosen cutoff parameter. We then analyze the second QND measurement  $\mathbf{F}^{(2)}$  of the selected data (figure(b)) to detect spin squeezing and entanglement. We illustrate this with data from a sample with  $N_A = 1.1 \times 10^6$  atoms and  $C = 1$ . Axes in (a) & (b) have units of  $10^3$  spins. Solid blue circles (a) and (b) have a radius  $\sqrt{CN_A}$ . In the insets we plot a histogram of the first and second measurements. The selected data are plotted in orange, and the dashed blue line in (b) indicates the cutoff. (c) Spin squeezing parameter  $\xi^2$  (orange diamonds) calculated from the second QND measurement of the selected data as a function of the cutoff parameter  $C$ . For reference, the same parameter calculated from the first QND measurement is also plotted (black circles). Inset: number of selected data points included as a function of the cutoff parameter.

## References

- [1] M. Lewenstein, *et al.* Adv. Phys. **56**, 243 (2007)
- [2] D. A. Lidar, *et al.* Phys. Rev. Lett. **81**, 2594 (1998)
- [3] I. Urizar-Lanz, *et al.* Phys. Rev. A **88**, 013626(2013)
- [4] G. Toth, M.W. Mitchell New J. Phys. **12** 053007(2010)
- [5] R.J. Sewell, *et al.* Phys. Rev. Lett. **109**, 253605 (2012)
- [6] N. Behbood, *et al.* Phys. Rev. Lett. **111**, 103601(2013)
- [7] N.Behbood, *et al.* arXiv:1403.1964 [quant-ph]

## Optomechanical self-structuring in cold atoms

G. Labeyrie<sup>1</sup>, E. Tesio<sup>2</sup>, P. Gomes<sup>2</sup>, G.-L. Oppo<sup>2</sup>, W.J. Firth<sup>2</sup>, G.R.M. Robb<sup>2</sup>, A.S. Arnold<sup>2</sup>, R. Kaiser<sup>1</sup>, and T. Ackemann<sup>2</sup>

<sup>1</sup>*Institut Non Linéaire de Nice, UMR 7335 CNRS, 1361 route des Lucioles, 06560 Valbonne, France*

<sup>2</sup>*SUPA and Department of Physics, University of Strathclyde, Glasgow G4 0NG, Scotland, UK*

Presenting Author: pedro.gomes@strath.ac.uk

Optomechanics has attracted a lot of interest recently due to the combined control of light and mechanical modes. Spontaneous optomechanical self-organization was observed in a variety of non-linear systems such as atomic ensembles in a cavity [1].

We are looking in a single mirror scheme where a single pump beam and a mirror placed after the atomic cloud induce spontaneous self-organization observed on a plane transverse to the beam propagation. Previous investigations that showed continuous symmetry breaking on both translation and rotation relied on spatial modulation on the internal states of the atoms. Recently it was predicted that dipole forces alone could induce the same kind of transverse self-organization based on the atomic density without intrinsic optical non-linearities [2].

We report on the observation of spontaneous self-structuring in cold atoms released from a magneto-optical trap [3]. The trap was initially loaded with  $6 \times 10^{10}$  atoms of  $^{87}\text{Rb}$ . The structures emerge in blue-detuned pump light as hexagons (blue in the Fig. 1, online) and in the atomic density as honeycombs (red in the Fig. 1, online) - the atoms are expelled from the intensity maximums. The set-up relies on the conversion from phase to amplitude modulation by diffraction (Talbot effect) and the length-scale of these structures is continuously tuned with the mirror distance. Two mechanisms come into play in these experiments: the already known internal states non-linearity and the new optomechanical nonlinearity. We identified regimes where each mechanism is dominant as well as the mixed case by comparing the structures in both the pump and in a probe beam sent a few tens of microseconds after pump extinction. In the optomechanical dominant regime, we observed in the probe the dynamical growth and decay of atomic structures in the order of magnitude comparable to the atomic motion at ultracold atoms temperatures.

We also present analysis on the structures contrast and wave-vector dependence on detuning and intensity.

### References

- [1] H. Ritsch *et al.* Rev. Mod. Phys. **85**, 553–601 (2013)
- [2] E. Tesio *et al.* Phys. Rev. A **86** 031801(R) (2012)
- [3] G. Labeyrie *et al.* Nature Photon. **8** 321–325 (2014)

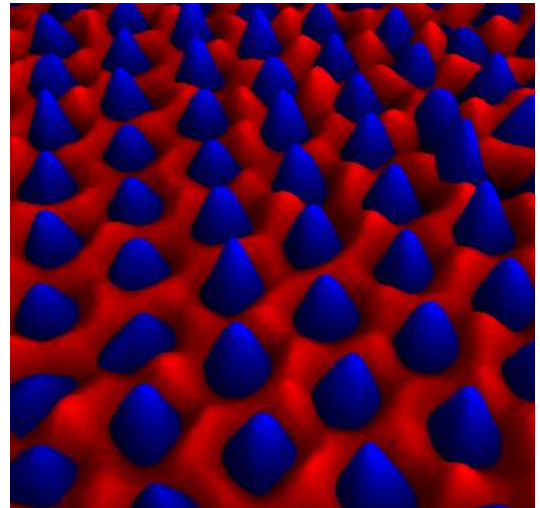


**Figure 1:** (Color online) Complementary honeycomb self-structuring of the atomic density imaged on the red-detuned probe beam (red) and hexagonal light patterns in the transmitted blue-detuned pump beam (blue).

# Condensate Phase Microscopy

A. Kosior<sup>1</sup> and K. Sacha<sup>1</sup>

<sup>1</sup>Marian Smoluchowski Institute of Physics, Jagiellonian University in Kraków, Poland

Presenting Author: krzysztof.sacha@uj.edu.pl

We show that the phase of a Bose-Einstein condensate wave-function of ultra-cold atoms in an optical lattice potential in two-dimensions can be detected [1]. The time-of-flight images, obtained in a free expansion of initially trapped atoms, are related to the initial distribution of atomic momenta but the information on the phase is lost. However, the initial atomic cloud is bounded and this information, in addition to the time-of-flight images, is sufficient in order to employ the phase retrieval algorithms. We analyze the phase retrieval methods for model wave-functions in a case of a Bose-Einstein condensate in a triangular optical lattice in the presence of artificial gauge fields.

In crystallography, electron microscopy and astronomical imaging, computationally retrieving the phase of diffraction patterns is remarkably successful [2]. The examples range from the biological cells imaging to the evaluation of the aberrations in the Hubble space telescope. In the cold atoms problems, it is not an external wave that diffracts on a measured object and is subsequently detected, but the matter wave itself is the *object* to be reconstructed.

## References

- [1] A. Kosior and K. Sacha, Phys. Rev. Lett. **112**, 045302 (2014).  
 [2] S. Marchesini, Rev. Sci. Instrum. **78**, 011301 (2007).

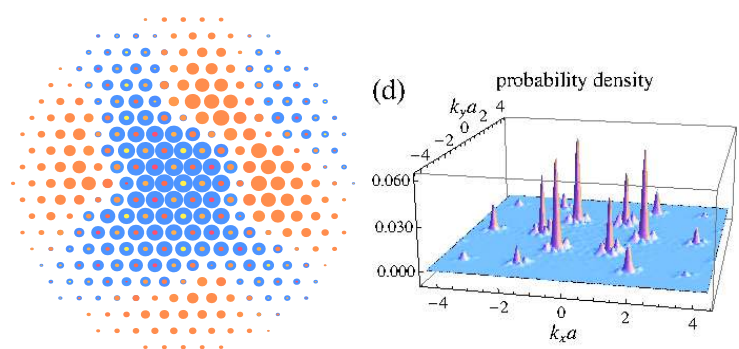


**Figure 1:** Left panel shows domain structures formed by cold atoms in the presence of a triangular optical lattice with negative tunneling amplitudes. The domains are obtained from the retrieved wave-function corresponding to the time-of-flight image presented in the right panel [1].

## Ultra-high flux atom-lasers

V. Bolpasi<sup>1,2</sup>, N.K. Efremidis<sup>1,3</sup>, M.J. Morrissey<sup>1,4</sup>, P.C. Condylis<sup>1,5</sup>, D. Sahagun<sup>1,5</sup>, M. Baker<sup>1,6</sup>, and W. von Klitzing<sup>1</sup>

<sup>1</sup>IESL-FORTH, Vassilika Vouton, GR-71110 Heraklion, Greece

<sup>2</sup>Physics Department, University of Crete, GR711 03, Heraklion, Crete, Greece

<sup>3</sup>Applied Mathematics Department, University of Crete, P.O. Box 2208, 71003, Heraklion, Greece

<sup>4</sup>Quantum Research Group, University of KwaZulu Natal, Westville, Durban 4000, South Africa

<sup>5</sup>Centre for Quantum Technologies, National University of Singapore, 3 Science Drive 2, Singapore 117543, Singapore

<sup>6</sup>School of Mathematics and Physics, The University of Queensland, Brisbane QLD 4072, Australia

Presenting Author: atomlaser@bec.gr

We couple strongly the magnetic hyperfine states of the atoms using a strong rf-field and use this to trap Bose-Einstein condensates in time-dependent adiabatic potentials (TDAP). We manipulate these potentials such that a well collimated, extremely bright atom laser emerges from a small spot just below the condensate.

Traditionally atom lasers are produced by a weak rf-field or a weak Raman beam, which resonantly outcouples a small fraction from within the BEC. The atoms then traverse the BEC and accelerate downwards under the influence of gravity. The maximum flux achievable from a given condensate increases with the strength of the coupling field. At high field strengths, however, it is fundamentally limited by the emergence of bound states [1].

The flux of the TDAP atom laser does not suffer from such limits, which allowed us to demonstrate a record flux of  $7.4 \times 10^7$  atoms/s. In term of flux per trapped atom this is more than an order of magnitude larger than any other continuously outcoupled atom laser achieved so far [1].

Furthermore, we produce the coldest thermal beam to date (200 nK). Finally, we observe, for the first time, an atom beam containing both an atom laser and a thermal atom beam.

We acknowledge the financial support of the Future and Emerging Technologies (FET) programme within the 7th Framework Programme for Research of the European Commission, under FET grant number: FP7-ICT-601180 (MatterWave).

### References

- [1] J. E. Debs *et al.* Phys. Rev. A **81**:2 013618 (2010)  
 [2] Supplementary material at <http://www.bec.gr/publication>

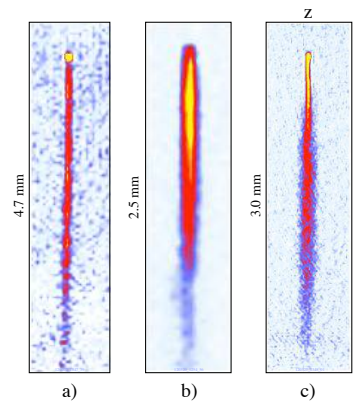


**Figure 1:** Images of atom-lasers after time-of-flight expansion. a) Pure atom laser of 2ms duration with a divergence of only 10 mrad. b) Atom laser with a flux of up to  $7.4 \times 10^7$  atoms/s. c) Atom beam combining atom laser and thermal emission. Please note the different vertical scales in the three plots. Supplementary material can be found here [2].

## Quantum magnetism with a Bose-Einstein Condensate

A. de Paz<sup>1</sup>, A. Sharma<sup>1</sup>, A. Chotia<sup>1</sup>, E. Maréchal<sup>1</sup>, P. Pedri<sup>1</sup>, L. Vernac<sup>1</sup>, B. Laburthe-Tolra<sup>1</sup>, and  
O. Gorceix<sup>1</sup>

<sup>1</sup>*Laboratoire de Physique des Lasers, CNRS and Université Paris 13, Sorbonne Paris Cité, UMR7538, F-93430 Villetaneuse, France*

Presenting Author: olivier.gorceix@univ-paris13.fr

Ultra-cold atomic gases are attracting considerable interest thanks to the many opportunities they provide to explore novel domains in quantum physics. Physicists from various disciplines gather to explore problems at the interfaces of AMO physics with condensed matter and statistical physics. Magnetic high-spin atoms such as chromium provide a test-bed to study the effects of long-range interactions in quantum many-body problems as well as the interplay between internal and external degrees of freedom. We report on two series of experiments using a spin-3 chromium Bose-Einstein condensate. In a first series, we demonstrate the stabilization of this quantum gas against dipolar relaxation loss processes by transferring the BEC in a 3D optical lattice. We also demonstrate how dipolar relaxation then acquires a resonant character as a function of the ambient magnetic field [1]. In another series of experiments, we observe for the first time magnetic dipolar interaction driven spin dynamics [2]. Starting from a Mott state, spin exchange oscillations are observed on two distinct timescales. Rapid oscillations result from contact interactions between atoms located in the same lattice sites. Slow oscillations result from dipolar interactions between atoms sitting at different sites of the lattice. Our work pioneers the experimental realization of quantum magnetism where dynamics is driven by long-range spin-spin interactions between distant lattice sites.

### References

- [1] A. de Paz *et al.* Phys. Rev. A **87**, 051609 Rapid (2013)
- [2] A. de Paz *et al.* Phys. Rev. Lett. **111**, 185305 (2013)

# Coherent superflash effect in cold atoms: Revealing forward scattering field in optically dense medium

C.C. Kwong<sup>1</sup>, T. Yang<sup>2</sup>, D. Delande<sup>3</sup>, R. Pierrat<sup>4</sup>, and D. Wilkowski<sup>1,2,5</sup>

<sup>1</sup>PAP, School of Physical and Mathematical Sciences, Nanyang Technological University, 637371 Singapore, Singapore.

<sup>2</sup>Centre for Quantum Technologies, National University of Singapore, 117543 Singapore, Singapore

<sup>3</sup>Laboratoire Kastler Brossel, UPMC-Paris 6, ENS, CNRS; 4 Place Jussieu, 75005 Paris, France

<sup>4</sup>Institut Langevin, ESPCI ParisTech, CNRS UMR 7587, 10 rue Vauquelin, 75005 Paris, France.

<sup>5</sup>Institut Non Linéaire de Nice, Université de Nice Sophia-Antipolis, CNRS, 06560 Valbonne, France

Presenting Author: david.wilkowski@ntu.edu.sg

The coherent transmission of a wave, through absorbing medium, results of interference between the incident field and the forward scattering field. This basic and well established process was experimentally observed in the case of an electromagnetic wave transmitted through a resonant atomic cold cloud [1]. Since the forward scattering field is build up with the incident field, one may states that the amplitude of the former cannot be larger than the latter. We recently demonstrate that this intuitive picture is incorrect [2]. This result recasts our understanding of coherent wave transport in optically dense medium.

We will discuss in detail how the complex transmitted field can be reconstructed using fast transient phenomena on Strontium intercombination line with cold atoms. An example of such a reconstruction is given in Fig. 1. Moreover, if the probe laser is abruptly switched off, we observe a coherent superflash of light at the output of the optically dense medium. Its intensity can be up to four times the incoming probe intensity. This superflash allows us to measure the coherence properties of the forward scattering field. We finally discuss potential application of optically dense medium for phase discrimination and for narrow pulse generation with high repetition rate.

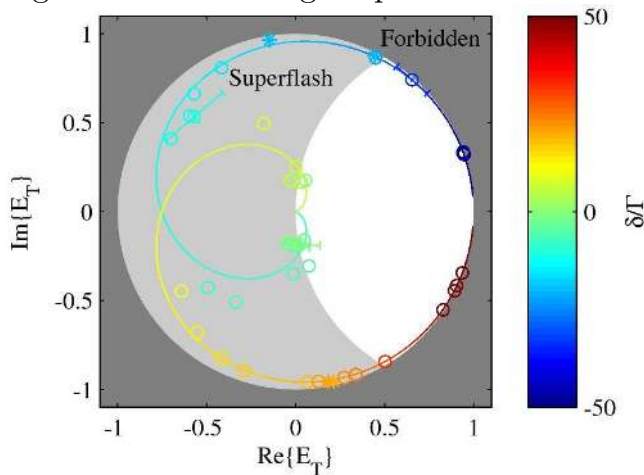


**Figure 1:** Reconstruction, as function of the probe frequency detuning, of the transmitted field in a cold cloud with an optical density of 19. The open circles are the data points and the plain curve the theoretical prediction.

## References

- [1] M. Chalony, R. Pierrat, D. Delande and D. Wilkowski, Phys. Rev. A 84, 011401(R) (2011).  
 [2] C. C. Kwong, T. Yang, P. Mysore, K. Pandey, D. Delande, R. Pierrat, and D. Wilkowski, *to be issued in 2014*.

## A 13-fold improved value for the electron mass

F. Köhler<sup>1,2,3</sup>, S. Sturm<sup>2</sup>, A. Wagner<sup>2</sup>, G. Werth<sup>4</sup>, W. Quint<sup>1,3</sup>, and K. Blaum<sup>2</sup>

<sup>1</sup>*GSI Helmholtzzentrum für Schwerionenforschung, D-64291, Darmstadt*

<sup>2</sup>*Max-Planck-Institut für Kernphysik, D-69117, Heidelberg*

<sup>3</sup>*Ruprecht-Karls-Universität, D-69117, Heidelberg*

<sup>4</sup>*Johannes Gutenberg-Universität, D-55122, Mainz*

Presenting Author: [florian.koehler.email@googlemail.com](mailto:florian.koehler.email@googlemail.com)

The mass of the electron is a key parameter of the Standard Model of physics. Its value is fundamental for the structure of matter on atomic and molecular scales; a high-precision value is relevant for the most stringent tests of quantum electrodynamics [1,2,3].

Here we use an indirect method similar to [4,5] to determine the atomic mass of the electron by measuring the spin-precession frequency of an electron bound to a carbon nucleus in a 3.7 T magnetic field. The single hydrogen-like carbon ion has been trapped for several months in a Penning trap apparatus. While probing the spin-precession frequency, the magnetic field has been measured simultaneously with a novel phase-sensitive detection technique, PnA (Pulse and Amplify) [6], working at ultra-low temperatures. The spin-state is determined by applying the continuous Stern-Gerlach effect.

This approach requires the theoretical knowledge of the bound electron  $g$ -factor, which has been calculated to a precision better than  $10^{-11}$ . Combining this state-of-the-art QED calculation and our measurement of the ratio of the electron spin-precession frequency to the ion cyclotron frequency, we can derive the electron mass [7]. With a relative uncertainty of  $3 \cdot 10^{-11}$  we have improved the electron mass by a factor of 13 with respect to the present CODATA value [8].

In this talk the measurement of the electron mass will be presented and the current status of our BS-QED tests will be summarized.

### References

- [1] R. Bouchendira *et al.* Phys. Rev. Lett. **106**, 080801 (2011)
- [2] D. Hanneke *et al.* Phys. Rev. Lett. **100**, 120801 (2008)
- [3] S. Sturm *et al.* Phys. Rev. Lett. **107**, 023002 (2011)
- [4] H. Häffner *et al.* Phys. Rev. Lett. **85**, 5308 (2000)
- [5] J. Verdú *et al.* Phys. Rev. Lett. **92**, 093002 (2004)
- [6] S. Sturm *et al.* Phys. Rev. Lett. **107**, 143003 (2011)
- [7] S. Sturm *et al.* Nature **506**, 13026 (2014)
- [8] P.J. Mohr *et al.* Rev. Mod. Phys. **84**, 1527 (2012)

# Experimental Tests of Macroscopic Quantum Superposition

H. Ulbricht<sup>1</sup>

<sup>1</sup>*Physics and Astronomy, University of Southampton, SO17 1BJ, Southampton, UK*

Presenting Author: [hendrik.ulbricht@soton.ac.uk](mailto:hendrik.ulbricht@soton.ac.uk)

New technological developments allow to explore the quantum properties of very complex systems, bringing the question of whether also macroscopic systems share such features, within experimental reach. The interest in this question is increased by the fact that, on the theory side, many suggest that the quantum superposition principle is not exact, departures from it being the larger, the more macroscopic the system [1]. Testing the superposition principle intrinsically also means to test suggested extensions of quantum theory, so-called collapse models. We will report on three new proposals to experimentally test the superposition principle with nanoparticle interferometry [2], optomechanical devices [3] and by spectroscopic experiments in the frequency domain [4, 5]. We will also report on the status of optical levitation and cooling experiments with nanoparticles in our labs, towards an Earth bound matter-wave interferometer to test the superposition principle for a particle mass of one million amu (atomic mass unit).

## References

- [1] Bassi, A., K. Lochan, S. Satin, T.P. Singh, and H. Ulbricht, *Models of Wave-function Collapse, Underlying Theories, and Experimental Tests*, Rev. Mod. Phys. **85**, 471 - 527 (2013).
- [2] Bateman, J., S. Nimmrichter, K. Hornberger, and H. Ulbricht, *Near-field interferometry of a free-falling nanoparticle from a point-like source*, arXiv:1312.0500 (2013).
- [3] Xuereb, A., H. Ulbricht, and M. Paternostro, *Optomechanical interface for matter-wave interferometry*, Sci. Rep. **3**, 3378 (2013).
- [4] Bahrami, M., A. Bassi, and H. Ulbricht, *Testing the quantum superposition principle in the frequency domain*, Phys. Rev. **A 89**, 032127 (2014),
- [5] Bahrami, M., M. Paternostro, A. Bassi, and H. Ulbricht *Non-interferometric Test of Collapse Models in Optomechanical Systems*, arXiv:1402.5421 (2014).

## Collective suppression of light scattering in a cold atomic ensemble

Y.R.P. Sortais<sup>1</sup>, J. Pellegrino<sup>1</sup>, R. Bourgain<sup>1</sup>, S. Jennewein<sup>1</sup>, A. Browaeys<sup>1</sup>, S.D. Jenkins<sup>2</sup>, and  
J. Ruostekoski<sup>2</sup>

<sup>1</sup>*Laboratoire Charles Fabry, Institut d'Optique, CNRS, Univ. Paris Sud, 2 avenue Augustin Fresnel, 91127 Palaiseau cedex, France*

<sup>2</sup>*Mathematical Sciences, Univ. Southampton, Southampton SO17 1BJ, United Kingdom*

Presenting Author: yvan.sortais@institutoptique.fr

When resonant emitters, such as atoms, molecules, or quantum dots, with a transition at a wavelength  $\lambda$  are confined inside a volume smaller than  $\lambda^3$ , they are coupled via strong dipole-dipole interactions. In this regime, the response of the ensemble to near-resonant light is collective and originates from the excitation of collective eigenstates of the system, such as super- and sub-radiant modes [1,2]. Dipole-dipole interactions profoundly affect the response of the system, as they modify the decay rate and shift the energy of each state in a different way, leading, e.g., to the collective Lamb shift [3,4]. The collective scattering of light can strongly differ from the case of an assembly of noninteracting emitters [5] and has been predicted to be suppressed for a dense gas of cold two-level atoms [6].

Here, I will present the first observation of the collective suppression of light scattering by a cold sample of  $^{87}\text{Rb}$  atoms with a size comparable to the wavelength of their optical transition [7]. Starting from a single atom and gradually increasing the number of atoms up to a few hundreds, we observe the emergence of a strong collective suppression of light scattering due to the increasing dipole-dipole interactions. Consistently with this suppression, we observe a broadening of the optical transition at  $\lambda = 780$  nm as well as a small red shift. We find that our measurements are compatible with numerical simulations of the response of the system in the low excitation limit, accounting for all the scattering processes between atomic dipoles and the internal level structure of the atoms. Ongoing investigations of the temporal response of the system, and comparisons to the case of a single atom [8], should also provide insight into the interplay between dipole-dipole interactions and collective scattering.

### References

- [1] R.H. Dicke, *Phys. Rev.* **93**, 99 (1954).
- [2] M. Gross and S. Haroche, *Phys. Rep.* **93**, 301 (1982).
- [3] R. Friedberg, S.R. Hartmann, and J.T. Manassah, *Phys. Rep.* **7**, 101 (1973).
- [4] M.O. Scully, *Phys. Rev. Lett.* **102**, 143601 (2009).
- [5] R.H. Lehmann, *Phys. Rev. A* **2**, 883 (1970).
- [6] T. Bienaimé *et al*, *Fortschr. Phys.* **61**, 377 (2013).
- [7] J. Pellegrino *et al*, arXiv:0914817 (2014).
- [8] R. Bourgain *et al*, *Opt. Lett.* **38**, 1963 (2013).

# A new method to measure photoabsorption cross-sections questions the value of the photodetachment cross-section of $\text{H}^-$

C. Blondel<sup>1</sup>, M. Vandevraye<sup>1</sup>, Ph. Babilotte<sup>1</sup>, and C. Drag<sup>1</sup>

<sup>1</sup>*Laboratoire Aimé-Cotton, Centre national de la recherche scientifique, F-91405 Orsay, France*

Presenting Author: christophe.blondel@u-psud.fr

A new method is described to measure photoexcitation cross-sections, relying on the asymptotic behavior of the signal in the saturated regime, when excitation is provided by a Gaussian laser beam. The method is implemented on a negative ion beam, with a single-mode pulsed Nd:YAG laser, to measure the photodetachment cross-section of the atomic anion  $\text{H}^-$ , at the wavelength 1064 nm.

This is the first laser measurement of the photodetachment cross-section of  $\text{H}^-$ . This cross-section is of primary importance both as the photodetachment cross-section of the most elementary negative ion and as a key parameter for the production of fast neutral  $\text{H}^0$  or  $\text{D}^0$  atoms, for plasma heating in the ITER and DEMO projects, by photodetachment from accelerated anions. A more classical numerical fitting method, including both the linear and the saturated regime, confirms a  $4.5(6) \times 10^{-21} \text{m}^2$  value, whereas most calculations performed for the last 50 years, including the most recent ones [1], have found  $3.6 \pm 1 \times 10^{-21} \text{m}^2$ , in agreement with the older experiments [2,3]. Meanwhile, a few calculations relying on the adiabatic approximation in hyperspherical coordinates happened to find a  $4.2 \times 10^{-21} \text{m}^2$  value [4,5], which would be compatible with our measurement.

The present result could suggest to revisit ab initio calculations of the  $\text{H}^-$  system and set more stringent constraints on the models used to represent  $\text{H}^-$  in atomic and molecular processes.

## References

- [1] A.M. Frolov, J. Phys. B: At. Mol. Opt. Phys. **37** 853 (2004)
- [2] L.M. Branscomb and S.J. Smith, Phys. Rev. **98** 1028 (1955)
- [3] H.-P. Popp and S. Kruse, J. Quant. Spectrosc. Radiat. Transfer **16** 683 (1976)
- [4] M.G.J. Fink and P. Zoller, J. Phys. B: At. Mol. Phys. **18** L373 (1985)
- [5] C.-H. Park, A.F. Starace, J. Tan and C.-D. Lin, Phys. Rev. A **33** 1000 (1986)

# Measurement of the X-ray emission anisotropies in the resonant photorecombination into highly charged ions

C. Shah<sup>1</sup>, P. Amaro<sup>1</sup>, R. Steinbrügge<sup>2</sup>, S. Bernitt<sup>2</sup>, Z. Harman<sup>2</sup>, S. Fritzsche<sup>3</sup>, A. Surzhykov<sup>4</sup>, J.R. Crespo López-Urrutia<sup>2</sup>, and S. Tashenov<sup>1</sup>

<sup>1</sup>*Physikalisches Institut, Im Neuenheimer feld 226, 69120 Heidelberg, Germany*

<sup>2</sup>*Max-Planck-Institut für Kernphysik, Saupfercheckweg 1, 69117 Heidelberg, Germany*

<sup>3</sup>*Friedrich-Schiller-Universität Jena, Fürstengraben 1, 07743 Jena, Germany*

<sup>4</sup>*Helmholtz-Institut, Helmholtzweg 4, 07743 Jena, Germany*

Presenting Author: chintan@physi.uni-heidelberg.de

We report the first systematic measurement of the photon angular distribution in the inter-shell dielectronic recombination (DR) and trielectronic recombination (TR) into highly charged ions. Iron and krypton ions in the He-like through O-like charge states were produced in an electron beam ion trap, and the electron-ion collision energy was scanned over the K-shell recombination resonances. An excellent electron energy resolution of 6.5 eV FWHM at 5 keV for iron and 11.5 eV FWHM at 9 keV for krypton was achieved.

The X rays emitted in the decay of resonantly excited states were simultaneously recorded by two germanium detectors which were mounted along and perpendicular to the electron beam propagation directions. The intensities of K-shell X-ray transitions were recorded as a function of electron beam energy. The measured photon emission asymmetries indicate the alignment of the corresponding excited states. Moreover, the alignment properties of the weaker processes such as TR were measured for the first time.

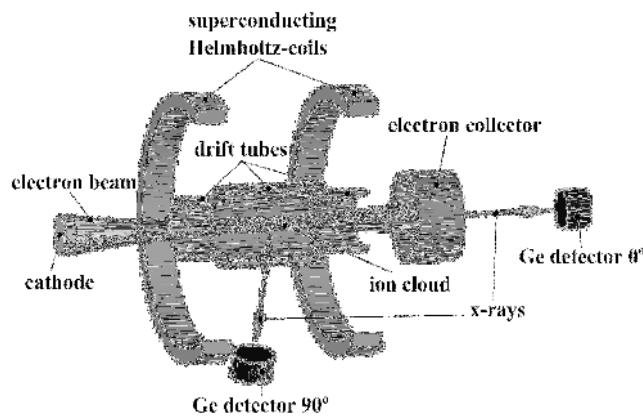


Figure 1: Scheme of the experimental setup.

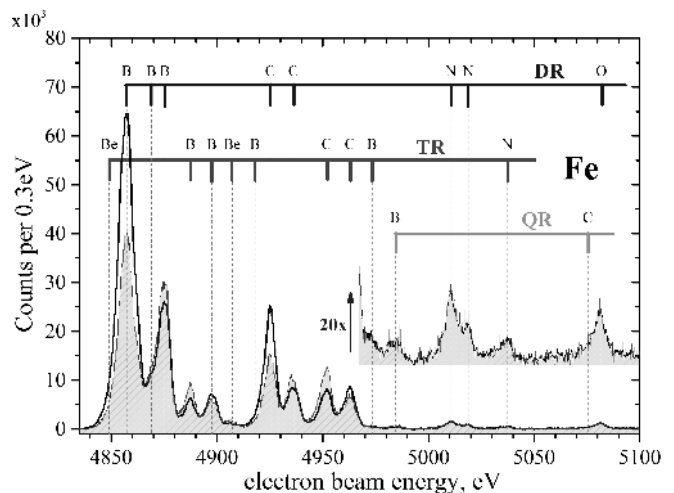


Figure 2: X-ray intensity as a function of the electron beam energy. The solid line shows the X-ray intensity perpendicular to the electron beam propagation direction, whereas the filled area indicates intensity along the electron beam propagation direction. Vertical markers represent the resonant recombination processes and corresponding initial charge state of the ions.

The measured X-ray emission anisotropies probe the electron-electron interaction in the strong field of the ion, e.g. they are highly sensitive to the Breit interaction. These results benchmark dedicated multiconfiguration Dirac-Fock electronic structure calculations and can be applied for polarization diagnostics of hot astrophysical and laboratory fusion plasmas.

# Experimental and theoretical study of 3-photon ionization He(1s2s <sup>3</sup>S) and He(1s2p <sup>3</sup>P)

M. Génévriez<sup>1</sup>, X. Urbain<sup>1</sup>, M. Brouri<sup>1</sup>, K. Dunseath<sup>2</sup>, and M. Terao-Dunseath<sup>2</sup>

<sup>1</sup> Institut de la Matière Condensée et des Nanosciences, Université Catholique de Louvain, Bât. M. de Hemptinne, Chemin du Cyclotron 2, 1348 Louvain-la-Neuve, Belgium

<sup>2</sup> Institut de Physique de Rennes, UMR 6251 CNRS-Université de Rennes 1, Bât. 11B, Campus de Beaulieu, F-35042 Rennes Cedex, France

Presenting Author: matthieu.genevriez@uclouvain.be

While the photoionization of atoms in the ground state has been intensively studied, less is known concerning photoionization of excited states, particularly multiphoton ionization [1,2,3]. We report here the results of an experimental and a theoretical study of the three-photon ionization of the 1s2s <sup>3</sup>S<sup>e</sup> and 1s2p <sup>3</sup>P<sup>o</sup> states of helium by a laser operating in the green and red regions of the visible spectrum.

In the experiment, He<sup>-</sup> ions are first formed in the 1s2s2p <sup>4</sup>P<sup>o</sup> state by collisions of fast helium ions with cesium. A pulsed dye laser pumped by the second or third harmonics of a Nd:YAG laser is then used to photodetach an electron, leaving an atom of helium in either the 1s2p <sup>3</sup>P<sup>o</sup> or the 1s2s <sup>3</sup>S<sup>e</sup> state. These are subsequently ionized by the absorption of three more photons. By tuning the wavelength of the laser, the ion yield from either of the two excited states can be measured. In the work reported here, the wavelength is varied within the 530-560 nm and 685-730 nm ranges in order to probe, respectively, the 1s2s <sup>3</sup>S<sup>e</sup> and 1s2p <sup>3</sup>P<sup>o</sup> states. Dependence of the ionization on the photon flux and the laser polarization is also studied by varying the laser peak intensity between  $1.25 \times 10^9 \text{ W cm}^{-2}$  and  $3.6 \times 10^{10} \text{ W cm}^{-2}$  and by changing the polarization state from linear to circular. The experimental results show two series of asymmetric peaks, associated to two-photon resonances with *ns* and *nd* Rydberg states for He(1s2s <sup>3</sup>S<sup>e</sup>) and with *np* and *nf* Rydberg states for He(1s2p <sup>3</sup>P<sup>o</sup>). For the latter, a series of peaks has tails towards higher photon energies while the other has tails changing direction below 706.7 nm.

A model Hamiltonian [4] is built using matrix elements from DVR and QDT calculations and checked against a full, *ab initio* *R*-matrix Floquet calculation. The time-dependent Schrödinger equation is numerically integrated to reproduce the experimental spectra with different pulse peak intensities. The series of peaks are consistently reproduced over the large wavelength ranges considered, both in shape and position.

For the 1s2p <sup>3</sup>P<sup>o</sup> ( $M_L = 0$ ) state, the 1s2p <sup>3</sup>P<sup>o</sup> and 1s3s <sup>3</sup>S<sup>e</sup> states are coupled by a one-photon interaction, and hence are strongly mixed over a relatively wide range of laser wavelengths. This dressing is absent in the case  $M_L = \pm 1$ . Ionization is shown to occur *via* two resonantly enhanced multiphoton ionization (REMPI) schemes: a (1+1+1) scheme for  $M_L = 0$ , never encountered before in atomic multiphoton ionization, and a (2+1) scheme for  $M_L = \pm 1$ . He(1s2s <sup>3</sup>S<sup>e</sup>) exhibits a much simpler (2+1) REMPI behaviour as a function of the laser wavelength and intensity. The laser polarization has also an important effect on the ionization yield and highlights, as for the ionization of He(1s2p <sup>3</sup>P<sup>o</sup>), the influence of the magnetic quantum number.

## References

- [1] P. Antoine, N.-E. Essarroukh, J. Jureta, *et al.* J. Phys. B **29**, 5367 (1996)
- [2] M. Gisselbrecht, D. Descamps, C. Lyngå, *et al.* Phys. Rev. Lett. **82**, 4607 (1999)
- [3] M. Madine, H.W. van der Hart J. Phys. B **38**, 3963 (2005)
- [4] H. Baker Phys. Rev. A **30**, 773 (1984)

# Non-resonant two-photon excitation to high Rydberg states

T.E. Wall<sup>1</sup>, D.B. Cassidy<sup>1</sup>, and S.D. Hogan<sup>1</sup>

<sup>1</sup>Dept. of Physics and Astronomy, University College London, Gower Street, London WC1E 6BT, UK

Presenting Author: t.wall@ucl.ac.uk

The imbalance of matter and antimatter in the universe is one of the great mysteries of modern physics. One test that might shed light on this puzzle is a measurement of how antimatter acts in a gravitational field. We are building an experiment to test antimatter gravity by measuring the free-fall of positronium [1]. Limited by annihilation, the ground state of triplet Ps has a lifetime of 142 ns, allowing free-fall of only around 100 fm (if  $\bar{g} = g$ ). However, Rydberg states have negligible annihilation rates, with lifetimes limited only by radiative decay. In experimentally feasible conditions these could be on the order of 10 ms, long enough to permit observable free-fall. Atoms in these highly excited states can also possess extremely large electric dipole moments, allowing manipulation with inhomogeneous electric fields [2].

Typical methods of Ps generation produce very hot atoms ( $v/c \sim 10^{-3}$ ), resulting in significant Doppler broadening (e.g.,  $\sim 0.5$  THz for 1s–2p). Efficient production of Rydberg Ps has been achieved with broad bandwidth (85 GHz) lasers that give reasonable overlap with these large Doppler profiles [3]. However, this technique limits the resolution and prevents accurate state selection at higher  $n$ .

To overcome this we plan to implement non-resonant Doppler-free two-photon excitation with much narrower bandwidth (3 GHz) pulsed dye lasers. This scheme allows state-selectivity at high- $n$ , opening up possibilities for transfer to higher angular momentum states. As a demonstration of this scheme we have performed non-resonant two-photon Rydberg excitation in a pulsed supersonic beam of helium. Using circularly polarized light we have driven transitions from the  $1s2s\ 2^3S_1$  state to the  $1snd$  Rydberg states in the range from  $n = 20$  up to  $n \simeq 100$ , resolving states up to  $n = 76$  (Fig. 1). We shall describe the effects of a range of experimental parameters, including polarization, dc electric fields and laser pulse energy. We discuss the application of this scheme to Ps and present calculations of the two-photon transition rates to Ps Rydberg states. In addition to the preparation of Rydberg Ps, non-resonant two-photon excitation schemes of this kind also have applications in precision spectroscopy of molecules and tests of QED [4].

## References

- [1] A. P. Mills Jr., M. Leventhal, Nucl. Instr. Meth. B **192**, 102–106 (2002)
- [2] E. Vliegen *et al.*, Phys. Rev. Lett. **92**, 033005 (2004)
- [3] D. B. Cassidy *et al.*, Phys. Rev. Lett. **108**, 043401 (2012)
- [4] D. Sprecher *et al.*, Faraday Discuss. **150**, 51–70 (2011)

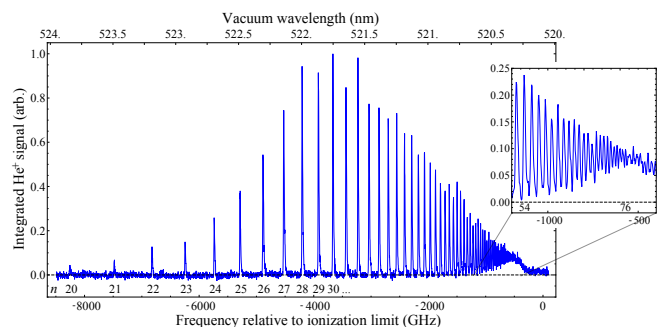


**Figure 1:** Helium Rydberg spectrum of  $m = 2$  states from  $n = 20$  up to the ionization limit, produced by non-resonant two-photon excitation. Inset: The spectrum shown in detail for states with  $54 \leq n \leq 76$ .

# Contribution of multiple capture processes in slow collisions of highly charged ions with a many-electron target

M. Trassinelli<sup>1</sup>, A. Salehzadeh<sup>2</sup>, T. Kirchner<sup>2</sup>, C. Prigent<sup>1</sup>, E. Lamour<sup>1</sup>, J.-P. Rozet<sup>1</sup>, S. Steydli<sup>1</sup>, and D. Vernhet<sup>1</sup>

<sup>1</sup>Sorbonne Universités, CNRS, UPMC Univ Paris 06, UMR 7588, Institut des NanoSciences de Paris, F-75005, Paris, France

<sup>2</sup>Department of Physics and Astronomy, York University, Toronto, Ontario, Canada M3J 1P3

Presenting Author: martino.trassinelli@insp.jussieu.fr

The dominant process in low-energy ion-atom collisions is electron transfer. If a highly charged projectile collides with a many-electron target, multiple capture is possible and multiply excited projectile states can be formed. This gives rise to a complex de-excitation cascade that involves both Auger and radiative transitions. Unless one would do a “complete experiment” that measures all relevant photon and ion charge state coincidences (and possibly Auger electrons as well) it is difficult to obtain complete information on such a collision system from measurements alone. Similarly, the predictive power of theoretical calculations is limited simply because a full first-principles calculation of the many-electron dynamics is not feasible.

We have investigated quasi-symmetric collision systems, such as 15 keV/q Ar<sup>17+</sup>–Ar, collisions both experimentally and theoretically. The experiments make use of low- and high-resolution X-ray spectroscopy and resolve the whole heliumlike Ar<sup>16+</sup> Lyman series from  $n = 2$  to  $n = 10$  [1]. The theoretical calculations are based on the assumption that the collisional capture and the post-collisional Auger and radiative decays can be viewed as being independent. The capture calculations are carried out on the level of the independent electron model using the two-center basis generator method (TC-BGM) and including projectile states up to the 10th shell in the basis [2]. The cross sections obtained for shell-specific multiple capture are fed into an Auger decay scheme [3].

Figure 1 shows our main result. For  $n \geq 7$  multiple capture is negligible and both sets of theoretical intensities coincide. They are at variance with the experimental data for  $n = 8$  and  $n = 10$ , possibly because of the limited basis set used in the TC-BGM calculations. For  $2 < n < 7$  the situation is quite different: Here, the theoretical results that include the multiple capture contributions are in very good agreement with the experimental data, while those which ignore them yield considerably lower intensities. This demonstrates quite clearly that multiple capture processes play an important role in this type of collision systems.

## References

- [1] M. Trassinelli *et al.* J. Phys. B **45** 085202 (2012)
- [2] A. Salehzadeh and T. Kirchner J. Phys. B **46**, 025201 (2013)
- [3] R. Ali *et al.* Phys. Rev. A **49** 3586 (1994)

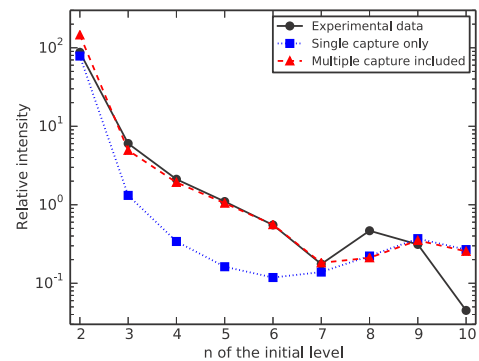


**Figure 1:** Experimental and calculated X-ray intensities for  $1snp \rightarrow 1s^2$  transitions in Ar<sup>16+</sup> following electron capture in 15 keV/q Ar<sup>16+</sup>–Ar collisions (see text for details).

# Measurement of the gravitational constant $G$ by atom interferometry

G. Rosi<sup>1</sup>, F. Sorrentino<sup>1</sup>, G.M. Tino<sup>1</sup>, L. Cacciapuoti<sup>2</sup>, and M. Prevedelli<sup>3</sup>

<sup>1</sup>Dipartimento di Fisica e Astronomia & INFN, Università di Firenze, via Sansone 1 50019 Sesto Fiorentino (FI), Italy

<sup>2</sup>European Space Agency, Research and Scientific Support Department, Keplerlaan 1, 2200 AG Noordwijk, The Netherlands

<sup>3</sup>Dipartimento di Fisica e Astronomia, Università di Bologna, viale Berti Pichat 6/2, 40127, Bologna, Italy

Presenting Author: sorrentino@fi.infn.it

We will report on the accurate measurement of the gravitational constant  $G$  with an atomic sensor. The experiment is based on a light-pulse atom interferometry gravity gradiometer detecting the gravitational field generated by a well characterized set of source masses (fig. 1).

<sup>87</sup>Rb atoms, trapped and cooled in a magneto-optical trap (MOT), are launched in a vertical vacuum tube, producing an atomic fountain. Near the apogees of the atomic trajectories, a measurement of their vertical acceleration is performed by a Raman interferometry scheme. External source masses are positioned in two different configurations ( $C_1$  and  $C_2$ ) and the induced phase shift is measured as a function of masses positions.

After a preliminary measurement with  $\sim 0.1\%$  precision [1], we recently operated several upgrades to improve the sensitivity and the control on sources of systematic errors [2]. We achieve a short term sensitivity of  $3 \times 10^{-9} \text{ g}/\sqrt{\text{Hz}}$  to differential gravity acceleration, limited by the quantum projection noise of the instrument. Active control of the most critical parameters allows to reach a resolution of  $5 \times 10^{-11} \text{ g}$  after 8000 s on the measurement of differential gravity acceleration. Fig. 1 shows the data used for the determination of  $G$ . The modulation of the differential phase shift produced by the source mass is well visible and can be resolved with a signal-to-noise ratio of 1000 after about one hour. The resulting value of the differential phase shift is  $0.547870(63)$  rad from which, after evaluation of systematic shifts and errors, we obtained the value of  $G = 6.67191(99) \times 10^{-11} \text{ m}^3 \text{ kg}^{-1} \text{ s}^{-2}$ .

This work was supported by INFN (MAGIA experiment)

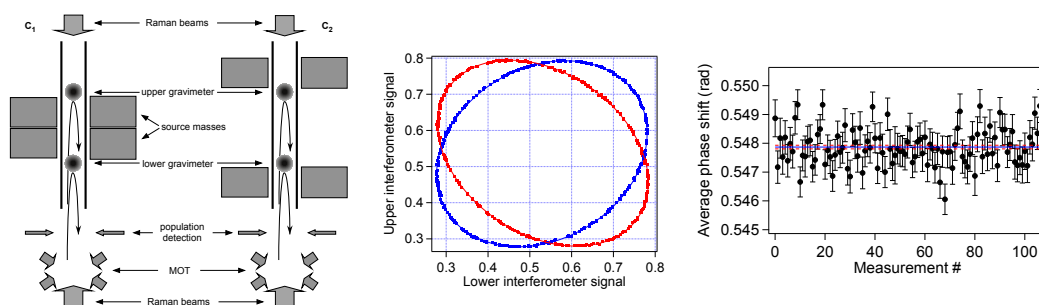


**Figure 1:** Left: scheme of the MAGIA experiment. Center: typical Lissajous figures obtained by plotting the output signal of the upper atom interferometer vs the lower one for the two configurations of the source masses:  $C_1$  (red) and  $C_2$  (blue). Left: Results of the measurements to determine  $G$ . Each point is the difference of the phase angle recorded for the two configurations of the source masses. The data acquisition for each point took about one hour. These data were recorded in different days spanning over one week in July 2013. The error bars are given by the combined error on the ellipse angles.

## References

- [1] G. Lamporesi et al., *Determination of the Newtonian Gravitational Constant Using Atom Interferometry*, Phys. Rev. Lett. **100** 050801 (2008).
- [2] F. Sorrentino et al., *Sensitivity limits of a Raman atom interferometer as a gravity gradiometer*, Phys. Rev. A **89** 023607 (2014).

# Wavefunction Microscopy: Simple Atoms under Magnification

F. Lépine<sup>1</sup>, S. Cohen<sup>2</sup>, M.J.J. Vrakking<sup>3</sup>, and C. Bordas<sup>1</sup>

<sup>1</sup>*Institut Lumière Matière, Université Lyon 1 & CNRS, 69621 Villeurbanne Cedex, France*

<sup>2</sup>*Physics Department, University of Ioannina, 45110 Ioannina, Greece*

<sup>3</sup>*Max-Born-Institut, Max Born Strasse 2A, D-12489 Berlin, Germany*

Presenting Author: christian.bordas@univ-lyon1.fr

The wavefunction is the main entity used to describe microscopic properties of matter in quantum mechanics. However, in general, its direct measurement is still an inaccessible quest. Observing directly, in real-space, the square modulus of the wavefunction (probability density) is from this point of view the first step to a direct insight into this elusive object.

In order to observe directly the square modulus of an atomic wavefunction, it must first be expanded to a macroscopic scale. Photoionization in the presence of an electric field provides such a magnification, allowing the wavefunction to propagate at large distance, and ensuring at the same time the boundedness along one coordinate. Therefore, simply measuring the spatial distribution of the electron flux using a high-resolution velocity map imaging spectrometer may allow, under appropriate conditions, to observe the square modulus of the electron wavefunction as suggested in [1]. In addition, an atom in an external electric field possesses quasi-discrete Stark resonances in the continuum. Therefore, not only the continuum wavefunction can be observed, but the wavefunction of a quasi-bound state bearing intrinsic properties of the atom may be visualized.

By exciting simple atoms like lithium [2] or hydrogen [3] in the presence of an electric field, we obtained the first experimental wavefunction microscopy images where signatures of quasi-bound states were evident. In this communication, we report such experiments where the nodal structure of the atomic state is directly observed, exhibiting a clear contrast between continuum and resonance features.

## References

- [1] V.D. Kondratovitch and V.N. Ostrovsky, *J. Phys. B* **17**, 1981 (1984), **17**, 2011 (1984), **23**, 21 (1990), **23**, 3785 (1990).
- [2] S. Cohen *et al.* *Phys. Rev. Lett.* **110**, 183001 (2013).
- [3] A.S. Stodolna *et al.* *Phys. Rev. Lett.* **110**, 213001 (2013).

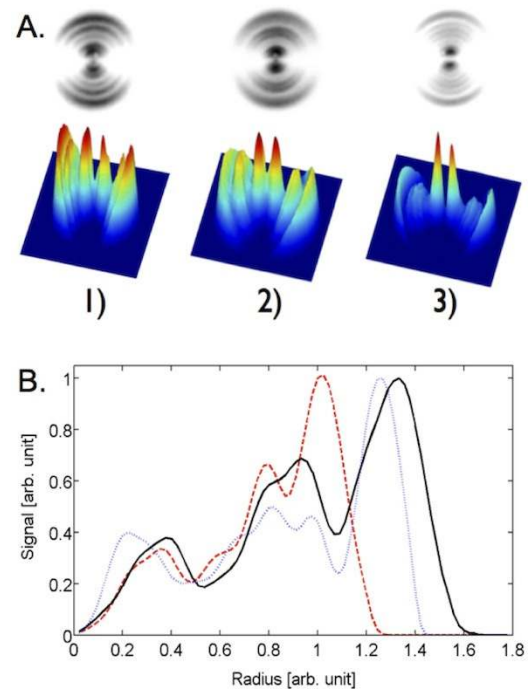


**Figure 1:** (A) 2D and 3D representation of experimental images in one-photon ionization of lithium.  $F=1000$  V/cm: (1) below, (2) on, and (3) above the ( $n=6$ ,  $m=1$ ) resonance. (B) radial distribution: the image is larger on-resonance (black curve) owing to tunnel ionization.

## Quantum interferometry in the time-domain with massive particles

P. Geyer<sup>1</sup>, N. Dörre<sup>1</sup>, P. Haslinger<sup>1</sup>, J. Rodewald<sup>1</sup>, S. Nimmrichter<sup>1</sup>, and M. Arndt<sup>1</sup>

<sup>1</sup>University of Vienna, Faculty of Physics, QuNaBioS & VCQ, Austria.

Presenting Author: philipp.geyer@univie.ac.at

Matter wave interferometry is a versatile tool for testing the foundations of quantum physics as well as for precision measurements. We have recently developed a universal **O**ptical the **T**ime-domain **M**atter-wave (**OTIMA**) Talbot-Lau interferometer[1, 2]. It is implemented using three pulsed standing light waves which act as absorptive gratings. Particles traversing the grating antinodes can be selectively removed via ionization or fragmentation.

Three VUV excimer lasers emit light at 157.6 nm with a pulse length of about 6 ns. A single mirror reflects all three laser beams to form three stable and mechanically coupled standing light waves. In our recent experimental realization a pulsed molecular nozzle source (Even Lavié valve) seeds organic molecules into an adiabatically expanding noble gas jet to generate a spectrum of cold clusters which are subjected to the interferometer pulses and detected in a time-of-flight mass spectrometer.

We have performed various experiments with organic clusters to demonstrate the versatility and universal applicability of this new interferometer scheme. It is suitable for nanoparticles that ionize or fragment (i.e. are susceptible to beam depletion) with one or two 157 nm photons. Many types of clusters (metallic, organic, semiconducting), a large range of complex molecules as well as many atomic species are candidate particles for future experiments.

The use of pulsed optical gratings makes it a suitable instrument for high-mass particles which aim at testing the linearity of quantum physics, as well as at probing novel decoherence effects such as fragmentation decoherence or continuous spontaneous localization [5,6].

The instrument opens also new avenues to quantum-enhanced measurements using deflectometry, absorption or photodissociation spectroscopy.

### References

- [1] P. Haslinger, N. Dörre, P. Geyer, J. Rodewald, S. Nimmrichter and M. Arndt, *Nature* 9, 144 (2013)
- [2] K. Hornberger, *et al.*, *Rev. Mod. Phys.* 84, 157 (2012)
- [3] S. Nimmrichter, *et al.*, *New. J. Phys.* 13, 075002 (2011)
- [4] S. B. Cahn, *et al.*, *Phys. Rev. Lett.* 79, 784 (1997)
- [5] S. L. Adler and A. Bassi, *Science* 325, 275 (2009)
- [6] S. Nimmrichter, *et al.*, *Phys. Rev. A* 83, 043621 (2011)

## Transverse Focusing Effects in the Zeeman Deceleration of Hydrogen Atoms

K. Dulitz<sup>1</sup>, A. Tauschinsky<sup>1</sup>, M. Motsch<sup>2</sup>, N. Vanhaecke<sup>3,4</sup>, and T.P. Softley<sup>1</sup>

<sup>1</sup>*Department of Chemistry, University of Oxford, Chemistry Research Laboratory, Mansfield Road, Oxford, OX1 3TA, UK*

<sup>1</sup>*Laboratorium für Physikalische Chemie, ETH Zürich, 8093 Zürich, Switzerland*

<sup>1</sup>*Fritz-Haber-Institut der Max-Planck-Gesellschaft, Faradayweg 4-6, 14195 Berlin, Germany*

<sup>1</sup>*Laboratoire Aimé Cotton, CNRS, Université Paris-Sud, ENS Cachan, 91405 Orsay, France*

Presenting Author: [katrin.dulitz@chem.ox.ac.uk](mailto:katrin.dulitz@chem.ox.ac.uk)

Zeeman deceleration is an experimental technique in which inhomogeneous, time-dependent magnetic fields inside an array of solenoid coils are used to manipulate the velocity of a supersonic beam [1, 2]. We have built and characterised a 12-stage Zeeman decelerator for hydrogen atoms in Oxford. We will present experimental results illustrating that the overall acceptance in a Zeeman decelerator can be significantly increased by applying a low, anti-parallel magnetic field to one of the coils so as to form a temporally varying quadrupole field which improves transverse particle confinement [3]. The results show excellent agreement with three-dimensional numerical particle trajectory simulations, and they suggest the use of a modified coil configuration to improve transverse focusing during the deceleration process.

We will also report on current work which is directed towards the magnetic deceleration of metastable species using a pulsed electron gun system.

### References

- [1] N. Vanhaecke *et al.* Phys. Rev. A **75**, 031402 (2007)
- [2] E. Narevicius *et al.* Phys. Rev. A **77**, 051401 (2008)
- [3] K. Dulitz *et al.* J. Chem. Phys. **140**, 104201 (2014)

# Hybrid Atom-Optical Interferometry for Gravitational Wave Detection and Geophysics

R. Geiger<sup>1,4</sup>, W. Chaibi<sup>2,4</sup>, B. Canuel<sup>3,4</sup>, A. Bertoldi<sup>3,4</sup>, A. Landragin<sup>1,4</sup>, L. Amand<sup>1,4</sup>, S. Gaffet<sup>5,4</sup>,  
E. Cormier<sup>6,4</sup>, and P. Bouyer<sup>3,4</sup>

<sup>1</sup>*SYRTE, Observatoire de Paris, Université Pierre et Marie Curie, CNRS UMR 8630, 61 avenue de l'Observatoire, 75014 Paris, France*

<sup>2</sup>*ARTEMIS, Observatoire de la Côte d'Azur, CNRS UMR 7250*

<sup>3</sup>*LP2N, Institut d'Optique d'Aquitaine, CNRS UMR 5298, 2 Allée René Laroumagne, 33405 Talence Cedex, France*

<sup>4</sup>*MIGA consortium, Matter wave-laser Interferometry Gravitation Antenna*

<sup>5</sup>*Laboratoire souterrain à Bas Bruit (LSBB) - CNRS UMS 3538, OCA, La Grande Combe, F-84400 Rustrel*

<sup>6</sup>*Centre Lasers Intenses et Applications, Université de Bordeaux 1 - CEA - CNRS UMR 5107, 351 Cours de La Libération, 33405 Talence Cedex, France*

Presenting Author: remi.geiger@obspm.fr

Position fluctuations of the optics limit the sensitivity of ground-based gravitational wave detectors based on optical interferometry at low frequencies ( $f \lesssim 10$  Hz). They prevent from investigating a large bandwidth of various potential astrophysical sources. In terrestrial experiments, these fluctuations are mainly due to seismic noise of the interferometer optics and to gravitational noise caused by fluctuations of the mass distribution in the surrounding of the instrument.

In this presentation, we will describe a new type of instrument which strongly rejects position fluctuations of the optics and can extend the sensitivity of ground-based gravitational wave detectors to the milli-Hertz range. Our proposition uses light-pulse atom interferometry combined with optical interferometry. We will show how the instrument can be used as a high sensitivity sensor of the local gravity and present its potential applications in geophysics. Then, we will describe the measurement protocol to extract a gravitational wave signal, with expected strain sensitivities lower than  $10^{-19}$  in the  $[0.01 - 1]$  Hz frequency domain, at 100 s integration time.

The proposed instrument is under realization in the framework of the MIGA consortium [1]. It will consist of 200 meter long optical cavities hosting three atom interferometer inertial sensors, and will be set up in 2016 at the low noise underground laboratory LSBB situated in France. We will present the status of its design and of the realizations of the atom interferometers.

## References

[1] <https://sites.google.com/site/migaproject/home>

## Three-body recombination for vanishing scattering lengths

S. Kokkelmans<sup>1</sup>, Z. Shotan<sup>2</sup>, O. Machtey<sup>2</sup>, and L. Khaykovich<sup>2</sup>

<sup>1</sup>*Eindhoven University of Technology, P.O. Box 513, 5600 MB Eindhoven, The Netherlands*

<sup>2</sup>*Department of Physics, Bar-Ilan University, Ramat-Gan, 52900 Israel*

Presenting Author: s.kokkelmans@tue.nl

Efimov physics in ultracold gases is described very well by universal scaling laws, based on the scattering length. Another important parameter in this respect is the van der Waals length, which was only recently found to define the binding energies of the Efimov trimers. While the scattering length can be tuned magnetically via a Feshbach resonance, the van der Waals length is constant and connected to the radial range of the potential. However, experimental hints at non-universal behavior, when going away from resonance, are quite badly understood. The next leading coefficient in the scattering phase shift, the effective range parameter, gives an indication of this non-universality, but at the same time it can also be strongly dependent on the magnetic field. An extreme case in the non-universal regime is the zero-crossing of a Feshbach resonance. Here the scattering length vanishes, while the effective range goes to infinity. Therefore both parameters cannot directly describe three-body recombination at this point.

We investigate both experimentally and theoretically three-body recombination, for two different zero crossings in an ultracold gas of <sup>7</sup>Li. One zero crossing is associated to a broad resonance, while the other one is connected to a narrow resonance. We see a clear experimental difference for the two resonances, and we give an explanation for the behavior in terms of a new theoretical effective length parameter. This parameter is described in terms of the finite range of the two-body potential, given by the van der Waals length, and by the width of the resonance.

## Detection of Negative Charge Carriers in Superfluid Helium Droplets: The Metastable Anions $\text{He}^{-*}$ and $\text{He}_2^{-*}$

A. Mauracher<sup>1</sup>, M. Daxner<sup>1</sup>, J. Postler<sup>1</sup>, S.E. Huber<sup>1</sup>, S. Denifl<sup>1</sup>, P. Scheier<sup>1</sup>, and J.P. Toennies<sup>2</sup>

<sup>1</sup>Institute for Ion and Applied Physics, University of Innsbruck, Technikerstr. 25 / 3, A-6020 Innsbruck

<sup>2</sup>Max Planck Institut für Dynamik und Selbstorganisation, Am Fassberg 17, D-37077 Göttingen

Presenting Author: johannes.postler@uibk.ac.at

We observed the creation of helium anions upon electron impact on helium nano droplets in three distinct resonances in the energy range of about 22 eV to 25 eV. These energies coincide very well with the resonances for the formation of negatively charged HND reported by Henne and Toennies [1].

The observed resonances were explained by elastic scattering of an electron with a helium atom, exciting the latter into its metastable  $2^3S$  state and leaving behind an electron bubble. However, it now seems more reasonable to explain this behaviour via formation of  $\text{He}^-$ , which is heliophilic and therefore readily stays inside the droplet.

Moreover, most parent anion formation processes of molecules embedded in HNDs show a “repetition” of low energy resonances around 22 eV which were attributed to ionization by aforementioned electron bubbles until now [2]. However, the new experimental data suggests that this phenomenon can be explained via the formation of  $\text{He}^-$  and subsequent ionization due to charge transfer.

We can prove the higher mobility of  $\text{He}^-$  compared to  $\text{He}_2^-$  by doping the HND with  $\text{SF}_6$ . While the  $\text{He}_2^-$  signal is only slightly affected, the  $\text{He}^-$  yield drops significantly. This can be explained by the ability of  $\text{He}^-$  to reach the  $\text{SF}_6$  molecule, which resides in the center of the droplet, whereas  $\text{He}_2^-$  is not mobile enough and moreover will stay at the surface of the HND.

The formation process of  $\text{He}^-$ , its properties and the consequences on the interpretation of previous studies will be presented in this contribution.

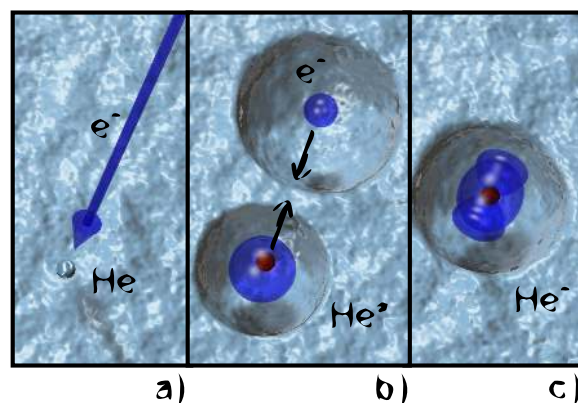


Figure 1: Artists impression of the creation steps of the helium anion

### References

- [1] U. Henne and J. P. Toennies, J. Chem. Phys. 108, 9327 (1998)
- [2] S. Denifl et al., Phys. Rev. Lett. 97, 043201 (2006).

## Three different approaches to cavity-enhanced spectroscopy

A. Cygan<sup>1</sup>, P. Wcisło<sup>1</sup>, S. Wójtewicz<sup>1</sup>, P. Masłowski<sup>1</sup>, R.S. Trawiński<sup>1</sup>, R. Ciuryło<sup>1</sup>, and D. Lisak<sup>1</sup>

<sup>1</sup>*Institute of Physics, Faculty of Physics, Astronomy and Informatics, Nicolaus Copernicus University, Grudziadzka 5/7, 87-100 Toruń, Poland*

Presenting Author: piotr.wcislo@fizyka.umk.pl

We present a comparison of three techniques of precise measurements of molecular spectra. The first one is well established frequency-stabilized cavity ring-down spectroscopy (FS-CRDS) [1-3]. The second method is an improved version of cavity mode-width spectroscopy (CMWS) [4,5]. The third method is based on the measurements of the cavity free spectral range, which is perturbed by a presence of the molecular transition. The first two techniques measure the absorption of the sample, while the third one its dispersion.

The measurement of a particular molecular transition with three independent techniques may be used to estimate an upper limit of the systematic errors introduced by these methods. Such comparison is of great importance for the line-shape analysis of experimental spectra, where one of the most challenging task is to distinguish the systematic error coming from experimental imperfections from these caused by the wrong choice of the line-shape model, see e.g. [6].

CRDS and CMWS techniques are complementary, in the sense that they achieve their best precision in different pressure ranges. For low concentrations the best precision is achieved with the CRDS technique, where the ring-down times are long and hence they can be well determined. In the opposite case, where the absorption is high, the precision of CMWS is enhanced [5]. The third method, based on the measurement of radio frequency seems to be completely insensitive to nonlinearity in detection system of the cavity transmission signal.

We tested these three methods on the CO rovibrational transitions from the ( $3 \leftarrow 0$ ) band, which are located in the spectral region around  $6201 \text{ cm}^{-1}$ .

The research is a part of the program of the National Laboratory FAMO in Toruń, Poland. The research is partially supported by the Foundation for Polish Science TEAM and HOMING PLUS Projects co-financed by the EU European Regional Development Fund, and is partially supported by the National Science Centre, Project No. DEC-2011/01/B/ST2/00491. A. Cygan is partially supported by the Foundation for Polish Science START Project.

### References

- [1] D. Long *et al.* Chem. Phys. Lett. **536**, 1–8 (2012)
- [2] A. Cygan *et al.* Eur. Phys. J. Spec. Top. **222**, 2119–2142 (2013)
- [3] S. Wójtewicz *et al.* J. Quant. Spectrosc. Radiat. Transfer **130**, 191–200 (2013)
- [4] D. A. Long *et al.* Appl. Phys. B **114**, 489–495 (2014)
- [5] A. Cygan *et al.* Opt. Express **21**, 29744–29754 (2013)
- [6] S. Wójtewicz *et al.* Phys. Rev. A **84**, 032511 (2011)

# Deceleration, cooling and trapping of SrF molecules for precision spectroscopy

S.C. Mathavan<sup>1</sup>, C. Meinema<sup>1</sup>, J.E. van den Berg<sup>1</sup>, H.L. Bethlem<sup>2</sup>, and S. Hoekstra<sup>1</sup>

<sup>1</sup>University of Groningen, The Netherlands

<sup>2</sup>Laserlab, VU Amsterdam, The Netherlands

Presenting Author: s.chirayath.mathavan@rug.nl

Heavy diatomic molecules can have hugely enhanced sensitivity for the study of fundamental symmetries and interactions, such as the search for an electron-EDM or parity violation. We work on the development of methods to cool and trap selected molecules suited for such precision measurements, since the ultimate sensitivity could be reached in an experiment exploiting the long coherence time offered by cold, trapped molecules.

We present the first results on the deceleration of SrF molecules [1, 3] in a traveling-wave Stark decelerator (Figure 1). Traditional Stark decelerators suffer from overfocusing, leading to losses. This makes it very inefficient to use such a device for the deceleration of heavy diatomics, such as SrF. A long traveling-wave decelerator, which is inherently stable, is therefore built in our lab. Using arbitrary waveform generators and high voltage amplifiers we can create true 3D moving electric traps inside the decelerator, that can be brought to a complete standstill in the laboratory [2]. After deceleration, we will laser cool the molecules to prepare them for a parity violation measurement. We report the status of the experiment and present our plans for cooling and precision spectroscopy using cold and/or trapped molecules.

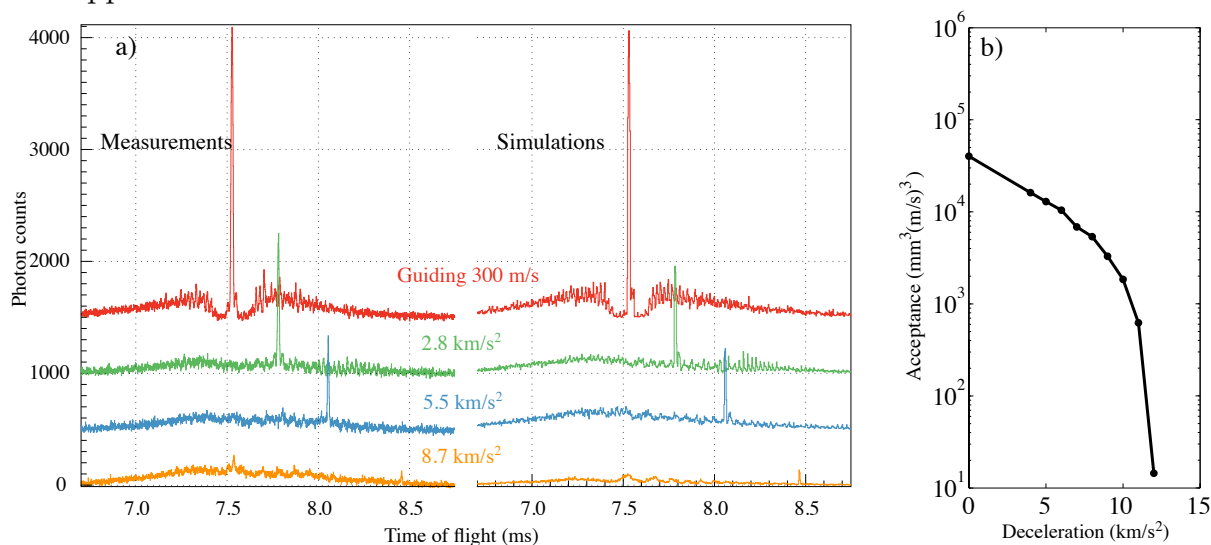


**Figure 1:** a) A time-of-flight measurement (left) compared with trajectory simulations (right) showing the deceleration of SrF molecules. b) Simulation results that illustrate the unavoidable decrease of acceptance with increasing deceleration strength. The observed deceleration matches the design efficiency.

## References

- [1] J. E. van den Berg, S. H. Turkesteen, E. B. Prinsen, S. Hoekstra, *Deceleration and trapping of heavy diatomic molecules using a ring-decelerator*, The European Physical Journal D, 66(9), 235 (2012)
- [2] M. Quintero-Perez, P. Jansen, T.E. Wall, J.E. van den Berg, S. Hoekstra, H.L. Bethlem, *Static Trapping of Polar Molecules in a Traveling-wave Decelerator*, Physical Review Letters 110, 133003 (2013).
- [3] J.E. van den Berg, S.C. Mathavan, C. Meinema, J. Nauta, T.H. Nijbroek, K. Jungmann, H.L. Bethlem, S. Hoekstra, *Traveling-wave deceleration of SrF molecules*, J. Mol. Spec., Special issue on Spectroscopic tests of fundamental physics (2014)

## Ion clouds in radio-frequency linear traps: transport and phase transitions

M.R. Kamsap<sup>1</sup>, J. Pedregosa-Gutierrez<sup>1</sup>, C. Champenois<sup>1</sup>, D. Guyomarc'h<sup>1</sup>, M. Houssin<sup>1</sup>, and M. Knoop<sup>1</sup>

<sup>1</sup>*Aix Marseille Université, CNRS, PIIM UMR 7345, 13397, Marseille, France*

Presenting Author: jofre.pedregosa@univ-amu.fr

An ion cloud confined in a linear RF-quadrupole trap is an example of a non-neutral plasma, a plasma consisting of particles with a single sign of charge. Its thermal equilibrium state has been widely studied by Dubin, O’Neil and co-workers in the context of large ion clouds in Penning traps and extrapolated to ions in RF-quadrupole traps (for a complete review, see [1]) and even to ions in multipole traps [2]. We are interested in the study of the dynamics of large ion clouds, in particular of out-of-equilibrium issues. For that purpose we have set-up a double linear RF-trap, being composed of three trapping zones of different potential geometries along a common  $z$ -axis [3].

One of the important issues in this configuration is the transport of an ion cloud by the translation of the trapping potential, with the objective of being as fast as possible without losing ions. Among others, the transport duration is a critical parameter in order to increase the frequency stability of microwave ion clock like the NASA prototype dedicated to Deep Space Navigation and soon to be tested in a flight demonstration mission [4]. In our trap, the geometry induces a deformation of the trapping potential during translation, which is responsible for heating of the center of mass motion as well as of motion in the center of mass frame. Although the electric field along the ion path is not known precisely, we will show that it is possible to transport an ensemble of several tens of thousands of ions over distances of a few centimeters in times as short as 100  $\mu$ s, losing only few % of the ions. The observed dependence of the heating of the cloud with the duration of its transport will also be presented and compared to molecular dynamics simulations [5].

Moreover, we are interested in the phase transition that cold ions encounter when they are laser-cooled. The structural organization of cold ions depends on their density, temperature and storage potential. We will show recent results about large ion crystals made of calcium ions in quadrupole traps and preliminary results concerning cold ions in an octupole trap. If their density is high enough, cold ions in a linear octupole trap are expected to organize in a hollow structure, formed of concentric tubes [6].

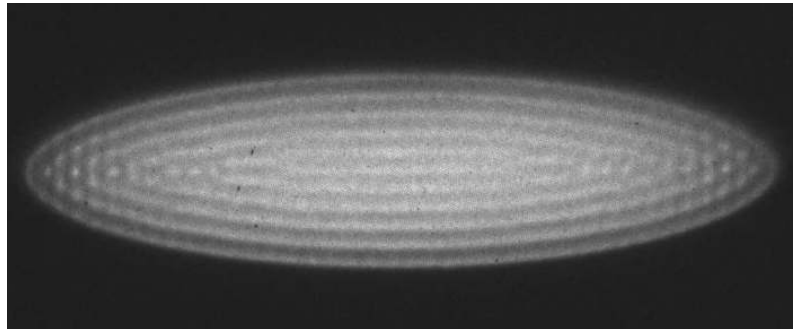


**Figure 1:** *Picture of a Coulomb crystal made of few thousands of calcium ions, laser cooled in a linear quadrupole trap*

### References

- [1] Daniel H. E. Dubin and T. M. O’Neil, *Rev. Mod. Phys.* **71** p. 87, (1999)
- [2] C. Champenois, *J. Phys. B*, **42** 154002 (2009)
- [3] C. Champenois, *et al.*, *AIP Conference Proceedings*, **1521** pp 210-219 (2013)
- [4] <http://www.jpl.nasa.gov/news/news.php?release=2012-100>
- [5] J. Pedregosa-Gutierrez *et al.*, submitted
- [6] F. Calvo *et al.*, *Phys. Rev. A* **80**, 063401 (2009)

## High-resolution Focussed Ion Beam by laser cooling and compression of a thermal atomic beam

S.H.W. Wouters<sup>1</sup>, G. ten Haaf<sup>1</sup>, J.F.M. van Rens<sup>1</sup>, S.B. van der Geer<sup>1,2</sup>, O.J. Luiten<sup>1</sup>, P.H.A. Mutsaers<sup>1</sup>, and E.J.D. Vredenbregt<sup>1</sup>

<sup>1</sup>Coherence and Quantum Technology group, Department of Applied Physics, Eindhoven University of Technology, PO Box 513, 5600 MB Eindhoven, Netherlands  
<sup>2</sup>Pulsar Physics, www.pulsar.nl

Presenting Author: s.h.w.wouters@tue.nl

In order to improve the resolution of nano-fabrication using Focused Ion Beams (FIBs) we are developing an ultra-cold ion source based on photo-ionization of a laser-intensified atomic beam. Initial calculations have shown that an ion beam with a brightness of  $10^7$  A/m<sup>2</sup> sr eV and a longitudinal energy spread of less than 1 eV can be achieved at a current up to 10 pA. Combined with high performance focusing optics, this would lead to a nanometer-sized spot at which sample manipulation can be performed.

The starting point is a high-flux atom source which consists of a Knudsen cell connected to a collimating tube. The brightness of the atomic beam is increased by laser cooling and compression in the transverse direction by means of a magneto-optical compressor. The resulting cold beam of atoms is photo-ionized inside an electric field to suppress disorder-induced heating caused by the non-uniform Coulomb interactions between the ions. The ion beam is then focussed to a nanometer-sized spot by means of an electrostatic lens column.

Numerical calculations have been performed on the magneto-optical compressor in order to find an optimal set of parameters. These reveal that a length of only 60 mm is sufficient for cooling and compressing the atomic beam to a brightness higher than  $10^7$  A/m<sup>2</sup> sr eV at an equivalent flux up to 1 nA. Furthermore, a model was set up to describe the effect of both the disorder-induced heating of the ions and of the lens aberrations on the final spot size. This was verified using particle tracking simulations incorporating a realistic ionization and acceleration structure. It was shown that spot sizes smaller than 1 nm can be achieved at currents up to a few pA or 5 nm at currents up to 20 pA which is better than the state of the art Liquid Metal Ion Source based FIBs.

We will report on simulations and on the experimental realization of the high-flux Knudsen cell with collimation tube and the magneto-optical compressor.

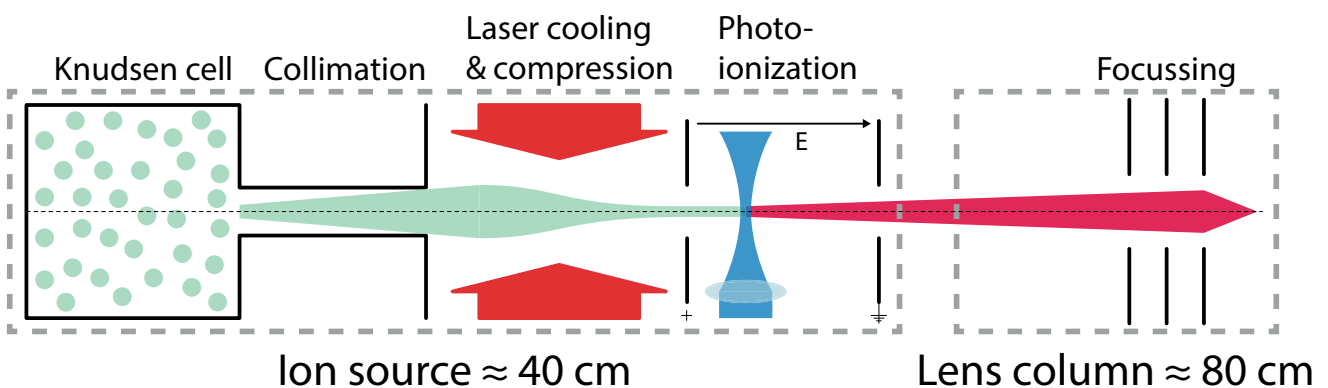


Figure 1: Schematic drawing of the Atomic Beam Laser-cooled Ion Source.

### References

# Towards Laser Cooling of Negative Ions

E. Jordan<sup>1</sup>, G. Cerchiari<sup>1</sup>, and A. Kellerbauer<sup>1</sup>

<sup>1</sup>Max Planck Institute for Nuclear Physics, Heidelberg, Germany

Presenting Author: elena.jordan@mpi-hd.mpg.de

Ultra-cold negative ions could be used in a wide field of applications, since other negative ion species could be cooled sympathetically by loading them in the same trap [1]. To date laser cooling of negative ions has never been demonstrated experimentally, because most atomic negative ions are weakly bound systems without bound excited states. There are few exceptions with opposite-parity excited states that allow electric dipole transitions [2]. We want to demonstrate the first laser cooling of atomic anions. In order to identify suitable candidates we study them by high-resolution laser spectroscopy. Previously the transition frequencies and transition cross-sections of various Os isotopes have been determined [3]. The Einstein  $A$  coefficient of the relevant transition was found to be low  $A \approx 330 \text{ s}^{-1}$ . In addition, the Landé  $g$  factors of the ground and excited state as well as the Zeeman splitting have been determined experimentally [4, 5]. Since it has been theoretically predicted that  $\text{La}^-$  is a promising candidate for laser cooling [2, 6], we are now studying  $\text{La}^-$  by infrared laser photo-detachment spectroscopy. For spectroscopy laser beam and ion beam are superimposed collinearly and the neutrals from two-photon detachment are counted. In this report we will present first measurement results (Fig. 1).

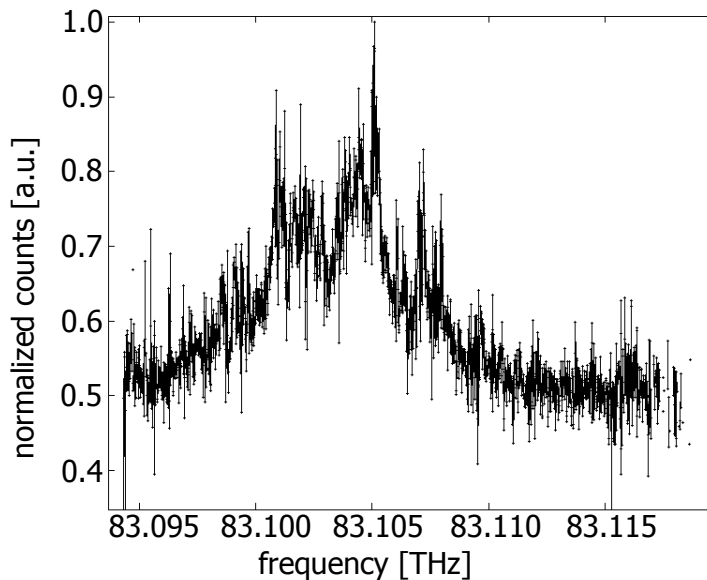


**Figure 1:** Neutralized La atom counts from two-photon detachment of a  $\text{La}^-$  beam vs. laser frequency. Preliminary data.

## References

- [1] A. Kellerbauer, J. Walz, *New J. Phys.* **8** 45 (2006)
- [2] S. M. O'Malley, D. R. Beck, *Phys. Rev. A* **81**, 032503 (2010)
- [3] U. Warring *et al.*, *PRL* **102**, 043001 (2009)
- [4] A. Fischer *et al.*, *Phys. Rev. Lett.* **104** (2010) 073004
- [5] A. Kellerbauer *et al.*, *Phys. Rev. A* **89** (2014), to appear
- [6] L. Pan, D. R. Beck, *Phys. Rev. A* **82**, 014501 (2010)

## Transfer ionization in collisions of bare nuclei with light atoms

O.Yu. Andreev<sup>1</sup>, E.A. Mistonova<sup>1</sup>, and A.B. Voitkiv<sup>2</sup>

<sup>1</sup>*Faculty of Physics, St. Petersburg State University, ul. Ulyanovskaya 1, Peterhof, St. Petersburg, 198504, Russia*

<sup>2</sup>*Max-Planck-Institute für Kernphysik, D-69117 Heidelberg, Germany*

Presenting Author: olyuan@gmail.com

In a collision between an ion (projectile) and an atom with two or more electrons (target) one of atomic electrons can be captured into a bound state of the ion while another electron be emitted. Such a process is called transfer ionization.

There are few basic mechanisms contributing to transfer ionization in fast collisions. Depending on whether the electron-electron interaction (correlation) is crucial or not these mechanisms can be subdivided into correlated and uncorrelated ones. The uncorrelated mechanisms include so called independent capture–ionization and capture–shake-off whereas the correlated ones are electron-electron Thomas [1] and electron-electron Auger [2-5].

A non-relativistic theory of transfer ionization in fast collisions (including both correlated and uncorrelated channels) was presented in [2-4]. This theory can be applied when the typical velocities of the electrons in their initial and final bound states are much less than the collision velocity.

We present calculation of the double-differential cross section of the correlated transfer ionization in relativistic collisions between bare nuclei and light atoms [5]. Nuclei with the nuclear charge  $30 \leq Z \leq 92$  are considered. The calculation is performed within the relativistic QED theory.

This process is profoundly influenced by the generalized Breit interaction already at modest relativistic impact energies. This interaction qualitatively changes the shape of the emission pattern and strongly increases the emission. These effects can be verified experimentally by detecting high-energy electrons emitted in the laboratory frame under large angles ( $\sim 120^\circ - 180^\circ$ ) with respect to the motion of the highly charged ion.

### References

- [1] L. H. Thomas Proc. R. Soc. **14**, 561-576 (1927)
- [2] A. B. Voitkiv J. Phys. B **41**, 195201 (2008)
- [3] A. B. Voitkiv, B. Najjari, and J. Ullrich Phys. Rev. Lett. **101**, 223201 (2008)
- [4] A. B. Voitkiv, X. Ma Phys. Rev. A **86**, 012709 (2012)
- [5] O. Yu. Andreev, E. A. Mistonova, and A. B. Voitkiv Phys. Rev. Lett. **112**, 103202 (2014)

## Polarizabilities of Actinides and Lanthanides

A. Kozlov<sup>1</sup>, V.V. Flambaum<sup>1</sup>, and V.A. Dzuba<sup>1</sup>

<sup>1</sup>University of NSW, Sydney, Australia

Presenting Author: alexx.kozloff@gmail.com

Polarizability of single atoms has been a subject of investigation for a long period of time. It determines interaction of atom with light which is used in optical lattice trapping and optical lattice based atomic clocks<sup>1</sup>, van der Waals forces between atoms and atom-walls interaction. Experimental measurements and theoretical calculations of polarizability for few-electron elements reach as high as one percent discrepancy. Although for more complicated many valence electron systems there's almost no experimental data nor theoretical predictions due to complexity of such a calculations.

We focus on polarizability calculations for ground and few excited states of lanthanides and actinides. These elements are of the great experimental interest for ultraprecise atomic clocks [1,2], searches for variation of fundamental constants and parity non-conservation [3], application in study of quantum gasses [4,5]. Calculations for atoms with opened f-shell are very complicated and usually have poor accuracy. There is no published data for most of actinides and lanthanides and the accuracy of unpublished results [6] is not determined. We calculate scalar polarizabilities for ground and first few excited states as well as tensor polarizabilities of ground states of opened f-shell elements.

The main consequence of our result is that scalar polarizabilities of different components of the same multiplet does not depend on values of their total angular momentum. This statement holds if electron shell occupation numbers don't differ much. It means that method works better for low lying levels, where the density of states is low enough as well as configuration mixing. Another requirement is absence of close levels of opposite parity that contribute to polarizability of one of the states of multiplet. This means that energy intervals between different components of the same configuration should be smaller than energy intervals between configuration and levels of opposite parity that contributes to its polarizability.

### References

- [1] B. J. Bloom *et al.*, Nature, doi:10.1038/nature12941 (2014)
- [2] A. Kozlov, V. A. Dzuba, V. V. Flambaum Phys. Rev. A. **88** 032509 (2013)
- [3] M. Leifer *et al.*, Phys. Rev. Lett. **111** 060801 (2013)
- [4] M. Mingwu *et al.*, Phys. Rev. Lett. **107** 190401 (2011)
- [5] K. Aikawa *et al.*, Phys. Rev. Lett. **108** 120802 (2012)
- [6] G. D. Doolen Los Alamos Nat. Lab. unpublished

# On the breakdown of the electric dipole approximation for hard X-ray photoionization cross sections

Ph.V. Demekhin<sup>1</sup>

<sup>1</sup>*Institute of Physics, University of Kassel, Heinrich-Plett-Str. 40, D-34132 Kassel, Germany*

Presenting Author: demekhin@physik.uni-kassel.de

The concept of the electric dipole approximation (EDA) for the interaction of matter with electromagnetic radiation is fundamental to all branches of spectroscopy and is described in nearly all textbooks on quantum mechanics. The EDA assumes that the radiation field, i.e., the plane wave expanded in a Taylor series as  $e^{i\mathbf{k}\cdot\mathbf{r}} = 1 + i\mathbf{k}\cdot\mathbf{r} - \frac{1}{2}(\mathbf{k}\cdot\mathbf{r})^2 + \dots$ , can be truncated to unity. In this situation, all higher order multiplet interactions, like electric quadrupole, magnetic dipole, etc., are neglected. In the IR, optical, UV, and VUV spectroscopies, the EDA is well justified for total cross sections by the following two realistic assumptions: (i) photoelectron velocities are extremely small compared to the speed of light which makes relativistic effects negligible, and (ii) the wavelength of the light is much larger than the orbitals from which electrons are ejected, eliminating contributions of higher terms in the Taylor expansion.

In the X-ray photoelectron spectroscopy, many extensive theoretical and experimental studies of the limits of the EDA have been reported (see, e.g., review [1]). In almost all studies, breakdowns of the EDA are manifested as deviations from dipolar angular distributions of photoelectrons [1]. The latter are known to be much more sensitive to the relative contributions from different photoelectron partial waves than the total cross sections. Therefore, relatively moderate contributions of higher multiplet interactions, which are nearly invisible in the total cross sections in soft X-ray range, become observable in the photoelectron angular distribution parameters. In hard X-ray limit, the EDA breaks down essentially completely, and nondipole contributions must also be visible in the total cross sections. Unfortunately, a low fluence of synchrotron radiation makes the direct observation of these effects in hard X-ray region rather unlikely, since photoionization cross sections usually decrease rapidly with the incident photon energy.

The situation becomes very promising by the advent of X-ray free electron lasers (XFELs). Nowadays, XFELs produce hard X-rays up to about 20 keV with peak brightness nearly ten orders of magnitude higher than the conventional synchrotron sources. XFELs enable single-shot femtosecond diffractive imaging [2] with the main application to biologically relevant molecules, which consist mainly of low and intermediate  $Z$  elements. What can be expected as an outcome of such experiments? Obviously, photons of high energy will mainly interact with deepest atomic shells, whose ionization potentials are below the photon energy. These deep atomic shells (e.g., K- and L- shells of intermediate  $Z$  elements from third or fourth row) are strongly localized compared to the 1s-orbital of hydrogen. An important physical question immediately arises, does the EDA breakdown vary for different low and intermediate  $Z$  elements? In particular, is the error introduced to the total ionization cross section by the EDA dependent on the atomic structure and charge, and for which elements this error can be neglected for a given hard X-ray photon energy?

Here, we investigate the breakdown of the EDA for K- and L- photoionization of H, He, Be, Ne, Ar, and Kr atoms by hard X-ray radiation, which is within the reach of present or planned XFELs. Numerical calculations [3], performed in the relativistic Pauli-Fock approximation, demonstrate that the computed *relative* contributions of the nondipole interactions to the cross sections grow as a function of the photoelectron kinetic energy almost equally for the 1s and 2s shells of all considered atoms. The same holds for the 2p shells of Ne, Ar, and Kr. We, thus, confirm analytical predictions of the Born approximation suggesting that in the considered energy range the *relative* error introduced to the ionization cross section of low and intermediate  $Z$  elements by the electric dipole approximation is almost independent of the spatial extent of the absorbing atomic orbital.

## References

- [1] D.W. Lindle and O. Hemmers, J. Electron. Spectr. Relat. Phenom. **100**, 297 (1999)
- [2] H.N. Chapman, *et al.*, Nature Phys. **2**, 839 (2006)
- [3] Ph.V. Demekhin, J. Phys. B **47**, 025602 (2014)

## Finding pathways for creation of cold molecules by laser spectroscopy

I. Temelkov<sup>1,2</sup>, H. Knöckel<sup>1</sup>, A. Pashov<sup>2</sup>, and E. Tiemann<sup>1</sup>

<sup>1</sup>*QUEST and Institute for Quantumoptics, Leibniz University Hanover, Welfengarten 1, 30175 Hanover*

<sup>2</sup>*Department of Physics, Sofia University, 5 James Bourchier Blvd, 1164 Sofia, Bulgaria*

Presenting Author: i\_temelkov@phys.uni-sofia.bg

The diatomic alkali molecules are of serious interest for the cold matter physics. This research is focused on developing a model for efficient transfer of  $^{23}\text{Na}^{39}\text{K}$  molecules from the  $\text{Na}(3s)+\text{K}(4s)$  asymptote to the lowest levels of the singlet ground state. The experiment is done in an ultrasonic beam apparatus, using a  $\Lambda$ -scheme with fixed pump and scanning dump laser. The signals are observed as dark lines on a constant fluorescence. The intermediate level is chosen to be strongly perturbed by the  $B^1\Pi - c^3\Sigma^+$  states mixing [1], helping to overcome the singlet-triplet transfer prohibition. In the beam NaK is created in its singlet ground state and the transfer is driven to the triplet state, but this scheme can work also in the reversed direction. Precise potential energy curves for singlet and triplet ground state already exist from previous work of our group [2]. We observe highly resolved hyperfine spectra of various rovibrational levels (from  $v=2$  up to the asymptote, for  $N=4,6,8$ ) of the  $a^3\Sigma^+$  state with resolution better than 10MHz. Two different theoretical models are used in parallel to describe the observations. The first one is based on molecular parameters. The other uses potential curves, taking into account all couplings as functions of the internuclear distance and calculating the energy levels for all the quantum numbers in a coupled state model. With these results an efficient pathway for the creation of cold NaK molecules is demonstrated.

### References

- [1] H. Katô et. al. J. Chem. Phys. **93**(4), 2228–2237 (1990)
- [2] A. Gerdes, M. Hobein, H. Knöckel and E. Tiemann Eur. Phys. J. D **49**(1), 67–73 (2008)

# The M1-to-E2 and E1-to-M2 cross-susceptibilities of the Dirac one-electron atom

P. Stefańska<sup>1</sup> and R. Szmytkowski<sup>1</sup>

<sup>1</sup>Atomic Physics Division, Department of Atomic, Molecular and Optical Physics, Faculty of Applied Physics and Mathematics, Gdańsk University of Technology, Narutowicza 11/12, 80-233 Gdańsk, Poland

Presenting Author: pstefanska@mif.pg.gda.pl

We consider a Dirac one-electron atom placed in a weak, static, uniform magnetic  $\mathbf{B}$  [or electric  $\mathbf{F}$ ] field. We show that, to the first order in the strength of the perturbing field, the only electric  $\mathcal{Q}^{(1)}$  [or magnetic  $\mathcal{M}^{(1)}$ ] multipole moment induced by the field in the ground state of the atom is the quadrupole one. The coordinate-free form of these tensors are respectively

$$\mathcal{Q}_{2\mu}^{(1)} = (4\pi\epsilon_0) c \alpha_{M1 \rightarrow E2} \left[ \frac{3}{4}(\boldsymbol{\nu}_\mu \mathbf{B} + \mathbf{B} \boldsymbol{\nu}_\mu) - \frac{1}{2}(\boldsymbol{\nu}_\mu \cdot \mathbf{B}) \mathcal{I} \right] \quad (1)$$

and

$$\mathcal{M}_2^{(1)} = (4\pi\epsilon_0) c \alpha_{E1 \rightarrow M2} \left[ \frac{3}{4}(\boldsymbol{\nu} \mathbf{F} + \mathbf{F} \boldsymbol{\nu}) - \frac{1}{2}(\boldsymbol{\nu} \cdot \mathbf{F}) \mathcal{I} \right], \quad (2)$$

where  $\mathcal{I}$  is the unit dyad,  $\boldsymbol{\nu}_\mu$  is the unit vector parallel (when  $\mu = +1/2$ ) or antiparallel (when  $\mu = -1/2$ ) to the field vector  $\mathbf{B}$ , while  $\boldsymbol{\nu}$  is the unit vector antiparallel to the permanent magnetic dipole moment of the atom.

The coefficients  $\alpha_{M1 \rightarrow E2}$  and  $\alpha_{E1 \rightarrow M2}$  appearing above are the magnetic-dipole-to-electric-quadrupole and the electric-dipole-to-magnetic-quadrupole cross-susceptibilities of the atom, respectively. Using the Sturmian expansion of the generalized Dirac–Coulomb Green function [1], we derive closed-form expressions for these two quantities. The results are of the form

$$\alpha_{M1 \rightarrow E2} = \frac{\alpha a_0^4 \Gamma(2\gamma_1 + 5)}{Z^4 720 \Gamma(2\gamma_1)} [(\gamma_1 + 1)\mathcal{R} - 1] \quad \text{and} \quad \alpha_{E1 \rightarrow M2} = -\frac{\alpha a_0^4 \Gamma(2\gamma_1 + 5)}{Z^4 240 \Gamma(2\gamma_1)} [(\gamma_1 - 2)\mathcal{R} - 1], \quad (3)$$

where we have defined

$$\mathcal{R} = \frac{(\gamma_1 + \gamma_2)\Gamma(\gamma_1 + \gamma_2 + 2)\Gamma(\gamma_1 + \gamma_2 + 3)}{\gamma_1 \Gamma(2\gamma_1 + 5)\Gamma(2\gamma_2 + 1)} {}_3F_2 \left( \begin{matrix} \gamma_2 - \gamma_1 - 2, \gamma_2 - \gamma_1 - 1, \gamma_2 - \gamma_1 \\ \gamma_2 - \gamma_1 + 1, 2\gamma_2 + 1 \end{matrix}; 1 \right). \quad (4)$$

Here  $\Gamma(z)$  is the Euler's gamma function,  $\gamma_\kappa = \sqrt{\kappa^2 - (\alpha Z)^2}$ ,  $\alpha$  denotes the Sommerfeld fine structure constant, while  ${}_3F_2$  is the generalized hypergeometric function.

In the nonrelativistic limit,  $\alpha_{M1 \rightarrow E2}$  tends to zero. This agrees with earlier calculations [4–6] of that quantity, based on the Schrödinger or Pauli equation for the electron, which predicted the *quadratic* dependence of the induced electric quadrupole moment on the magnetic induction  $B$ .

The first of the authors very recently received a more general result for  $\alpha_{M1 \rightarrow E2}$ , which describes this quantity for an arbitrary excited state of the atom. [7]

## References

- [1] R. Szmytkowski J. Phys. B **30**, 825–861 (1997) [erratum: **30**, 2747 (1997)]
- [2] R. Szmytkowski, P. Stefańska Phys. Rev. A **85**, 042502/1–6 (2012)
- [3] R. Szmytkowski, P. Stefańska Phys. Rev. A **89**, 012501/1–7 (2014)
- [4] C. A. Coulson, M. J. Stephen Proc. Phys. Soc. A **69**, 777–782 (1956)
- [5] A. V. Turbiner Yad. Fiz. **46**, 204–218 (1987)
- [6] A. Y. Potekhin, A. V. Turbiner Phys. Rev. A **63**, 065402/1–4 (2001)
- [7] P. Stefańska, (PhD Thesis, Gdańsk University of Technology, 2014)

## Influence of external fields on the hydrogen atom in some problems of astrophysics

D. Solovyev<sup>1</sup>, V. Dubrovich<sup>2,3</sup>, L. Labzowsky<sup>1,4</sup>, and G. Plunien<sup>5</sup>

<sup>1</sup>*Department of Physics, Saint-Petersburg State University, Petrodvorets, Oulianovskaya 1, 198504, St. Petersburg, Russia*

<sup>2</sup>*St. Petersburg Branch of Special Astrophysical Observatory, Russian Academy of Sciences, 196140, St. Petersburg, Russia*

<sup>3</sup>*Nizhny Novgorod State Technical University n. a. R. E Alekseev, LCN, GSP-41, Minin str. 24, 603950, N. Novgorod, Russia*

<sup>4</sup>*Petersburg Nuclear Physics Institute, 188300, Gatchina, St. Petersburg, Russia*

<sup>5</sup>*Institut für Theoretische Physik, Technische Universität Dresden, Mommsenstrasse 13, D-01062 Dresden, Germany*

Presenting Author: solovyev.d@gmail.com

Investigation of the cosmic microwave background (CMB) formation processes is one of the most actual problem at present time. In view of detailed theoretical description of the CMB we analyzed the response of the hydrogen atom to the external photon fields. Field characteristics are defined via conditions corresponding to the recombination era of universe. Approximation of three-level atom with the different schemes of levels ( $\Xi$ -, V- and  $\Lambda$ -scheme) was used to describe the "atom - fields" interaction. It is found that the phenomena of the electromagnetically induced transparency (EIT) take place when the CMB radiation is considered as a source of field. Modification of the optical depth entering in the Sobolev escape probability is required

$$p_{ij}(\tau_S) \rightarrow p_{ij}(\tau_S \cdot (1 + f)) \quad (1)$$

It is shown that the additional terms expressed by the function  $f$  contribute on the level of 1% in resonance [1], [2].

The effects of influence of an external field on the hydrogen atom in astrophysics can be addressed to investigation of the interstellar medium (ISM). In particular, modification of the Sobolev escape probability Eq. (1) can be applied for the theoretical description of the 21 cm line profile in the ISM. As the another kind of phenomenon we have evaluated the Bloch-Siegert shift for the different values of magnetic field's strengths when the stars with the strong surface magnetic fields are taken as a powerful pumping source of radiation. It is found that the additional shift of resonant frequency should be taken into account in the search for the time variation of the fundamental constants. The influence of the electromagnetic field should be considered carefully in each special case for the frequency determination [3].

### References

- [1] D. Solovyev, V. Dubrovich and G. Plunien J. Phys. B: At. Mol. Opt. Phys. **45** 215001 (2012)
- [2] D. Solovyev and V. Dubrovich accepted in Central European Journal of Physics (2014)
- [3] D. Solovyev, Phys. Lett. A **377** 2573–2576 (2013)

# Above-threshold detachment of $\text{Si}^-$ by few-cycle femtosecond laser pulses

S.M.K. Law<sup>1</sup> and S.F.C. Shearer<sup>1</sup>

<sup>1</sup>Centre for Theoretical Atomic, Molecular and Optical Physics, Queen's University Belfast, Belfast BT7 1NN, N. Ireland

Presenting Author: f.shearer@qub.ac.uk

The recent adiabatic saddle point approach of Shearer and Monteith [1] is extended to multiphoton detachment of negative ions with outer half-filled  $np^3$  subshells. This theory is applied to investigate strong field photodetachment dynamics of  $\text{Si}^-$  ions exposed to few-cycle femtosecond laser pulses, without taking into account the rescattering mechanism. The present theory can be modified to take into account the spatiotemporal intensity distribution of the laser focus and saturation effects. To date, there are relatively few studies on photodetachment cross sections for  $\text{Si}^-$  in the literature [3-5]. The aim of the present work is to provide for the first time, detailed information on strong field photodetachment dynamics of  $\text{Si}^-$  by mid-infrared femtosecond laser pulses.

This study focuses on numerical calculations for mid-infrared few cycle laser pulses with wavelengths of 1340 nm and 1985 nm at intensities of  $1.4 \times 10^{12}$  W/cm<sup>2</sup> and  $3.5 \times 10^{12}$  W/cm<sup>2</sup>. In this work as in [1] we assume an ir laser with frequency  $\omega$ , polarized along the  $\hat{\mathbf{z}}$  axis, whose time-dependent vector potential is given by,

$$\mathbf{A}(t) = A(t)\hat{\mathbf{z}} = A_0 \left[ \sin^2 \left( \frac{\omega t}{2N} \right) \sin(\omega t + \alpha) \right] \hat{\mathbf{z}}. \quad (1)$$

At higher intensities of order  $10^{13}$  W/cm<sup>2</sup>, the present few-cycle regime fails and we need to use an infinitely long flat pulse to describe the photodetachment process accurately. This may be due to the fact that the Keldysh parameter has only a well defined meaning in the long pulse limit [6]. In this case we consider the intensity of  $7.6 \times 10^{13}$  W/cm<sup>2</sup> and take the laser field  $\mathbf{F}(t)$  to be defined as,

$$\mathbf{F}(t) = F(t)\hat{\mathbf{z}} = [F \cos \omega t] \hat{\mathbf{z}}. \quad (2)$$

The calculations involve summation over channels with different values of  $m = 0, \pm 1$  simulated separately and with the statistical averaging of channels associated with the three final triplet atomic states,  $^3P_2$ ,  $^3P_1$  and  $^3P_0$  of Si respectively.

Analysis of electron momentum distribution probability maps reveal a remarkably detailed concentric-ring structure of above threshold detachment. This is attributed to electronic quantum wave-packet interference effects.

Above threshold detachment of photoangular distributions (PADs) as functions of laser intensity and wavelength near channel closings are also investigated and found to be sensitive to initial-state symmetry as in [1-2].

Additionally it is observed that the profile of the photoelectron emission spectra calculated within the current few-cycle laser pulse regime is strongly influenced by the carrier envelop phase (CEP), thus indicating it is a powerful tool for extracting information about the mechanism underlying photodetachment of  $\text{Si}^-$  on a femtosecond time scale.

## References

- [1] S. F. C. Shearer and M. R. Monteith, Phys. Rev. A **88**, 033415, (2013).
- [2] S. F. C. Shearer and C. R. J. Addis, Phys. Rev. A **85**, 063409, (2012).
- [3] G. F. Gribakin, A. A. Gribakina, B. V. Gul'tsev, *et al.*, J. Phys. B: At. Mol. Opt. Phys. **25**, 1757, (1992).
- [4] P. Balling, P. Kristensen, H. Stapelfeldt, *et al.*, J. Phys. B: At. Mol. Opt. Phys. **26**, 3531, (1993).
- [5] L. Veseth, J. Phys. B: At. Mol. Opt. Phys. **32**, 5725, (1999).
- [6] L. V. Keldysh, J. Exp. Theor. Phys. **47**, 1945, (1964).

## Strong competition between velocity-changing and phase/state changing collisions in H<sub>2</sub> spectra perturbed by Ar

P. Wcisło<sup>1</sup>, F. Thibault<sup>2</sup>, H. Cybulski<sup>1</sup>, and R. Ciuryło<sup>1</sup>

<sup>1</sup>Institute of Physics, Astronomy and Informatics, Nicolaus Copernicus University, Grudziadzka 5/7, 87-100 Toruń, Poland

<sup>2</sup>Institut de Physique de Rennes, UMR CNRS 6251, Université de Rennes 1, Campus de Beaulieu, Bât.11B, F-35042 Rennes, France

Presenting Author: piotr.wcislo@fizyka.umk.pl

For the H<sub>2</sub>/D<sub>2</sub>-Ar systems, fundamental discrepancies between thermally averaged collisional broadening obtained from experimentally determined law [1,2] and from *ab initio* close-coupling (CC) calculations were reported [3-5]. For instance at room temperature the broadening of the Q(1) line calculated from the experimental law was almost two times larger than the theoretical one.

To resolve the problem of these huge discrepancies we performed highly accurate calculations of the H<sub>2</sub>-Ar potential energy surface (PES) by employing the RCCSD(T) method in combination with the large aug-cc-pCVQZ basis and the 332211 midbond basis set (in the calculations the stretching of the H<sub>2</sub> bond was considered). However, we found that the broadening of the H<sub>2</sub> Q(1) line determined from the CC calculations based on the new PES is even less consistent with the value from experimental law than the previous CC calculations based on less accurate, earlier PES [6]. Next, we modified the line-shape model replacing the phenomenological model of the velocity-changing collisions by much more physical *ab initio* billiard-ball model, for which it was already shown that it provides appropriate description of the velocity-changing collisions for the H<sub>2</sub>-Ar system [7]. We found that this approach gives the H<sub>2</sub> Q(1) line broadening, for the mixture of 5% of H<sub>2</sub> and 95% of Ar, very close to experimental values, see Fig. 1. Our model not only properly handles the dynamics of optically active molecules (in particular a strong competition between velocity-changing and phase/state-changing collisions), but also constitutes a first step toward application of advanced *ab initio* line-shape models in ultra-accurate optical metrology based on molecular spectroscopy.

### References

- [1] J. P. Berger *et al.* Phys. Rev. A **49**, 3396–3406 (1994)
- [2] F. Chaussard *et al.* J. Chem. Phys. **112**, 158–166 (2000)
- [3] L. Waldron, W.-K. Liu, J. Chin. Chem. Soc. **48**, 439–448 (2001)
- [4] L. Waldron, W.-K. Liu, R. J. Le Roy, J. Mol. Struct. **591**, 245–253 (2002)
- [5] H. Tran, F. Thibault, J.-M. Hartmann, J. Quant. Spectrosc. Radiat. Transfer **112**, 1035–1042 (2011)
- [6] C. Bissonnette *et al.* J. Chem. Phys. **105**, 2639–2653 (1996)
- [7] P. Wcisło *et al.*, submitted to Phys. Chem. Chem. Phys. (2014)

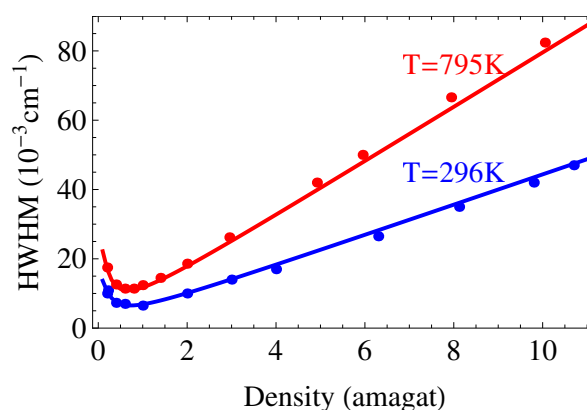


**Figure 1:** HWHM of the H<sub>2</sub> Q(1) line as a function of density for mixture of 5% H<sub>2</sub> and 95% Ar. Dots represent experimental results [2], while the lines correspond to our *ab initio* calculations.

# Laser cooling of magnesium atoms with increased ultracold fraction

A.E. Bonert<sup>1</sup>, D.V. Brazhnikov<sup>1,2</sup>, A.N. Goncharov<sup>1,2,3</sup>, A.M. Shilov<sup>1,2</sup>, A.V. Taichenachev<sup>1,2</sup>, and V.I. Yudin<sup>1,2,3</sup>

<sup>1</sup>*Institute of Laser Physics SB RAS, Novosibirsk 630090, Russia*

<sup>2</sup>*Novosibirsk State University, Novosibirsk 630090, Russia*

<sup>3</sup>*Novosibirsk State Technical University, Novosibirsk 630073, Russia*

Presenting Author: phd7@rambler.ru

At present, there are several atomic candidates for designing a new-generation optical-lattice-based frequency standard: Yb, Sr, Hg, Ca and Mg. The problem of deep laser cooling of large number of these atoms is very urgent and important for quantum metrology and other interesting applications. Scientists have already reached success with the first four elements ( $T \sim 1 \mu\text{K}$ ), but long time that problem has not been solved for magnesium atoms [1,2]. Recently the group of experimentalists from Hunnover University [3] has managed to cool  $^{24}\text{Mg}$  down to  $5 \mu\text{K}$ , but only 5000 of ultracold atoms have been accumulated in a dipole trap. It is about 0.05% from initial number of cold atoms in a magneto-optical trap.

We present the theoretical analysis of sub-Doppler laser cooling of  $^{24}\text{Mg}$  atoms using dipole transition  $3^3\text{P}_2 \rightarrow 3^3\text{D}_3$  under two counterpropagating light waves with opposite circular polarizations (1D  $\sigma^+\sigma^-$  configuration). For numerical calculations the standard semi-classical approach based on the Fokker-Planck equation for linear momentum distribution of atoms is exploited. The distributions are gained beyond the limits of slow atoms approximation and for arbitrary light field intensity. The absence of these limits allows us to determine the optimal parameters of light field to maximize a fraction of ultracold atoms ( $T \approx 5\text{-}10 \mu\text{K}$ ) in a whole atomic cloud. In particular, at certain conditions the fraction can reach the value of 50% (see Fig.1). In 3D case the profile at Fig.1 may quantitatively change, but we believe that existence of some optimum with the large percentage also should present. So, solution of the existing problems in deep laser cooling of large number of magnesium atoms has obvious prospects for atomic optics and quantum metrology.

The work was supported by the Russian Foundation for Basic Research (14-02-00806, 14-02-00712, 14-02-00939, 12-02-00403, 12-02-00454), by the Presidential Grants (MK-4680.2014.2 and NSh-4096.2014.2), by the grant of Novosibirsk City Administration, by the Russian Academy of Sciences and the Presidium of SB RAS, by the Russian Ministry of Education and Science.

## References

- [1] N. Rehbein *et al.* Phys. Rev. A **76** 043406 (2007)
- [2] T. E. Mehlstäubler *et al.* Phys. Rev. A **77** 021402 (2008)
- [3] M. Riedmann *et al.* Phys. Rev. A **86** 043416 (2012)

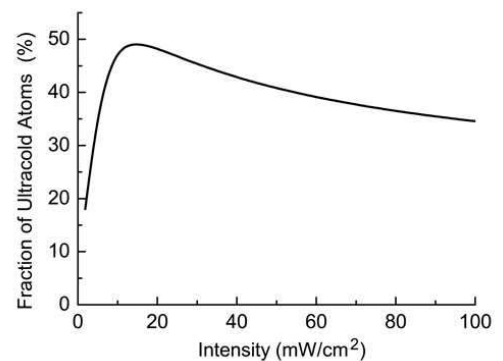


**Figure 1:** Fraction of ultracold atoms in a cold atomic cloud, detuning equals to  $-2\gamma$ .

## Differential cross section of dielectronic recombination with H-like uranium

K.N. Lyaschenko<sup>1</sup> and O.Yu. Andreev<sup>1</sup>

<sup>1</sup>*Faculty of Physics, St. Petersburg State University, ul. Ulyanovskaya 1, Petergof, St. Petersburg, 198504, Russia*

Presenting Author: laywer92@mail.ru

Investigation of the dielectronic recombination with H-like uranium within the framework of QED is presented. We consider process where the initial state is presented by a one-electron ion of uranium being in the ground state and by an incident electron. The energy of the initial state is close to the energies of double-excited states  $((2s, 2s), (2s, 2p), (2p, 2p))$ . The final state is given by a two-electron ion in one of the single-excited states  $((1s, 2s), (1s, 2p))$  and by emitted photon. The process of dielectronic recombination is a resonant process. The resonances in the cross section correspond to the double excited states. In the resonant area the dielectronic recombination gives the main contribution to the cross section.

The calculation is performed with employment of the line-profile approach [1,2]. The one-photon exchange correction for the low-lying states is taken into account in all orders of the QED perturbation theory. The electron self-energy and vacuum polarization corrections are considered in the first order of the perturbation theory.

We present results of the calculation of the total and differential cross section. The polarization properties are also considered and the Stokes parameters are presented. The contribution of the Breit interaction to the cross section and to the Stokes parameters is investigated. The results are compared with available experimental and theoretical data.

### References

- [1] O. Yu. Andreev, L. N. Labzowsky, G. Plumien, D. A. Solovyev Phys. Rep. **455**, 135–246 (2008)
- [2] O. Yu. Andreev, L. N. Labzowsky, A. V. Prigorovsky Phys. Rev. A **80**, 042514 (2009)

# 4d<sup>9</sup>np resonant Auger effect in Xe: interchannel interaction as a dominant effect in the population of high angular momentum final ionic states

B.M. Lagutin<sup>1</sup>, I.D. Petrov<sup>1</sup>, V.L. Sukhorukov<sup>2</sup>, A. Ehresmann<sup>3</sup>, K.-H. Schartner<sup>4</sup>, and H. Schmoranzer<sup>5</sup>

<sup>1</sup>Rostov State Transport University, 344038, Rostov-on-Don, Russia

<sup>2</sup>Institute of Physics, Southern Federal University, 344090, Rostov-on-Don, Russia

<sup>3</sup>Institut für Physik, Universität Kassel, D-34132 Kassel, Germany

<sup>4</sup>I. Physikalisches Institut, Justus-Liebig-Universität, D-35392 Giessen, Germany

<sup>5</sup>Fachbereich Physik, Technische Universität Kaiserslautern, D-67653 Kaiserslautern, Germany

Presenting Author: sukhorukov\_v@mail.ru

Radiationless decay of the photon-excited inner-shell atomic resonance is known as the resonance Auger effect (RAE). The intensities of the spectral lines and the photoelectron angular distribution (PAD) have been studied intensively for the rare-gas atoms (see, e.g., recent review [1]). Large differences between measured and calculated PAD parameters for the high total angular momentum ( $J=5/2, 7/2$ ) ionic states (in some cases even the sign is opposite, see experimental dots for  $\beta_{el}$  in Fig. 1) have been observed [2,3]. However, the reason of the discrepancy was not clearly understood before the present investigation.

The interaction between different decay channels of the 4d<sup>9</sup>6p resonances in Xe was investigated theoretically within the configuration interaction Pauli-Fock approximation with core polarization (CIPFCP) [4]. The strong impact of the 4d<sup>9</sup>5s<sup>2</sup>5p<sup>6</sup>6p-4d<sup>10</sup>5s<sup>1</sup>5p<sup>5</sup>6p $\epsilon$ f decay channel on other decay channels was revealed. This influence is associated with the resonance-like dependence of the 5s5p-4d $\epsilon$ f decay amplitude on the energy of the  $\epsilon$ f-electron and has the same origin as the well-known giant resonance in the 4d photoabsorption of Xe, i.e. the potential barrier effect.

The interaction between the 4d<sup>10</sup>5s<sup>1</sup>5p<sup>5</sup>6p $\epsilon$ f and 4d<sup>10</sup>5s<sup>2</sup>5p<sup>4</sup>6p $\epsilon$ g decay channels decreases the 5p5p-4d $\epsilon$ g amplitude by a factor of about 3 (Fig. 2) and results in strong changes of the photoionization cross section and (even in sign) polarization parameters  $\beta_{el}$ , alignment  $A_{20}$  and orientation  $O_{10}$  of the Xe 5p<sup>4</sup>mp levels with large values of the total angular momentum for which the 4d<sup>10</sup>5s<sup>2</sup>5p<sup>4</sup>6p $\epsilon$ g channel is dominating. This conclusion is confirmed by the good agreement between the measured  $\beta_{el}$ ,  $A_{20}$  and  $O_{10}$  parameters [2,3] and those computed taking into account the interchannel interaction (Fig. 1)

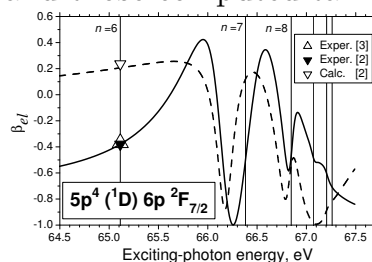


**Figure 1:** Computed and measured PAD parameters for the  $5p^4(^1D)6p^2F_{7/2}$  level. Dashed (without) and solid (with interchannel interaction) curves – present calculations. Vertical lines – positions of the  $4d^9_{5/2}np_{3/2}$  resonances.

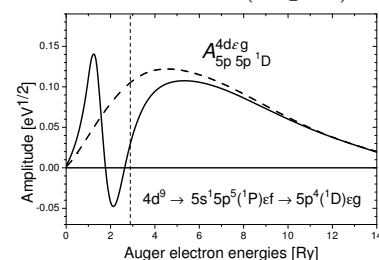


**Figure 2:** Auger amplitudes for the 5p5p-4d $\epsilon$ g decay channel computed without (dashed line) and with (solid line) influence of the 5s5p-4d $\epsilon$ f decay channel. Vertical line – position of the  $4d^9_{5/2}np$  resonance in the respective continuum.

## References

- [1] N.M. Kabachnik *et al.* Phys. Rep. **451**, 155–233 (2007)
- [2] S.M. Huttula *et al.* Chem. Phys. **289** 81–91 (2003)
- [3] J. Söderström *et al.* New J. Phys. **13** 073014 (2011)
- [4] V. L. Sukhorukov *et al.* J. Phys. B: At. Mol. Opt. Phys. **45** 092001 (2012)

# Manifestation of the 4d- $\epsilon f$ giant resonance in the $N_{4,5}OO$ Auger effect in Xe

I.D. Petrov<sup>1</sup>, B.M. Lagutin<sup>1</sup>, V.L. Sukhorukov<sup>2</sup>, A. Ehresmann<sup>3</sup>, and H. Schmoranzner<sup>4</sup>

<sup>1</sup>Rostov State Transport University, 344038, Rostov-on-Don, Russia

<sup>2</sup>Institute of Physics, Southern Federal University, 344090, Rostov-on-Don, Russia

<sup>3</sup>Institut für Physik, Universität Kassel, D-34132 Kassel, Germany

<sup>4</sup>Fachbereich Physik, Technische Universität Kaiserslautern, D-67653 Kaiserslautern, Germany

Presenting Author: sukhorukov\_v@mail.ru

The high resolution  $N_{4,5}OO$  Auger spectrum of Xe [1] is a challenge example to check the degree of ability of the theoretical approximations. There exists substantial difference between theory and experiment even in the most sophisticated investigation of Kivimäki *et al.* [2] (see Fig. 1). In our recent work on the 4d<sup>9</sup>6p resonant Auger decay of Xe [3] we revealed that the partial 5p5p-4d $\epsilon g$  decay amplitude is strongly influenced by the 5s5p-4d $\epsilon f$  channel. This finding motivated us to revive the theoretical study of the normal  $N_{4,5}OO$  Auger decay in Xe.

We applied the configuration interaction Pauli-Fock approximation with core polarization (CIPFCP) [4]. The following many-electron effects appeared to be very important: (i) inter-channel interaction of all final-state Auger channels; (ii) polarization of the core by the outgoing electron; (iii) dipole polarization of the electron shells described by the 5p5p-5s( $n/\epsilon$ ) $\ell$  excitations [5]; (iv) reduction of the effective Coulomb interaction via inclusion of highly-excited configurations [5]. Taking into account these effects, especially the interaction between the 5s<sup>2</sup>5p<sup>4</sup>(<sup>1</sup>D) $\epsilon g$  and 5s<sup>1</sup>5p<sup>5</sup>(<sup>1</sup>P) $\epsilon f$  decay channels, reduced the probability of the 5p5p-4d $\epsilon g$  Auger decay by more than an order of magnitude.

Computed widths of the  $N_4$  and  $N_5$  levels agree with the measured ones within 2%. The shape of the computed  $N_{4,5}OO$  Auger spectrum (Fig. 1) and the Auger-electron angular distribution parameters are also in much better agreement with the measured values than the previous theoretical data.

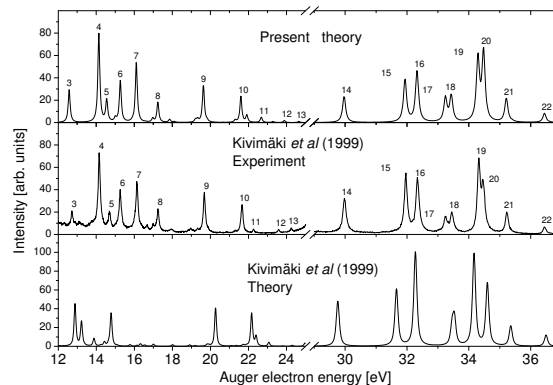


**Figure 1:** Experimental ([2], middle panel) and theoretical (present calculation - upper panel, [2] - lower panel)  $N_{4,5}OO$  spectra of Xe corresponding to the exciting-photon energy of 95.1 eV.

## References

- [1] L. O. Werme, T. Bergmark, K. Siegbahn Phys. Scr. **6**, 141–150 (1972)
- [2] A. Kivimäki *et al.* J. Electr. Spectr. Relat. Phenom. **101-103** 43-47 (1999)
- [3] B. M. Lagutin *et al.* J. Phys. B: At. Mol. Opt. Phys. **45** 245006 (2012)
- [4] V. L. Sukhorukov *et al.* J. Phys. B: At. Mol. Opt. Phys. **45** 092001 (2012)
- [5] B. M. Lagutin *et al.* J. Phys. B: At. Mol. Opt. Phys. **29** 937–976 (1996)

# Nature of photoemission in the range of the 5s-photoelectron spectrum of iridium

A.T. Kozakov<sup>1</sup>, A.V. Nikolsky<sup>1</sup>, K.A. Googlev<sup>1</sup>, I.D. Petrov<sup>2</sup>, B.M. Lagutin<sup>2</sup>, V.L. Sukhorukov<sup>1</sup>,  
H. Huckfeldt<sup>3,4</sup>, D. Holzinger<sup>3,4</sup>, A. Gaul<sup>3,4</sup>, and A. Ehresmann<sup>3,4</sup>

<sup>1</sup>*Institute of Physics, Southern Federal University, 344090, Rostov-on-Don, Russia*

<sup>2</sup>*Rostov State Transport University, 344038, Rostov-on-Don, Russia*

<sup>3</sup>*Institut für Physik, Universität Kassel, D-34132 Kassel, Germany*

<sup>4</sup>*Center for Interdiscipl. Nanostruct. Sci. and Technology, D-34132 Kassel, Germany*

Presenting Author: sukhorukov\_v@mail.ru

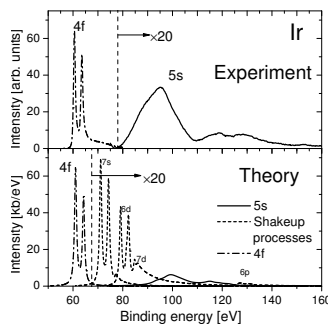


**Figure 1:** Photoelectron spectrum of 4f- and 5s-shells of Ir. Intensity of the spectra is scaled by 20 at the right side of the vertical dashed line.

The 4f and 5s X-ray photoelectron spectra (XPES) of the iridium metal excited by monochromatized Al  $K_{\alpha}$  radiation were measured using the X-ray photoelectron microprobe ESCALAB-250. These spectra are presented in the upper panel of Fig. 1. The integral intensity of the measured 5s spectrum amounts to 21.7% of the 4f spectrum intensity, whereas the estimate using the Hartree-Fock-Slater data of Yeh and Lindau [1] yields for this ratio about 3% only.

In the present work we calculated the 4f and 5s XPES of Ir using the configuration interaction Pauli-Fock approximation with core polarization (CIPFCP) [2]. The spectra were computed applying the isolated-atom model. The 5s XPES was computed in the  $5s^2 5p^6 5d^7 6s^2 (^4F_{9/2})$  ground state, whereas in the calculation of the 4f XPES the 5d-shell was treated as a spherical one. The most important many-electrons effects influencing the 5s- $\epsilon p$  photoemission were found to be: (i) dipole polarization of electron shells (DPES), described by the  $5p5p$ - $5s5d$ ,  $4f5p$ - $5s5d$  and  $4f4f$ - $5s5d$  excitations of the  $5s^1 5d^7$  ionic state and contributing multiplet structure of the 5s XPES; (ii) intershell correlations described by the interaction between the  $5s$ - $\epsilon p$ ,  $4f$ - $\epsilon(d/g)$ , and  $5p$ - $\epsilon(s/d)$  channels and contributing about 3% to the  $5s$ - $\epsilon p$  photoionization cross section; (iii) double-electron single-photon correlational transitions  $4f5p$ - $5d\epsilon\ell$  ( $\ell = 1, 3, 5, 7$ ) through the  $4f^{13} 5p^6 5d^7 \epsilon'\ell'$  intermediate channels contributing satellites which have binding energies in the range of 110-140 eV and 16% of the 5s XPES intensity.

Computed 4f and 5s XPES are presented in the lower panel of Fig. 1. For better clarity, the theoretical binding energies were decreased by 9 eV. The integral intensity of the computed 5s XPES amounts to 3.4% only of the 4f XPES intensity. We suppose that the 5s-photoionization is not a dominant process forming the spectrum in the 80–140 energy range. In order to reveal an additional mechanism of the photoemission in this energy range, we calculated the shake excitation/ionization processes of the outer 5p-, 5d- and 6s- electrons accompanied by creation of the 4f vacancy. They were calculated within the sudden approximation and are presented in the lower panel of Fig. 1 by dashed curves. The integral intensity of the XPES in the 5s-energy range amounts to 18,6% of the 4f-XPES intensity, which is close to the experimental value. However, the shape of the theoretical spectrum differs from the experimental one. This discrepancy can be connected with the limitations of the isolated-atom model.

## References

- [1] J. J. Yeh and I. Lindau *At. Data and Nucl. Data Tables* **32**, 1–155 (1985)
- [2] V. L. Sukhorukov *et al. J. Phys. B: At. Mol. Opt. Phys.* **45** 092001 (2012)

# Resonant electron-capture in ion-atom collisions: Fraunhofer diffraction pattern

H. Agueny<sup>2,1</sup>, A. Makhoute<sup>1</sup>, and A. Dubois<sup>2</sup>

<sup>1</sup>*UFR de Physique du Rayonnement et des Interactions Laser-Matière, Faculté des Sciences. Université Moulay Ismail, B.P. 11201, Zitoune, Meknès, Morocco*

<sup>2</sup>*Laboratoire de Chimie Physique-Matière et Rayonnement, Université Pierre et Marie Curie, UMR 7614, 11 Rue Pierre et Marie Curie, 75231 Paris Cedex 05, France*

Presenting Author: h.agueny@gmail.com

Diffraction with atomic matter waves is a rich branch of atomic physics and quantum optics. It has been investigated in the first time by Estermann and Stern [1] in which helium atoms were reflected and diffracted from the surface of a *LiF* crystal.

Recently, diffraction patterns have been observed experimentally for electron processes in ion-atom collisions. For instance, Wang *et al.* [2] have observed oscillations in the angular distribution of projectile for single electron-capture in  $He^{2+}$ -*He* collisions at intermediate energies. These structures are attributed to Fraunhofer diffraction. At low projectile energies, this phenomenon has already been observed by van der poel *et al.* [3] for  $Li^+$ -*Na* single electron-capture collisions. However, to the best of our knowledge, this phenomenon has not been identified and discussed theoretically before in connection with double electron-capture in slow and intermediate  $He^{2+}$ -*He* collisions.

In the conference, we shall investigate the presence of the Fraunhofer diffraction patterns in the resonant electron-capture process in  $He^{2+}$ -*He* collisions for energies ranging from 10 to 75 *keV/u* ( $v=0.6-1.7$  a.u.). To study this collision system, a semi-classical close-coupling (SCCC) approach is used to solve the time-dependent Schrödinger equation where the electron-electron correlation is taken into account. Differential cross sections (DCS) are calculated by using eikonal method [4,5] in which the probability amplitudes from the SCCC calculations are augmented by a coulombic phase. Our DCS will be discussed, where the observed diffraction patterns (Fig. 1) can be interpreted as resulting from diffraction of matter waves of projectile  $He^{2+}$  by target *He*.

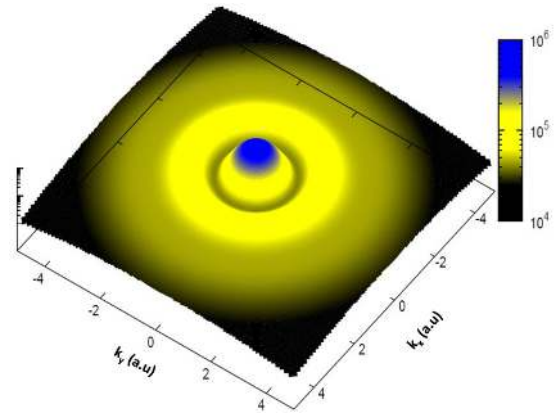


**Figure 1:** (color online). Two-dimensional differential cross sections in the transverse plane at the collision energy 25 *keV/u* a.u. for double electron-capture collision:  
 $He^{2+} + He(1s^2) \rightarrow He(1s^2) + He^{2+}$

## References

- [1] I. Estermann and A. Stern *Z. Phys.* **61**, 95 (1930)
- [2] Q. Wang *et al.* *J. Phys. B* **45**, 025202 (2012)
- [3] M. van der Poel *et al.* *Phys. Rev. Lett.* **87**, 123201 (2001)
- [4] B. H. Bransden and M.R.C. McDowell, *Charge exchange and the theory of ion-atom collisions* (Clarendon Press, Oxford, 1992)
- [5] A. Dubois, S. E. Nielsen, J. P. Hansen *J. Phys. B* **26**, 705 (1993)

## Using highly charged ions to probe possible variations in the fine-structure constant

J.C. Berengut<sup>1</sup>, V.A. Dzuba<sup>1</sup>, V.V. Flambaum<sup>1</sup>, and A. Ong<sup>1</sup>

<sup>1</sup>*School of Physics, University of New South Wales, Sydney 2052, Australia*

Presenting Author: jcb@phys.unsw.edu.au

The sensitivity of an atomic transition to variations in the fine structure constant,  $\alpha = e^2/\hbar c$ , scales proportionally to the ionisation energy. Therefore highly charged ions can be much more sensitive probes of space-time  $\alpha$ -variation than atoms or near-neutral ions.

To be competitive with current limits on time-variation of  $\alpha$  in the laboratory, optical transitions should be used. To maximise sensitivity, the transition should be between orbitals with different principal quantum number and different angular momentum in highly charged ions. Optical transitions such as this can occur in a limited subset of highly charged ions when the orbitals involved are nearly degenerate [1,2]. We have identified several such systems and shown that the transitions have a number of properties that could make them suitable reference transitions for atomic clocks with high accuracy [3,4].

We present recent theoretical developments on the identification and characterisation of the most promising systems for a highly charged ion clock. In addition, transitions in  $\text{Ir}^{17+}$ , first proposed as a clock candidate in [2], are being studied using the Heidelberg Electron Beam Ion Trap. We will report on the experimental progress and the implications for a functional clock.

### References

- [1] J. C. Berengut, V. A. Dzuba, V. V. Flambaum, *Phys. Rev. Lett.* **105**, 120801 (2010)
- [2] J. C. Berengut *et al.*, *Phys. Rev. Lett.* **106**, 210802 (2011)
- [3] J. C. Berengut *et al.*, *Phys. Rev. A.* **86**, 022517 (2012)
- [4] J. C. Berengut *et al.*, *Phys. Rev. Lett.* **109**, 070802 (2012)

## Limits on the dependence of the fine-structure constant on gravitational potential from white-dwarf spectra

J.C. Berengut<sup>1</sup>, V.V. Flambaum<sup>1</sup>, A. Ong<sup>1</sup>, J.K. Webb<sup>1</sup>, J.D. Barrow<sup>2</sup>, M.A. Barstow<sup>3</sup>, S.P. Preval<sup>3</sup>, and J.B. Holberg<sup>4</sup>

<sup>1</sup>*School of Physics, University of New South Wales, Sydney 2052, Australia*

<sup>2</sup>*DAMTP, Centre for Mathematical Sciences, University of Cambridge, Cambridge CB3 0WA, United Kingdom*

<sup>3</sup>*Department of Physics and Astronomy, University of Leicester, University Road, Leicester LE1 7RH, United Kingdom*

<sup>4</sup>*Lunar and Planetary Laboratory, University of Arizona, Sonett Space Science Building, Tucson, Arizona 85721, USA*

Presenting Author: jcb@phys.unsw.edu.au

We propose a new probe of the dependence of the fine-structure constant on a strong gravitational field using sensitive transitions in the absorption spectra of white-dwarf stars [1]. The sensitivity of an atomic transition to variations in the fine structure constant,  $\alpha = e^2/\hbar c$ , increases with the ionisation degree. In our study, we used around 100 far-UV transitions in Fe v and Ni v observed in the white-dwarf star G191-B2B by the Hubble Space Telescope Imaging Spectrograph.

These iron and nickel ions reside in the atmosphere of the white dwarf and the observed features are formed in its outer layers, near the surface of white dwarf. Consequently, the ions experience the strong downward surface gravity of the star, but are supported against this by the transfer of momentum from high-energy photons, a process termed “radiative levitation”. The dimensionless gravitational potential for these ions (relative to the laboratory) is  $\Delta\phi \approx 5 \times 10^{-5}$ .

We obtained the limit on the change in  $\alpha$  due to this gravitational field as  $\Delta\alpha/\alpha = (4.2 \pm 1.6) \times 10^{-5}$  and  $(-6.1 \pm 5.8) \times 10^{-5}$  for Fe v and Ni v spectra, respectively. This constrains theories where light scalar fields change parameters of the Standard Model (such as  $\alpha$ ).

Finally, we also calculated isotope shifts for these transitions, which can be used to constrain models of chemical evolution of our galaxy [2].

### References

[1] J. C. Berengut *et al.*, Phys. Rev. Lett. **111**, 010801 (2013)

[2] A. Ong, J. C. Berengut, V. V. Flambaum, Phys. Rev. A **88**, 052517 (2013)

# Confirmation of New Even-parity Energy Levels of La I by Laser-Induced Fluorescence Spectroscopy

Gö. Başar<sup>1</sup>, Gü. Başar<sup>1</sup>, I.K. Öztürk<sup>1</sup>, F. Güzelçimen<sup>1</sup>, A. Er<sup>1</sup>, S. Kröger<sup>2</sup>, and L. Windholz<sup>3</sup>

<sup>1</sup>*Faculty of Science, Physics Department, Istanbul University, Tr-34134 Vezneciler, Istanbul, Turkey*

<sup>2</sup>*Hochschule für Technik und Wirtschaft Berlin, Wilhelminenhofstr. 75A, D-12459 Berlin, Germany*

<sup>3</sup>*Institute of Experimental Physics, Graz University of Technology, Petersgasse 16, A-8010 Graz, Austria*

Presenting Author: gbasar@istanbul.edu.tr

In continuation of the previous work done at the Institute of Experimental Physics of Graz University of Technology [1], we tried to confirm new even-parity energy levels of atomic Lanthanum (La I) by at least one laser excitation in the near infrared wavelength region at the Laser Spectroscopy Laboratory of Istanbul University. The levels were found when performing laser-spectroscopic investigations in the yellow spectral range. Despite of all efforts no further excitation of these levels - and thus no confirmation of their existence - was possible in the visible range.

We performed laser-induced fluorescence spectroscopy, using a continuous wave tunable titan-sapphire laser (Coherent MBR-110 pumped by Coherent Verdi 18 W) as narrow-band light source and a hollow cathode discharge lamp (described in ref. [2]) as source of free La atoms. We investigated the hyperfine structure of seven La I lines in the wavelength region of 750 nm to 865 nm ( $11\,560\text{ cm}^{-1}$  to  $13\,330\text{ cm}^{-1}$ ). Laser-induced fluorescence signals were filtered with a grating monochromator (McPherson 207) and detected with a photomultiplier (Hamamatsu PM R928) for all current lines.

On the basis of yet not confirmed data of new levels, possible excitation transitions within the range of our laser system as well as possible fluorescence wavelengths were calculated (as decay lines from the new energy levels) using the classification program [3]. Then we tried to excite and detect the proposed transitions, but not all these trials were successful. Finally seven spectral lines could be excited with the laser light and detected by laser-induced fluorescence.

We succeeded in confirming five levels. The magnetic dipole hyperfine constant  $A$  for the new levels could be obtained by fitting the recorded hyperfine patterns with the computer program Fitter [4] (the quadrupole hyperfine constant  $B$  was assumed to be zero, since the La nucleus has a very small electric quadrupole moment). The results for energy,  $J$  value, parity and magnetic dipole hyperfine constant  $A$  agree well with the preliminary values.

| new even level |                             |           |
|----------------|-----------------------------|-----------|
| $J$            | energy ( $\text{cm}^{-1}$ ) | $A$ (MHz) |
| 3/2            | 25 558.770                  | 250 (5)   |
| 9/2            | 32 448.352                  | 360 (3)   |
| 9/2            | 43 199.08                   | 100 (2)   |
| 5/2            | 42 041.20                   | 58 (10)   |
| 3/2            | 42 819.72                   | -32 (2)   |

**Table 1:** *New even energy levels of La I*

## References

- [1] L. Windholz, Graz University of Technology, unpublished (2014)
- [2] D. Messnarz, G. H. Guthöhrlein, Eur. Phys. J. D, 12 269 (2000)
- [3] L. Windholz, G. H. Guthöhrlein, Phys. Scr. T, 105 55 (2003)
- [4] G. H. Guthöhrlein, University of Bundeswehr Hamburg, unpublished (2004)

# Production and detection of phase modulation of matter waves

B. Decamps<sup>1</sup>, J. Gillot<sup>1</sup>, A. Gauguet<sup>1</sup>, J. Vigué<sup>1</sup>, and M. Büchner<sup>1</sup>

<sup>1</sup>Laboratoire Collisions Agrégats Réactivité-IRSAMC, Université de Toulouse-UPS and CNRS UMR 5589, F-31062, Toulouse, France

Presenting Author: matthias.buchner@irsamc.ups-tlse.fr

It is theoretically possible to produce any linear superposition of quantum states with a well-defined phase and this possibility is widely used in matter wave interferometry. However, the superposition of motional states of free propagating particles with different kinetic energies has rarely been produced and detected, because there is no widely applicable technique to produce such a superposition. We have used the matter-wave analogue of the Kerr effect for light to modulate the phase of the waves propagating in the two arms of an atom interferometer: time-dependent electric fields produce these phase modulations thanks to the polarizability energy shift of the atom ground state. These phase modulations are detected on the interferometer output signal as shown in Figure 1. A sinusoidal electric field with a frequency of 21 Hz is applied and we can observe the first and second harmonics (see Figures 1 and 2)

When we apply two modulations at the same frequency  $\nu$ , we detect a modulation involving up to many harmonics of this frequency when the modulation phase amplitude is large. When we apply modulations at two different frequencies  $\nu_1$  and  $\nu_2$ , the interferometer output signal present beats at the frequency  $\nu_1 - \nu_2$  and at its harmonics, even if  $\nu_1$  and  $\nu_2$  are large with respect to the detector bandwidth and the dispersion of the atom time-of-flight from the modulation region to the detector. All the experimental results are in excellent agreement with theoretical expectations; in particular, the delay between modulation and detection is well explained by the fact that the signal propagates with the atom group velocity. Finally, we have used this technique to transmit signals, either digital or analogic.

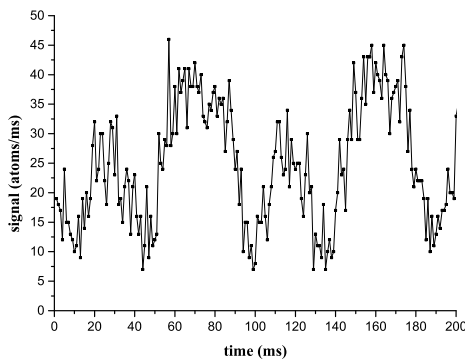


**Figure 1:** Signal of the atom interferometer as a function of time. The count period is 1 ms. We apply a sinusoidal electric field on one interferometer arm, which induces a periodic phase shift. We can clearly distinguish the first and second harmonics.

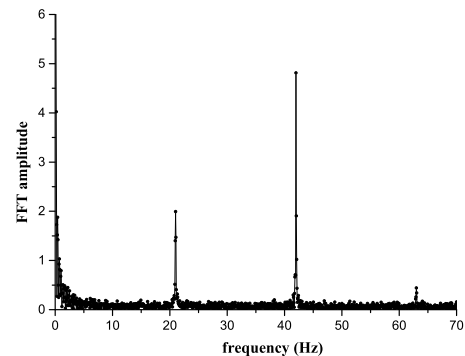


**Figure 2:** FFT amplitude of the interferometric signal. The first and second harmonics are well resolved and a small contribution of the third order can be recognized.

# Atom interferometry measurements of the He-McKellar-Wilkins and the Aharonov-Casher geometric phases

J. Gillot<sup>1</sup>, S. Lepoutre<sup>1</sup>, A. Gauguet<sup>1</sup>, J. Vigué<sup>1</sup>, and M. Büchner<sup>1</sup>

<sup>1</sup>Laboratoire Collisions Agrégats Réactivité-IRSAMC, Université de Toulouse-UPS and CNRS UMR 5589, F-31062, Toulouse, France

Presenting Author: matthias.buchner@irsamc.ups-tlse.fr

We present measurements of the He-McKellar-Wilkins (HMW) and Aharonov-Casher (AC) geometrical phases by atom interferometry. Our atom interferometer working with <sup>7</sup>Li allows the spatial separation between the two interferometer arms of about 100 μm [1]. We apply opposite electric fields, proportional to a voltage V, on the two arms and a homogenous magnetic field, proportional to a current I. We prepare the <sup>7</sup>Li atoms in their  $F = 2$ ,  $m_F = \pm 2$  ground state sublevel by optical pumping. This preparation allows the suppression of stray phases and the measurement of both the HMW and the AC phase shift in one experiment. The HMW phase shift does not depend on the magnetic hyperfine state, while the AC phase shift changes sign with  $m_F$  and we use these different behaviours to separate both phases. We measured these phases for three different atom velocities  $v_m$ , the results are in good agreement with the predicted values and are independent of  $v_m$  [2,3]. This independence is an important characteristic of a geometric phase. Fig. 1 and 2 summarize our results for the HMW and the AC phases, resp.

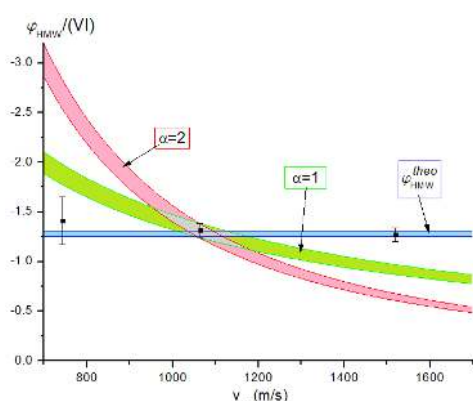


**Figure 1:** Plot of the slope of the HMW phase  $\varphi_{HMW}/(V I)$  (in units of  $10^{-6}$  rad/VA) as a function of the mean atom velocity  $v_m$ . The experimental results are compared to the theoretical value, represented with its error bar by the blue horizontal band. The shaded areas represent what would be the phase if, starting from its value at 1062 m/s, the HMW phase was varying like  $1/v^\alpha$  with  $\alpha = 1$  (green) or  $\alpha = 2$  (pink).

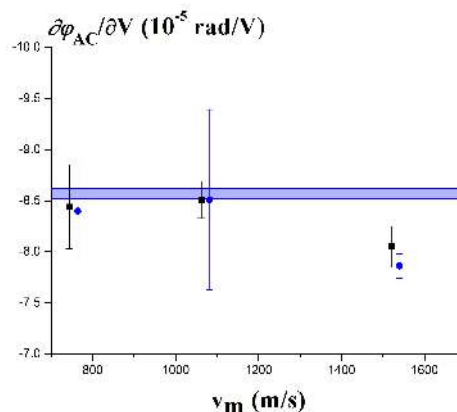


**Figure 2:** Plot of the slope of the AC phase  $\varphi_{AC}/(V)$  as a function of the mean atom velocity  $v_m$ . The experimental results are compared to the theoretical values calculated with the assumption of a perfect optical pumping, represented with its error bar by the blue horizontal band, and to the corrected theoretical ones, taking into account the limited optical pumping efficiency.

## References

- [1] A. Miffre, M. Jacquy, M. Büchner, G. Tréneç, and J. Vigué, Eur. Phys. J. D **33**, 99 (2005)
- [2] J. Gillot, S. Lepoutre, A. Gauguet, M. Büchner and J. Vigué, Phys. Rev. Lett. **111**, 030401 (2013)
- [3] J. Gillot, S. Lepoutre, A. Gauguet, J. Vigué and M. Büchner, submitted to Eur. Phys. J. D, <http://arxiv.org/pdf/1312.3453.pdf>

# Strong correlation between the electron spin orientation and bremsstrahlung linear polarization observed in the relativistic regime

O. Kovtun<sup>1</sup>, S. Tashenov<sup>1</sup>, V. Tioukine<sup>2</sup>, A. Surzhykov<sup>3</sup>, V.A. Yerokhin<sup>3,4</sup>, and B. Cederwall<sup>5</sup>

<sup>1</sup>Physikalisches Institut der Universität Heidelberg, Germany

<sup>2</sup>Institut für Kernphysik Johannes Gutenberg-Universität Mainz, Germany

<sup>3</sup>Helmholtz-Institut Jena, Germany

<sup>4</sup>Center for Advanced Studies, St. Petersburg State Polytechnical University, Russia

<sup>5</sup>Royal Institute of Technology, Stockholm, Sweden

Presenting Author: kovtun@physi.uni-heidelberg.de

Atomic field bremsstrahlung is one of the dominant radiation processes in relativistic collisions of electrons with atoms. It arises due to the decelerated motion of the electron scattered in the Coulomb field of the atomic nucleus. The radiation, emitted in the form of x-rays and gamma-rays, is strongly polarized. Polarization reveals details of the dynamics of the scattering electron. Experiments at the electron energy of 100 keV have shown that the x-ray polarization plane generally does not coincide with the reaction plane when the incoming electrons are spin-polarized. The latter is defined by the incoming electron and the emitted x-ray propagation directions. When the electron spin is confined to the reaction plane, the plane of x-ray polarization tilts with respect to the reaction plane [1,2,3]. These observations point to the effect of the spin-orbit interaction in electron scattering and bremsstrahlung.

The spin-effect, observed in previous experiments, was small, causing a few degrees tilt of the polarization plane. On the other hand, due to the relativistic nature of the spin-orbit interaction, it is expected that this effect should be markedly increased at higher energies [4,5]. We have studied bremsstrahlung produced by polarized electrons with 2 MeV kinetic energy colliding with a thin gold target. Gamma-ray linear polarization was measured with the Compton polarimetry technique applied to a segmented germanium detector, see Fig. 1. The Compton-recoiled electron and the scattered gamma-ray were detected in time-coincidence in separate detector pixels. This allowed sampling of the complete azimuthal angular distribution of the scattered gamma-rays and determination of the polarization angle. Moreover, in the same experiment, we have developed the technique of ambient radiation background suppression based on Compton imaging.

The experiment revealed a dramatically increased polarization correlation – for the electron beams polarised along and opposite to their propagation directions, the measured tilts of the gamma-ray polarization plane were  $49 \pm 6$  and  $125 \pm 6$  deg, respectively. These results are in agreement with the full-order relativistic calculations. They demonstrate a prominent role of the electron spin interactions in the process of bremsstrahlung as well as Coulomb scattering.

## References

- [1] S. Tashenov *et al.* Phys. Rev. Lett. **107**, 173201 (2011)
- [2] R. Maertin *et al.* Phys. Rev. Lett. **108**, 264801 (2012)
- [3] S. Tashenov *et al.* Phys. Rev. A **87**, 022707 (2013)
- [4] H.K. Tseng, R.H. Pratt, Phys. Rev. A **7**, 1502 (1973)
- [5] V.A. Yerokhin, A. Surzhykov, Phys. Rev. A **82**, 062702 (2010)

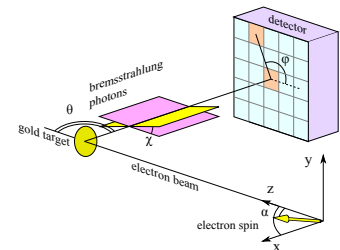


Figure 1: Scheme of the experiment.

# Zeeman effect investigations in $^{142}\text{Nd II}$ using Collinear Ion Beam Laser Spectroscopy

S. Werbowy<sup>1,3</sup>, H. Hühnermann<sup>2,3</sup>, J. Kwela<sup>1</sup>, and L. Windholz<sup>3</sup>

<sup>1</sup>*Institute of Experimental Physics, University of Gdansk, ul. Wita Stwosza 57, 80-952 Gdansk, Poland)*

<sup>2</sup>*Department of Physics, University of Marburg, Renthof 5, 35037 Marburg, Germany*

<sup>3</sup>*Institut für Experimentalphysik, Technische Universität Graz, Petersgasse 16, 8010 Graz, Austria*

Presenting Author: windholz@tugraz.at

High resolution Zeeman spectra of the hyperfine structure of ionic spectral lines of the 142 isotope of neodymium were observed using a Collinear Ion Beam Laser Spectroscopy technique (CLIBS). Nd ions with mass number 142 were selected by means of a separator magnet and accelerated to a kinetic energy of about 19 keV. The ion beam was then overlapped with a counter-propagating laser beam, tuned and stabilized close to the investigated transition including the Doppler shift. In the interaction chamber the ions are additionally accelerated with a scanning voltage in the range 0-3500 V (corresponding to a wave number shift of  $0.75\text{ cm}^{-1}$ ), allowing to perform Doppler tuning instead of changing the frequency of the laser. The technique allows to achieve line widths of ca. 60 MHz and to tune the Zeeman patterns with a step size of 5 MHz.

To produce a strong magnetic field perpendicular to the ion beam inside the interaction chamber, and to avoid vacuum contaminations, we used strong permanent neodymium magnets. The field strength was measured by a Hall-effect Gauss-meter and by the Zeeman effect of the  $^{138}\text{Ba(II)}$  ( $5d\ ^2D_{3/2} - 6p\ ^2P_{3/2}$ ) transition at 585.368 nm, where the Lande-factors  $g$  of the combining levels are known with very high precision. We produced a magnetic field of 330 Gauss perpendicular to the ion beam, uniform through the entire interaction region. Despite the fact that this field is perpendicular to the moving ions, the deflection of the ions having high mass and high kinetic energy is minor, and has no influence on the experiment.

For our investigations, we chose the Nd isotope 142 ( $I = 0$ ) to avoid difficulties in analysis due to hyperfine structure splitting. The analysis of the experimental spectra of 12 Nd II transitions having wavelengths between 568.853 nm and 589.153 nm (in air) allowed us to determine the Lande-factors for 21 energy levels. 8 of them belong to the  $4f^45d$  configuration, 10 to  $4f^46p$  and 3 to  $4f^35d^2$ . Our results are compared with other investigations, in which standard experimental techniques for Zeeman effect measurements were used, having smaller resolution, but applying much higher magnetic field strengths.

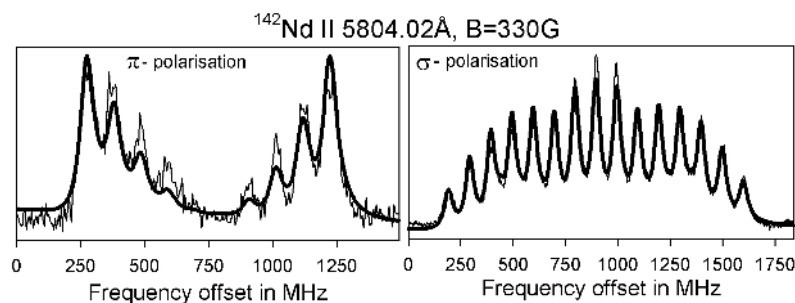


**Figure 1:** Zeeman splitting of the Nd II - line 5804.02 Å  
(transition between levels  $6005.33\text{ cm}^{-1}$  ( $a^6\ K_{9/2}$ ;  $g = 0.559$ ) and  $23230.0\text{ cm}^{-1}$  ( $z^6\ K_{9/2}$ ;  $g = 0.785$ )).

*This work was supported by grants of Wissenschaftlich-Technische Zusammenarbeit Österreich-Polen, no. Pl 21/2012 and Pl 12/2014.*

# New energy levels of the La Atom found by a combination of several spectroscopic techniques

L. Windholz<sup>1</sup>, B. Gamper<sup>1</sup>, T. Binder<sup>1</sup>, and J. Dembczynski<sup>2</sup>

<sup>1</sup>*Institute for Experimental Physics, Graz University of Technology, Petersgasse 16, 8010 Graz, Austria*

<sup>2</sup>*Chair of Quantum Engineering and Metrology, TU Poznan, PL-60-965 Poznan, Poland*

Presenting Author: windholz@tugraz.at

We report on a combination of optogalvanic spectroscopy, laser-induced fluorescence (LIF) spectroscopy, emission spectroscopy using a grating monochromator, and Fourier-transform spectroscopy. The methods were used to search for up to now unknown energy levels of neutral La. As source of free La atoms, we use a hollow cathode lamp, for excitation the radiation of cw dye lasers operating with different dyes [1].

When exciting transitions to high-lying energy levels of the La atom by means of laser light, we noticed that optogalvanic (OG) spectroscopy is very sensitive, and one can observe much more lines than one would expect. For example, between 6808 and 6812 Å there is 1 line listed in the MIT wavelength tables [2], while we could excite 12 lines.

Thus we decided to make a continuous wavelength scan over a wide spectral region, using a cw dye laser, operating with R6G. It was possible to scan the laser from 610 to 560 nm. Altogether, more than 1500 spectral lines were found, most of them showing a nicely resolved hyperfine (hf) structure pattern. For the classification of these lines, we use a computer program 'Elemente' [3], which suggests transitions having the right wave number (within a chosen interval) and which shows expected hf patterns, since the hf constants of all known La levels meanwhile are determined. When no suggestion is given, we assume that a new, up to now unknown level is involved. In such case, we set the laser wavelength to the highest peak of the unclassified pattern and search for laser-induced fluorescence (LIF) lines. Here we have to distinguish between some cases:

(1) We find no fluorescence line. This may be the case if the excited transition is the only one strong line, or if the LIF lines are in the infrared or ultraviolet region outside our detection range. The excited transition stays unclassified.

(2) We find some LIF lines which are in phase with the chopped exciting laser light. This phase gives us the information that the emission of the LIF takes place from the upper level of the transitions. For finding more exactly the fluorescence wavelengths, we perform the following procedure: The laser wavelength is set to optimal excitation (with help of the OG signal). Then the monochromator dispersing the LIF light is scanned and gives a signal when LIF light passes to the photomultiplier. A second chopper in front of the monochromator entrance slit and a second Lock-In amplifier allows to record simultaneously the emission spectrum of the hollow cathode lamp. The recorded spectrum is then compared with a high-resolution Fourier-transform spectrum. In this way we can determine LIF wavelengths with an uncertainty of less than 0.1 Å, despite of the fact that the resolution of the monochromator is 0.5 Å and the reading of the monochromator scale is accurate to only  $\pm 2$  Å. Using all available information (excitation and LIF wavelengths, estimated J values and hf constants from a simulation of the observed hf pattern) it is in most cases possible to find the data of the new level involved in the transition.

(3) We find some LIF lines which have opposite phase compared to the chopped exciting laser light. Such lines are observed when the lower level of the laser excitation serves as the upper level of a strong transition to a very low-lying La level. The energy of the new level can be found by adding the transition wave number to the energy of the level marked by this LIF line.

(4) Sometimes we find a huge number of LIF lines (e.g. when exciting 6520.64 Å, more than 200 LIF-lines). In such cases we have to assume that the upper levels of the observed LIF transitions are populated by collisional energy transfer. Then it may be very difficult to find out where the new level is located.

The experiments are performed to have reliable data for a semi-empirical description of the wave functions of La levels.

## References

- [1] I. Siddiqui, S. Khan, B. Gamper, J. Dembczynski and L. Windholz, J. Phys. B 46, 065002 (2013)
- [2] Wavelength Tables, edited by G.R. Harrison (The M.I.T. Press, 1969)
- [3] L. Windholz and G. H. Guthöhrlein, Physica Scripta T105, 55 (2003)

# New Energy Levels of the Pr Atom found by Analyzing a Fourier Transform Spectrum

Z. Uddin<sup>1,2</sup>, L. Windholz<sup>1</sup>, G.H. Guthöhrlein<sup>1,3</sup>, S. Zehra<sup>2</sup>, and S. Jilani<sup>2</sup>

<sup>1</sup>*Institute for Experimental Physics, Graz University of Technology, Petersgasse 16, 8010 Graz, Austria*

<sup>2</sup>*Department of Physics, University of Karachi, Pakistan*

<sup>3</sup>*Universität der Bundeswehr Hamburg, Hamburg, Germany*

Presenting Author: windholz@tugraz.at

Using a high-resolution Fourier transform spectrum [1], prominent but up to now not classified spectral lines in the near infrared spectral region, which showed sufficiently resolved hyperfine (hf) patterns, were studied. If the hf pattern of the line under investigation could be simulated reliably, we got from the hf structure the total angular momenta and the hyperfine constants A of the involved levels (the quadrupole hyperfine constant B can be assumed to be zero). Searching now in our database of Pr levels for levels having proper J and A, we could identify one of the combining levels. The energy of the other one can then be calculated using the center of gravity (cg) wave number of the line. A newly found level must explain with high accuracy other spectral lines with respect to their cg wavelength and to the hyperfine pattern. Sometimes also energies and A-values of known levels were corrected (e.g. level  $21424.11 \text{ cm}^{-1}$ ,  $J=7/2$ ,  $A=435 \text{ MHz}$ , as given in ref. [2], was changed to  $21424.059 \text{ cm}^{-1}$ ,  $J=7/2$ ,  $A=502(3) \text{ MHz}$ ). Some of the newly found levels are listed in Table 1, together with the explained lines.

| new odd level |                             |         | explained line              |           |         | lower even level |                             |           |         |
|---------------|-----------------------------|---------|-----------------------------|-----------|---------|------------------|-----------------------------|-----------|---------|
| J             | energy ( $\text{cm}^{-1}$ ) | A (MHz) | wavelength ( $\text{\AA}$ ) | C         | Int     | J                | energy ( $\text{cm}^{-1}$ ) | A (MHz)   | B (MHz) |
| 9/2           | 21438.488                   | 1040(5) | 6789.618                    | nl        | 6       | 11/2             | 6714.184                    | 474.692   | -29.633 |
|               |                             |         | 7813.607                    |           | 12      | 9/2              | 8643.824                    | 797(2)    | -       |
|               |                             |         | 7928.395                    | nl        | 8       | 11/2             | 8829.063                    | 769(1)    | -30(20) |
|               |                             |         | 8214.829                    | nl        | 15      | 11/2             | 9268.726                    | 977(1)    | -24(20) |
|               |                             |         | 8498.565                    | nl        | 3       | 11/2             | 9675.029                    | 683(1)    | -       |
|               |                             |         | 9433.968                    | nl        | 5       | 11/2             | 10841.407                   | 530(3)    | -       |
|               |                             |         | 9490.053                    | nl        | 5       | 11/2             | 10904.034                   | 301(1)    | -20(10) |
|               |                             |         | 9749.525                    |           | 11      | 9/2              | 11184.396                   | 692(1)    | 15(30)  |
|               |                             |         | 9835.661                    | nl        | 18      | 7/2              | 11274.229                   | 1286(1)   | -10(20) |
|               |                             |         | 11/2                        | 22077.806 | 1038(4) | 5665.569         |                             | 70        | 9/2     |
| 6919.618      |                             | 14      |                             |           |         | 13/2             | 7630.132                    | 776.286   | -43.592 |
| 7925.918      |                             | 11      |                             |           |         | 13/2             | 9464.440                    | 1056(1)   | -15(10) |
| 5/2           | 24500.390                   | 760(10) | 5539.063                    | nl        | 41      | 5/2              | 6451.808                    | 1189.6(6) | -5(5)   |
|               |                             |         | 6855.784                    | nl        | 7       | 7/2              | 9918.190                    | 1057.4(5) | 22(6)   |
|               |                             |         | 7777.498                    | nl        | 4       | 5/2              | 11646.312                   | 1317(10)  | -       |
|               |                             |         | 8413.293                    | nl        | 4       | 7/2              | 12617.700                   | 883(2)    | -       |
|               |                             |         | 8790.599                    |           | 5       | 5/2              | 13127.722                   | 156(1)    | 0(10)   |
|               |                             |         | 9711.652                    | nl        | 7       | 3/2              | 14206.294                   | 184(2)    | -       |
|               |                             |         | 9816.012                    |           | 9       | 5/2              | 14315.745                   | 1063(2)   | -       |

**Table 1:** New levels and classified lines. C comment: nl means the line is not contained in commonly used wavelengths tables, e.g ref. [3].

## References

- [1] B.Gamper, Z.Uddin, M.Jahangir, *et al.* J. Phys. B: At. Mol. Opt. Phys. **44** (2011) 045003 (7pp)
- [2] A.Ginibre, PhD Thesis Université de Paris-sud (1988)
- [3] Wavelength Tables, edited by G.R. Harrison (The M.I.T. Press, 1969)

# Investigation of Fourier Transform Spectrum of Niobium in Argon Discharge in the near-infrared

A. Er<sup>1</sup>, Gö. Başar<sup>1</sup>, I.K. Öztürk<sup>1</sup>, F. Güzelçimen<sup>1</sup>, M. Tamanis<sup>2</sup>, R. Ferber<sup>2</sup>, and S. Kröger<sup>3</sup>

<sup>1</sup>*Faculty of Science, Physics Department, Istanbul University, Tr-34134 Vezneciler, Istanbul, Turkey*

<sup>2</sup>*Laser Centre, The University of Latvia, Rainis Boulevard 19, LV-1586 Riga, Latvia*

<sup>3</sup>*Hochschule für Technik und Wirtschaft Berlin, Wilhelminenhofstr. 75A, D-12459 Berlin, Germany*

Presenting Author: alever@istanbul.edu.tr

The aim of present work is to classify the spectral niobium lines in the near-infrared region by means of hyperfine structure. The most extensive wavelength lists for niobium [1] are limited to wavelengths below 1 090 nm for Nb I and 700 nm Nb II. In the NIST Atomic Spectra Database [2] only wavelengths below 890 nm are listed. The present work extends the wavelength range to the near infrared up to 1 700 nm.

Nb with the atomic number 41 has only one stable isotope, <sup>93</sup>Nb, which is characterized by a nuclear spin quantum number of  $I=9/2$  [3]. In the present work, Nb spectrum produced in hollow cathode discharge lamp has been recorded in the wavelength range from 833 nm to 1 700 nm (from 5 900 cm<sup>-1</sup> to 12 000 cm<sup>-1</sup>) using a high resolution Fourier transform spectrometer (Bruker IFS 125HR) at the Laser Centre of the University of Latvia. The hollow-cathode discharge was running in an argon atmosphere. Both Niobium and Argon lines were observed in the spectrum.

In total 829 spectral lines were detected. Using the Classification Programme [4], which contains a list of levels from [1, 5-11], 103 lines could be classified as Nb I transitions and only one line as Nb II transition. 43 of these Nb I transitions and the Nb II transition were classified for the first time; 36 of the classified Nb I transitions and the Nb II transition have not been listed in the literature before. Furthermore 347 lines are assigned as Ar I lines and 234 as Ar II lines, of which 41 and 20, respectively, were assigned for the first time. Remaining 144 spectral lines could not be classified, 10 of which could be assigned as Nb lines, because of their hyperfine pattern. Seven of unclassified lines have been observed also in the La-Ar-spectrum in [12] and therefore are very possibly Ar lines.

## Acknowledgements:

MT and RF acknowledge support from the Latvian Science Council grant Nr 119/2012.

## References

- [1] C. I. Humphreys, W. F. Meggers, *J. Res. Natl Bur. Stand.* **34**, 478 (1945)
- [2] NIST Atomic Spectra Database, Version 5: <http://www.nist.gov/pml/data/asd.cfm>
- [3] C.M. Lederer and V.S. Shirley, *Tables of Isotopes* (7th edn, New York:Wiley, 1978)
- [4] L. Windholz, G. H. Guthöhrlein, *Phy. Scripta* **T105**, 55 (2003)
- [5] S. Kröger, A. Bouzed, *Eur. Phys. J. D* **23**, 63 (2003)
- [6] S. Kröger, O. Scharf, G.H. Guthöhrlein, *Europhys. Lett.*, **66**, 344 (2004)
- [7] S. Kröger *et al.*, *Eur. Phys. J. D* **41**, 61 (2007)
- [8] I.K. Öztürk, G. Başar *et al.*, in preparation (2014)
- [9] L. Minnhagen, *Ark. Fys.* **25**, 203 (1963)
- [10] P. Palmeri, E. Biémont, *Phys. Scr.* **51**, 76 (1995)
- [11] E. B. Saloman, 2010, *J. Chem. Ref. Data* **39**, 033101 (2010)
- [12] F. Güzelçimen, G. Başar *et al.*, *Astrophys. J. Suppl. Series* **208**, 18 (2013)

## Investigation of the hyperfine structure of atomic vanadium for energetically high-lying levels up to 45 000 cm<sup>-1</sup>

F. Güzelçimen<sup>1</sup>, N. Al-Labady<sup>1</sup>, Gö. Başar<sup>1</sup>, I.K. Öztürk<sup>1</sup>, A. Er<sup>1</sup>, S. Kröger<sup>2</sup>, M. Tamanis<sup>3</sup>, and R. Ferber<sup>3</sup>

<sup>1</sup>Faculty of Science, Physics Department, Istanbul University, Tr-34134 Vezneciler, Istanbul, Turkey

<sup>2</sup>Hochschule für Technik und Wirtschaft Berlin, Wilhelmshofstr. 75A, D-12459 Berlin, Germany

<sup>3</sup>Laser Centre, The University of Latvia, Rainis Boulevard 19, LV-1586 Riga, Latvia

Presenting Author: feyzag@istanbul.edu.tr

The focus of present work is to extend the data of magnetic dipole hyperfine structure constant  $A$  for energy levels of atomic vanadium up to 45 000 cm<sup>-1</sup> of atomic vanadium. Using the Fourier Transform spectrometer (Bruker IFS 125HR), which is located at the Laser Centre of the University of Latvia, spectra of vanadium-argon plasma were recorded in the spectral range from 12 000 cm<sup>-1</sup> to 30 000 cm<sup>-1</sup> with resolution of 0.03 cm<sup>-1</sup>. The vanadium plasma was produced in a hollow cathode discharge. The hollow cathode lamp was cooled by liquid nitrogen in order to reduce the Doppler broadening.

For the purpose of the present study, transitions have been chosen, between such energy levels, for which the constant  $A$  of one of them was unknown. The hyperfine structure of 60 atomic vanadium lines lying in the spectral range from 14 000 cm<sup>-1</sup> to 28 000 cm<sup>-1</sup> (360 nm to 706 nm) were analysed. The classification and the wavelength of the center of gravity of the investigated lines were taken from [1]. The computer program Fitter [2] was used to determine the magnetic dipole hyperfine structure constant  $A$  by fitting the hyperfine structure of spectral lines with a Voigt profile function. For each line, the  $A$  constant for one of the two involved levels was well-known from literature [3-9] and was fixed during the fit.

We could newly determine the magnetic dipole hyperfine structure constant  $A$  for 18 energy levels of even parity belonging to the configurations  $3d^34s^2$ ,  $3d^44s$ ,  $3d^44d$ ,  $3d^34s4d$  and  $3d^34s5s$ , as well as for 37 energy levels of odd parity belonging to the configurations  $3d^44p$  and  $3d^34s4p$ . With our new results, the hyperfine structure constants for all experimentally known energy levels of both parities up to 45 000 cm<sup>-1</sup> are now available for atomic vanadium.

### Acknowledgements:

GB acknowledges support from the Istanbul University Scientific Research Project with project No. BYP 3537. MT and RF acknowledge support from the Latvian State Programme grant Nr 2014.10-4/VPP-2/5.

### References

- [1] A.P. Thorne, J.C. Pickering, J. Semeniuk, *Astrophys. J. Suppl.* 192:11 1 (2011)
- [2] G. H. Guthöhrlein, University of Bundeswehr Hamburg, unpublished (2004)
- [3] U. Johann, J. Dembczynski, W. Ertmer, *Z. Phys.* A303 7 (1981)
- [4] P. Unkel *et al.*, *Z. Phys.*, 11 259 (1989)
- [5] H. El-Kashef, N. Ludwig, *Phys. Scr. B*, 179 103 (1992)
- [6] P. Palmeri *et al.*, *J. Phys.B: At. Mol. Opt. Phys.* 28 3741 (1995)
- [7] P. Palmeri *et al.*, *Phys. Scr.* 55 586 (1997)
- [8] P. H. Lefebvre, H.P. Garnir, E. Biemont, *Phys. Scr.* 66 363 (2002)
- [9] F. Güzelçimen *et al.*, *Astrophys. J. Suppl. Series*, accepted. (2014)

## Theoretical oscillator strengths for the Sc I

I.K. Öztürk<sup>1</sup>, B. Atalay<sup>2</sup>, G. Çelik<sup>3</sup>, F. Güzelçimen<sup>1</sup>, A. Er<sup>1</sup>, Gö. Başar<sup>1</sup>, and S. Kröger<sup>4</sup>

<sup>1</sup>Faculty of Science, Physics Department, Istanbul University, Tr-34134 Vezneciler, Istanbul, Turkey

<sup>2</sup>Canakkale Onsekiz Mart University, Faculty of Arts and Sciences, Department of Physics, 17100 Canakkale, Turkey

<sup>3</sup>Selçuk University, Faculty of Science, Department of Physics, Campus 42075 Konya, Turkey

<sup>4</sup>Hochschule für Technik und Wirtschaft Berlin, Wilhelminenhofstr. 75A, D-12459 Berlin, Germany

Presenting Author: [ikanat@istanbul.edu.tr](mailto:ikanat@istanbul.edu.tr)

The atomic transition probabilities and also oscillator strengths are very important fundamental parameters in the fields of atomic spectroscopy, astronomy. In particular, accurate oscillator strengths are necessary for the determination of the elemental abundances in stars. Scandium (Sc) is apparently a much more abundant element in the sun and certain stars than on earth. It is one of the elements with only one stable isotope. This isotope has the mass number 45 and nuclear spin  $I = 7/2$  [1].

The electric dipole transition probabilities and the oscillator strengths of neutral Scandium have been calculated using the Cowan code [2] and the quantum defect orbital (QDO) theory [3] for the wavelength region from 400 nm to 580 nm. The transition probability and the oscillator strength results obtained in this work are mostly in agreement with the data obtained from different theoretical methods given in the literature [4, 5, 6]. In this study, 24 transition probabilities have been given for the first time.

### References

- [1] W. H. Parkinson, E. M. Reeves, F. S. Tomkins, Proc. R. Soc. London Ser. A **351**, 569 (1976)
- [2] R. D. Cowan, *The Theory of Atomic Structure and Spectra* (University of California Press, Berkeley, 1981)
- [3] G. Simons, J. Chem. Phys. **60**, 645 (1974)
- [4] C. H. Corliss, W R Bozman, *Experimental Transition Probabilities for Spectral Lines of Seventy Elements*, (U.S.N.B.S. Monograph 53, U.S. Govt Printing Office, Washington, DC 1962)
- [5] W.L. Wiese, J.R. Fuhr, J. Phys. Chem. Ref. Data **4**, 263 (1975)
- [6] J. E. Lawler, J. T. Dakin, J. Opt. Soc. Am. B, **6**, 1457 (1989)

## Behaviour of atomic transitions of Rb $D_2$ line in strong magnetic fields

A. Tonoyan<sup>1,2</sup>, A. Sargsyan<sup>1</sup>, H. Hakhumyan<sup>1</sup>, Y. Pashayan-Leroy<sup>2</sup>, C. Leroy<sup>2</sup>, and D. Sarkisyan<sup>1</sup>

<sup>1</sup>*Institute for Physical Research, NAS of Armenia, Ashtarak, 0203, Armenia*

<sup>2</sup>*Laboratoire Interdisciplinaire Carnot de Bourgogne, UMR CNRS 6303, Université de Bourgogne, 21078 Dijon Cedex, France*

Presenting Author: aratonoyan@gmail.com

It is well known that the energy levels of atoms in external magnetic fields undergo splitting into a large number of a Zeeman sublevels which are strongly frequency shifted. Simultaneously, external magnetic fields cause changes in atomic transition probabilities. There is a huge number of applications of magneto-optical processes in atomic vapor of alkali metals [1, 2]. An efficient “ $\lambda/2$ -method” (is the resonant wavelength of laser radiation) based on nanometric-thin cell filled with Rb is implemented to study the splitting of hyperfine transitions of  $^{85}\text{Rb}$  and  $^{87}\text{Rb}$   $D_2$  line in an external magnetic field in the range of  $B = 3 \text{ kG} - 7 \text{ kG}$ . It is experimentally demonstrated that from 38 (22) Zeeman transitions allowed at low  $B$ -field in  $^{85}\text{Rb}$  ( $^{87}\text{Rb}$ ) spectra in the case of  $\sigma^+$  polarized laser radiation, only 12 (8) remain at  $B > 5 \text{ kG}$ , caused by decoupling of the total electronic momentum  $J$  and the nuclear spin momentum  $I$  (hyperfine Paschen-Back (HPB) regime) (Fig. 1a). In particular, the  $\lambda/2$ -method has allowed us to resolve 20 atomic transitions (which are regrouped in two separate groups of 10 atomic transitions each) and to determine their frequency positions, fixed (within each group) frequency slopes, as well as the probability characteristics of the transitions (Fig. 1b). The experiment agrees well with the theory. Possible applications are described.

**Figure 1:** a) Diagram of  $^{85}\text{Rb}$  (left side) ( $I = 5/2$ ), and  $^{87}\text{Rb}$  (right side) ( $I = 3/2$ )  $D_2$  line transitions for  $\sigma^+$  laser excitation in HPB regime. The selection rules:  $\Delta m_J = +1$ ;  $\Delta m_I = 0$ . For  $^{85}\text{Rb}$  there are 12 transitions marked by the respective numbers 3 – 6, 8, 9, 12, 13, 15, 16, 17 and 19; for  $^{87}\text{Rb}$  there are 8 transitions marked by the respective numbers 1, 2, 7, 10, 11, 14, 18, and 20. b) Frequency positions of the Rb  $D_2$  line atomic transitions 1 – 20 versus the magnetic field. Solid lines are the calculated curves and black squares are the experimental results (with an error of 3%). At  $B > 4.5 \text{ kG}$  the transitions are regrouped to form two groups of ten transitions each.

### References

- [1] D. Budker, W. Gawlik, D. F. Kimball *et al.* Rev. Mod. Phys. **74**, 1153 (2002).
- [2] A. Sargsyan, G. Hakhumyan, C. Leroy *et al.* Opt. Lett. **37**, 1379–1381 (2012).

## Localization of Atomic Populations due to Field of Running Waves

E. Efremova<sup>1</sup>, M. Gordeev<sup>2</sup>, and Yu. Rozhdestvensky<sup>2</sup>

<sup>1</sup>*Saint-Petersburg State University, department of Physics, Ulanovskaya st 3, Staryi Peterhoff, Saint-Petersburg, Russia 198504*

<sup>2</sup>*Saint-Petersburg National Research University of Information Technologies, Mechanics and Optics, department of Laser optics, Kronversky prospect 49A, Saint-Petersburg, Russia, 197101*

Presenting Author: mxmgordeev@gmail.com

This work is devoted to investigation of the one aspect of the fundamental problem of an interaction laser radiation with the matter. This problem is spatial localization of atomic populations due to fields of few running waves.

We first propose in our work two - dimensional spatial localization of atomic population in medium with tripod - like configuration of levels under influence of the field only of running waves. Three running waves propagate in one plane with angles equals  $120^\circ$  to each other and form the system of a standing waves in this plane. In the field of thus standing waves one can localize atomic populations. Moreover, the degree of such a localization may achieve a hundreds of the wavelength of the incident radiation.

We demonstrated that an excitation of the central transition of the tripod-like system using a field of multidirectional linearly polarized running waves is the necessary condition of the population dependence from spatial coordinates in the XY - plane. The two - dimensional shapes that appear in this system can have very complicated structure such as "double - craters". Besides, we have demonstrated the possibility to obtain the phenomenon of coherent population trapping (CPT) that shows a good conformity of our method and numerical calculations with existing theory.

### References

- [1] S. Qamar, S.-Y. Zhu, M.S. Zubairy Phys. Rev. A **61**, 063806 (2000)
- [2] G.S. Agarwal and K.T. Kapale J. Phys. B: At. Mol. Opt. Phys. **39**, 3437–3446 (2006)
- [3] J. Xu and X. Hu J. Phys. B: At. Mol. Opt. Phys. **40**, 1451–1459 (2007)
- [4] V. Ivanov and Yu. Rozhdestvensky Phys. Rev. A **81**, 033809 (2010)

## Probing near field thermal emission with atoms

A. Laliotis<sup>1</sup>, T. Passerat de Silans<sup>2,1</sup>, I. Maurin<sup>1</sup>, M. Ducloy<sup>1</sup>, and D. Bloch<sup>1</sup>

<sup>1</sup>Laboratoire de Physique des Lasers, UMR 7538 du CNRS et de l'Université Paris 13, 99 Av. J.B. Clément, 93430 Villetaneuse, France

<sup>2</sup>Laboratório de Superfície, DF-CCEN, Cx. Postal 5086 Universidade Federal de Paraíba, 58051-900 João Pessoa, Paraíba, Brazil

Presenting Author: athanasios.laliotis@univ-paris13.fr

In the electrostatic or van der Waals (vdW) regime, the Casimir-Polder interaction is usually described as the classical interaction between a fluctuating dipole and its image. This shifts the atomic energy levels by  $-C_3/z^3$ ,  $C_3$  being the vdW coefficient and  $z$  the atom-surface distance. The above picture fails to account for thermal effects. Contrary to the far field regime [1], near field thermal effects are intricately linked to the dielectric properties of the surface. Dielectrics support evanescent surface modes whose density peaks around the surface polariton resonance frequency. As a result the thermal excitation of the surface modes creates intense nearly monochromatic electromagnetic fields [2] that evanescently decay away from the surface of the dielectric.

Here we show that excited state atoms are sensitive to the near field emission of hot surfaces. By means of selective reflection spectroscopy we probe  $Cs(7D_{3/2})$  atoms next to a sapphire surface ( $\approx 100nm$ ) and measure the  $C_3$  (vdW) coefficient of the atom-surface interaction [3]. Using a high temperature all sapphire vapour cell, we explore temperatures ranging from 500K to 1000K. The evanescent thermal fields at the sapphire surface resonance at  $12.1\mu m$  couple with the  $7D_{3/2} \rightarrow 5F_{5/2}$  virtual atomic transition at  $10.8\mu m$ . As a consequence the surface induced red shift of the  $7D_{3/2}$  level is increased by a factor of 2. Our findings are summarised in Fig.1 which shows the measured temperature dependence of the  $C_3$  coefficient (red dots) as a function of temperature along with the theoretical predictions (dashed line). A very good agreement between theory and experiment is observed.

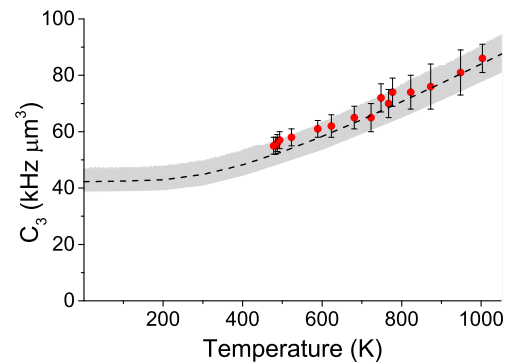


**Figure 1:** The temperature dependence of the  $C_3$  coefficient. The grey shaded area represents the uncertainty on the theoretical predictions.

The influence of temperature reveals the QED nature of the van der Waals interaction and may provide a way to control forces between neutral atoms and surfaces including their complete cancellation or change of sign. This could have important implications on fundamental measurements or technological applications, such as atom trapping close to nanofibers [4] or atom chips. This work was partly supported by Capes-Cofecub Ph 740/12

### References

- [1] J.M. Obrecht, R.J. Wild, M. Antezza *et al.* Phys. Rev. Lett **98**, 063201 (2007)
- [2] A. V. Shechegrov, K. Joulain, R. Carminati *et al.* Phys. Rev. Lett **85**, 1548-1551 (2010)
- [3] A. Laliotis T. Passerat de Silans, I. Maurin *et al.* arXiv:1403.3898 (2014)
- [4] E. Vetsch, D. Reitz, G. Sagué *et al.* Phys. Rev. Lett **104**, 203603 (2010)

# Electron–impact study of O<sub>2</sub> molecule: *R*-matrix method

J. Singh<sup>1</sup> and K.L. Baluja<sup>2</sup>

<sup>1</sup>*Keshav Mahavidyalaya, University of Delhi, Pitam pura, Delhi-110034, India.*

<sup>2</sup>*Department of Physics and Astrophysics, University of Delhi, Delhi-110007, India.*

Presenting Author: rajvanshi\_jasmeet@yahoo.co.in

Molecular oxygen plays a fundamental role in the physics and chemistry of earth's atmosphere [1]. A detailed information about collisions between low-energy electrons and oxygen molecules is required in studies of the physics of planetary atmosphere, gaseous discharges, and both astrophysical and laboratory plasmas [2]. It is the electronic transition from the  $X^3\Sigma_g^-$  state of oxygen to the  $a^1\Delta_g$  and  $b^1\Sigma_g^+$  states which give rise to the infrared and red bands in the atmospheric spectrum. The long life time of the metastable state ( $a^1\Delta_g$ ) of oxygen, which make scattering from an excited molecular target state possible [3].

We have computed elastic differential, momentum-transfer, excitation, and ionization cross sections for electron-impact on O<sub>2</sub> molecule, which are computed using the *R*-matrix method [4–5]. The results of the static exchange, correlated one-state, 22-state close-coupling approximation are presented. We have detected a stable anionic bound state  $^2\Pi_g$  of O<sub>2</sub><sup>−</sup>, with a vertical electron affinity value of 0.389 eV for O<sub>2</sub> which is in good agreement, with theoretical value 0.390 eV [6], and experimental value of  $0.451 \pm 0.007$  eV [7]. We detected two shape resonances of  $^2\Pi_u$  symmetry in the excitation cross sections of the  $^1\Delta_g$  and  $^1\Sigma_g^+$  excited states and compared our results with [8]. The dissociative nature of these resonances is explored by performing scattering calculations in which O-O bond is stretched. The variation of position and width of these resonances as a function of internuclear distance is in good agreement with previous results of [9]. These resonances support dissociative attachment yielding O, O<sup>−</sup> in dissociation of O<sub>2</sub>. We have reasonable agreement with the previous calculations [2] for vertical excitation energies. The ionization cross sections are calculated in the binary-encounter Bethe model and compared with previous results [10]. The results of DCSs, at 3, 5, 7 and 9 eV, are comparable to the results of [11]. We have included up to *g*-partial wave ( $l = 4$ ) in the scattering calculations. The Born-correction for dipole-allowed transition ( $X^3\Sigma_g^-$  to  $B^3\Sigma_u^-$ ) [12] has been carried out to account for the contribution of partial waves higher than *g* wave ( $l = 4$ ). The scattering length of O<sub>2</sub> molecule is calculated which is  $1.989 a_0$ .

## References

- [1] T. G. Slanger *Science* **265**, 1817 (1994)
- [2] A. G. Middleton *et al.* *J. Phys. B* **27**, 4057 (1994)
- [3] M. A. Khakoo *et al.* *J. Phys. B: At. Mol. Phys.* **16**, L317 (1983)
- [4] J. Tennyson, *Phys. Rep.* **491**, 29 (2010)
- [5] P. G. Burke, *R-Matrix Theory of Atomic Collisions: Application to Atomic, Molecular and Optical Processes*, (Springer, 2011)
- [6] R. Gonzalez-Luque *et al.* *Chem. Phys. Lett.* **204**, 323 (1993)
- [7] M. J. Travers, D. C. Cowless, G. B. Ellison *Chem. Phys. Lett.* **164**, 449 (1989)
- [8] C. J. Noble, P. G. Burke *Phys. Rev. Lett.* **68**, 2011 (1992)
- [9] K. Higgins, C. J. Noble, P. G. Burke *J. Phys. B: At. Mol. Opt. Phys.* **27**, 3203 (1994)
- [10] K. N. Joshipura, B. K. Antony, M. Vinodkumar *J. Phys. B: At. Mol. Opt. Phys.* **35**, 4211 (2002)
- [11] L. E. Machado *et al.* *Phys. Rev. A* **60**, 1199 (1999)
- [12] G. Herzberg, *Spectra of Diatomic Molecules*, vol I (Princeton, NJ: Van Nostrand, 1950) 2nd ed

## Vanishing the delay of a light pulse induced by propagation in matter

F. Tommasi<sup>1</sup>, E. Ignesti<sup>1</sup>, L. Fini<sup>1,2</sup>, and S. Cavalieri<sup>1,2</sup>

<sup>1</sup>*Dipartimento di Fisica e Astronomia, Università di Firenze, Via Giovanni Sansone 1 I-50019 Sesto Fiorentino, Italy*

<sup>2</sup>*European Laboratory for Non-Linear Spectroscopy (LENs), Università di Firenze, Via Nello Carrara 1, I-50019 Sesto Fiorentino, Italy*

Presenting Author: cavalieri@fi.infn.it

Any transmission line of some extent presents two key steps: propagation in a slow media (respect to the vacuum) with reduction of the signal amplitude and a further propagation in an amplifying media. The aim is to recover the delay induced by propagation in matter.

Our idea is to combine, in a proof of principle experiment, the delay induced in a slow light propagation with a subsequent “superluminal” propagation in an amplifying medium. In addition we show that this possibility can be optically controlled [1].

In recent years, research in controlling propagation dynamics of optical pulses has been able to achieving extremely low group velocities (“slow-light”- regime) [2] or superluminal group velocities (“fast-light”-regime) [3]. In the fast-light case, the pulse peak is in advance in propagation respect to vacuum-case, in a way consistently with special relativity and causality [4]. We showed theoretically [5] and experimentally [6,7] that is possible to achieve an incoherent optical control of propagation dynamics of an optical pulse both in slow-light case and in fast-light case for a pulse of 3 ns of time duration.

The experimental set-up consists in two cells filled with hot sodium vapor at low pressure and two control pulses, resonant with different atomic transitions, in order to produce a passive medium in the first cell and an active medium in the second one. In a subsequent time, a probe pulse, with central wavelength tuned near resonance with an atomic transition, experiments an extra-delay in the first cell, because of normal dispersion properties probed in the passive medium, and an advance in the second one, because of anomalous dispersion zone in the active medium.

Results showed that the second fast-light stage can be controlled by the control pulse to not only completely recover the previously induced delay in the first slow light stage, but also produces an advance, respect vacuum propagation, equals to the case of the first stage switched off.

In this way the previous history of the pulse propagation can be canceled in a timescale of 1.0 ns.

Our experiment may also lead to interesting scenarios in optical signal transmission, with adding to the necessary amplification stage an optical control upon the recover of the propagation delay.

### References

- [1] R. W. Boyd, D. J. Gauthier *Science* **326** 1074 (2009)
- [2] Y. Okawachi *et al. Phys. Rev. Lett.* **94** 153902 (2005)
- [3] L.J.Wang, A. Kuzmich, A. Dogariu *Nature* **406** 277–279 (2000)
- [4] Brillouin L. *Wave Propagation and Group Velocity* (Academic, New York, 1960)
- [5] M. V. Tognetti *et al. Phys. Rev. A* **81** 023812 (2006)
- [6] E. Ignesti *et al. Phys. Rev. A* **86** 063818 (2012)
- [7] E. Ignesti *et al. Phys. Rev. A* **87** 033828 (2013)

## Line intensities and pressure broadening coefficients in the $\nu_1$ band of N<sub>2</sub>O molecule using IR spectroscopy : N<sub>2</sub>, O<sub>2</sub> and Ar bath gas effect

Et. Es-sebbar<sup>1,2</sup>, M. Deli<sup>1</sup>, and A. Farooq<sup>1</sup>

<sup>1</sup>*Chemical Kinetics Laser Sensors Laboratory, Clean Combustion Research Center, Division of Physical Sciences and Engineering , King Abdullah University of Science and Technology ( KAUST), Thuwal 23955- 6900, Saudi Arabia*

Presenting Author: Ettouhami.Essebbar@kaust.edu.sa

Nitrous oxide molecule (N<sub>2</sub>O), considered a potent greenhouse gas, is an important trace atmospheric constituent with high abundance. In higher altitudes, N<sub>2</sub>O plays a crucial role in the chemistry of troposphere and stratosphere involving ultraviolet solar photon absorption. Accurate knowledge of the spectroscopic parameters of N<sub>2</sub>O including line intensities, foreign– broadening coefficients is needed for monitoring its abundance in Earth’s atmosphere. The current study deals with precise measurements of absolute intensities and collisional broadening coefficients in the  $\nu_1$  band of N<sub>2</sub>O molecule in the presence of N<sub>2</sub>, O<sub>2</sub> and Ar as foreign gases. Moreover, collisional broadening coefficients of air may also be derived from the N<sub>2</sub>– and O<sub>2</sub>–broadening contributions by considering an ideal atmospheric composition. Studies are performed at room temperature for ten rotational transitions accessible to our laser system near 4.5  $\mu m$  (i.e. 2186 – 2202 cm<sup>-1</sup> spectral range) using infrared absorption spectroscopy. To retrieve the spectroscopic parameters for each individual transition, the measured absorption line shape was simulated using Voigt and Galatry profiles. The obtained results were compared with previous experimental data available in the literature. Our data agree well with existing values, the discrepancies being less than 5 % for most of the probed transitions. The spectroscopic data are very useful for the design of diagnostic sensor used to monitor the abundance of N<sub>2</sub>O in the atmosphere.

# Precision measurement of muonium hyperfine splitting at J-PARC

S. Kanda<sup>1</sup>

the J-PARC MuHFS Collaboration

<sup>1</sup>Department of Physics, University of Tokyo, 7-3-1 Hongo, Bunkyo-ku, Tokyo 113-0033, Japan

Presenting Author: kanda@post.kek.jp

Muonium is the bound state of a positive muon and an electron. In the standard model of particle physics, muonium is considered as the two-body system of structureless leptons. At J-PARC (Japan Proton Accelerator Research Complex), we are going to perform a precision measurement of muonium’s ground state hyperfine splitting (MuHFS). MuHFS is the most precise probe for test of the bound state QED and determination of the ratio of muon’s magnetic moment to proton’s one. The experimental methodology is microwave spectroscopy of muonium. Figure 1 shows the conceptual overview of the experiment. Spectroscopy of the energy states can be performed by measurement of positron asymmetry from muonium decay. Precision of the latest experimental result [1] was mostly statistically limited (more than 90% of total uncertainty). Hence, higher statistics is essential to the higher precision of measurement. Our goal is more than 10 times accuracy with 200 times of statistics relative to the latest experiment. For improvement of precision, we use the J-PARC’s highest intensity pulsed muon beam [2] and highly segmented positron detector with SiPM (Silicon PhotoMultiplier) [3]. For further improvement, we reduce systematic uncertainty by using a longer cavity, a high precision superconducting magnet, and online/offline beam profile monitor. In this presentation, we discuss the experimental overview and R&D status of each components.

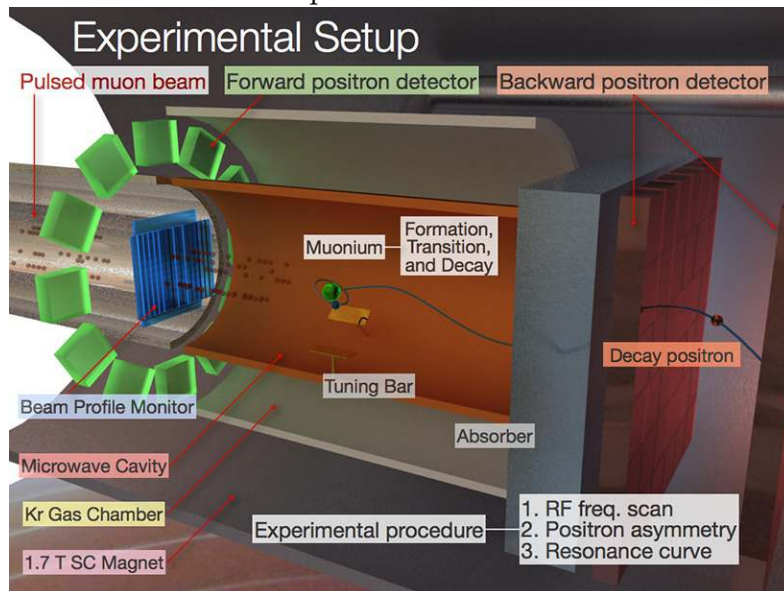


Figure 1: *Experimental Overview*

## References

- [1] W. Liu et al., PRL. 82, 711 (1999).
- [2] A. Toyoda et al. J.Phys.Conf.Ser. 408 (2013) 012073
- [3] S. Kanda et al, KEK-MSL Progress Report 2012B0117 (2013)

## Positron binding to polar molecules

G.F. Gribakin<sup>1</sup> and A.R. Swann<sup>1</sup><sup>1</sup>*School of Mathematics and Physics, Queen's University Belfast, Belfast BT7 1NN, UK*

Presenting Author: g.gribakin@qub.ac.uk

Before a positron annihilates with an electron in a polyatomic molecule, it usually enters into a quasibound state [1]. A wealth of experimental data on positron-molecule binding are now available. It shows that the binding energy  $\varepsilon_b$  is strongly enhanced in molecules with large permanent dipole moments [2]. However, there are few calculations of positron binding, and due to the difficulty in treating the electronic states in the presence of a positron, these calculations are not generally considered precise [3].

In this work we study positron-molecule binding theoretically using a simple model. The molecule is modelled as an impenetrable sphere of radius  $r_0$  with a static point dipole  $\mathbf{D}$  moment at its centre. Outside the sphere the positron experiences the point dipole's potential:

$$V(\mathbf{r}) = \begin{cases} \infty & \text{if } r \leq r_0, \\ \mathbf{D} \cdot \mathbf{r}/r^3 & \text{if } r > r_0. \end{cases} \quad (1)$$

For this potential the radial Schrödinger equation can be solved analytically in terms of Bessel functions, with the angular part diagonalized numerically. The application of appropriate boundary conditions leads to a simple relationship between  $\varepsilon_b$  and  $r_0$ , and we consider  $r_0$  as a fitting parameter. Using existing experimental data on binding energies leads to unphysically small values of  $r_0$  for all of the molecules studied. This suggests that electron-positron correlations neglected in (1) play a large role in determining the binding energy. We account for these using the polarization potential  $-\alpha/2r^4$  (where  $\alpha$  is the molecular dipole polarizability) via perturbation theory; the first-order correction to the binding energy is

$$\Delta\varepsilon_b = \int |\psi(\mathbf{r})|^2 (\alpha/2r^4) d^3\mathbf{r}, \quad (2)$$

where  $\psi(\mathbf{r})$  is the ground-state positron wave function. This has enabled accurate predictions of  $\varepsilon_b$  to be made for a range of organic molecules and hydrogen cyanide, whose binding energy cannot be measured experimentally but has been calculated with the diffusion Monte Carlo (DMC) method [4].

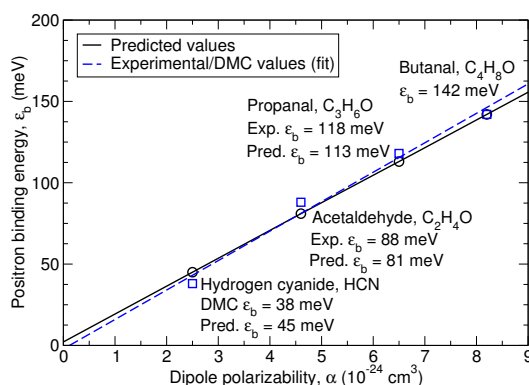


**Figure 1:** Comparison of predicted  $\varepsilon_b$  obtained using  $D = 2.7$  debye and  $r_0 = 0.58$  a.u. for aldehydes and hydrogen cyanide (circles) with experimental values for aldehydes and DMC for HCN (squares).

## References

- [1] G. F. Gribakin, J. A. Young, and C. M. Surko, *Rev. Mod. Phys.* **82**, 2557 (2010)
- [2] J. R. Danielson, J. J. Gosselin, and C. M. Surko, *Phys. Rev. Lett.* **104**, 233201 (2010)
- [3] J. R. Danielson *et al.*, *Phys. Rev. A* **85**, 022709 (2012)
- [4] Y. Kita *et al.*, *J. Chem. Phys.* **131**, 134310 (2009)

## Quantum cascade laser emission width narrowing at the kHz level by means of optical feedback

E. Fasci<sup>1</sup>, N. Collucelli<sup>2</sup>, A. Gambetta<sup>2</sup>, M. Cassinero<sup>2</sup>, M. Marangoni<sup>2</sup>, P. Laporta<sup>2</sup>, L. Gianfrani<sup>1</sup>,  
A. Castrillo<sup>1</sup>, and G. Galzerano<sup>2</sup>

<sup>1</sup>*Dipartimento di Matematica e Fisica, Seconda Università di Napoli, Viale Lincoln 5, 81100 Caserta, Italy*

<sup>2</sup>*Istituto di Fotonica e Nanotecnologie - CNR and Dipartimento di Fisica - Politecnico di Milano, Piazza Leonardo da Vinci 32, 20133 Milano, Italy*

Presenting Author: antonio.castrillo@unina2.it

Quantum Cascade Lasers (QCL), in particular room-temperature distributed-feedback lasers, are becoming the usual sources for accessing the mid-IR molecular fingerprint spectral region. For advanced applications in precision spectroscopy a great effort is aimed at further improving their spectral purity performance. Indeed, although the intrinsic emission linewidth of a QCL can be as low as a few hundreds of hertz [1, 2], excess technical noise, such as the pump current noise, broadens the QCL emission linewidth by several orders of magnitude up to few megahertz for 1-ms observation times. For this reason, different electronic feedback techniques have been implemented to narrow the QCL linewidth down to the 10-kHz level, such as locking to the side of a molecular line [3], to an optical cavity [4], as well as phase locking QCLs to thulium frequency comb [5]. Even better results have been obtained using electronic feedback from a molecular sub-Doppler reference [6].

In this work, we demonstrate the kHz linewidth narrowing of a room-temperature distributed feedback QCL, tunable in the range from 8.56 to 8.63  $\mu\text{m}$ . In particular, the QCL is frequency locked to a high-finesse V-shaped cavity by the optical feedback method [7-11]. This simple and robust technique allows us to narrow the 1-ms QCL linewidth from 3 MHz down to  $\sim 2$  kHz. A preliminary characterization of the frequency stability of the QCL source, performed by using a properly developed mid-IR optical frequency comb [12], demonstrated a relative frequency stability of  $10^{-10}$  for an integration time of 100 ms.

The proposed QCL source will be a powerful tool for high-resolution molecular spectroscopy and optical frequency standard in the mid-IR spectral region. In particular, the QCL laser will be used for the absolute measurement of the line center frequency of a two-photon transition in a molecular beam of  $\text{CHF}_3$ , allowing for a determination of the possible variation of the electron to proton mass ratio at level of  $10^{-15}\text{yr}^{-1}$  [13].

### References

- [1] S. Bartalini *et al.* Opt. Express **19**, 17996-18003 (2011)
- [2] L. Tombez *et al.* Opt. Lett. **36**, 3109-3111 (2011)
- [3] R. M. Williams *et al.* Opt. Lett. **24**, 1844-1846 (1999)
- [4] M. S. Taubman, T. L. Myers, B. D. Cannon, R. M. Williams Spectrochim. Acta Part A **60**, 3457-3468 (2004)
- [5] A. A. Mills *et al.* Opt. Lett. **37**, 4083-4085 (2012)
- [6] F. Cappelli *et al.* Opt. Lett. **37**, 4811-4813 (2012)
- [7] B. Dahmani, L. Hollberg, R. Drullinger Opt. Lett. **12**, 876-878 (1987)
- [8] P. Laurent, A. Clairon, and C. Breant IEEE J. Quantum Electron. **QE-25**, 1131 (1989)
- [9] A. Hemmerich, D. H. McIntyre, C. Zimmermann, T. W. Hänsch, Opt. Lett. **15**, 372-374 (1990)
- [10] J. Morville, S. Kassi, M. Chenevier, D. Romanini Appl. Phys. B **80**, 10271038 (2005)
- [11] G. Maisons, P. Gorrotxategi-Carbajo, M. Carras, D. Romanini Opt. Lett. **35**, 3607-3609 (2010)
- [12] A. Gambetta *et al.* Opt. Lett. **38**, 1155-1157 (2013)
- [13] FIRB projects RBFR1006TZ-2 and RBFR1006TZ-3 funded by the Italian Ministry for Education, University and Research (MIUR)

# An efficient calculation of the scattering wavefunction and phase shift

V.V. Meshkov<sup>1</sup> and A.V. Stolyarov<sup>1</sup>

<sup>1</sup>Department of Chemistry, Lomonosov Moscow State University, 119991, Moscow, Russia

Presenting Author: meshkov@laser.chem.msu.ru

The scattering phase shift is a key characteristic of the colliding particles in quantum scattering theory. It is widely used to determine the metastable states, the scattering lengths as well as thermodynamic and transport properties of gases. The phase shift  $\eta_l$  is determined from the asymptotic form of the radial wavefunction  $\psi(r) \simeq A \sin(kr + \eta_l + \pi l/2)$ , where  $k$  is the relative wave vector of the colliding particles and  $l$  is the rotational quantum number. We show that if the wavefunction is represented in the form  $f(r) \sin(kr) + g(r) \cos(kr)$ , where  $f(r) \simeq f_0 + f_1/r + \dots$  and  $g(r) \simeq g_0 + g_1/r + \dots$  when  $r \rightarrow \infty$ , then the substitution of the radial variable  $r = -(1+x)/x$  define the functions  $f(r(x))$  and  $g(r(x))$  in the finite domain  $x \in [-1, 0]$  by the coupled equations

$$\begin{cases} -f''_{xx} - \frac{2}{x}f'_x + \frac{2k}{x^2}g'_x + \left[ \frac{l(l+1)}{x^2} + \frac{2\mu V(r(x))}{\hbar^2 x^4} \right] f(x) = 0 \\ -g''_{xx} - \frac{2}{x}g'_x - \frac{2k}{x^2}f'_x + \left[ \frac{l(l+1)}{x^2} + \frac{2\mu V(r(x))}{\hbar^2 x^4} \right] g(x) = 0 \end{cases}$$

which could be efficiently solved of by means of polynomial collocation method [1] ( $'$  denotes differentiation with respect  $x$ ,  $V(r)$  is interatomic potential). Thus it allows one to define the wavefunction  $\psi(r)$  on the whole interval of interatomic distances  $r \in [0, +\infty)$  and to determine the phase shift as  $\eta_l = \arctan(g(x=0)/f(x=0))$  at the end of the interval. The mapping method has been already used for calculation bound levels and scattering lengths [2,3]. It poses the exponential convergence rate with respect to number of collocation points  $N$  (see Fig. 1). The multi-channel version of the method is applied for highly accurate calculation of the resonance position and width of quasi-bound levels above dissociation limits of KCs, RbCs and KRb molecules.

The work was the partially supported by the Russian Foundation for Basic Research (Project N13-03-00466).

## References

- [1] J. P. Boyd, *Chebyshev and Fourier Spectral Methods* (DOVER Publications, Inc., New York, 2000)
- [2] V.V. Meshkov, A.V. Stolyarov, R.J. Le Roy J. Chem. Phys, **135**, 154108, (2011)
- [3] V.V. Meshkov, A.V. Stolyarov, R.J. Le Roy Phys. Rev. A, **78**, 052510 (2008)

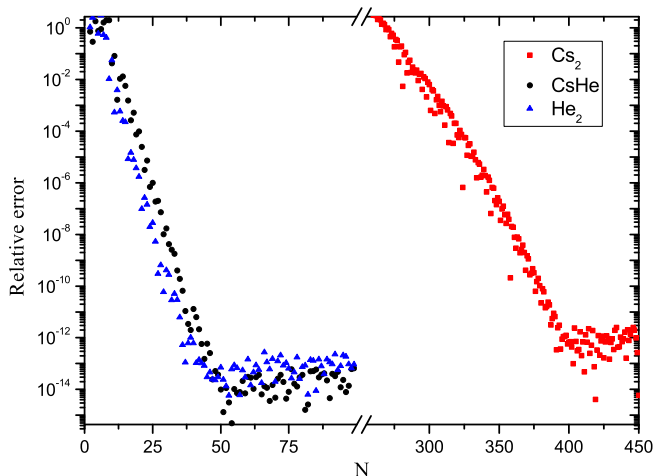


**Figure 1:** Relative errors in phase shift obtained for  $Cs_2$ ,  $CsHe$  and  $He_2$  potentials ( $E=1000 \text{ cm}^{-1}$ ,  $l=25$ ) as function of the number of grid points ( $N$ ) used in the polynomial collocation method.

## Zeeman splitting in lithium-like and boron-like ions

D.A. Glazov<sup>1,2</sup>, A.V. Volotka<sup>1,2</sup>, V.A. Agababaev<sup>1</sup>, M.M. Sokolov<sup>1</sup>, A.A. Shchepetnov<sup>1</sup>, V.M. Shabaev<sup>1</sup>,  
I.I. Tupitsyn<sup>1</sup>, and G. Plunien<sup>2</sup>

<sup>1</sup>*Department of Physics, St. Petersburg State University, Oulianovskaya 1, Petrodvorets, 198504 St. Petersburg, Russia*

<sup>2</sup>*Institut für Theoretische Physik, Technische Universität Dresden, Mommsenstraße 13, D-01062 Dresden, Germany*

Presenting Author: glazov.d.a@gmail.com

The  $g$  factor of hydrogen-like ions proved to be a sensitive tool for determination of fundamental constants [1]. First ppb-precision measurement for lithium-like system has been accomplished recently [2]. Experiments with heavy boron-like ions can provide independent determination of the fine structure constant [3]. The ARTEMIS experiment presently being performed at GSI aims at measurement of the Zeeman splitting in boron-like argon [4]. Apart from the  $g$  factors of the ground and first excited states, it will be sensitive to the non-linear effects in magnetic field.

We present the most recent theoretical results for the  $g$  factor of medium- $Z$  lithium-like and boron-like ions and for the contributions of second and third order in magnetic field to the Zeeman splitting in boron-like ions. The  $g$  factor of lithium-like ions is improved by the rigorous evaluation of the screened-QED and two-photon-exchange corrections. The  $g$  factor of boron-like ions includes the first-order QED corrections, the one-photon exchange, the higher-order correlation effects in the Breit approximation, and the recoil correction.

### References

- [1] S. Sturm *et al.* Nature **506**, 467 (2014)
- [2] A. Wagner *et al.* Phys. Rev. Lett. **110**, 033003 (2013)
- [3] V. M. Shabaev *et al.* Phys. Rev. Lett. **96**, 253002 (2006)
- [4] D. von Lindenfels *et al.* Phys. Rev. A. **87**, 023412 (2013)

# Basis Set Optimization Method for Rydberg States – GTO Basis Sets for He and Be

J. Šmydke<sup>1</sup> and P.R. Kaprálová-Ždánková<sup>1</sup>

<sup>1</sup>*J. Heyrovský Institute of Physical Chemistry, Academy of Sciences of the Czech Republic, Prague*

Presenting Author: jan.smydke@jh-inst.cas.cz

A new method to optimize basis sets suitable for Rydberg states investigation has been suggested and applied [1,2] to Gaussian basis of helium and beryllium atoms. It is based on a variational optimization of *the improved virtual orbitals* [3], which lead to dominant configurations in the CI excited states expansion and thus more properly describe excited states than the standard Hartree-Fock orbitals.

We have also introduced *the exponentially tempered Gaussian basis set* scheme (ExTG)

$$\log_{10} \zeta_k = a 10^{-bk} + c; \quad k = 0 \dots (N - 1) \quad (1)$$

which naturally emerged after a series of improved virtual orbitals had consecutively been optimized. Compared to *the even tempered Gaussian* scheme (ETG)

$$\log_{10} \zeta_k = a k + b; \quad k = 0 \dots (N - 1), \quad (2)$$

the ExTG basis increases density of diffuse Gaussians and achieves the same quality with much smaller number of basis functions.

The calculated CI and EOM-CC excitation energies were compared to other basis set results and to experiment. The helium basis set was also employed in a complex scaled calculation of resonances with excellent results approaching quality of the Coulomb-Sturmian basis set.

## References

- [1] P.-R. Kaprálová-Ždánková, J. Šmydke, J. Chem. Phys. **138**, 024105 (2013)
- [2] P.-R. Kaprálová-Ždánková, J. Šmydke, S. Civiš, J. Chem. Phys. **139**, 104314 (2013)
- [3] W. J. Hunt, W. A. Goddard III, Chem. Phys. Lett. **3**, 414 (1969)

## Search for a parity violation effect in chiral molecules: old dream and new perspectives

S.K. Tokunaga<sup>1,2</sup>, A. Shelkovnikov<sup>1,2</sup>, P.L.T. Sow<sup>2,1</sup>, S. Mejri<sup>1,2</sup>, O. Lopez<sup>2,1</sup>, A. Goncharov<sup>1,2</sup>, B. Argence<sup>1,2</sup>, C. Daussy<sup>1,2</sup>, A. Amy-Klein<sup>1,2</sup>, C. Chardonnet<sup>2,1</sup>, and B. Darquié<sup>2,1</sup>

<sup>1</sup>Université Paris 13, Sorbonne Paris Cité, Laboratoire de Physique des Lasers, Villetaneuse, France

<sup>2</sup>CNRS, UMR 7538, LPL, Villetaneuse, France

Presenting Author: benoit.darquie@univ-paris13.fr

Parity violation (PV) effects have so far never been observed in chiral molecules. Originating from the weak nuclear force, PV should lead to a frequency difference in the rovibrational spectra of the two enantiomers of a chiral molecule. However the smallness of the effect represents a very difficult experimental challenge. The measurement of PV in molecules is interesting for a range of subjects across the board. It is a probe of the weak interaction and would thus serve as a test of the standard model of physics. But it has also been suggested to be connected to biomolecular homochirality, a strong quantity imbalance observed on earth between left- and right-handed biomolecules. We have been working towards measuring this difference using Ramsey interferometry in the mid-infrared (at around 10  $\mu\text{m}$ ) using ultra-narrow line width CO<sub>2</sub> lasers referenced to atomic clocks in Paris via an optical link. We expect to reach a fractional sensitivity of around  $10^{-15}$  ( $\sim 10$  mHz) on the frequency difference between enantiomers [1].

We present the results of preliminary investigations conducted on methyltrioxorhenium (MTO), an achiral test molecule whose chiral derivatives have recently been synthesized and are estimated to have a  $\sim 10^{-14}$  level PV effect [2]. We report on the high-resolution spectroscopy of MTO [3,4], both in a cell and in a supersonic beam (Fig. 1). This work has enabled us to identify several key elements of the current experiment needing improvement prior to making a PV measurement. The first is the lack of tunability of our CO<sub>2</sub> lasers. We present our on-going work towards the replacement of the CO<sub>2</sub> lasers with quantum cascade lasers (QCLs) [5] the very latest mid-infrared laser technology which offer broad and continuous tuning. Secondly, the current molecular beam source only yields a modest flux for species such as MTO which are solid at room temperature. We plan to overcome this by developing a buffer-gas-beam source and report on our latest efforts to implement buffer-gas cooling on polyatomic species such as MTO.

### References

- [1] B. Darquié *et al.* Chirality **22**, 870–884 (2010)
- [2] N. Saleh *et al.* Phys. Chem. Chem. Phys. **15**, 10952–10959 (2013)
- [3] C. Stoeffler *et al.* Phys. Chem. Chem. Phys. **13**, 854–863 (2011)
- [4] S. K. Tokunaga *et al.* Mol. Phys. **111**, 2363–2373 (2013)
- [5] P. L. T. Sow *et al.* arXiv:1404.1162 [physics.optics] (2014)

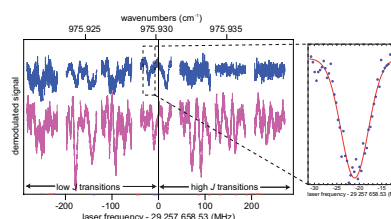


**Figure 1:** Linear absorption spectroscopy of a MTO-seeded supersonic jet, in the vicinity the R(20) CO<sub>2</sub> laser line frequency (0 MHz on the bottom axis). Lower pink curve: translational temperature  $\geq 5$  K. Upper blue curve: translational temperature  $\sim 1$  K. The inset is a zoom on a single line.

## Atomic Parity Violation in a single trapped Ra<sup>+</sup> ion.

A. Mohanty<sup>1</sup>, E.A. Dijck<sup>1</sup>, M. Nuñez Portela<sup>1</sup>, A. Valappol<sup>1</sup>, A.T. Grier<sup>1</sup>, O. Böll<sup>1</sup>, S. Hoekstra<sup>1</sup>, K. Jungmann<sup>1</sup>, C.J.G. Onderwater<sup>1</sup>, R.G.E. Timmermans<sup>1</sup>, L. Willmann<sup>1</sup>, and H.W. Wilschut<sup>1</sup>

<sup>1</sup>University of Groningen, Zernikelaan 25, 9747 AA Groningen, The Netherlands

Presenting Author: a.mohanty@rug.nl

Atomic Parity Violation (APV) provides for determining electroweak parameters in the Standard Model. In particular, the weak mixing angle ( $\sin^2\theta_W$ ) can be determined from single trapped Ra<sup>+</sup> ion [1]. This experiment at the lowest accessible momentum transfer provides for a sensitive test of the running of the electroweak mixing angle. The effects of weak interactions can be measured in Ra<sup>+</sup> by exploiting the properties of light shift in the  $7s^2S_{1/2} - 6d^2D_{3/2}$  transition. Light shifts permit the mapping of weak interaction effects on the energy splitting of the magnetic sub-levels in the Ra<sup>+</sup> ion.

A particular experimental requirement for an APV experiment is the localization of the ion within a fraction of an optical wavelength in the presence of two light fields of known frequency. Alkaline earth metal ions are very well suited for such experiments, because atomic structure calculations are possible to the required sub-percent level of precision [2]. The contribution of the weak interactions grow significantly faster than the third power of the atomic number Z. Therefore the heaviest alkaline earth element Radium (Z=88) has been chosen for our experiment. In Ra<sup>+</sup>, the weak interaction contributions are about 50 times larger than in the so far best investigated atom, i.e. Cs. A 5-fold improvement in the weak mixing angle appears possible within less than one week of measurement time.

High precision optical frequency metrology is possible with single trapped ions, which is a key ingredient for the measurement. Several Radium isotopes for our experiment have been produced at the TRIμP facility at KVI. In preparation of the parity experiment we have already determined the hyperfine structure of the  $6d^2D_{3/2}$  states [3], the isotope shift of the  $6d^2D_{3/2} - 7p^2P_{1/2}$  transition in the isotopes  $^{209-214}\text{Ra}^+$  [4] as well as the lifetime of the  $6d^2D_{5/2}$  state. These measurements agree well with theory at a level of a few percent [5,6].

We present here the status of the experiment, where the Ba<sup>+</sup> ion serves as a precursor. The lifetime of the  $5d^2D_{5/2}$  state in a single trapped Ba<sup>+</sup> ion has been precisely measured. The determination of the light shift in the  $5d^2D_{3/2} - 6s^2S_{1/2}$  transition in this system is the next step on the way towards single trapped Ra<sup>+</sup> ion APV experiment. The preparation of an offline  $^{223}\text{Ra}$  source is in progress. The setup for a single Ra<sup>+</sup> ion parity experiment is also well suited for realizing a most stable optical clock.

### References

- [1] N. Fortson, Phys. Rev. Lett. **70**, 2383-2386 (1993)
- [2] B. K. Sahoo, Phys. Rev. A **79**, 052512 (2009)
- [3] O. O. Versolato *et al.*, Phys. Lett. A. **375**, 3130 (2011)
- [4] G. S. Giri *et al.*, Phys. Rev. A. **84**, 020503 (2011)
- [5] L. W. Wansbeck *et al.*, Phys. Rev. C. **86**, 015503 (2012)
- [6] M. Nuñez Portela *et al.*, Appl. Phys. B. **114**, 173-182 (2014)

# Measurement of the forbidden $2\ ^3S_1 \rightarrow 2\ ^1P_1$ transition in quantum degenerate helium

R.P.M.J.W. Notermans<sup>1</sup>, R.J. Rengelink<sup>1</sup>, and W. Vassen<sup>1</sup>

<sup>1</sup>LaserLaB, Department of Physics and Astronomy, VU University Amsterdam, the Netherlands

Presenting Author: w.vassen@vu.nl

There is a longstanding 6.8 (3.0) MHz discrepancy between QED theory and the experimental value of the ionization energy of the  $2\ ^1P_1$  state in helium. We present the first measurement of the forbidden 887-nm  $2\ ^3S_1 - 2\ ^1P_1$  transition in a quantum degenerate gas of  $^4\text{He}^*$  [1], using the experimental setup as used to measure the doubly forbidden  $2\ ^3S \rightarrow 2\ ^1S$  transition by van Rooij *et al.* [2]. The low temperature of the gas ( $\sim 1\ \mu\text{K}$ ) allows us to observe the transition at its natural linewidth of 287 MHz and control systematic frequency shifts with kHz accuracy.

From our measurements we obtain the transition frequency with a relative accuracy of  $1.6 \times 10^{-9}$  and determine the ionization energy of the  $2\ ^1P_1$  state with  $6.7 \times 10^{-10}$  relative accuracy. Our result deviates  $> 3\sigma$  from the currently most accurate QED theory for the  $2\ ^1P_1$  ionization energy [3]. Recent measurements of the  $2\ ^1S_0 \rightarrow 2\ ^1P_1$  [4] and  $2\ ^1P_1 \rightarrow 3\ ^1D_2$  [5] transition frequencies by Luo *et al.*, which are performed in a RF discharge cell, allow an independent determination of the  $2\ ^1P_1$  ionization energy and agree with our work. This discrepancy with theory is shown in Fig. 1 and indicates that a renewed effort on the QED calculations is required.

Furthermore, as the transition is observed at its natural linewidth, our measurement allows for the most accurate determination of the lifetime of the  $2\ ^1P_1$  state to date. The determined lifetime of  $0.551\ (0.004)_{\text{stat}}\ ({}^{+0.013}_{-0.000})_{\text{syst}}$  ns is in agreement with theory and previous determinations that are based on completely different techniques.

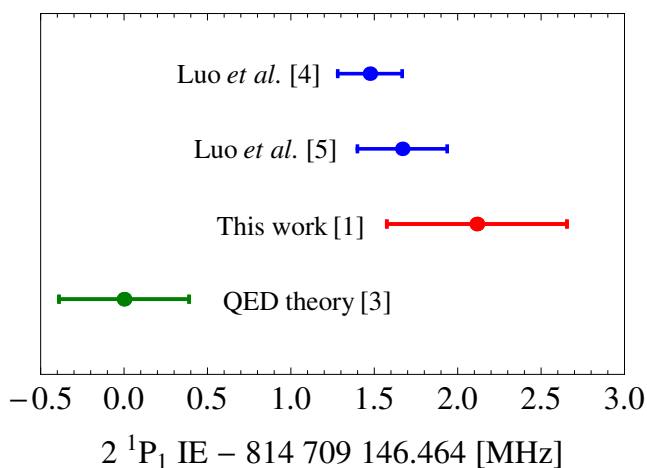


**Figure 1:** Comparison of our experimental determination of the  $2\ ^1P_1$  ionization energy [1] with other experiments by Luo *et al.* [4–5] and QED theory by Yerokhin and Pachucki [3].

## References

- [1] R.P.M.J.W. Notermans, W. Vassen, arXiv:1404.1759v1 [physics.atom-ph]
- [2] R. van Rooij *et al.*, Science **333**, 196 (2011)
- [3] V.A. Yerokhin, K. Pachucki, Phys. Rev. A **81** 022507 (2010)
- [4] P.-L. Luo *et al.*, Phys. Rev. Lett. **111** 013002 (2013); Phys. Rev. Lett. **111** 0179901(E) (2013)
- [5] P.-L. Luo *et al.*, Phys. Rev. A **88** 054501 (2013)

# Radiative data of lowly-ionized iron-peak elements for transitions of astrophysical interest

V. Fivet<sup>1</sup>, P. Quinet<sup>1,2</sup>, and M. Bautista<sup>3</sup>

<sup>1</sup>*Astrophysique et Spectroscopie, Université de Mons - UMONS, B7000 Mons, Belgium*

<sup>2</sup>*IPNAS, Université de Liège, B4000 Liège, Belgium*

<sup>3</sup>*Department of Physics, Western Michigan University, Kalamazoo MI 49008, USA*

Presenting Author: quinet@umons.ac.be

Accurate fine-structure atomic data for the Fe-peak elements (Sc, Ti, V, Cr, Mn, Fe, Co and Ni) are essential for interpreting astronomical spectra currently available. The lowly-ionized spectra of several iron group elements have been observed in nebular and stellar environments [1-2]. Yet, our present knowledge of their atomic structure is lagging behind the avalanche of high-quality spectra arising from these ions.

We present our systematic approach for studying the electronic structures and radiative rates of forbidden lines of doubly-ionized iron peak elements. The magnetic dipole (M1) and electric quadrupole (E2) transition probabilities are computed using the pseudo-relativistic Hartree-Fock (HFR) code of Cowan [3] and the central Thomas-Fermi-Dirac-Amaldi potential approximation implemented in AUTOSTRUCTURE [4] using a new method of optimization for the potential scaling parameters. The extensive sets of results obtained using these two theoretical approaches are then compared to the rare experimental and theoretical data available in the literature for these ions in order to assess the advantages and shortcomings of each method and provide astrophysicists with a comprehensive set of reliable radiative data.

## References

- [1] A. Mesa-Delgado *et al.*, MNRAS **395**, 855 (2009)
- [2] T. Zethson *et al.*, A&A **540**, A133 (2012)
- [3] R. D. Cowan, *The Theory of Atomic Structure and Spectra* (Univ. California Press, Berkeley, 1981)
- [4] N.R. Badnell, J. Phys. B: At. Mol. Phys **30**, 1 (1997)

# QED tests of heliumlike systems with X-ray laser spectroscopy

J.R. Crespo López-Urrutia<sup>1</sup>, S. Bernitt<sup>1</sup>, J.K. Rudolph<sup>1</sup>, R. Steinbrügge<sup>1</sup>, S.W. Epp<sup>2</sup>, and J. Ullrich<sup>3</sup>

<sup>1</sup>Max-Planck-Institut für Kernphysik, D-69117, Heidelberg

<sup>2</sup>Max-Planck-Institut für Struktur und Dynamik der Materie, D-22607 Hamburg

<sup>3</sup>Physikalisch-Technische Bundesanstalt, D-38116 Braunschweig

Presenting Author: crespojr@mpi-hd.mpg.de

Emission spectroscopy in electron beam ion traps has been the main tool for precision studies of highly charged ions (HCI), delivering essential data on their level structure and, in a few instances, also on the related transition probabilities. Its essential limitation arises from the unavoidable compromise between achievable resolution and signal strength in the observation of isotropically emitting sources. This shortcoming is circumvented, much like in optical laser spectroscopy, by the recently introduced method of resonant fluorescence spectroscopy of HCI at highly collimated X-ray sources, such as synchrotrons and free-electron lasers. Here, the advantages of the large linear photon energy dispersion achievable with very large monochromators, and the high spectral purity of the sources due to the use of insertion devices, allow one to reach a resolution akin to the highest ones reported in emission spectroscopy works but with much shorter data acquisition times.

Our experimental investigations on the oscillator strengths of the most intense L-shell transitions of Fe<sup>16+</sup> at around 800 eV [1] using the free-electron laser LCLS have led to a better understanding of a long-standing astrophysical controversy. Furthermore, using highly monochromatized synchrotron radiation from PETRA III we have also resonantly excited the ions Fe<sup>18+..24+</sup> [2] and Kr<sup>34+</sup> at photon energies around 6.6 keV and 13.1 keV, respectively, with substantially improved accuracy. These results strongly support state-of-the-art QED calculations of two-electron systems [3], which had recently been contested [4]. Moreover, the achieved resolution was sufficient for determining the natural line widths of several K $\alpha$ ? transitions in Fe ions for the first time. Such X-ray lines are the underlying spectral constituents of the relativistically broadened and shifted fluorescence features observed in active galactic nuclei with central massive black holes, and in their jets. Modelling such astrophysical spectra, and those of future missions like *Athena+*, will require improved and benchmarked atomic physics input data.

Further enhancements of our method will include the use of higher-resolving monochromators and free-electron lasers seeding schemes, as well as the linkage of HCI transitions to Mößbauer nuclear transitions and metrological wavelength standards. We are currently testing the long sought-after [5] sympathetic cooling of HCI in our novel cryogenic Paul trap CryPTE<sub>x</sub> [6] using Be<sup>+</sup> ion Coulomb crystals to lower the ion temperature by a factor of more than one million. In combination with various improved fluorescence detection schemes based on photon recoil [7], we expect further enhancements of the current experimental capabilities. In this way, more stringent tests of the QED calculations in fundamental systems such as hydrogenlike and heliumlike ions will become possible. In the long run, direct frequency determinations in the X-ray region could provide new insights in the physics of those strong-field QED systems.

## References

- [1] S. Bernitt *et al.*, Nature, **492**, 225 (2012)
- [2] J. K. Rudolph *et al.*, Phys. Rev. Lett. **111**, 103002 (2013)
- [3] A. N. Artemyev *et al.*, Phys. Rev. A **71**, 062104 (2005)
- [4] C. Chantler *et al.*, Phys. Rev. Lett. **109**, 153001 (2012); see also comment: S. W. Epp, Phys. Rev. Lett. **110**, 159301 (2013), and reply: C. Chantler *et al.*, Phys. Rev. Lett. **110**, 159302 (2013)
- [5] L. Gruber *et al.*, Phys. Rev. Lett. **86**, 636 (2001)
- [6] M. Schwarz *et al.*, Rev. Sci. Instrum. **83**, 083115 (2012); O.O. Versolato *et al.*, Hyperfine Interact. **214**, 189 (2013); O. O. Versolato *et al.*, Phys. Rev. Lett. **111**, 053002 (2013); A. K. Hansen *et al.*, Nature **508**, 76 (2014)
- [7] P. O. Schmidt *et al.*, Science **309**, 749 (2005); Yong Wan *et al.*, Nature Comm. **5**, 3096 (2014); D. B. Hume, *et al.*, Phys. Rev. Lett. **107**, 243902 (2011); M. Drewsen, priv. comm.

# Correlation Channels in Sequential Double Ionisation

J. Kaushal<sup>1</sup>, H. Rey<sup>2</sup>, O. Smirnova<sup>1</sup>, and H. van der Hart<sup>2</sup>

<sup>1</sup>Max Born Institute, Max Born Strasse 2a, 12489 Berlin, Germany

<sup>2</sup>Queen's University Belfast, Belfast, United Kingdom

Presenting Author: jivesh.kaushal@mbi-berlin.de

We present a quantum mechanical method to study the effects of Correlation channels on Sequential Double Ionisation (SDI) in strong elliptical fields. Recent experiments [1] have shown that the independent electron approximation is not sufficient to explain the observed electron spectrum and release time of electrons in SDI from laser fields with high intensities and close to circular ellipticities.

Classical methods [2, 3] to explain the different imprints of correlation effects, for example, oscillation in ratio of yield for parallel to anti-parallel electrons, evolution of three to four band structure in the recoil ion momentum distribution with laser intensity, and correlated angular distributions for the emitted electrons have been developed but we present the first quantum mechanical treatment of the phenomenon.

Our method is based on the recently developed analytical  $R$ -matrix (ARM) method [4, 5], wherein we partition the configuration space into a core dominated and laser field dominated region, and along with it use the eikonal-Volkov approximated (EVA) [6] electron states to describe the wavefunction for the continuum electrons, taking into account the long-range Coulomb potential effects from the residual ion. In order to incorporate effects of ion transitions caused by correlation potential existing between the first ionising electron and the residual ion being left behind, we use the method outlined in [7] to include multielectron effects, thus going beyond the Single Active Electron (SAE) approximation for SDI. We also extend the method to apply to effects of the correlation potential on the quantum trajectories.

The correlation amplitude, which can be expressed as the ratio of the indirect-to-direct ionisation amplitude [7], is shown in Fig. 1. Since the ionisation to the ground of  $\text{Ar}^{++}$  is many orders of magnitude more likely from the  $^1S$  than  $^2P_{3/2}$ , the correlated channel is the dominant pathway for SDI in Argon.

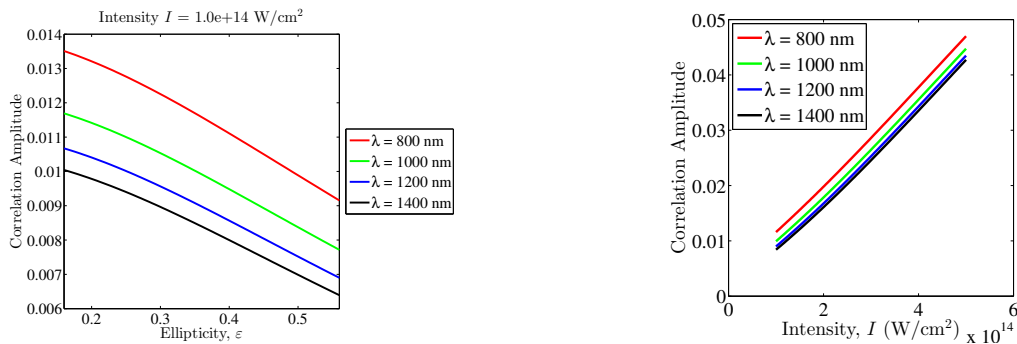


**Figure 1:** Variation of correlation amplitude with ellipticity and field strength for laser induced coupling between  $^1S$  and  $^2P_{3/2}$  state of  $\text{Ar}^+$ , that contributes to correlated sequential ionisation pathway.

## References

- [1] A. N. Pfeiffer *et al.*, New J. Physics **13**, 093008 (2011).
- [2] X. Wang and J. H. Eberly, arxiv:1102.0221v1.
- [3] Y. Zhou, C. Huang, Q. Liao, and P. Liu, Phys. Rev. Lett. **109**, 053004 (2012); Y. Zhou, Q. Zhang, C. Huang, and P. Liu, Phys. Rev. A **86**, 043427 (2012); Y. Zhou, C. Huang, and P. Liu, Opt. Express **20**, 20201 (2012).
- [4] L. Torlina and O. Smirnova, Phys. Rev. A **86**, 043408 (2012).
- [5] J. Kaushal and O. Smirnova, Phys. Rev. A **88**, 013421 (2013).
- [6] O. Smirnova, M. Spanner, and M. Yu. Ivanov, Phys. Rev. A **77**, 033407 (2008).
- [7] L. Torlina, M. Yu. Ivanov, Z. B. Walters, and O. Smirnova, Phys. Rev. A **86**, 043409 (2012).

# Towards single-atom-resolved detection of strongly correlated fermions in an optical lattice

J. Hinney<sup>1</sup>, E. Haller<sup>1</sup>, J. Hudson<sup>1</sup>, A. Kelly<sup>1</sup>, D. Cotta<sup>1</sup>, G. Bruce<sup>1,2</sup>, and S. Kuhr<sup>1</sup>

<sup>1</sup>*Department of Physics, University of Strathclyde, Glasgow, United Kingdom*

<sup>2</sup>*School of Physics & Astronomy, University of St Andrews, St Andrews, United Kingdom*

Presenting Author: jakob.g.hinney@strath.ac.uk

Motivated by the recent achievement of single-site-resolved imaging and manipulation of strongly correlated bosonic systems in an optical lattice [1,2], we illustrate our progress to realize single-atom imaging for fermionic <sup>40</sup>K. Detecting and manipulating strongly correlated fermionic systems at the level of a single atom will further exploit the potential of ultracold atoms as a quantum simulator for the Fermi-Hubbard model.

Atoms from a two-stage magneto-optical trap of <sup>87</sup>Rb and <sup>40</sup>K are loaded into a magnetic trap, before evaporative cooling and transport in an optical trap delivers a quantum degenerate gas to a 3-dimensional optical lattice. By selective removal of atoms from all lattice planes but the one at the focal plane of a NA = 0.68 microscope objective, we will resolve the distribution and evolution of atoms across individual sites of the 2D lattice using fluorescence imaging. We plan to use this novel detection method to characterize, e.g., temperature, spin-structure, or entropy distribution of quantum phases such as fermionic Mott insulators, Band insulators, metallic phases or Néel antiferromagnets.

## References

- [1] W. S. Bakr, J. I. Gillen, A. Peng, S. Fölling, M. Greiner *Nature* **462**, 74–78 (2009)
- [2] J. F. Sherson, C. Weitenberg, M. Endres, M. Cheneau, I. Bloch, S. Kuhr *Nature* **467** 68–72 (2010)

# Accurate relativistic properties of hydrogenic atoms with the Lagrange-mesh method

D. Baye<sup>1</sup>, L. Filippin<sup>2</sup>, and M. Godefroid<sup>2</sup>

<sup>1</sup>*Physique Quantique, C. P. 165/82, and Physique Nucléaire Théorique et Physique Mathématique, C. P. 229, Université Libre de Bruxelles (ULB), B-1050 Brussels, Belgium*

<sup>2</sup>*Chimie Quantique et Photophysique, C. P. 160/09, Université Libre de Bruxelles (ULB), B-1050 Brussels, Belgium*

Presenting Author: Livio.Filippin@ulb.ac.be

The Lagrange-mesh method is an approximate variational calculation using a special basis of  $N$  functions, called Lagrange functions, related to a set of  $N$  mesh points and the Gauss quadrature associated with this mesh [1]. It combines the high accuracy of a variational approximation and the simplicity of a calculation on a mesh [2,3]. The Lagrange functions are infinitely differentiable functions that vanish at all points of this mesh, except one. Used as a variational basis in a quantum-mechanical calculation, these functions lead to a simple algebraic system when matrix elements are calculated with the associated Gauss quadrature. The variational equations take the form of mesh equations with a diagonal representation of the potential only depending on values of this potential at the mesh points [1,3]. The most striking property of the Lagrange-mesh method is that, in spite of its simplicity, the obtained energies and wave functions can be as accurate with the Gauss quadrature approximation as in the original variational method with an exact calculation of the matrix elements [2,3]. It has been applied to various problems in atomic and nuclear physics.

For the exactly solvable Coulomb-Dirac problem describing hydrogenic atoms, numerically exact energies and wave functions, i.e. exact up to rounding errors, are obtained for any state and for any nuclear charge with very small numbers of mesh points [4]. Tests with the Yukawa potential provide very accurate results with a number of mesh points for which the computation seems instantaneous. The approximate wave functions provide mean values of powers of the coordinate that are also extremely precise. These results can be compared with very accurate benchmark calculations [5].

A more stringent test of wave functions is given by the calculation of polarizabilities. For the non relativistic hydrogen atom, numerically exact polarizabilities can be found with the Lagrange-mesh method for small numbers of mesh points [6]. Work is in progress to extend this study to the relativistic case, for which very accurate values are available for comparison [7]. In this case, exact static dipole polarizabilities are known only for the ground state [8] and the  $2s$  excited state of the hydrogen atom [8,9]. Our aim is to calculate accurate numerical polarizabilities from the Dirac equation with the Lagrange-mesh method. We will use the obtained energies and wave functions from Ref. [4] to study multipolar polarizabilities of the ground state and some excited states in the hydrogenic and Yukawa cases.

## References

- [1] D. Baye and P.-H. Heenen, *J. Phys. A* **19**, 2041 (1986)
- [2] D. Baye, M. Hesse, and M. Vincke, *Phys. Rev. E* **65**, 026701 (2002)
- [3] D. Baye, *Phys. Status Solidi (B)* **243**, 1095 (2006)
- [4] D. Baye, L. Filippin, and M. Godefroid, *Phys. Rev. E* **89**, 043305 (2014)
- [5] C. Krauthauser and R. N. Hill, *Can. J. Phys.* **80**, 181 (2002)
- [6] D. Baye, *Phys. Rev. A* **86**, 062514 (2012)
- [7] L.-Y. Tang *et al.*, *Phys. Rev. A* **86**, 012505 (2012)
- [8] V. Yakhontov, *Phys. Rev. Lett.* **91**, 093001 (2003)
- [9] R. Szymtkowski and K. Mielewczyk, *J. Phys. B* **37**, 3961 (2004)

# Alignment to orientation conversion of rubidium atoms under D<sub>2</sub> excitation in an external magnetic field: experiment and theory

M. Auzinsh<sup>1</sup>, A. Berzins<sup>1</sup>, R. Ferber<sup>1</sup>, F. Gahbauer<sup>1</sup>, L. Kalvans<sup>1</sup>, A. Mozers<sup>1</sup>, and A. Spiss<sup>1</sup>

<sup>1</sup>Laser Centre, University of Latvia, Rainis Blvd. 19, LV - 1586 Riga, Latvia

Presenting Author: marcis.auzins@lu.lv

We present results from a theoretical and experimental investigation of level-crossing spectra of rubidium atoms at D<sub>2</sub> excitation for crossings of levels whose projection  $m_F$  of the total angular momentum  $F$  on the quantization axis differ by one ( $\Delta m = 1$ ). The crossings occur when the levels are shifted by the nonlinear Zeeman effect in an external magnetic field  $\mathbf{B}$  whose direction defines the quantization axis. When two levels with  $\Delta m = 1$  cross they can be coherently excited by linearly polarized laser radiation whose polarization vector  $\mathbf{E}$  forms an angle of  $\pi/4$  with respect to the magnetic field  $\mathbf{B}$ . In this geometrical configuration, we observe laser induced fluorescence (LIF) emitted in the direction that is perpendicular to both  $\mathbf{E}$  and  $\mathbf{B}$  in order to observe the LIF signal as a function of magnetic field. The level-crossings lead to the emission of partially circularly polarized fluorescence light in the observation direction. The change in the detected circularly polarized LIF implies that the aligned angular momentum state created by the exciting laser radiation has been transformed into an oriented state under the influence of the external magnetic field.

We have extended the theoretical model and improved the experiment in comparison to previous studies [1], in particular so as to be able to study excitation at higher laser power densities while observing the individual circularly polarized light components. The theoretical model is based on the optical Bloch equations and takes into account all neighbouring hyperfine levels, the splitting of magnetic sublevels in the external magnetic field, and the Doppler effect [2]. The theoretical model is able to describe the experimentally measured signals for magnetic fields up to 85 G and laser power densities of 6 mW/cm<sup>2</sup>. We thank Latvian Council of Science project 119/2012 for financial support.

## References

- [1] J. Alnis *et al.* Phys.Rev.A **63**, 023407 (2001)
- [2] M. Auzinsh *et al.* Phys.Rev.A **79**, 053404 (2009)

## Experimental measurements and an improved theoretical description of magneto-optical signals of the cesium D<sub>1</sub> transition in an extremely thin cell

M. Auzinsh<sup>1</sup>, A. Berzins<sup>1</sup>, R. Ferber<sup>1</sup>, F. Gahbauer<sup>1</sup>, U. Kalninsh<sup>1</sup>, L. Kalvans<sup>1</sup>, A. Papoyan<sup>2</sup>, R. Rundans<sup>1</sup>, and D. Sarkisyan<sup>2</sup>

<sup>1</sup>Laser Centre, The University of Latvia, 19 Rainis Boulevard, LV-1586 Riga, Latvia

<sup>2</sup>Institute for Physical Research, NAS of Armenia, Ashtarak-0203, Armenia

Presenting Author: Marcis.Auzins@lu.lv

The extremely thin cell (ETC) is characterized by walls that are separated by a distance that varies from few hundred nanometres to approximately 1  $\mu\text{m}$  [1]. Obtaining and modelling theoretically magneto-optical signals in an ETC presents various challenges. Previous attempts to model the experimental signals obtained good agreement between experiment and theory for rather narrow magnetic field scans. However, satisfactory agreement could not be achieved for larger magnetic field values [2]. In order to improve the theoretical model, we have expanded it to account for effects associated with particles flying through the laser beam in a much more refined way. The laser beam profile was split into multiple sections, each of which had its own characteristic laser beam intensity and transit relaxation rate. This approach allowed us to treat the wings of the laser beam profile, where the laser intensity is much lower than in the centre of the beam. Furthermore, a new approach to atom-wall collisions was applied by averaging over different velocity groups for the velocity in the direction perpendicular to the cell walls. To test the new features of the theoretical model in detail we chose the Cs D1 line, for which magneto-optical resonances have not been studied in an ETC, and which provides a simple system to test the physical effects that take place in this type of cell.

Magneto-optical signals were observed in fluorescence from one side of the ETC. The detector collected fluorescence light emitted in a direction that was nearly perpendicular to the laser beam. Although the fluorescence signal is weak, it is easier to separate it from the background, and its intensity is less subject to the interference effects that result from the etalon formed by the ETC walls and that are pronounced in absorption signals. The ETC was placed at the centre of a three-axis Helmholtz coil system. Two pairs of coils were used to compensate the earth's magnetic field, and the third coil was used to scan the magnetic field from -55G to 55G. To achieve detectable signals, the ETC was placed in small oven that was built in such a way that it practically produced no stray magnetic fields. To gain insight into processes within the ETC and to test the model, we measured the dependence of the signal on temperature, laser power, and cell thickness for different transitions. The experimental results were compared to theoretical calculations.

This work was supported by Latvian Science Council grant 119/2012.

### References

- [1] D. Sarkisyan *et al.* Opt. Commun. 200, 201 (2001)
- [2] M. Auzinsh *et al.* Phys. Rev A **81** 033408 (2010)

## The identification of stable dark states of a single nitrogen vacancy (NV) center surrounded by several $^{13}\text{C}$ atoms in a diamond lattice

M. Auzinsh<sup>1</sup>, L. Kalvans<sup>1</sup>, R. Lazda<sup>1</sup>, J. Smits<sup>1</sup>, and L. Busaite<sup>1</sup>

<sup>1</sup>*Laser Center, University of Latvia, Zellu street 8, Riga, Latvia*

Presenting Author: marcis.auzinsh@lu.lv

Initially the spin Hamiltonian method [1,2] is applied for a system composed of a single nitrogen-vacancy (NV) center in a diamond and several  $^{13}\text{C}$  atoms at nearby lattice sites. The NV centers have spin  $S = 1$ , whereas the  $^{13}\text{C}$  atoms have spin  $S = 1/2$ . The eigenvalues and eigenfunctions of the ground state of said system are calculated.

Then those eigenfunctions that could be related to a  $\Lambda$  scheme formed by a two-photon resonance excited by a single microwave source are identified.

Afterwards we examine whether the two-photon resonance criterion remains valid as the magnetic field value is changed by the interaction of  $^{13}\text{C}$  atoms located at more distant lattice sites. If so, a stable dark state is identified. Finally we evaluate if the dark state's position with respect to the microwave frequency remains stable as the magnetic field is changed. Thus we attempt to explain certain characteristics of the ODMR spectra obtained from a  $^{13}\text{C}$  isotopically enriched diamond crystal.

This research is kindly supported by NATO Science for Peace project CBP.MD.SFPP.98839: "Novel Magnetic Sensors and Techniques for Security Applications."

### References

- [1] A. P. Nizovtsev, Kilin S. Ya., Pushkarchuk V. A. Optics and Spectroscopy V **108**, 239–246 (2010)
- [2] A. P. Nizovtsev, Kilin S. Ya., Pushkarchuk V. A. Optics and Spectroscopy V **108**, 230–238 (2010)

## The $g$ -factors of lithiumlike $^{40,48}\text{Ca}^{17+}$ and their isotopic effect

F. Köhler<sup>1,2,3</sup>, J. Hou<sup>2</sup>, S. Sturm<sup>2</sup>, A. Wagner<sup>2</sup>, G. Werth<sup>4</sup>, W. Quint<sup>1,3</sup>, and K. Blaum<sup>2</sup>

<sup>1</sup>GSI Helmholtzzentrum für Schwerionenforschung, D-64291, Darmstadt

<sup>2</sup>Max-Planck-Institut für Kernphysik, D-69117, Heidelberg

<sup>3</sup>Ruprecht-Karls-Universität, D-69117, Heidelberg

<sup>4</sup>Johannes Gutenberg-Universität, D-55122, Mainz

Presenting Author: florian.koehler.email@googlemail.com

High-precision measurements of the gyromagnetic factor ( $g$ -factor) of an electron bound to a nucleus - a hydrogenlike ion - provide the opportunity to determine fundamental constants [1] and to test the theory of quantum electrodynamics of bound systems (BS-QED). The most stringent test of BS-QED in a strong electric field ( $\approx 2 \cdot 10^{-15}$  V/m) has been performed by measuring the  $g$ -factor of hydrogenlike silicon  $^{28}\text{Si}^{13+}$  with a relative uncertainty of  $7 \cdot 10^{-11}$  [2]. The comparison of the measured  $g$ -factor of lithiumlike silicon,  $^{28}\text{Si}^{11+}$ , with its theoretical prediction enabled the most stringent test of electron-electron interaction [3].

To test BS-QED under even stronger conditions we are currently measuring bound electron  $g$ -factors with heavier nuclei. The comparison of the  $g$ -factors of lithiumlike  $^{40}\text{Ca}^{17+}$  and lithiumlike  $^{48}\text{Ca}^{17+}$  will provide the first direct measurement of the isotopic effect. The dominant contribution to the isotopic effect is the recoil correction [4].

To produce the different isotopes in a closed setup we use a miniature electron-beam-ion-source with an enriched calcium-target. After the creation-process the single ion is trapped for several months in a triple Penning trap apparatus. The  $g$ -factor is determined by measuring the ratio between the spin-precession frequency of the bound electron to the cyclotron frequency of the ion. The spin-state is determined by applying the continuous Stern-Gerlach effect. The cyclotron frequency is measured with a novel phase-sensitive detection technique, PnA (Pulse and Amplify) [5], working at ultra-low temperatures.

The experimental setup, the measurement principle, detection methods and the status of the  $g$ -factor measurements of different calcium isotopes will be presented.

### References

- [1] S. Sturm *et al.* Nature **506**, 13026 (2014)
- [2] S. Sturm *et al.* Phys. Rev. Lett. **107**, 023002 (2011)
- [3] A. Wagner *et al.* Phys. Rev. Lett. **110**, 033003 (2013)
- [4] V.M. Shabaev Phys. Rev. A **64**, 052104 (2001)
- [5] S. Sturm *et al.* Phys. Rev. Lett. **107**, 143003 (2011)

# The self-energy of bound electron

J. Zamastil<sup>1</sup> and V. Patkóš<sup>1</sup>

<sup>1</sup>Department of Chemical Physics and Optics, Charles University, Faculty of Mathematics and Physics, Ke Karlovu 3, 121 16 Prague 2, Czech Republic

Presenting Author: patkosv@email.cz

In present time accuracy of spectroscopic measurements achieved fantastic accuracy 1 part in 10 to the power 14. If these measurements are followed by theoretical calculations of similar accuracy we can test quantum electrodynamics and part of the standard model responsible for parity violating weak forces by comparing theory and experiment and set some of the basic physical constants like Rydberg constant, mass and radius of nucleus, constant of fine structure etc. For achieving this kind of accuracy of calculations one must take into account the so called radiation corrections and in particular the most important of them, the self-energy of bound electron. Our method is based on one single assumption, namely that except for the part of the time component of the electron four-momentum corresponding to the electron rest mass, the exchange of four-momentum between the virtual electron and photon can be treated perturbatively. This assumption holds very well, except for the electron virtual states with very high three-momentum. It can be shown that for such virtual states one can always rearrange the pertinent expression in a way that allows the electron to be treated as free. The fraction of the free-particle approximation contained in the relativistic multipole expansion carried out to a given order can be precisely determined. By taking the method up to the ninth order and estimating the remainder of the series, the result obtained for the ground state of the hydrogen atom differs from the other result of comparable accuracy by 2 parts in 10<sup>9</sup>. This amounts to the difference of 18 Hz for 2s – 1s transition in hydrogen. This is by four orders smaller than the uncertainty in determination of the proton radius.

For years the self-energy for the atoms with low nuclear charges has been calculated via the series in powers of  $Z\alpha$

$$\Delta E = \frac{m\alpha(Z\alpha)^4}{\pi n^3 s^3} F(Z\alpha, n, l_j). \quad (1)$$

The more recent methods used to calculate self-energy are based on the partial wave expansion. However, for atoms with low nuclear charges this method converges very slowly. Nonetheless, the most accurate results obtained so far for the hydrogen atom were obtained in [1] by means of this expansion. In that paper several millions of partial waves were considered. For each partial wave there is a three-dimensional integration to be performed numerically

Our method is based on the assumption that the four-momentum of the bound electron in virtual states is dominated by the four-momentum of the electron at rest:

$$\frac{1}{k^2 - 2k \cdot \varepsilon + H - 2k \cdot (\Pi - \varepsilon)} = \frac{1}{z - \tilde{H}_0 - \lambda \tilde{H}_1}, \quad (2)$$

where  $\varepsilon$  is the four-momentum of electron at rest,  $k$  is the four-momentum of photon and  $\Pi$  is the four-momentum of virtual electron. Only few terms have to be taken in order to get the desired accuracy. The only integrals to be performed numerically are one-dimensional integrals over the electron wave numbers of the continuous part of the spectrum. Taking the method to the ninth order we obtain results

| Term  | $F(\alpha, 1, 0)$ |
|-------|-------------------|
| Lead  | 10.315870916      |
| Total | 10.316793675(50)  |
| Other | 10.316793650(1)   |

**Table 1:** Lead order stands for the first two terms in the expansion. Total is the method taken to the ninth order. Other stands for the result taken from [1].

## References

- [1] U. D. Jentschura et al, Phys. Rev. A **63**, 042512 (2001).  
(2001). See also U. D. Jentschura et al, Phys. Rev. Lett. **82**, 53 (1999).
- [2] J. Zamastil and V. Patkóš, Phys. Rev. A **86**, 042514 (2012).
- [3] J. Zamastil and V. Patkóš, Phys. Rev. A **88**, 032501 (2013).

# Modification of The Atomic Scattering Factor in Electric Field

S.Y. Yousif Al-Mulla<sup>1</sup>

<sup>1</sup>University of Borås/College of Engineering/ S-50190 Borås/ Sweden

Presenting Author: Samir.Al-Mulla@hb.se

Quantum mechanical calculations of a modification of the X-ray scattering form factor of an atom/ion in an electric field using a three parameter wave function have been performed. These calculations are compared with the previous two parameter wave function calculations. The X-ray atomic scattering factor for an unperturbed atom with N electron is given by:

$$f_0 = \sum_{j=1}^N \psi_0^* \exp(i\chi S \cdot r_j) \psi_0 d\tau = \sum_{j=1}^N \psi_0^* \exp(iK r_j \cos \theta_j) \psi_0 d\tau$$

In the presence of an electric field F, the wave function is perturbed,

$$f = f_0 + i f_1 F + O(F^2) \text{ where } i f_1 F = 2F \sum_{j=1}^N \int \psi_0^* \exp(iKS \cdot r_j) \psi_1 d\tau$$

We use the Kirkwood - Pople-Schofield approach for the wave function

$$\psi = \psi_0 \left[ 1 + \sum_j u(r_j) \right] \text{ where } u(r) = F(\mu r + \nu r^2 + \eta r^3) \text{ and the } f_1 \text{ is given by}$$

$$i f_1 F = 2F \sum_i \sum_j \psi_0^* \exp(iKS \cdot r_j) (\mu r_i + \nu r_i^2 + \eta r_i^3) \cos \theta_i \psi_0 d\tau$$

The optimal values of  $\mu$ ,  $\nu$  and  $\eta$  are determined variationally and calculated from various moments of the unperturbed charge distribution using a single Slater determinant.

|     | Ne    |       | Na <sup>+</sup> |       | Fe <sup>-</sup> |       |
|-----|-------|-------|-----------------|-------|-----------------|-------|
| K   | (a)   | (b)   | (a)             | (b)   | (a)             | (b)   |
| 0.2 | 0.522 | 0.524 | 0.206           | 0.207 | 2.19            | 2.21  |
| 0.6 | 1.330 | 1.314 | 0.563           | 0.542 | 4.520           | 4.450 |
| 1.0 | 1.620 | 1.581 | 0.775           | 0.743 | 3.932           | 3.661 |
| 1.4 | 1.450 | 1.391 | 0.821           | 0.806 | 2.378           | 2.239 |
| 1.8 | 1.043 | 1.004 | 0.731           | 0.716 | 0.991           | 0.930 |
| 2.2 | 0.604 | 0.583 | 0.566           | 0.560 | 0.012           | 0.006 |
| 2.6 | 0.206 | 0.201 | 0.383           | 0.371 |                 |       |
| 3.0 | 0.023 | 0.020 | 0.211           | 0.200 |                 |       |

(a) Two parameter wave function

(b) Three parameter wave function

**Table 1:** The magnitude of the modified X-ray scattering factor per unit applied field with scattering vector K in inverse atomic units.

## References

- [1] J.A.D. Matthew, S.Y. Yousif, Acta Crys. A **40**, 716 (1984).
- [2] J.A.D. Matthew, S.Y. Yousif, Molec. Phys. **51**, 175 (1984).
- [3] K. Andersson, A. Sadlej, J. Phys. Rev. A **46**, 2356 (1992).
- [4] S.Y. Yousif Al-Mulla, Physica Scripta **61**, 417 (2000).

## Rubidium spectroscopy in high magnetic fields

S. Scotto<sup>1,2</sup>, R. Battesti<sup>1</sup>, M. Fouché<sup>1</sup>, E. Arimondo<sup>1,2</sup>, D. Ciampini<sup>2</sup>, and C. Rizzo<sup>1</sup>

<sup>1</sup>*Laboratoire National des Champs Magnétiques Intenses (UPR 3228, CNRS-UPS-UJF-INSA), 31400 Toulouse, France*

<sup>2</sup>*Dipartimento di Fisica 'E. Fermi', Università di Pisa, Largo Pontecorvo 3, 56127 Pisa, IT*

Presenting Author: stefano.scotto@lncmi.cnrs.fr

Alkali atoms have been extensively studied in the field of atomic spectroscopy. Here we present spectroscopical data of a rubidium vapor immersed in a static magnetic field generated by permanent magnets. This kind of investigations could in principle open possibilities in high magnetic field metrology (greater than 100 G) with optical probes. This challenge directly leads to the measurement of Landé g-factors for excited states of alkalis, which are nowadays poorly known. Landé g-factor has a long history of improvement in experimental determinations and theoretical calculations. For a free electron, while Dirac equation predicts a value of  $g_e = 2$ , quantum electrodynamics corrects this value reaching a very good agreement between theory and experiments. In a bound state, such as an atom, we have to consider the Landé  $g_J$  factor relative to the J total angular momentum. Schroedinger level atomic physics predicts its value, a combination of the free-electron value and the value associated to the orbital angular momentum. Deviations from that prediction are produced by core-valence correlation, relativistic effects and bound-state QED, these effects being of the order of  $10^{-5} - 10^{-6}$ .

## Towards the hyperfine spectroscopy of ground-state antihydrogen atoms

M. Tajima<sup>1</sup>, N. Kuroda<sup>1</sup>, S. Ulmer<sup>2</sup>, D.J. Murtagh<sup>3</sup>, S. Van Gorp<sup>3</sup>, Y. Nagata<sup>3</sup>, M. Diermaier<sup>4</sup>, S. Federmann<sup>5</sup>, M. Leali<sup>6,7</sup>, C. Malbrunot<sup>(4),5</sup>, V. Mascagna<sup>6,7</sup>, O. Massiczek<sup>4</sup>, K. Michishio<sup>8</sup>, T. Mizutani<sup>1</sup>, A. Mohri<sup>3</sup>, H. Nagahama<sup>1</sup>, M. Ohtsuka<sup>1</sup>, B. Radics<sup>3</sup>, S. Sakurai<sup>9</sup>, C. Sauerzopf<sup>4</sup>, K. Suzuki<sup>4</sup>, H.A. Torii<sup>1</sup>, L. Venturelli<sup>6,7</sup>, B. Wünschek<sup>4</sup>, J. Zmeskal<sup>4</sup>, N. Zurlo<sup>6,7</sup>, H. Higaki<sup>9</sup>, Y. Kanai<sup>3</sup>, E. Lodi Rizzini<sup>6,7</sup>, Y. Nagashima<sup>8</sup>, Y. Matsuda<sup>1</sup>, E. Widmann<sup>4</sup>, and Y. Yamazaki<sup>1,3</sup>

<sup>1</sup>*Institute of Physics, Graduate School of Arts and Sciences, University of Tokyo, Tokyo 153-8902, Japan*

<sup>2</sup>*Ulmer Initiative Research Unit, RIKEN, Saitama 351-0198, Japan*

<sup>3</sup>*Atomic Physics Laboratory, RIKEN, Saitama 351-0198, Japan*

<sup>4</sup>*Stefan-Meyer-Institut für Subatomare Physik, Österreichische Akademie der Wissenschaften, Wien 1090, Austria*

<sup>5</sup>*CERN, Genève 1211, Switzerland*

<sup>6</sup>*Dipartimento di Ingegneria dell'Informazione, Università di Brescia, Brescia 25133, Italy*

<sup>7</sup>*Istituto Nazionale di Fisica Nucleare, Gruppo Collegato di Brescia, Brescia 25133, Italy*

<sup>8</sup>*Department of Physics, Tokyo University of Science, Tokyo 162-8601, Japan*

<sup>9</sup>*Graduate School of Advanced Sciences of Matter, Hiroshima University, Hiroshima 739-8530, Japan*

Presenting Author: tajima@radphys4.c.u-tokyo.ac.jp

A precise comparison of both hydrogen and its counterpart antihydrogen will provide a sensitive test of the CPT symmetry. The ASACUSA collaboration has developed a cusp trap system consisting of an antiproton trap, a positron source and trap, a cusp trap, and a spectrometer line to measure the hyperfine transition frequency of ground-state antihydrogen atoms at the CERN Antiproton Decelerator. In 2012, antihydrogen atoms were synthesized by injecting an ultra-slow antiproton beam into a positron plasma in the cusp trap. Figure 1 shows the electrical potential configuration on axis in the cusp trap. To counteract the axial separation of antiprotons and positrons, and to prolong the antihydrogen production period, an rf-assisted direct injection scheme was developed. As a result, we succeeded in detecting an beam of antihydrogen 2.7m downstream of the production region, where perturbing residual magnetic fields were small[1]. The next step towards the precision spectroscopy is to prepare more intense and colder beam. One possible improvement is to keep axial energy spread of antiprotons after the transportation as small as possible. During the AD shutdown in 2013, we developed such a scheme using protons. The axial energy spread of the proton beam was reduced by a factor of 6. The development of the antihydrogen beam source for in-flight spectroscopy as well as the optimization of extraction and transportation of antiprotons will be discussed.

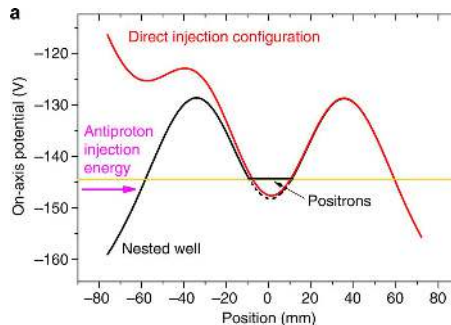


**Figure 1:** Illustration of the direct injection scheme, which is used to produce antihydrogen atoms. A positron plasma is confined and compressed at the center of the nested well. The potential is opened when antiprotons are injected into the positron plasma[1].

### References

[1] N. Kuroda *et al.* Nature Communications **5**:3089 (2014)

# Calculations of the hyperfine constants of $^{35}\text{Cl } 3p^4 4s^4 P$ and $3p^4 4p^4 D$

A. Touat<sup>1</sup>, M. Nemouchi<sup>1</sup>, T. Carette<sup>2</sup>, and M.R. Godefroid<sup>2</sup>

<sup>1</sup>Laboratoire d'Électronique Quantique, Faculté de Physique, Université des Sciences et Technologies Houari Boumediene, Algiers, Algeria

<sup>2</sup>Service de Chimie Quantique et Photophysique, CP160/09, Université Libre de Bruxelles, Brussels, Belgium

Presenting Author: atouat@usthb.dz

This work follows previous work on ab-initio calculations of hyperfine constants of some atomic states of nitrogen [1,2], fluorine [3,4] and oxygen [4]. For all these elements and also chlorine, hyperfine spectra was measured using saturation absorption spectroscopy [5-8]. In general a good agreement between theoretical and experimental values of the hyperfine constants were obtained. All calculations mentioned in [1-4] were performed using ATSP-2K [9] and GRASP-2K [10] codes.

For the first time the hyperfine structures of  $^{35}\text{Cl } 3p^4 4s^4 P_{1/2,3/2,5/2}$  and  $3p^4 4p^4 D_{1/2,3/2,5/2,7/2}$  are investigated theoretically. We use Multiconfiguration HartreeFock (MCHF) method, included in ATSP-2k code, comparing different correlation models. The influence of the relativistic effects on the hyperfine structures is investigated by using the Breit-Pauli approximation, also included in the ATSP-2k code.

The preliminary results show that the valence-valence correlation is the dominant effect, while the influence of relativistic effects on the hyperfine constants is negligible. These conclusions are made by comparing our theoretical results with experimental values [8] and between which there is a satisfactory agreement.

## References

- [1] P. Jönsson *et al.* J. Phys. B: At. Mol. Opt. Phys. **43**, 115006-12 (2010)
- [2] T. Carette *et al.* Eur. Phys. J. D **60**, 231-242 (2010)
- [3] T. Carette *et al.* Phys. Rev. A **88** 042501-9 (2013)
- [4] N. Aourir *et al.*, in preparation
- [5] R.M. Jennerich, A.N. Keiser, and D.A. Tate, Eur. Phys. J. D **40**, 81-89 (2006)
- [6] D. A. Tate and D. N. Aturaliye, Phys. Rev. A **56**, 1844-1854 (1997)
- [7] R. M. Jennerich and D. A. Tate, Phys. Rev. A, **62**, 042506-12 (2000)
- [8] D.A. Tate and J.P. Walton, Phys. Rev. A **59**, 1170-1177 (1999)
- [9] C. Froese Fischer *et al.* Comput. Phys. Commun. **176** 559- 579 (2007)
- [10] P. Jönsson *et al.* Comput. Phys. Commun. **184** 2197- 2203 (2013)

## Coincidence studies of electron impact excitation of Zn atoms

M. Piwiński<sup>1</sup>, Ł. Kłosowski<sup>1</sup>, D. Dziczek<sup>1</sup>, and S. Chwirot<sup>1</sup>

<sup>1</sup>*Institute of Physics, Faculty of Physics, Astronomy and Informatics, Nicolaus Copernicus University, Grudziadzka 5, 87-100 Torun, Poland*

Presenting Author: Mariusz.Piwinski@fizyka.umk.pl

In recent years there has been a growing interest in zinc as a replacement material for toxic mercury in discharge lamps [1]. However, insufficient knowledge of both the Zn properties and mechanisms of the collisional excitation of the atomic states of interest has been a serious obstacle to improving the Zn bulb technology. Due to limited experimental and theoretical data on electron scattering from zinc atoms, recently some attention has been focused in this direction [2,3,4].

The electron-photon coincidence experiment in the coherence analysis version was used to obtain the most detailed information about impact excitation of zinc atoms to  $4^1P_1$  state. The present work is a continuation of our research on electron impact excitation of Zn atom [2,3] and a part of broader studies concerning the atoms with two valence electrons outside relatively inert core like Ca [5], Cd [6,7] and He [8]. Geometry of the experiment which was typical for the coherence analysis technique and the experimental set-up and procedures were described in our earlier work [2].

Stokes and Electron Impact Coherence Parameters (EICPs) for electronic excitation of  $4^1P_1$  state of zinc atoms has been measured for incident electron energy of 60 eV. Examples of graphical representations of angular distributions of the electron charge cloud of the excited  $4^1P_1$  state of Zn corresponding to the values of the EICPs for angles  $10^\circ$  and  $20^\circ$  are presented in Figure 1.

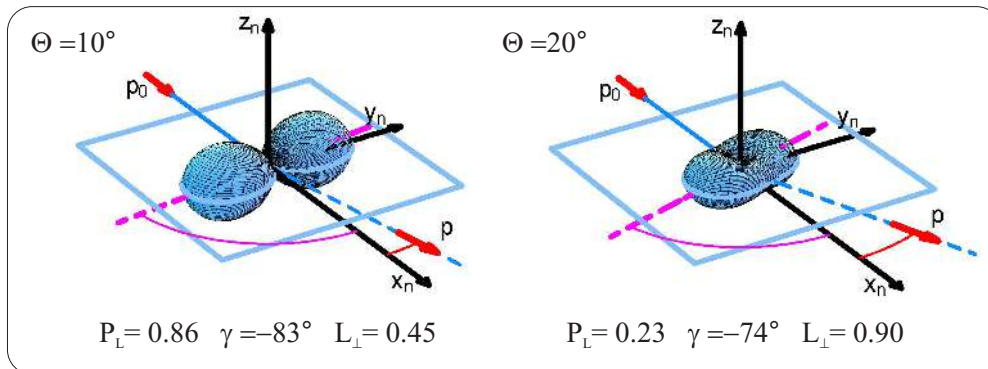


**Figure 1:** Graphical representations of angular distribution of electron charge cloud corresponding to the measured EICPs for Zn  $4^1P_1$  excitation by 60 eV electrons for scattering angles  $10^\circ$  and  $20^\circ$ .

### References

- [1] M. Born and M. Strösser *J. Phys. D: Appl. Phys.* **40**, 3823–3828 (2007)
- [2] M. Piwiński *et al.* *Phys. Rev. A* **86**, 052706 (2012)
- [3] M. Piwiński *et al.* *Eur. Phys. J.-Spec. Top.* **222**, 2273–2277 (2013)
- [4] Tapasi Das *et al.* *Phys. Lett. A* **378**, 641–643 (2014)
- [5] D. Dyl *et al.* *J. Phys. B: At. Mol. Opt. Phys.* **32**, 837–844 (1999)
- [6] M. Piwiński *et al.* *J. Phys. B: At. Mol. Opt. Phys.* **35**, 3821–3827 (2002)
- [7] M. Piwiński *et al.* *J. Phys. B: At. Mol. Opt. Phys.* **39**, 1945–1953 (2006)
- [8] Ł. Kłosowski *et al.* *Phys. Rev. A* **80**, 062709 (2009)

## Two-photon Excitation of high-lying 4d levels in FeII and oscillator strengths for non-LTE stellar atmosphere models

H. Hartman<sup>1,2</sup>, L. Engström<sup>3</sup>, H. Lundberg<sup>3</sup>, and H. Nilsson<sup>2</sup>

<sup>1</sup>*Applied Math and Materials Science, Malmö University, SE-20506 MALMÖ, SWEDEN*

<sup>2</sup>*Lund Observatory, Lund University, SE-22100 LUND, SWEDEN*

<sup>3</sup>*Department of Physics, Lund University, SE-22100 LUND, SWEDEN*

Presenting Author: lars.engstrom@fysik.lth.se

We report on experimental lifetimes for high-excitation 4d levels in FeII and oscillator strengths for the 4p-4d decays from these levels. These transitions are of importance for abundance studies and for non-LTE stellar atmosphere model. One step excitations can reach odd parity levels in the FeII energy level system. However, for higher excitation even parity levels, such as 4d or 5s, processes involving multiple photons must be used. We have utilized two-photon excitation, where the upper level has same parity as the lower level and the energy of the exciting laser tuned to half of the transition energy. The radiative lifetimes are combined with relative intensities for the decay channels, as measured from FTS spectroscopy of a hollow cathode discharge lamp.

We discuss the technique, report on experimental values and comparisons with calculations, and applications to stellar spectroscopy.

## The FERRUM project: Experimental Transition Probabilities from Highly Excited Even 5s Levels in Cr II

L. Engström<sup>1</sup>, H. Lundberg<sup>1</sup>, H. Nilsson<sup>2</sup>, H. Hartman<sup>2,3</sup>, and E. Bäckström<sup>4</sup>

<sup>1</sup>*Department of Physics, Lund University, SE-22100 LUND, SWEDEN*

<sup>2</sup>*Lund Observatory, Lund University, SE-22100 LUND, SWEDEN*

<sup>3</sup>*Applied Math and Materials Science, Malmö University, SE-20506 MALMÖ, SWEDEN*

<sup>4</sup>*Department of Physics, Stockholm University, SE-10691 STOCKHOLM, SWEDEN*

Presenting Author: lars.engstrom@fysik.lth.se

We report lifetime measurements of the 5 levels in the  $3d^4(a^5D)5s e^6D$  term in Cr II at an energy around  $83000 \text{ cm}^{-1}$  and  $\log(gf)$  values for 38 transitions from the investigated levels. The results are obtained using time-resolved laser-induced fluorescence on ions from a laser-produced plasma. Since the levels have the same parity as the low-lying states directly populated in the plasma, we used a two-photon excitation scheme. This process is greatly facilitated by the presence of the  $3d^4(a^5D)4p z^6F$  levels at roughly half the energy difference. The  $f$ -values are obtained by combining the experimental lifetimes with branching fractions derived using relative intensities from a hollow cathode lamp recorded with a Fourier Transform spectrometer.

We discuss the techniques, report on experimental values and comparisons with theoretical calculations.

# Computer modelling of intensities of helium Stark lines in regions of levels anticrossings.

R. Drozdowski<sup>1</sup>, J. Kwela<sup>1</sup>, and L. Windholz<sup>2</sup>

<sup>1</sup>*Institute of Experimental Physics, University of Gdańsk, ul. Wita Stwosza 57, 80-952 Gdańsk, Poland*

<sup>2</sup>*Institut für Experimentalphysik, Technische Universität Graz, Petersgasse 16, 8010 Graz, Austria*

Presenting Author: fizrd@ug.edu.pl

Studies of the Stark effect of noble gas atoms have been performed since the discovery of this effect in 1913. Nevertheless, these investigations were restricted to relatively low field strengths; thus, several effects, like levels-anticrossings, which appear in high electric fields, remained unnoticed and undescribed. Theoretical description of the Stark effect in high fields is very difficult and needs high computer power, since the electric field mixes states with different parities and different principal quantum numbers. Thus, calculation with huge energy matrices is necessary. Furthermore, many specific atomic data from other experiments or calculations are needed. For many years systematic experimental investigations of the Stark effect of the noble gases He, Ne, Ar, Kr and Xe have been performed in Graz. However, because of difficulties with theoretical interpretation of the spectra only a small part of the result has been published so far.

From the theoretical point of view the case of the lightest noble gas, He, is the most convenient for description. The structure of He is relatively well known and for higher atomic states the approximation of hydrogen-like wave function can be used.

In our earlier papers [1, 2] we presented experimental and theoretical investigations of shifts of lines from spectral series  $2^3P - n^3Q$  ( $n = 3 \div 10$ ,  $Q = S, P, D, \dots$ ),  $2^1S - n^1Q$  ( $n = 3 \div 9$ ,  $Q = S, P, D, \dots$ ) and  $2^1P - n^1Q$  ( $n = 3 \div 9$ ,  $Q = S, P, D, \dots$ ) in electric fields up to 1600 kV/cm. The applied fields were high enough that patterns belonging to neighboring principal quantum numbers overlapped each other - we observed interesting levels - anticrossings effects. These effects are reflected in a variation of intensities of the observed Stark lines. By matching various superpositions of the excited states in the intensity calculations we can follow results of observation. We performed computer simulations for the levels anticrossings regions between  $n = 6, 7$  and  $n = 7, 8$  in the second triplet series ( $2^3P - n^3Q$ ,  $Q = S, P, D, \dots$ ).

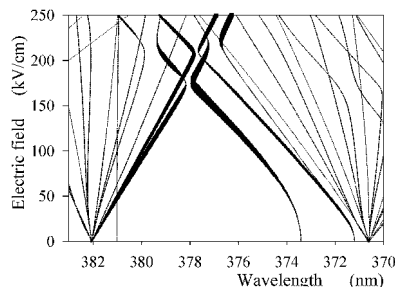


**Figure 1:** Intensities of four strongest Stark lines obtained in computer simulations for the anticrossing region  $n = 6, 7$ . We considered excitation of parabolic triplet states:  $|6401\rangle$ ,  $|6500\rangle$ ,  $|7060\rangle$  and  $|7051\rangle$ .

This work has been supported by the grant 008/2012/2013/2014 for Scientific and Technical Cooperation between Poland and Austria.

## References

- [1] L. Windholz *et al.* Phys. Scr. **78** 065303 (2008)
- [2] L. Windholz *et al.* J. Opt. Soc. Am. B **29** 934 (2012)

# A Widely Tunable 10 $\mu\text{m}$ QCL Locked to a Metrological Mid-IR Reference for Precision Molecular Spectroscopy

P.L.T Sow<sup>1,2</sup>, S. Mejri<sup>2,1</sup>, S.K Tokunaga<sup>2,1</sup>, O. Lopez<sup>1,2</sup>, A. Goncharov<sup>1,2,3</sup>, A. Argence<sup>1,2</sup>, C. Chardonnet<sup>1,2</sup>, A. Amy-Klein<sup>2,1</sup>, B. Darquié<sup>1,2</sup>, and C. Daussy<sup>2,1</sup>

<sup>1</sup>CNRS, UMR 7538, LPL, 93430 Villetaneuse, France

<sup>2</sup>Université Paris 13, Sorbonne Paris Cité, Laboratoire de Physique des Lasers, 93430 Villetaneuse, France

<sup>3</sup>Permanent address: Institute of Laser Physics of SB RAS, Pr. Lavrentyeva 13/3, Novosibirsk, 630090 Russia

Presenting Author: papalattabara.sow@univ-paris13.fr

The quantum cascade lasers (QCL) are popular sources for spectroscopy in the field of mid-infrared because of the wide range of wavelengths they can cover ( $3 \mu\text{m} < \lambda < 24 \mu\text{m}$ ) [1]. Several examples of spectroscopic measurements with spectrometers based on QCL have been reported [2].

We are currently developing a laser spectrometer based on a near-room-temperature distributed feedback QCL which emits around  $10 \mu\text{m}$ . The QCL source has been compared to an ultra-stable  $\text{CO}_2$  laser.

We characterized the free-running QCL and demonstrated a frequency noise roughly one order of magnitude lower than previously published characterizations of QCLs. A full width at half maximum (FWHM) of 60 kHz for the beat signal between the free-running QCL and a 1-kHz narrow  $\text{CO}_2$  laser was observed for 1 ms of integration time.

We have also demonstrated a narrowing of the QCL by a coherent phase-lock to a  $\text{CO}_2$  laser stabilized onto a saturated absorption line of  $\text{OsO}_4$ . The beat spectrum (see Fig. 1) between phase-locked QCL and  $\text{CO}_2$  laser recorded with a radio-frequency (RF) spectrum analyzer allowed us to estimate that more of 99% of the beat signal RF power is concentrated in the laser carrier. This allows to conclude that the QCL reproduces almost exactly the spectral characteristics of our ultra-stable  $\text{CO}_2$  laser (10-Hz line width, accuracy of a few tens of hertz). This results in record QCL line width of the order of 10 Hz, 3 to 4 orders of magnitude lower than a free-running QCL, and a relative stability at 1 s of about 1 Hz.

The phase-locked QCL was then used to record spectra of ammonia ( $\text{NH}_3$ ) and methyltrioxorhenium (MTO) (see Fig. 2) to demonstrate its potential for two main projects of our group: the determination of the Boltzmann constant,  $k_B$ , by Doppler spectroscopy of ammonia [3] and the first observation of parity violation in chiral molecules [4].

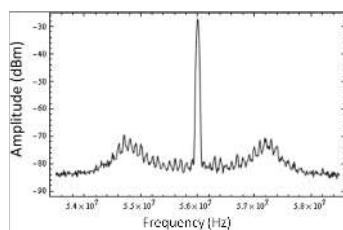


**Figure 1:** Beat signal spectrum between the frequency-stabilized  $\text{CO}_2$  laser and the phase-locked QCL recorded with a RF spectrum analyzer (30 kHz resolution band-width).

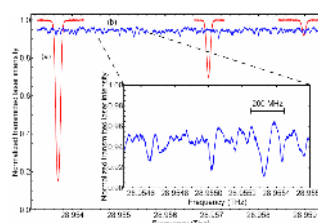


**Figure 2:** Linear absorption spectra of  $\text{NH}_3$  (red curve (a)) and MTO (blue curve (b))

## References

- [1] Kosterev *et al.*. Applied Physics B, **90(2)**, 165-176 (2008)
- [2] Wysocki *et al.*. Applied Physics B, **92(3)**, 305-311 (2008)
- [3] C. Lemarchand *et al.*. Metrologia **50** 623 (2013)
- [4] S. K. Tokunaga *et al.*. Molecular Physics 111, Issue 14-15, 2363–2373 (2013)

# Quantum State Preparation and Holography

S. Carlström<sup>1</sup>, J. Mauritsson<sup>1</sup>, and K.J. Schafer<sup>2</sup>

<sup>1</sup>Department of Physics, Lund University, PO Box 118, SE-22100 Lund, Sweden

<sup>2</sup>Department of Physics and Astronomy, Louisiana State University, Baton Rouge, LA 70803

Presenting Author: stefanos.carlstrom@fysik.lth.se

The ability to prepare and observe arbitrary quantum superpositions is an important step towards tailored chemistry. We explore the ability to use a tailored sequence of pulses to prepare an arbitrary electron wave packet (EWP) in He I. To observe that the desired wave packet was formed, we use a holographic technique, pioneered in [1, 2]: a XUV pump pulse ( $P_1$ ) is used to excite an ensemble of bound states simultaneously as a continuum EWP is produced. By applying a VUV probe pulse ( $P_3$ ) at a later time, the excited electrons can be ionized and interfere with the continuum wave packet. The tailoring is achieved by adding an extra pulse ( $P_2$ ) resonant with the 1s2p–1s3s transition of He I (see figure 1). By tuning the intensity of this control pulse, we are able to shift the population between the different states, later probed by  $P_3$  (see figure 2).

The calculations are done by solving the time-dependent Schrödinger equation in the single active electron approximation, with a very fast, newly developed GPU code that can process  $\sim 70$  k grid points/ms.

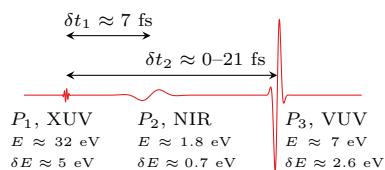


**Figure 1:** The pulse scheme:  $P_1$  is a XUV pump pulse, with broad bandwidth, capable of exciting/ionizing the atom to many bound/continuum states.  $P_2$  is a control pulse in resonance with a bound transition.  $P_3$  is a probe pulse, ionizing the remaining bound states into the continuum, where they will interfere with the states ionized by the pump pulse.

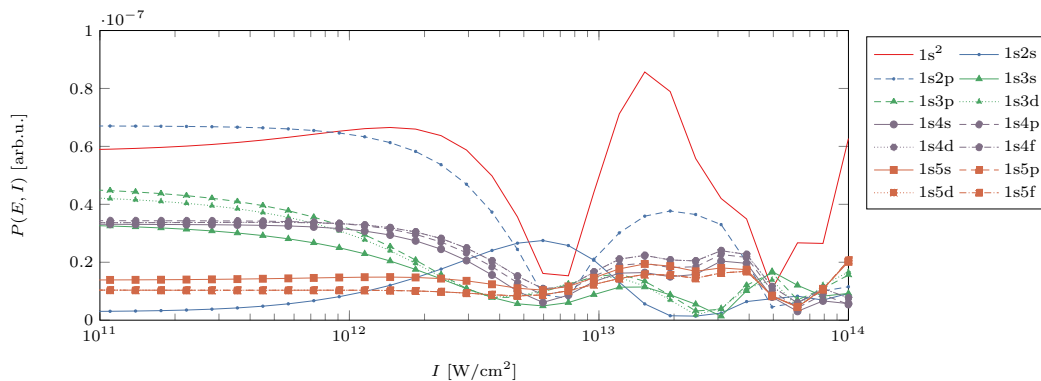


**Figure 2:** Amplitude of the different photoelectron peaks, corresponding to bound states of He I, as a function of control pulse ( $P_2$ ) intensity. The peaks are those found in the  $\beta_1$  coefficient in the Legendre decomposition of the angular photoelectron spectrum, corresponding to transitions driven with an odd number of photons.

## References

- [1] J. Mauritsson *et al.* Phys. Rev. Lett. **105** 053001 (2010), doi:10.1103/PhysRevLett.105.053001
- [2] K. Klünder *et al.* Phys. Rev. A **88**(3) 033404 (2013), doi:10.1103/PhysRevA.88.033404

# Excitation of singlet and triplet He states by neutral He - He collisions at intermediate energy range

R. Drozdowski<sup>1</sup>, E. Baszanowska<sup>2</sup>, P. Kamiński<sup>1</sup>, and G. von Oppen<sup>3</sup>

<sup>1</sup>Institute of Experimental Physics, University of Gdańsk, ul. Wita Stwosza 57, 80-952 Gdańsk, Poland

<sup>2</sup>Department of Physics, Gdynia Maritime University, ul. Morska 81-87, 81-225 Gdynia, Poland

<sup>3</sup>Institut für Atomare Physik und Fachdidaktik, Technische Universität Berlin, Hardenbergstrasse 36, D-10623 Berlin, Germany

Presenting Author: fizrd@ug.edu.pl

As was showed in several papers, the anticrossing spectroscopy has been useful to determine the states of He atoms excited by collisions with helium ion of intermediate energy. In this case, the electric field of helium ion strongly affects the evolution of the electron cloud of He atom at a longe distance. In contrast for He - He collision, the interaction between colliding objects occurs for the closest approach. Hoever, also in this case the excited helium atoms have a large electric dipole moments and the anticrossing spectroscopy is appropriate to analyze such post-collisional states.

In this work, the first time, the anticrossing spectra of the helium line  $\lambda(1s4l - 1s2p \ ^3P) = 447.2 \text{ nm}$  were measured for  $10 - 30 \text{ keV}$  helium atom - helium atom collisions. The post collisional He I states are superpositions of the zero-field eigenstates  $|1snl \ ^{1,3}L, M_L\rangle$  with different angular momenta. Therefore the transient atomic helium states can have highly asymmetric charge distribution with large electric dipole moments. By measuring the intensity  $I(F_z)$  of spectral line at electric field  $F_z$  applied to the collision volume the charge distribution can be determined [1]. Due to singlet and triplet anticrossings of Stark sublevels the characteristic anticrossing peaks appear giving especially detailed information about the post-collisional states of the excited He atoms [2]. The theoretical intensity functions were calculated taking into account cascade processes, the inhomogeneity of the axial electric field in the collision volume and the density distribution of the target He atoms [3]. Fitting the theoretical intensities to the measured ones, the post-collisional states of He atoms were determined. Figure 1 shows measured anticrossing spectra.

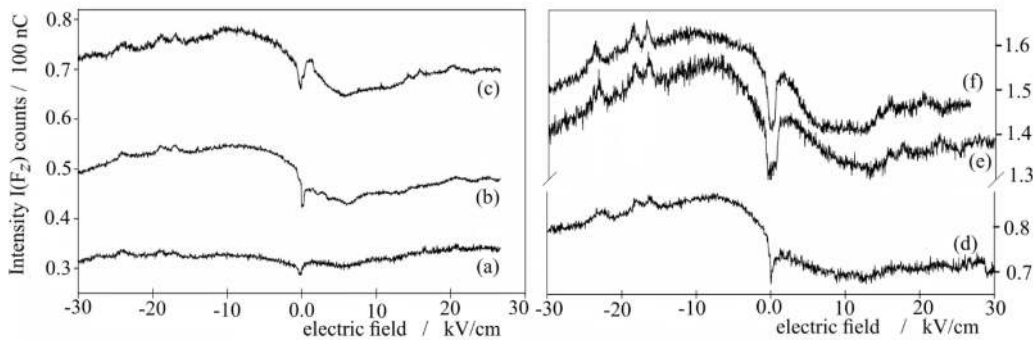


**Figure 1:** Anticrossing spectra  $I_{447}(F_z)$  measured for transition  $(1s4l \ ^3D^3F - 1s2p \ ^3P)$  for He - He collisions at impact energies of 10 keV (a), 15 keV (b), 20 keV (c), 24 keV (d), 26 keV (e), and 30 keV (f).

## References

- [1] C. C. Havener *et al.* Phys. Rev. Lett. **48** 926 (1982)
- [2] M. Busch *et al.* J. Phys B: At. Mol. Opt. Phys. **36** 4849 (2006)
- [3] E. Baszanowska *et al.* J. Phys B: At. Mol. Opt. Phys. **45** 115203 (2012)

# A transmission-line decelerator for atoms in high Rydberg states

P. Lancuba<sup>1</sup> and S.D. Hogan<sup>1</sup>

<sup>1</sup>*Department of Physics and Astronomy, University College London, London, United Kingdom*

Presenting Author: patrick.lancuba.12@ucl.ac.uk

A transmission-line decelerator, based upon the continuous motion of a set of three-dimensional electric traps above a planar array of surface-based electrodes, has been developed and demonstrated experimentally for the manipulation of samples in high Rydberg states. This device is ideally suited for accelerating, decelerating and trapping helium atoms initially travelling in fast ( $\sim 1950$  m/s) pulsed supersonic beams.

The decelerator design comprises an array of miniature metallic electrodes imprinted on an insulating substrate. These electrodes are located between two ground planes and therefore represent a segmented electrical transmission line. Deceleration is achieved by applying a set of pre-programmed oscillating electrical potentials to this array of electrodes, in a manner similar to that used in other chip-based Stark decelerators [1–3].

Our surface-based decelerator exploits the very large electric dipole moments, on the order of 10000 D, associated with Rydberg states of high principal quantum number, and can be readily combined with recently developed transmission-line guides [4] for comprehensive control of the translational motion of Rydberg atoms and molecules close to surfaces.

In general, surface-based devices for manipulating the translational motion and internal quantum states of Rydberg atoms and molecules have applications in hybrid approaches to quantum information processing involving Rydberg atoms and microwave circuits [5], in studies of Rydberg atom/molecule-surface interactions [6], and chemistry at low temperatures [7].

## References

- [1] S. D. Hogan, P. Allmendinger, H. Saßmannshausen, H. Schmutz, and F. Merkt, *Phys. Rev. Lett.* **108**, 063008 (2012)
- [2] S. A. Meek, H. Conrad, and G. Meijer, *Science*, **324**, 1699 (2009)
- [3] P. Allmendinger, J. A. Agner, H. Schmutz and F. Merkt, *Phys. Rev. A*, **88**, 043433 (2013)
- [4] P. Lancuba and S. D. Hogan, *Phys. Rev. A*, **88**, 043427 (2013)
- [5] S. D. Hogan, J. A. Agner, F. Merkt, T. Thiele, S. Filipp and A. Wallraff, *Phys. Rev. Lett.* **108**, 063004 (2012)
- [6] T. P. Softley, *Int. Rev. Phys. Chem.* **23**, 1 (2004)
- [7] M. T. Bell and T. P. Softley, *Mol. Phys.* **107**, 99 (2004)

# Measurements of anion lifetimes in the Double Electrostatic Ion Ring Experiment DESIREE: Preliminary results

O.M. Hole<sup>1</sup>, E. Bäckström<sup>1</sup>, M. Kaminska<sup>1</sup>, R. Nascimento<sup>1</sup>, J.D. Alexander<sup>1</sup>, M. Björkhage<sup>1</sup>, M. Blom<sup>1</sup>, L. Brännholm<sup>1</sup>, M. Gatchell<sup>1</sup>, P. Halldén<sup>1</sup>, F. Hellberg<sup>1</sup>, G. Källersjö<sup>1</sup>, A. Källberg<sup>1</sup>, S. Leontein<sup>1</sup>, L. Liljeby<sup>1</sup>, P. Löfgren<sup>1</sup>, A. Paál<sup>1</sup>, P. Reinhed<sup>1</sup>, S. Rosén<sup>1</sup>, A. Simonsson<sup>1</sup>, R.D. Thomas<sup>1</sup>, D. Hanstorp<sup>2</sup>, S. Mannervik<sup>1</sup>, H.T. Schmidt<sup>1</sup>, and H. Cederquist<sup>1</sup>

<sup>1</sup>Department of Physics, Stockholm University, SE-106 91 STOCKHOLM, Sweden

<sup>2</sup>Department of Physics, Göteborg University, SE-412 96 GÖTEBORG, Sweden

Presenting Author: odd.hole@fysik.su.se

The Double ElectroStatic Ion Ring ExpERiment (DESIREE) is a new tool with the primary goal of investigating interactions between internally cold anions and cations at very low center-of-mass energies [1,2]. The storage rings are situated within a cooled chamber ( $\sim 11$  K) which limits the amount of black-body radiation. This enables the storage of loosely bound atomic and molecular ions – ions that would rapidly photo-detach at ambient temperatures. The rings also have excellent vacuum conditions ( $10^{-14}$  mbar) which means that beams can be stored for long periods of time before they are lost due to collisions with the residual gas –  $1/e$  lifetimes of more than  $10^3$  seconds have been measured for several anions.

We are at present finalizing measurements of the lifetimes of the excited, metastable,  $^2P_{1/2}$  fine structure levels in the  $\text{Te}^-$ ,  $\text{Se}^-$ , and  $\text{S}^-$  ions yielding preliminary results of about half a second, a few seconds, and a few minutes respectively. These are the only excited states for these ions and they decay to the  $^2P_{3/2}$  ground states through magnetic dipole (M1) transitions. Our results appears to be consistent with earlier measurements and theory for  $\text{Te}^-$  [3,4] and  $\text{Se}^-$  [4], while no previous measurements of the  $\text{S}^-$  lifetime is available. This demonstrates that the excellent ion storage conditions in DESIREE enables lifetime studies in a new time domain presenting new challenges for theory.

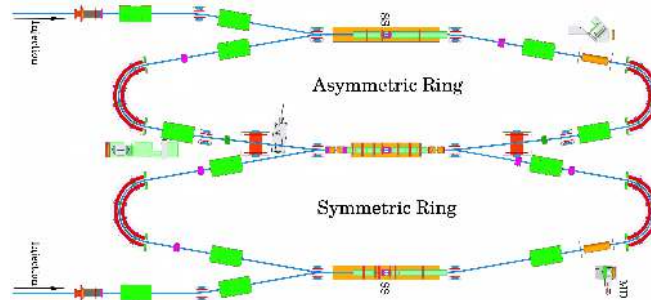


**Figure 1:** A schematic overview of the DESIREE ion optics [5]. The blue line represents the ion orbit. The measurements were done by probing the stored ion beam with a short laser pulse at the straight section (SS) of the symmetric ring. This neutralizes a minuscule fraction of the ions which could then be detected by the movable neutral detector (MD). By selecting a laser frequency that would only neutralize ions in the metastable state, we could thus monitor the population of ions in this state over time. This, together with measurements of the total ion beam lifetime, allows for the determination of the lifetimes of the metastable states.

## References

- [1] H. T. Schmidt *et al.* Rev. Sci. Instrum. **85** 055115-1-6 (2013)
- [2] R. D. Thomas *et al.* Rev. Sci. Instrum. **82** 065112-1-18 (2011)
- [3] A. Ellmann *et al.* Phys. Rev. Lett. **92** 253002-1-4 (2004)
- [4] P. Andersson *et al.* Phys. Rev. A **73** 032705-1-7 (2006)
- [5] <http://www.atom.fysik.su.se/index.php/research/experimental-group/desiree/test>

## Slow beams of cold molecular radicals for precision spectroscopy

J.S. Bumby<sup>1</sup>, J.A. Almond<sup>1</sup>, S. Skoff<sup>1</sup>, N. Fitch<sup>1</sup>, B.E. Sauer<sup>1</sup>, M.R. Tarbutt<sup>1</sup>, and E.A. Hinds<sup>1</sup>

<sup>1</sup>*Centre for Cold Matter, Imperial College London, London, SW7 2AZ*

Presenting Author: james.bumby08@imperial.ac.uk

Ultra-cold matter has a huge range of uses - from searches for new physics such as the measurement of the electron electric dipole moment (EDM) or variation of fundamental constants, to the exploration of exotic and degenerate phases of matter. Buffer gas cooling is a general method for cooling molecules to the 1 Kelvin level, and can produce molecular beams with speeds below 50m/s. Such beams are ideal for precision measurements where long interaction times are needed, or for further cooling (using laser cooling methods, for example).

We present a characterization of a buffer gas source of ytterbium monofluoride (YbF) molecules. Our source produces 5 billion ground state YbF radicals per steradian per pulse, with speeds in a range from 80 – 200  $ms^{-1}$  and translational and rotational temperatures of 4K. We consider how to load an optical molasses from this source, with the goal of producing ultracold YbF molecules for a vastly improved measurement of the electron EDM.

# Cavity optomechanics with photonic crystal nanomembrane

K. Makles<sup>1</sup>, I. Krasnokutskaja<sup>1</sup>, C. Caer<sup>1</sup>, S. Deleglise<sup>1</sup>, T. Briant<sup>1</sup>, P-F Cohadon<sup>1</sup>, A. Heidmann<sup>1</sup>, and M. Makles<sup>1</sup>

<sup>1</sup>Laboratoire Kastler Brossel, UPMC-ENS-CNRS, F-75252, Paris

Presenting Author: makles@spectro.jussieu.fr

We present a new generation of optomechanical device designed to reach the quantum ground state. It combines the high reflectivity of a photonic crystal, with the high mechanical Q-factor and low mass of a nanomembrane. Optomechanical coupling between a moving mirror and quantum fluctuations of light first appeared in the context of interferometric gravitational-wave detection. Since then, several schemes involving a cavity with a movable mirror subject to radiation pressure have been proposed to detect the quantum position fluctuations of a mechanical resonator. The zero-point motion detection of an oscillator requires high resonance frequencies (MHz to GHz) and low temperature (in the hundreds  $\mu K$  range) only achievable by combining cryogenic and active cooling techniques such as laser cooling or cold damping, and also a sufficient sensitivity to the displacement measurement (high finesse cavity).

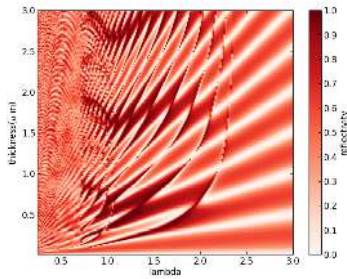


**Figure 1:** Simulation of reflectivity for various geometrical parameters of the crystal.

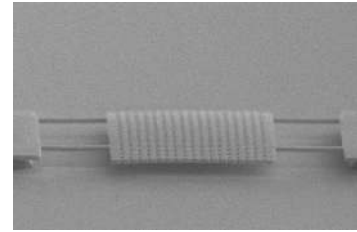


**Figure 2:** MEM view of a photonic crystal nanomembrane

Most of optomechanical devices are coated with dielectric multilayer and suffer from the low mechanical Q-factor and large mass due to the coating. In this way photonic nanomembrane thanks to the high optical reflectivity, low mass and perfect mechanical characteristics, seems to be a promising candidate for such application. High reflectivity is insured by photonic crystal which is designed to have almost a total reflection at normal incidence Fig. 1) and the absence of a coating makes possible to have a mass around 100 pg [1]. To build a cavity with such a small system ( $30 \times 30 \mu m^2$ ) (Fig. 2) we need a very small optical beam waist ( $3 \mu m$ ) therefore we have developed small radius of curvature coupling mirrors integrated in  $200 \mu m$  length cavity. The sensitivity of this cavity is at  $10^{-16} m/Hz^{1/2}$  level that is theoretically sufficient to observe the ground-state fluctuations. It has already allowed us to observe thermal noise.

We are currently developing a cold damping feedback loop in order to reduce the effective temperature of the membrane. Any active cooling relies on a viscous damping force that reduces the Q-factor of the resonator. It is then crucial to design a device with a very high initial Q-factor. Different geometries, materials, and stress in the membrane have been tested and we have achieved structures with Q-factor of 20000 at room temperature and 65000 at 20 K. We are also developing an integrated excitation scheme using capacitive coupling with the membrane. The small size of the nanomembrane give rise to a nonlinear behavior, which is due to the emergence of constraints generated by the large amplitude of displacements. We have observed both static nonlinear effect as bistability and dynamical effects such as phase conjugated generation or as the coupling between different modes of the membrane, which could be used in metrology to stabilize the oscillator frequency [2].

## References

- [1] T. Antoni, A. F. Kuhn, T. Briant, P.-F. Cohadon, A. Heidmann, R. Braive, A. Beveratos, I. Abram, L. Le Gratiet, I. Sagnes, and I. Robert-Philip *Opt. Lett.* **36** 3434 (2011)
- [2] T. Antoni, K. Makles, R. Braive, T. Briant, P.-F. Cohadon, I. Sagnes, I. Robert-Philip and A. Heidmann *et al.* *EPL* **100** 68005 (2012)

# Ultracold collisional processes in atomic traps

V.S. Melezhik<sup>1</sup>

<sup>1</sup>*Bogoliubov Laboratory of Theoretical Physics, Joint Institute for Nuclear Research, Dubna, Moscow Region 141980, Russian Federation*

Presenting Author: melezhik@theor.jinr.ru

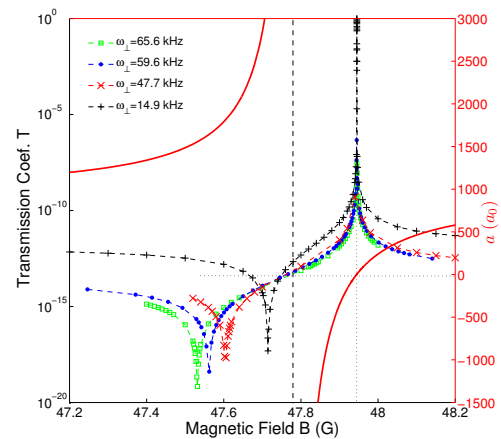
Impressive progress of the physics of ultracold quantum gases has stimulated the necessity of detailed and comprehensive investigations of collisional processes in the confined geometry of atomic traps. Here the free-space scattering theory is no longer valid and the development of the low-dimensional theory including the influence of the confinement is needed. In our works we have developed a computational method [1-3] for pair collisions in tight atomic waveguides and have found several novel effects in its application: the confinement-induced resonances (CIRs) in multimode regimes including effects of transverse excitations and deexcitations [2], the so-called dual CIR yielding a complete suppression of quantum scattering [1], and resonant molecule formation with a transferred energy to center-of-mass excitation while forming molecules [4]. Our calculations have also been used for planning and interpretation of the Innsbruck experiment on investigation of CIRs in ultracold Cs gas [5].

In the past two years we develop a theoretical model for Feshbach resonance shift and width induced by an atomic waveguide [6]. The Feshbach resonances of different tensorial structure have been used for experimental creation of the CIRs [5], however the modeling of CIRs was limited by the single-channel s-wave potentials [7]. We have calculated the shifts and widths of s-, d- and g-wave magnetic Feshbach resonances of Cs atoms in harmonic waveguides. In Figure the calculated transmission coefficient  $T$  as a function of magnetic field  $B$  and the waveguide frequency  $\omega_{\perp}$  is given near the d-wave Feshbach resonance 47.8G in Cs, where the free-space scattering length  $a(B)$  (solid curves in the Figure) diverges. We have found that  $a = 0.68a_{\perp} = 0.68\sqrt{\hbar/(\mu\omega_{\perp})}$  is fulfilled at the positions of the CIR (minimums of  $T$  in the Figure) for the Feshbach resonances of different tensorial structure. It holds in spite of the fact that this law was originally obtained in the framework of s-wave single-channel pseudopotential [7]. We have also found the linear dependence of the width of the resonance enhancement of the  $T$ -coefficient (at the point 47.95G in the Figure) on the atomic momentum and quadratic dependence on the trap width  $a_{\perp}$ . The found effect could potentially be used experimentally.

Recently, we have predicted [8] the dipolar confinement-induced resonances (DCIRs) at ultracold dipolar collisions in harmonic waveguides and quantitatively investigated the conditions for appearance of such resonances. Our model opens novel possibilities, which we plan to discuss briefly, for quantitative studies of anisotropic quantum scattering in the plane [9] and modeling quasi-2D scattering of polar molecules in “pancake” traps.

## References

- [1] V.S. Melezhik, J.I. Kim, P. Schmelcher Phys. Rev. A **76**, 053611–1–15 (2007)
- [2] S. Saeidian, V.S. Melezhik, P. Schmelcher Phys. Rev. A **77**, 042721–1–15 (2008)
- [3] V.S. Melezhik Phys. Atom. Nucl. **76**, 139–148 (2013)
- [4] V.S. Melezhik, P. Schmelcher New J. Phys. **11**, 073031–1–11 (2009)
- [5] E. Haller *et al.* Phys. Rev. Lett. **104**, 153203–1–4 (2010)
- [6] S. Saeidian, V.S. Melezhik, P. Schmelcher Phys. Rev. A **86**, 062713–1–9 (2012)
- [7] M. Olshanii Phys. Rev. Lett. **81**, 938–941 (1998)
- [8] P. Giannakeas, V.S. Melezhik, P. Schmelcher Phys. Rev. Lett. **111**, 183201 (2013)
- [9] E.A. Koval, O.A. Koval, V.S. Melezhik arXiv:1403.4432 (submitted to Phys. Rev. A)



## Three-body recombination at the scattering length's zero-crossings

O. Machtey<sup>1</sup>, Z. Shotan<sup>1</sup>, S. Kokkelmans<sup>2</sup>, and L. Khaykovich<sup>1</sup>

<sup>1</sup>*Department of Physics, Bar-Ilan University, Ramat-Gan, 52900 Israel*

<sup>2</sup>*Eindhoven University of Technology, P.O. Box 513, 5600 MB Eindhoven, The Netherlands*

Presenting Author: lev.khaykovich@biu.ac.il

We investigate the tree-body recombination rates in a gas of ultracold <sup>7</sup>Li atoms in the vicinity of scattering length's zero-crossings, e.g. when  $a \rightarrow 0$ . We show that although the two-body scattering length  $a$  and, thus, the two-body collisional cross-section vanish, the three-body recombination rates stay finite. Moreover, they can still be related to the relevant two-body parameters,  $a$  and  $R_e$ , where  $R_e$  is the effective range of the interaction potential.

Recently it has been shown that the two-body physics plays a decisive role in the universal few-body physics in ultracold gases, e. g. in the limit of  $a \rightarrow \infty$  [1 – 3]. Here we study the questions of how far the importance of two-body physics extends and what parameters govern the three-body processes in the opposite, non-universal limit, e.g. when the scattering length vanishes? These questions, to some extent, were addressed in recent theoretical studies in Refs. [4 – 6].

Assuming the dominance of the two-body physics in three-body processes, we start by considering the effective range expansion of the scattering phase shift  $\delta(k)$  in its usual form:  $k \cot(\delta(k)) = -1/a + R_e k^2/2$ . However, when  $a \rightarrow 0$  the first term diverges and to compensate this divergence the second term diverges as well ( $|R_e| \rightarrow \infty$ ), which makes the above expression inconvenient in this limit. A better form of the effective range expansion can be obtained from the standard expression with a simple algebra:  $-\tan(\delta(k))/k = a + R_e a^2 k^2/2$ . We show that although neither  $a$  nor  $R_e$  are good lengths at zero-crossings, their combination in the form of the effective recombination length  $L_e = (-R_e a^2/2)^{1/3}$  captures remarkably well the behaviour of the three-body recombination rates. No farther knowledge of the short-range two-body or three-body potentials are needed for this purpose. Moreover, while two-body collisional cross-section becomes energy dependent at zero-crossings, the tree-body recombination rate coefficient remains energy independent. In addition we show that  $L_e$  continues to be the dominate length in the inelastic three-body processes for larger scattering lengths up to a region where the universal three-body physics takes over and the leading length becomes  $a$ .

Having connected these new measurements with the previously reported results in the universal limit ( $a \rightarrow \infty$ ) [7] we can now predict the entire magnetic field dependence of the three-body recombination rates. We thus can point out a non-trivial magnetic field value at which they should vanish notifying a region where Bose-Einstein condensate's lifetime should be optimal.

### References

- [1] J. Wang, J. P. D'Incao, B. D. Esry and C. H. Greene, Phys. Rev. Lett. **108**, 263001 (2012)
- [2] R. Schmidt, S. P. Rath and W. Zwerger, Eur. Phys. J B **85**, 386 (2012)
- [3] P. K. Sorensen, D. V. Fedorov, A. S. Jensen and N. T. Zinner, Phys. Rev. A **86**, 052516 (2012)
- [4] D. S. Petrov, Phys. Rev. Lett. **93**, 143201 (2004)
- [5] M. Jona-Lasinio and L. Pricoupenko, Phys. Rev. Lett. **104**, 023201 (2010)
- [6] L. Pricoupenko and M. Jona-Lasinio, Phys. Rev. A **84**, 062712 (2011)
- [7] N. Gross, Z. Shotan, S. Kokkelmans and L. Khaykovich, Phys. Rev. Lett. **103**, 163202 (2009)

# Anisotropic optical trapping of ultracold erbium atoms

M. Lepers<sup>1</sup>, J.-F. Wyart<sup>1,2</sup>, and O. Dulieu<sup>1</sup>

<sup>1</sup>Lab. Aimé Cotton, CNRS/Univ. Paris-Sud/ENS Cachan, 91405 Orsay, France

<sup>2</sup>LERMA, Observatoire de Paris-Meudon, Univ. Pierre et Marie Curie, 92195 Meudon, France

Presenting Author: maxence.lepers@u-psud.fr

In the field of ultracold matter, dipolar quantum gases, which are composed of atoms or molecules with an intrinsic permanent electric or magnetic dipole moment, have drawn growing attention in the last few years. When they interact with each other or with an external electromagnetic field, such dipoles show an anisotropic behaviour, which means that the energy of interaction significantly depends on the relative orientation of the dipoles and the field polarization. In this respect, lanthanide atoms are of particular interest, since they possess a strong permanent magnetic dipole moment (up to 10 Bohr magnetons for dysprosium), which is due to their rich energy-level structure. The recent Bose-Einstein condensations of dysprosium [1] and erbium [2] testify to this increasing interest in lanthanides.

When confined in a dipole trap, ultracold atoms are submitted to a potential whose depth is proportional to the real part of their dynamic dipole polarizability. The atoms also experience photon scattering whose rate is proportional to the imaginary part of their dynamic dipole polarizability [3]. In this work we calculated the complex dynamic dipole polarizability of ground-state erbium, using the sum-over-state formula inherent to second-order perturbation theory. The summation is performed on transition energies and transition dipole moments from ground-state erbium, which are computed using the Racah-Slater least-square fitting procedure provided by the Cowan codes [4]. This allows us to predict 9 unobserved odd-parity energy levels of total angular momentum  $J = 5, 6$  and  $7$ , in the range  $25000\text{-}31000\text{ cm}^{-1}$  above the ground state.

Regarding the trapping potential, we find that ground-state erbium essentially behaves like a spherically-symmetric atom, in spite of its large electronic angular momentum. We also find a mostly isotropic van der Waals interaction between two ground-state erbium atoms, characterized by a coefficient  $C_6^{\text{iso}} = 1760\text{ a.u.}$ . On the contrary, the photon-scattering rate shows a pronounced anisotropy, since it strongly depends on the polarization of the trapping light [5].

## References

- [1] M. Lu *et al.* Phys. Rev. Lett. **107** 190401 (2011)
- [2] K. Aikawa *et al.* Phys. Rev. Lett. **108** 210401 (2012)
- [3] R. Grimm, M. Weidemüller, and Y.B. Ovchinnikov, At. Mol. Opt. Phys. **42**, 95 (2000)
- [4] R.D. Cowan, *The theory of atomic structure and spectra* (University of California Press, 1981)
- [5] M. Lepers, J.-F. Wyart, and O. Dulieu, Phys. Rev. A **89**, 022505 (2014)

# Anisotropic quantum scattering in plane

E.A. Koval<sup>1,2</sup>, O.A. Koval<sup>1</sup>, and V.S. Melezhik<sup>1,2</sup>

<sup>1</sup>*Bogoliubov Laboratory of Theoretical Physics, Joint Institute for Nuclear Research, Dubna, Moscow Region 141980, Russian Federation*

<sup>2</sup>*Department of Theoretical Physics, Dubna International University for Nature, Society and Man, Dubna, Moscow Region 141980, Russian Federation*

Presenting Author: e-cov@yandex.ru

We study the quantum scattering in two spatial dimensions (2D) [1]. Our computational scheme allows to quantitatively analyze the scattering parameters for the strong anisotropy of the interaction potential. High efficiency of the method is demonstrated for the 2D scattering on the cylindrical potential with the elliptical base and dipole-dipole collisions in the plane. We reproduce the result for the 2D scattering of polarized dipoles in binary collisions obtained recently by Ticknor [2] and explore the 2D collisions of unpolarized dipoles (see Figure 1). In Figure 2 the total cross section  $\sigma$  presented as a function of the angles  $\alpha$  and  $\beta$ . The cross section was calculated for the case  $Dq = 10$ , where  $D = md^2/(2\hbar^2)$  is the dipolar length and  $q = \sqrt{2mE}/\hbar$  is the relative momentum. We found progressive narrowing of the resonance area with a simultaneous decrease of the amplitudes of the resonance oscillations with increasing angle  $\beta$  from 0 to  $\pi$  due to the dominance of the repulsive feature of dipole-dipole potential for  $\beta \rightarrow \pi$ .

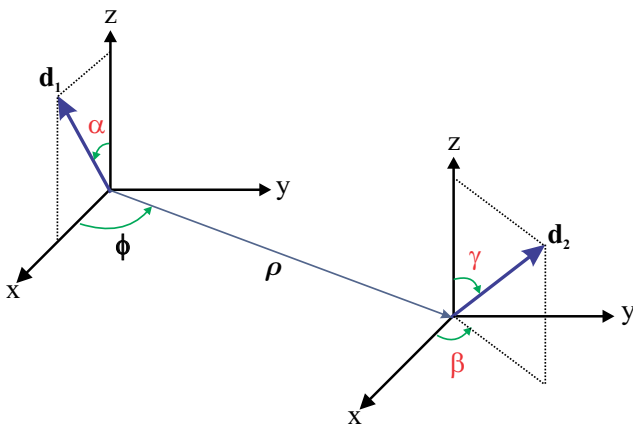


**Figure 1:** Collision in the plane  $XY$  of two arbitrarily oriented dipoles  $d_1$  and  $d_2$

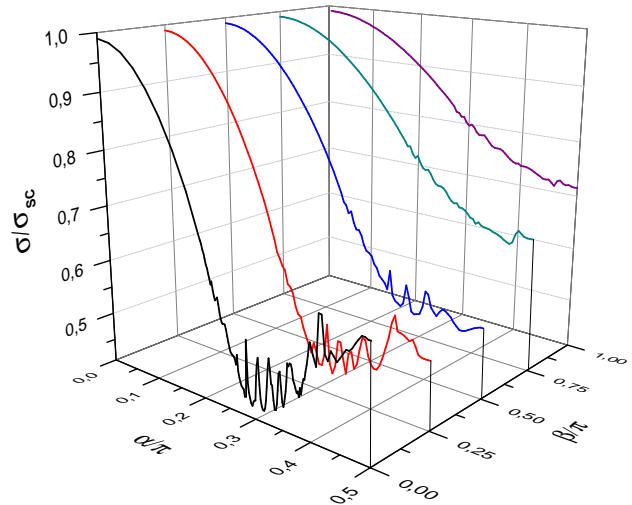


**Figure 2:** The total cross sections  $\sigma$  as a function of the dipole tilt angle  $\alpha = \gamma$  and the rotational angle  $\beta$  (cross sections are given in the units of  $\sigma_{sc} = \frac{4}{q}\sqrt{\pi Dq}$ )

## References

- [1] E. A. Koval, O. A. Koval, V. S. Melezhik, arXiv:1403.4432 (submitted to Phys. Rev. A)
- [2] C. Ticknor, Phys. Rev. A **84**, 032702 (2011)
- [3] V. S. Melezhik, J. Comput. Phys. **92**, 67-81 (1991)
- [4] D. S. Petrov and G. V. Shlyapnikov, Phys. Rev. A **64**, 012706 (2001).

# Control of few body resonant-transfer interactions in a cold Rydberg gas

P. Cheinet<sup>1</sup>, R. Faoro<sup>1</sup>, B. Pelle<sup>1</sup>, E. Arimondo<sup>2</sup>, and P. Pillet<sup>1</sup>

<sup>1</sup>Laboratoire Aimé Cotton, CNRS, ENS-Cachan, Bat. 505 Université Paris Sud, 91405 Orsay, France

<sup>2</sup>INO-CNR, Università di Pisa, Largo Pontecorvo 3, I-56127 Pisa, Italy

Presenting Author: patrick.cheinet@u-psud.fr

Observing the transition between 2-body and many-body physics in complex systems is a challenge as it is difficult to isolate few-body interactions from many-body interactions. Cold Rydberg atoms, which are known for their strong interaction properties [1], constitute in this prospect an interesting system to study many-body physics.

Previously in Laboratoire Aimé Cotton, we have succeeded [2] to isolate a 4-body interaction process appearing as a specific resonance of energy exchange between Rydberg atoms. This process originated from the coincident recombination of two 2-body energy exchange resonances [3] like the one in Eq. (1) called Förster resonance in analogy to FRET in biomolecules. Such a coincidence prevents *a priori* to extend this process to other systems, atoms or molecules. We have thus searched for more general processes.

$$2 \times np_{3/2}m \leftrightarrow ns + (n + 1)s \quad (1)$$

We will present here a new resonant 3-body energy transfer process in cesium Rydberg atoms. This process, presented in Eq. (2), is a revival of the known 2-body resonance in Eq. (1) induced by a much smaller energy exchange of a third atom changing only its magnetic sub-level.

$$3 \times np_{3/2}m \leftrightarrow ns + (n + 1)s + np_{3/2}m' \quad (2)$$

We have found that this exchange process is particularly strong and is present for any starting  $p_{3/2}$  state in cesium. For instance Fig. (1) presents these resonances from the  $32p_{3/2}m_{1/2}$  state: the 2-body resonance of Eq. (1) is expected at a field of 6.89V/cm and is used as field calibration. The 3-body process of Eq. (2) is then well observed at the expected field of 6.61V/cm with a large transfer to the  $s$  states.

Our observations are likely to have implications in various domains, from quantum physics to biology and new materials: This new FRET process could be used to design a 3-Qbit quantum gate or to provide an effective Quantum Non Demolition measurement of the entanglement between 2 atoms, measuring the 3<sup>rd</sup>. FRET is also widely used in biology as an imaging tool [4] which could be extended using additional molecules inducing 3-body FRET. Finally, 3-body FRET could help improving new solar cell technology which already tries to mimic light-harvesting.

## References

- [1] T. F. Gallagher, *Rydberg atoms* (Cambridge University Press, 1994)
- [2] J. H. Gurian *et al.* PRL **108** 023005 (2012)
- [3] K. A. Safinya *et al.* PRL **47** 405 (1981)
- [4] E. A. Jares-Erijman and T. Jovin, Nat. Biotech. **21**, 1387 (2003)

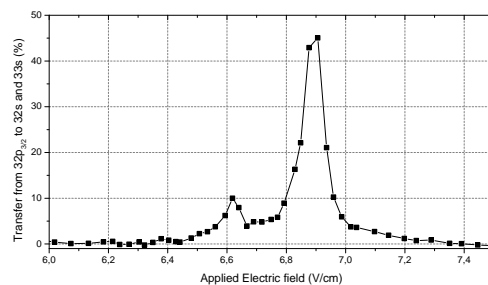


**Figure 1:** Resonant exchanges from  $32p_{3/2}m_{1/2}$ . The 2-body resonance is expected at 6.89V/cm while the 3-body resonance is calculated at 6.61V/cm.

## Theoretical study of the rare gases dimers

A.A. Korobitsin<sup>1</sup> and E.A. Kolganova<sup>1,2</sup>

<sup>1</sup>Bogoliubov Laboratory of Theoretical Physics, Joint Institute for Nuclear Research (JINR), Dubna, Moscow region, Russia

<sup>2</sup>University “Dubna”, Dubna, Moscow region, Russia

Presenting Author: koroaa@theor.jinr.ru

The rare gas clusters represent a typical example of van der Waals systems which unusual properties have recently attracted a lot of attention of many researchers. In fact, the development of the technology gives a possibility to study ultracold gases with fully controlled interatomic interaction and to find some universal correlations between observables [1]. To investigate Efimov phenomenon in three-atomic clusters it is necessary to have a good knowledge of dimer systems [2]. The spectrum of van der Waals rare gas dimers is considered in this presentation.

We calculated spectra and wave functions for pairs of atoms He, Ne, Ar, Kr, Xe and Rn. Calculations were performed for all possible homogeneous and heterogeneous pairs of rare gas atoms. The interatomic van der Waals potentials for the these pairs were determined using the Tang-Toennies [3], Aziz [4] and Lennard-Jones [5] potential models. It is necessary to point out that during purely theoretical *ab initio* computations of potential curves, their authors, as a rule, do not go beyond the presentation of potential values in the form of a table. Such numerical reports are often sufficient, because subsequent application of various parameter-fitting procedures yields fairly simple expressions, but for few-body calculations the analytic expression of potential is needed. The radial wave functions for the ground states of Ne – Rn dimers for the Tang-Toennies potential [3] are presented in the figure (Fig. 1).

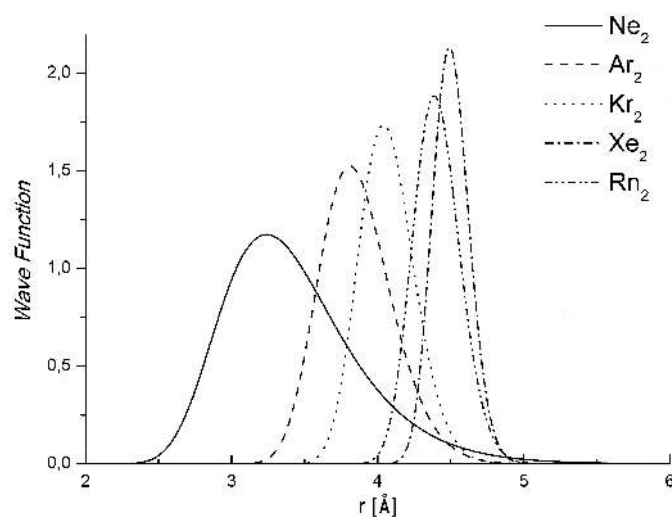


Figure 1: Radial wave functions of the ground states Ne – Rn dimers for TT potential [3].

### References

- [1] H.W. Hammer and L. Platter Ann. Rev. Nucl.Part.Sci. **60**, 207–236 (2010); V.Roudnev and M.Cavagner Phys.Rev.Lett. **108**, 110402 (2012); E.A. Kolganova Few-Body Syst. **4** (2014)
- [2] E.A. Kolganova, A.K. Motovilov and W. Sandhas Few-Body Syst. **51**, 249–257 (2011)
- [3] K.T. Tang and J.P. Toennies J.Chem.Phys. **118**, 4976-4983 (2003)
- [4] R.A. Aziz and M.J. Slaman, J. Chem. Phys. **94**, 8047–8053 (1991); D.A. Barrow, M.J. Slaman and R.A. Aziz J. Chem. Phys. **91**, 6348–6358 (1989); R.A. Aziz J. Chem. Phys. **99**, 4518–4525 (1993)
- [5] D.M. Leither, J.D. Doll and M. Whitnell J.Chem.Phys. **94**, 6644 - 6659 (1991)

# Modeling of bound states of quantum systems in a two-dimensional geometry of atomic traps

O.A. Koval<sup>1,2</sup> and E.A. Koval<sup>1,3</sup>

<sup>1</sup>*Bogoliubov Laboratory of Theoretical Physics, Joint Institute for Nuclear Research, Dubna, Moscow Region 141980, Russian Federation*

<sup>2</sup>*University Centre, Joint Institute for Nuclear Research, Dubna, Moscow Region 141980, Russian Federation*

<sup>3</sup>*Department of Theoretical Physics, Dubna International University for Nature, Society and Man, Dubna, Moscow Region 141980, Russian Federation*

Presenting Author: kov.oksana20@gmail.com

Numerical modeling of two-particle quantum systems in two-dimensional (2D) space is presented. The dependence of two atoms energy spectrum  $E$  on the scattering length  $a$  in the geometry of the confining trap was calculated. In the correspondent computational scheme we use conventional methods for solving the eigenvalue and the scattering problems. Agreement of numerical results with the analytical data, obtained in [1] with the zero-range potential approximation of the interatomic interaction, is illustrated by Figure 1. The calculated dependence of the energy levels of the two-particle system on the one-dimensional optical trap potential parameter and the scattering length is presented on Figure 2.

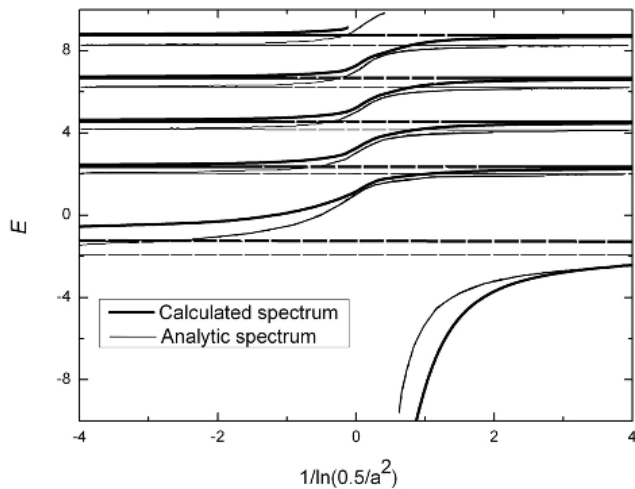


**Figure 1:** The dependence of the energy spectrum  $E$  of bound states calculated data and analytical data obtained by the author in [1], on the values of the quantity  $1/\ln(\frac{1}{2a^2})$ , at the frequency of the oscillator  $w = 1$ .

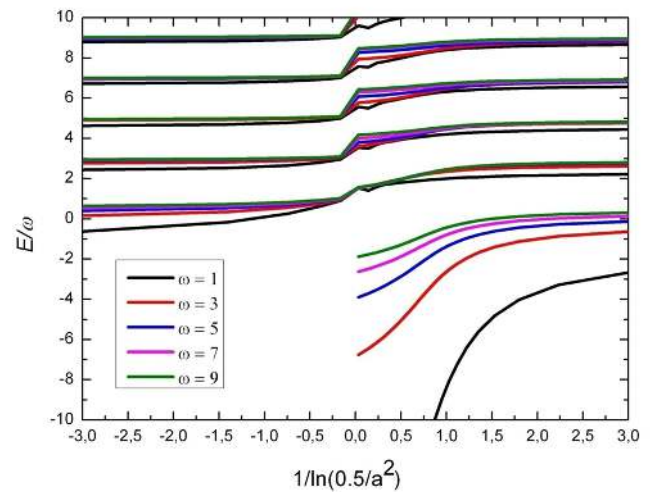


**Figure 2:** The dependence of the bound state energies on the frequency of the harmonic oscillator trap potential.

## References

- [1] Th. Busch *et al.* *Foundation of Physics* **28**, 549–559 (1998)
- [2] L.D. Landau, E.M. Lifshitz, *Quantum Mechanics* (Butterworth-Heinemann, Oxford, 1999)
- [3] V.S. Melezhik *J. Comput. Phys.* **92** 67–81 (1991)

# A continuous source of spin-polarized cold atoms

T. Vanderbruggen<sup>1</sup>, S. Palacios<sup>1</sup>, S. Coop<sup>1</sup>, N. Martinez<sup>1</sup>, and M.W. Mitchell<sup>1,2</sup>

<sup>1</sup>ICFO - Institut de Ciències Fòniques, Mediterranean Technology Park, 08860 Castelldefels (Barcelona), Spain

<sup>2</sup>ICREA - Institució Catalana de Recerca i Estudis Avançats, 08015 Barcelona, Spain

Presenting Author: thomas.vanderbruggen@icfo.es

We propose a new method to produce a continuous source of spin-polarized cold atoms [1] which are all-optically guided after their extraction from a magneto-optical trap (MOT), as depicted in Fig. 1 (a). The technique combines several physical effects and relies on light-shift engineering [Fig. 1 (b)], implemented using two coaxially overlapped optical beams each one driving a given transition of a three-level atom in a ladder configuration ( $\Xi$ -system). In a well-chosen scenario, the light-shift creates a state-dependent potential which implements the atom-diode [2] responsible for the continuous extraction of the atoms from a MOT into an all-optical guide.

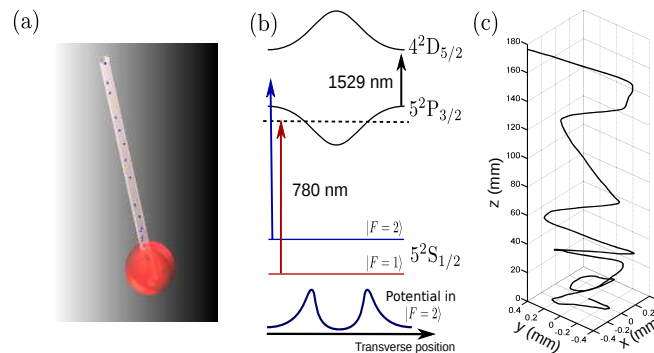


**Figure 1:** (a) Concept: a pipe-like potential is generated all-optically. It continuously extracts the atoms from a magneto-optical trap and guide them. (b) Relevant atomic levels of  $^{87}\text{Rb}$  versus the transverse direction. (c) Simulation of the propagation of an atom along the guide.

We performed a theoretical study by extending the Dalibard and Cohen-Tannoudji dressed-atom model [3] to the case of a doubly-driven  $\Xi$ -system. We analysed and quantified the dipole forces and the various sources of momentum diffusion in the resonant, non-perturbative, regime. In particular, from the Markovian evolution of the internal state, we obtain a general formula for the diffusion coefficient associated with the dipole force fluctuation.

We proposed and studied in detail the implementation of the method for  $^{87}\text{Rb}$  atoms. We show that, using  $\sigma^+$ -polarized fields driving the transitions  $5^2S_{1/2} \rightarrow 5^2P_{3/2}$  and  $5^2P_{3/2} \rightarrow 4^2D_{5/2}$  at 780 nm and 1529 nm respectively, a closed  $\Xi$ -system can be isolated within the complicated structure of  $^{87}\text{Rb}$ . Moreover, with this choice of transitions, the atoms will be optically pumped in a given Zeeman sub-state thus polarizing the atomic sample.

The theoretical results have then been used in a numerical simulation of Langevin-like equations [Fig. 1 (c)] to estimate the performance of the system both in terms of loading and guiding. We show that a large fraction of the atoms ( $\sim 20\%$ ) is guided over at least 5 cm, the mean velocity at this distance being 3.9 m/s with a dispersion of 2.1 m/s. This guided distance could deliver the atoms inside a magnetic shield that blocks the continuously operated MOT magnetic field.

The proposed method thus creates a continuous source of guided spin-polarized cold atoms. Such a source can be of particular interest for atom interferometry.

## References

- [1] T. Vanderbruggen and M. W. Mitchell, Phys. Rev. A **87**, 033410 (2013)
- [2] J. J. Thorn, E. A. Schoene, T. Li and D. A. Steck, Phys. Rev. Lett. **100**, 240407 (2008).
- [3] J. Dalibard and C. Cohen-Tannoudji, J. Opt. Soc. Am. B **2**, 1707 (1985).

## Superfluid transition in a 2D Bose gas with tunable interactions

M. Robert-de-Saint-Vincent<sup>1</sup>, R.J. Fletcher<sup>1</sup>, J. Man<sup>1</sup>, N. Navon<sup>1</sup>, R.P. Smith<sup>1</sup>, and Z. Hadzibabic<sup>1</sup>

<sup>1</sup>*Cavendish Laboratory, University of Cambridge, Cambridge CB30HE, United Kingdom*

Presenting Author: mrdsv2@cam.ac.uk

The superfluid character in quantum fluids can arise from a variety of mechanisms. Finite size two-dimensional Bose gases present a subtle interplay between Bose-Einstein Condensation, driven by quantum statistics, and the interaction-driven Berezinskii-Kosterlitz-Thouless phase transition, at which free vortices become suppressed and quasi-long range order emerges [1].

Here, we present experimental results on an ensemble of <sup>39</sup>K atoms in the degenerate regime, confined in 2D by an optical potential. The respective roles of quantum statistics and interactions are probed by tuning the strength of interactions through the use of Feshbach resonances, and observing the evolution of the phase coherence in the sample. The same system will allow future tests on the superfluid character of the system, for example through the study of persistent currents in a 2D toroidal geometry [2].

### References

- [1] Z. Hadzibabic, J. Dalibard, *Rivista del Nuovo Cimento* **34**, 389, (2011)
- [2] S. Beattie *et al.* *Phys. Rev. Lett* **110** 025301 (2013)

# Cavity-enhanced non-destructive detection of atomic populations in Optical Lattice Clocks

U. Eismann<sup>1</sup>, C. Shi<sup>1</sup>, J.-L. Robyr<sup>1</sup>, R. Le Targat<sup>1</sup>, and J. Lodewyck<sup>1</sup>

<sup>1</sup>LNE-SYRTE, Observatoire de Paris, 75014 Paris, France

Presenting Author: rodolphe.letargat@obspm.fr

In Optical Lattice Clocks (OLCs), an ultrastable laser probes a high quality factor atomic clock transition. The large number of neutral atoms addressed simultaneously opens the way towards unprecedented statistical uncertainties: the fractional stability could ultimately reach  $10^{-17}$  at one second when the clocks are solely limited by the atomic Quantum Projection Noise. Recently, a new generation of ultrastable lasers led to demonstrated stabilities as low as a few  $10^{-16}$  at one second [1,2,3].

An alternative approach to improve the stability is to detect the atomic populations in a non-destructive way, by measuring the phase shift induced by the atoms on a weak off-resonant laser beam [4]. The recycling of the atoms reduces drastically the dead time between each spectroscopy phase, and decreases significantly the sampling of the frequency noise of the ultrastable clock laser. We will present our strategy to implement a cavity based non-destructive detection: in our scheme, far detuned sidebands are resonantly coupled to an optical resonator, they are phase shifted by the atoms before being compared to the carrier reflected by the cavity and used as local oscillator.

We will compare this approach with the free space Mach-Zehnder interferometer approach we presented in [4]. We show how the signal-to-noise ratio is enhanced by the cavity effect, possibly allowing to reach a detection resolution better than the Quantum Projection Noise. Finally we discuss the implementation of this detection scheme in an operational OLC, as well as the possible impact of this technique on the uncertainty budget.

The perspective of improved stabilities of OLCs must be compatible with demonstrated uncertainty budgets. Therefore, to conclude, we'll present the comparisons between two independent OLCs at LNE-SYRTE and show that they are in agreement at a level surpassing the uncertainty on the current definition of the SI second [5]. It places them among the main contenders on the path to a possible redefinition of the second.

## References

- [1] B. J. Bloom *et al.*, Nature 12941, doi:10.1038 (2014)
- [2] N. Hinkley *et al.*, Science 341, p.1215 (2013)
- [3] C. Hagemann *et al.*, IEEE Trans. Instrum. Meas. 99, p.1 (2013)
- [4] J. Lodewyck *et al.*, Phys Rev. A 79 061401 (2009)
- [5] R. Le Targat *et al.*, Nature Communications 4, 2109 (2013)

# Generating synthetic gauge potentials by split driving of an optical lattice

C.E. Creffield<sup>1</sup> and F. Sols<sup>1</sup>

<sup>1</sup>*Departamento de Física de Materiales, Universidad Complutense de Madrid, E-28040, Madrid, Spain*

Presenting Author: c.creffield@fis.ucm.es

Ultracold atoms held in optical lattice potentials provide an almost ideal arena for the study of coherent quantum phenomena. We describe here a method to generate synthetic gauge potentials using the effect termed "coherent destruction of tunneling" to renormalise the value of the intersite tunneling [1]. Inspired by the well-known split-operator scheme used in quantum simulation, our approach uses two quickly alternating signals to engineer the appropriate Aharonov-Bohm phases, and permits the simulation of a uniform tunable magnetic field [2]. We explicitly demonstrate that our split-driving scheme reproduces the behavior of a charged quantum particle in a magnetic field over the complete range of field strengths, and produces the Hofstadter butterfly band-structure for the Floquet quasienergies.

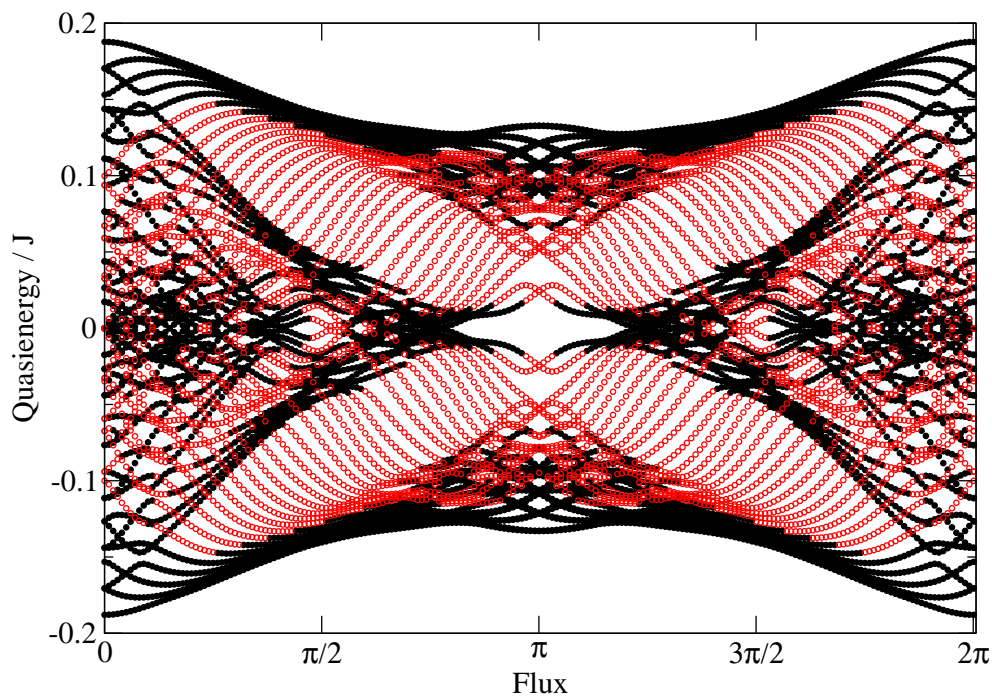


**Figure 1:** Floquet quasienergies for the split-driven system, showing the formation of the Hofstadter butterfly structure. Black (filled) circles show the bulk states, the red (unfilled) symbols the chiral transporting edge states.

## References

- [1] C.E. Creffield and F. Sols, Phys. Rev. A **84**, 023630 (2011)
- [2] C.E. Creffield and F. Sols, <http://arxiv.org/abs/1403.5915>

# Observing collective effects of Strontium in an optical cavity

M.R. Henriksen<sup>1</sup>, S.A. Schäffer<sup>1</sup>, B.T.R. Christensen<sup>1</sup>, P.G. Westergaard<sup>1,2</sup>, J. Ye<sup>3</sup>, and J.W. Thomsen<sup>1</sup>

<sup>1</sup>Niels Bohr Institute, Blegdamsvej 17, 2100 Copenhagen, Denmark

<sup>2</sup>Danish Fundamental Metrology; Matematiktorvet 307, 1. sal, DK-2800 Kgs. Lyngby, Denmark

<sup>3</sup>JILA, Department of Physics, 440 UCB, Boulder, Colorado 80309, USA

Presenting Author: schaffer@nbi.dk

The stability of the current state of the art optical atomic clocks are limited due to frequency noise of the interrogation oscillator caused by the Dick effect [1,2]. To improve future atomic clocks the frequency stability of the interrogation oscillator will need to be better than  $10^{-17}$  at 1s interrogation time [3-9].

Following [10-12], we investigate the possibility of exploiting collective effects to enhance the spectral purity of the local oscillator by directly interrogating cold atoms placed in a low finesse cavity. Multiple atoms strongly coupled to a single cavity mode may experience collective effects where the atomic sample acquires a collective phase with the cavity mode. This effect significantly enhances the phase response of this relatively simple system and offers a superior signal to noise ratio. Ultimately, this system may lead to a shot noise limited laser linewidth in the microhertz range [11].

Our experimental set-up consists of a standard Magneto Optical Trap (MOT) with  $5 \times 10^8$   $^{88}\text{Sr}$  atoms placed inside a low finesse cavity (fig. 1). The cavity enhances atom-light interaction by a factor on the order of the finesse ( $F = 80$ ) and direct spectroscopy on the weakly allowed intercombination line  $^1\text{S}_0 - ^3\text{P}_1$  ( $\Gamma = 7.6$  kHz) is performed. We lock the cavity to the probe laser ensuring a standing wave in the cavity at all times. Using the so-called NICE-OHMS technique [13-15], we measure the phase response of the atoms as we scan the frequency of our probe laser.

In order to push the current limitations further we are building a novel set-up in which a continuous jet of atoms should allow us to recreate this effect and further minimize the Dick effect.

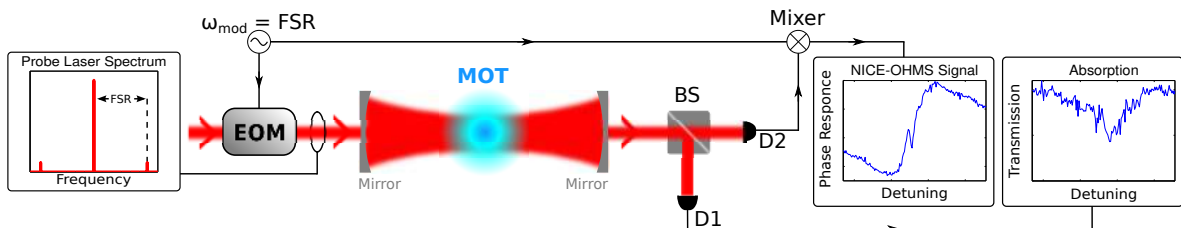


Figure 1: A modulated laser beam interacts with cold  $^{88}\text{Sr}$ -atoms and heterodyne detection is performed.

## References

- [1] G. Santarelli *et al.* IEEE Trans. Ultrason. Ferroelectr. Freq. Control **45**, 887 (1998).
- [2] P. Westergaard *et al.* IEEE Trans. Ultrason. Ferroelectr. Freq. Control **57**, 623 (2010).
- [3] T. Kessler *et al.* Nature Photonics **6**, 687-692 (2012).
- [4] M. J. Martin *et al.* Science **341**, 632-636 (2013).
- [5] M. Bishof *et al.* Phys. Rev. Lett. **111**, 093604 (2013).
- [6] B. J. Bloom *et al.* Nature **506**, 71-75 (2014).
- [7] N. Hinkley *et al.* Science **341**, 1215-1218 (2013).
- [8] R. Le Targat *et al.* Nat. Commun. **4**, 2109 (2013).
- [9] M. Takamoto *et al.* Nature **435**, 321-324 (2005).
- [10] M. J. Martin *et al.* Phys. Rev. A **84**, 063813 (2011).
- [11] D. Meiser *et al.* Phys Rev. Lett. **102**, 163601 (2009).
- [12] D. Meiser and M. Holland Phys. Rev. A. **81**, 033847 (2010).
- [13] J. Ye, L. S. Ma, J. L. Hall JOSA B **15** 6 (1998).
- [14] L. S. Ma *et al.* JOSA B **16** 2255 (1999).
- [15] H. Tanji-Suzuki *et al.* Adv. In Atomic, Molecular, and Opt. Phys. **60**, 201-237 (2011).

## Spectroscopies of dilute Fermi liquids

J.J. Kinnunen<sup>1</sup>

<sup>1</sup>*Aalto University School of Science, Finland*

Presenting Author: jami.kinnunen@aalto.fi

Ultracold atomic Fermi gases can form a superfluid at sufficiently low temperatures, with the atoms forming condensing bosonic pairs. Above the transition temperature, in the pseudogap state, these pairs are still believed to exist but in an uncondensed state. These ideas have been tested and experimentally verified using various spectroscopic methods, particularly radio-frequency- (rf-), momentum resolved rf-, and Bragg spectroscopies.

While the experiments and the related physics are well understood, in order to fully appreciate the role played by the pair formation, it is useful to have a contrasting theoretical formulation based on Fermi liquid theory (FLT). Unfortunately, the simplest such theory, which contains only Hartree-type energy shifts, provides qualitatively wrong results. However, the theory can be extended by including perturbative corrections.

Here, I will present such a theory by extending perturbatively the Brueckner-Goldstone theory used in Ref.[1] and using the theory for calculating spectroscopic signatures of dilute Fermi gases. This theory will also connect with the diagrammatic scheme proposed in Ref.[2] for spectroscopies in normal Fermi gases. The model can be used for studying spectroscopies in the cases where no well-defined pairs exist, such as highly imbalanced gases and high temperatures. In addition, it can be used as a comparison tool for the spectra obtained from the BCS superfluid theory.

### References

- [1] J. J. Kinnunen *Phys. Rev. A* **85**, 012701 (2012)
- [2] M. J. Leskinen, J. Kajala, J. J. Kinnunen *New J. Phys* **12**, 083041 (2010)

## A Double Magneto-Optical Trap for Hg and Rb

M. Witkowski<sup>1,2</sup>, S. Bilicki<sup>2</sup>, B. Nagórny<sup>2</sup>, B. Przewięźlikowski<sup>2</sup>, R. Munoz-Rodriguez<sup>2</sup>, P.S. Żuchowski<sup>2</sup>,  
R. Ciuryło<sup>2</sup>, and M. Zawada<sup>2</sup>

<sup>1</sup>*Institute of Physics, University of Opole, Oleska 48, PL-45-052 Opole, Poland*

<sup>2</sup>*Institute of Physics, Faculty of Physics, Astronomy and Informatics, Nicolaus Copernicus University, Grudziądzka 5,  
PL-87-100 Toruń, Poland*

Presenting Author: marcin\_w@fizyka.umk.pl

We present an experimental set-up of two species Hg-Rb magneto-optical trap (MOT). Rubidium atoms are very convenient for variety of experiments with ultracold samples including BEC, magnetic Feshbach resonances, photoassociation and many more [1]. The experimental methods for cooling and trapping Rb atoms are well developed and commonly used in many laboratories. On the other hand Hg atoms have a rare combination of features that makes them very interesting for cooling and trapping experiments: diversity of bosonic and fermionic isotopes, no hyperfine or fine structure in ground state, meta-stable states with extremely long life times, low Doppler and recoil temperatures. Moreover, due to very high weight Hg atom is a very good candidate for experimental tests of fundamental physics [2,3]. Because of small black body radiation shift and relatively high frequency of the clock transition it is also attractive for optically based metrology of time [5]. Nevertheless, experiments with cold Hg atoms are challenging due to very inconvenient wavelength (254 nm) of the cooling transition.

In bosons with the  $s^2$  configuration the clock transition  $^1S_0 - ^3P_0$  is strictly forbidden. The commonly used method to overcome this problem is to induce a coupling with  $^3P_0$  state which is optically accessible. In the Hg-Rb MOT, the presence of cold Rb atoms can be used to broaden the  $^1S_0 - ^3P_0$  clock transition in Hg. It was recently demonstrated [4] in an analogical SrRb system that the molecular states supported by the clock transition are dipole allowed at short range. Therefore, also the shifts and widths of the atomic transitions might be modified by a presence of the cold Rb atoms.

The preliminary studies of interactions in Hg MOT and between Hg and Rb MOTs are presented. The particular attention is given to the measurements of the scattering properties in various isotopes of the Hg atoms, such as thermalization rates, which provide information about the interaction potential, essential to predict the collisional shift of the Hg  $^1S_0 - ^3P_0$  clock transition [5–7]. The information about the interaction potential can also be obtained from loading curves of the MOT and from a photoassociation spectroscopy close to the  $^1S_0 - ^3P_1$  trapping transition. One of the goals of the presented experimental set-up is controlled production of ultracold homo- and heteronuclear molecules by the light-assisted photoassociation. We plan to take advantage of the Rb  $5S - 7S$  two-photon line at 760 nm as the photoassociation transition. The absolute frequency of this transition was measured recently by our group with the highest accuracy [8].

### References

- [1] E. A. Cornell, C. E. Wieman, Rev. Mod. Phys. **74**, 875–893 (2002)
- [2] E. Angstmann, V. Dzuba, V. Flambaum, Phys. Rev. A **70**, 014102 (2004)
- [3] M. Romalis *et al.* Phys. Rev. Lett. **86**, 2505–2508 (2001)
- [4] P. Żuchowski *et al.* arXiv:1402.0702 (2014)
- [5] H. Hachisu *et al.* Phys. Rev. Lett. **100**, 053001 (2008)
- [6] J. J. McFerran *et al.* Phys. Rev. Lett. **108**, 183004 (2012)
- [7] P. Villwock *et al.* Eur. Phys. J. D **65**, 251–255 (2011)
- [8] P. Morzyński *et al.* Opt. Lett. **38**, 4581–4584 (2013)

## Grating chips for quantum technologies.

J.P. McGilligan<sup>1</sup>, P.F. Griffin<sup>1</sup>, E. Riis<sup>1</sup>, and A.S. Arnold<sup>1</sup>

<sup>1</sup>*Department of Physics, SUPA, University of Strathclyde, Glasgow G4 0NG, UK*

Presenting Author: james.mcgilligan@strath.ac.uk

Laser cooled atomic samples have resulted in profound advances in frequency metrology, however the technology is typically complex and bulky. Micro-fabricated diffractive optical elements (DOEs) [1] can greatly facilitate the miniaturisation of magneto-optical traps (MOTs) for use in ultra-cold atom technology (Fig. 1). Here we present our latest results: precise optical characterisation of several new gratings, an investigation of phase-space properties in the MOT, and a magnetic trap loaded from the grating-based optical molasses.

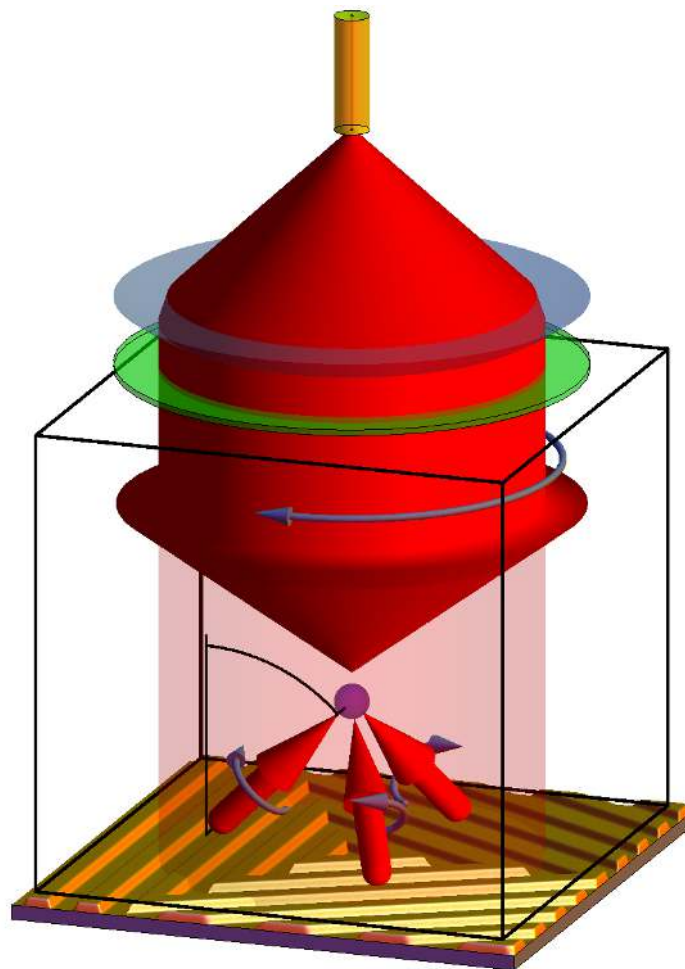


**Figure 1:** A diffractive optical elements (DOE) can transform a single circularly-polarised input beam into all required beams for an intensity-balanced magneto-optical trap [1]. This kind of chip was used to sub-Doppler cool atomic gases and subsequently load them into a magnetic trap.

### References

[1] C. C. Nshii et al, A surface-patterned chip as a strong source of ultra-cold atoms for quantum technologies, *nature nanotechnology Lett.* 47 (2013)

## Maximum Contrast Condensate Interference

C.H. Carson<sup>1</sup>, Yueyang Zhai<sup>1</sup>, P.F. Griffin<sup>1</sup>, E. Riis<sup>1</sup>, and A.S. Arnold<sup>1</sup>

<sup>1</sup>SUPA, Department of Physics, University of Strathclyde, Glasgow G4 0NG, United Kingdom

Presenting Author: christopher.carson@strath.ac.uk

We use magnetic levitation and a variable-separation dual optical plug to obtain clear spatial interference between two BECs axially separated by up to 0.25 mm. Fringes are observed using standard (i.e. non-tomographic) resonant absorption imaging [1]. The ‘magnifying’ effect of a weak inverted parabola potential on fringe separation is observed and agrees well with theory. With 160 ms levitation we can observe single-shot interference contrasts as high as 95% (see Figure 1 absorption image below), close to the theoretical limit due to pixellation of the sinusoidal fringes on our CCD camera. Interference patterns with fringe periods of 85  $\mu\text{m}$  (individual de Broglie wavelengths of 170  $\mu\text{m}$ ) are possible with 200 ms levitation. We are currently looking into other methods and geometries to split the BEC, one of these methods is to RF dress [2] our standard Ioffe-Pritchard trap [3] which would split the condensate radially [4]. Phase fluctuations are an inherent property in highly elongated BECs at finite temperature [5] which can degrade interferometry. Our long time-of-flight enables new levels of sensitivity to these fluctuations.

<http://photonics.phys.strath.ac.uk>.

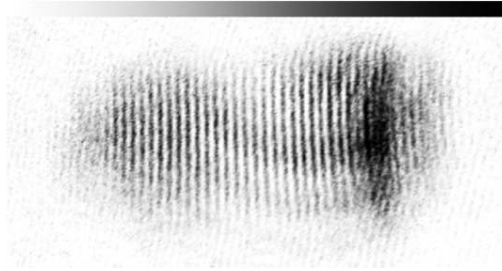


**Figure 1:** High contrast (95%) interference fringes between two initially separated condensates after 160 ms time-of-flight.

### References

- [1] M. E. Zawadzki, P. F. Griffin, E. Riis, and A. S. Arnold, Phys. Rev. A 81, 043608 (2010).
- [2] O. Zobay and B. M. Garraway, Phys. Rev. Lett. 86, 1195 (2000).
- [3] A. S. Arnold, C. S. Carvie and E. Riis, Phys. Rev. A. 73, 041606 (2006).
- [3] O. Zobay and B. M. Garraway, Phys. Rev. Lett. 86, 1195 (2000).
- [4] T. Schumm *et al.*, Nat. Phys. 1, 57 (2005).
- [5] S. Dettmer *et al.*, Phys. Rev. Lett. 87, 160406 (2001).

# Single atoms register in a micro-cavity for multi-particle entanglement

C. Leboutteiller<sup>1</sup>, S. Garcia<sup>1</sup>, F. Ferri<sup>1</sup>, J. Reichel<sup>1</sup>, and R. Long<sup>1</sup>

<sup>1</sup>Laboratoire Kastler Brossel, 24 rue Lhomond, 75005, Paris

Presenting Author: claire.leboutteiller@lkb.ens.fr

Motivated by applications in quantum-enhanced metrology and quantum information processing, we are building a cold atom experimental platform devoted to multi-particle entanglement generation with a high finesse fiber optical cavity as key feature. In this cavity, <sup>87</sup>Rb atoms resonant at 780nm, will be trapped at the antinodes of a 1560nm, i.e. twice 780nm, standing wave, forming a 1D lattice of equally and strongly coupled single atoms. In addition, a high numerical aperture lens will allow for single-site detection and addressing as shown on figure 1, and Raman transitions will be driven by transverse beams thanks to the large optical access to the cavity.

Quantum-enhanced metrology schemes can be explored and characterized in this setup, in particular dissipative preparation of spin squeezed atomic ensembles [1].

This system can also realise an effective Dicke model, as proposed in [2], which exhibits a quantum phase transition, already observed for large numbers of atoms [3][4]. With smaller atom number (10 to 50 atoms) we will be able to use quantum tomography techniques [5] to study the role of entanglement in the vicinity of the quantum phase transition as well as its scaling laws.

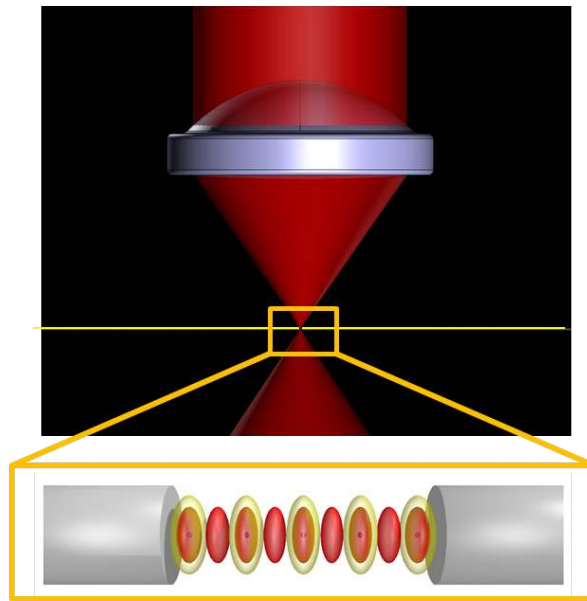


**Figure 1:** 1D lattice of <sup>87</sup>Rb single atoms in the fibered cavity with a high numerical aperture lens

## References

- [1] E.G. Dalla Torre *et al.* Physical Review Letters, **110**, 120402 (2013)
- [2] F. Dimer *et al.* Physical Review A, **75**, 013804 (2007)
- [3] K. Baumann *et al.* Nature, **464**, 09009 (2010)
- [4] M. P. Baden *et al.* arXiv:1404.0512v1 (2014)
- [5] F. Haas *et al.* Science, **344**, 180 (2014)

# Observation of spatio-temporal instabilities in a Magneto-Optical Trap

R. Romain<sup>1</sup>, P. Verkerk<sup>2</sup>, and D. Hennequin<sup>2</sup>

<sup>1</sup>*School of Physics & Astronomy, University of Nottingham, Nottingham NG7 2RD*

<sup>2</sup>*PhLAM institute, University of Lille, F-59655, Villeneuve d'Ascq*

Presenting Author: rudy.romain@gmail.com

Nowadays, Magneto-Optical Traps (MOTs) are mainly used as a source of cold atoms, for example, to study quantum phase transition, cold molecules or to build metrology setups. However, recent studies have shown that studying the MOT can be very useful because it is similar to plasma system [1,2]. MOT has the advantage of being a quite simple setup with high level control compared to plasma one, so it can be used as a model system.

We are interested in the dynamics of a cloud of cold atoms in a regime of stochastic instabilities. This regime was previously studied in a retro-reflected configuration [2]. In such a system, the mean variables are the number of trapped atoms and the position of the cloud center of mass. The stochastic instabilities are characterized by a noise amplification randomly in time. More precisely, the variable evolution presents a low noisy signal with bursts of large fluctuations. Inside a burst, frequencies around 100 Hz are observed.

In the present work, we want to go further than the previous study which only considered the temporal dynamics. We add a fast video camera to the detection system. This camera has a high sampling rate ( $> 1000$  pictures/s) and is thus suitable for our observation. I will develop the method used to extract information from the huge amount of data produced by the camera. We will show that only some spots inside the cloud are unstable and not the whole cloud. The number of spots and their distribution vary in time due to the stochastic origin of these instabilities. I will be able to model the atomic collective motion responsible of the unstable behavior.

## References

- [1] J. T. Mendonça *et al.* Phys. Rev. A **78** 013408 (2008)
- [2] R. Romain, D. Hennequin, P. Verkerk Eur. Phys. J. D **61**, 171–180 (2011)
- [3] A. Stefano, P. Verkerk, D. Hennequin Eur. Phys. J. D **30** 243–258 (2004)

## Tuning effective magnetic dipolar interactions in Rb spinor condensates

S. Palacios<sup>1</sup>, S. Coop<sup>1</sup>, T. Vanderbruggen<sup>1</sup>, N. Martinez<sup>1</sup>, and M.W. Mitchell<sup>1,2</sup>

<sup>1</sup>ICFO- The Institute of Photonic Sciences, Carl Friedrich Gauss 3, 08860 Castelldefels (Barcelona), Spain

<sup>2</sup>ICREA - Institució Catalana de Recerca i Estudis Avançats, 08015 Barcelona, Spain

Presenting Author: silvana.palacios@icfo.es

We describe our progress towards the all optical formation of a spinor condensate of Rb atoms in a quiet magnetic environment with residual fields  $< 10$  pT. Under such an environment the Zeeman energy is overshadowed by the weak magnetic dipole-dipole interaction (MDDI) energy of Rb: the interplay between MDDI and spin dependent contact interaction (SDCI) determines the ground state magnetization of the magnetic superfluid. The long range nature of MDDI couples the external and internal degrees of freedom, making the magnetization depends on the geometry of the confining trap. By changing the trap shape it is possible to explore different phase transitions that appear in the absence or presence of magnetic fields and gradients, and effectively tune the MDDI as shown in Fig. 1 [1].

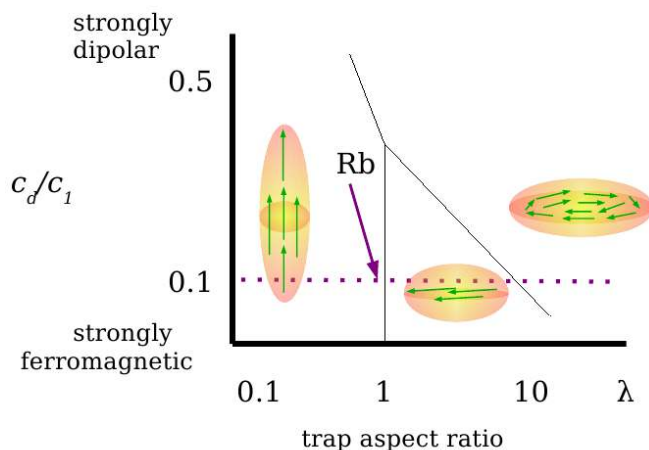


**Figure 1:** Phase diagram of dipolar spin-1 ferromagnetic condensates in the  $c_d/c_1 - \lambda$  space where  $c_d/c_1$  is the ratio between MDDI and SDCI strengths (about 0.1 for Rb) and  $\lambda$  the trap aspect ratio.

We confine  $^{87}\text{Rb}$  atoms in a dipole trap at 1560 nm formed by three crossing Gaussian beams. This trap induces not only a trapping potential but also a large differential light-shift between the ground state  $5^2S_{1/2}$  and the excited state  $5^2P_{3/2}$  (D2 line) due to strong contributions to the polarizability of the excited state through the  $5^2P_{3/2} - 4D_{3/2,5/2}$  transitions at 1529 nm. This light-shift is spatially dependent like the intensity distribution of the Gaussian beams, we exploit this effect in the characterization of the trap geometry. The magnetic field environment is actively controlled by compensating the fields measured by fluxgate detectors (noise  $< 10$  pT) around the vacuum chamber. By evaporating cooling we will condense atoms occupying the  $F=1$  ferromagnetic ground state and by changing the relative powers and waists of the dipole beams we will change the trap geometry.

### References

[1] S. Yi, H. Pu Phys. Rev. Lett. **97**, 020401 (2006)

# Modulation Transfer and Double-Resonance Optical Pumping with optical transitions in $^{87}\text{Rb}$

Y.N. Martinez de Escobar<sup>1</sup>, S. Palacios<sup>1</sup>, S. Coop<sup>1</sup>, T. Vanderburggen<sup>1</sup>, and M.W. Mitchell<sup>1</sup>

<sup>1</sup>ICFO - The Institute of Photonic Sciences, Castelldefels, Spain

Presenting Author: natali.martinez@icfo.es

We demonstrate modulation transfer from a pump to a probe beam via non-linear processes in  $^{87}\text{Rb}$  using both the  $5\text{S}_{1/2}$ - $5\text{P}_{3/2}$  and  $5\text{S}_{1/2}$ - $5\text{P}_{3/2}$ - $4\text{D}_{3/2,5/2}$  ladder transition schemes. This technique, when used in spectroscopy, produces Sub-Doppler spectroscopic lineshapes free of unwanted background offsets that typically shift the zero-crossing of the signal. Modulation transfer spectroscopy (MTS) on the  $5\text{S}_{1/2}$ - $5\text{P}_{3/2}$  transition displays characteristics observed in similar setups [1]; we demonstrate for the first time modulation transfer on the excited  $5\text{P}_{3/2}$ - $4\text{D}$  transitions. These transitions are important since they correspond to an absolute standard reference for C-band telecom wavelengths (1529 to 1565 nm). We obtain suitable MTS error signals for the  $5\text{S}_{1/2}$ - $5\text{P}_{3/2}$  and  $5\text{P}_{3/2}$ - $4\text{D}$  transitions, and confirm that the unique features of MTS are preserved even on the excited transitions. The narrow dispersion signals allow us to frequency stabilize narrow-linewidth fiber lasers at 1529 nm and 1560 nm (Fig. 1A).

Two-photon optical pumping on the ladder transition also allows us to measure the decay rate of the  $5\text{P}_{3/2}$ - $4\text{D}$  transitions. As shown in Fig. 1B, instead of monitoring atoms excited (by laser L1) into the intermediate state  $5\text{P}_{3/2}$  with laser L2 (expected to be low for a state with a large decay rate), the double-resonance optical pumping (DROP) mechanism provides a loss channel for atoms resonant with the two-photon cycling transition, returning them to a ground state not resonant with L1; an increase in transmission of L1 therefore coincides with the double resonance transition, providing an improved SNR on sub-Doppler spectrum for the  $5\text{P}_{3/2}$ - $4\text{D}$  transitions. We report on our preliminary measurements and expected uncertainty budget of the decay rates.

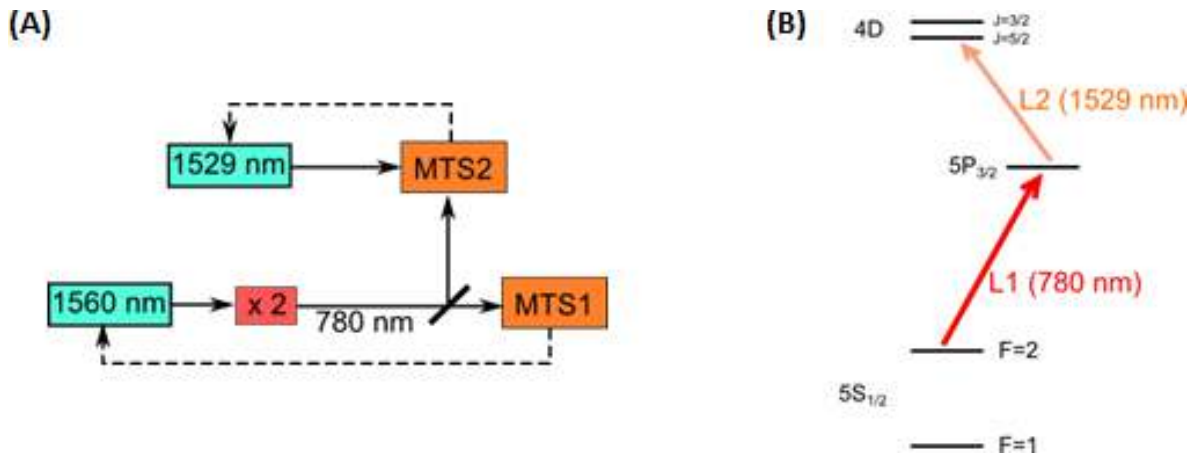


**Figure 1:** (A) Schematic depicting the laser frequency stabilization approach in our experiment. (B) Atomic transitions involved in MTS and DROP spectroscopy (see text).

## References

- [1] D. J. McCarron, S. A. King, S. L. Cornish Meas. Sci. Technol. **19**, 105601 (2008)

# Quantum Tunneling in a Quasi-periodically Driven Optical Lattice

C. Yuce<sup>1</sup>

<sup>1</sup>*Physics Department, Anadolu University, Turkey*

Presenting Author: cyuce@anadolu.edu.tr

We investigate quantum tunneling phenomena for an optical lattice subjected to a bichromatic ac force. We show that incommensurability of the frequencies leads to super Bloch oscillation. We propose directed super Bloch oscillation for the quasi periodically driven optical lattice. We study the dynamical localization and photon assisted tunneling for a periodical and quasi-periodical ac force.

## References

[1] C. Yuce Eur. Phys. Lett., **103**, 30011 (2013)

# Spontaneous coherence of magnons in spin-polarized atomic hydrogen gas

O. Vainio<sup>1</sup>, L. Lehtonen<sup>1</sup>, J. Järvinen<sup>1</sup>, J. Ahokas<sup>1</sup>, S. Sheludiyakov<sup>1</sup>, D. Zvezdov<sup>1,2</sup>, K.-A. Suominen<sup>1</sup>, and S. Vasiliev<sup>1</sup>

<sup>1</sup>*Department of Physics and Astronomy, University of Turku, 20014 Turku, Finland*

<sup>1</sup>*Kazan Federal University, 420008, 18 Kremlyovskaya St, Kazan, Russia*

Presenting Author: otto.vainio@utu.fi

A macroscopic occupation of the ground state and long-range correlations between particles are the hallmarks of Bose-Einstein condensation in cold atomic gases. Similar phenomena are also observed in systems of wave-like excitations (quasiparticles) such as photons, excitons, and spin waves (magnons). Spin waves in cold gases are propagating perturbations of spins, manifesting as travelling fluctuations of the macroscopic magnetization. The propagation results from the cumulative effect of the identical spin rotation (ISR) effect due to exchange interaction. In spin-polarized atomic hydrogen gas magnons can be trapped and controlled by magnetic forces in a manner similar to ordinary atoms with magnetic moments. We show that at high hydrogen gas densities the magnons accumulate in their ground state and exhibit long-term coherence, profoundly changing the electron spin resonance spectra of the atomic hydrogen gas.

In our experiments the gas of atomic hydrogen is hydraulically compressed to high densities of  $5 \cdot 10^{18} \text{ cm}^{-3}$  at temperatures 0.2 - 0.6 K in a magnetic field of 4.6 T. We observed a variety of spin wave modes caused by the ISR effect with strong dependence on the spatial profile of the polarizing magnetic field. The ISR magnons of atomic hydrogen are high field seeking excitations, and are trapped in regions of strong magnetic field [1]. We demonstrate confinement of magnons in two magnetic traps of distinct geometries, toroidal and spherical, the latter combined with a linear magnetic field gradient. Above a critical value of the hydrogen atom density a sharp and prominent peak emerged in the CW ESR spectrum. We also recorded pulsed ESR spectra where the gas was probed with a small tipping angle resonance excitation. In the resulting free induction decay signals a similar feature was observed: a rapid decay and a subsequent refocusing of the transversal magnetization into a slowly-decaying single-frequency tail. We interpret these effects as signs of spontaneous coherence and argue for an explanation in terms of Bose-Einstein condensation of magnons.

## References

[1] O. Vainio *et al.* PRL **108** 185304 (2012)

## Emergence of nonlinearity in bosonic ultracold gases

B. Vemersch<sup>1,2</sup> and J.C. Garreau<sup>1</sup>

<sup>1</sup>Laboratoire de Physique des Lasers, Atomes et Molécules, CNRS, Université Lille 1, F-59655, Villeneuve d'Ascq

<sup>2</sup>Institute for Quantum Optics and Quantum Information of the Austrian Academy of Sciences, A-6020 Innsbruck, Austria

Presenting Author: jean-claude.garreau@univ-lille1.fr

The advent of Bose-Einstein condensation and the possibility of creating experimentally ultracold quantum-degenerate atomic gases opened new and fascinating perspectives for the study of weakly interacting quantum systems. In the case of ultracold bosonic gases, the possibility of generating a mesoscopic quantum-coherent state is particularly interesting. At very low – yet experimentally accessible – temperatures, such systems can be described with very good accuracy by a nonlinear version of the Schrödinger equation, namely the mean-field Gross-Pitaevskii equation, in which a nonlinear term accounts for coherent particle-particle interactions. This means that such systems can in principle display “quasiclassical” chaos, i.e., chaotic dynamics associated to exponential sensitivity to initial conditions, which is forbidden by the usual (linear) Schrödinger equation. One thus faces a paradox: The exact description of a boson gas corresponds to a (very complex) many-body problem which can be reduced to a system of coupled *linear* equations, and thus *cannot* display quasiclassical chaos! In going from the many-body formulation to the mean-field approximation, quasiclassical behavior has emerged, i.e., symmetries of the many body system have been broken. In the present work, we use a toy model consisting of a Bose-Einstein condensate confined to three adjacent sites of a tilted lattice, which constitutes a “minimal” system presenting quasiclassical chaos. We compare the dynamics of such a system obtained by numerical integration of the many-body problem with that observed by numerical integration of the Gross-Pitaevskii equation. This sheds some light on the emergence of the nonlinearity, and hints for possible explanations of the above-mentioned paradox.

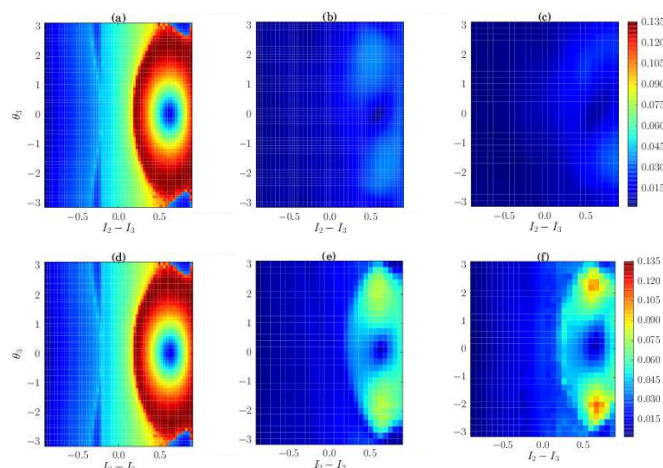


**Figure 1:** Variance of the wave packet position calculated according to various methods: Gross-Pitaevskii equation (left column), Lanczos diagonalization (center column), and truncated Husimi representation (right column), and with different number of particles, 30 (top row) and 400 (bottom row). The red areas correspond to quasiclassical chaos, easily spotted in the Gross-Pitaevskii simulation, but clearly depending on the particle number for many-body approaches.

# Light-Shift Tomography of an Optical Dipole Trap

S. Coop<sup>1</sup>, S. Palacios<sup>1</sup>, N. Martinez<sup>1</sup>, T. Vanderbruggen<sup>1</sup>, and M.W. Mitchell<sup>1,2</sup>

<sup>1</sup>ICFO - The Institute of Photonic Sciences, Av. Carl Friedrich Gauss 3, 08860 Castelldefels (Barcelona), Spain

<sup>2</sup>ICREA - Institució Catalana de Recerca i Estudis Avançats, 08015 Barcelona, Spain

Presenting Author: simon.coop@icfo.es

Here we describe a technique for directly characterising an optical dipole trap called *light-shift tomography* [1]. The intense trapping light induces a significant AC Stark shift on the atoms, and if the trap wavelength is appropriately close to an excited state transition this shift is much stronger for the excited state than the ground state. In our experiment we use <sup>87</sup>Rb and light at 1560 nm, which is close to the 5P<sub>3/2</sub>–4D<sub>5/2</sub> transition at 1529 nm. This proximity to an excited state transition strongly affects the polarisability of the excited state, and so the Stark shift is about 42 times stronger on the 5P<sub>3/2</sub> excited state than the 5S<sub>1/2</sub> ground state (Fig. 1). The differential light-shift means the resonance frequency of the atom is dependent on its position in the laser beam. By probing at different frequencies, one can ‘see’ atoms at different positions in the trap, and the probe detuning can be used to infer the local trapping light intensity. A measurement of the position of resonant atoms versus frequency effectively maps the isopotentials of the trap in-situ, from which one can reconstruct the trap shape, width, and depth (Fig. 2). This method also has the advantage of being able to measure non-harmonic potentials, unlike e.g. measuring trap frequencies. Here we present an explanation of this effect, our results in using this technique to make a 3D reconstruction of our trap, and point out some limitations and sources of systematic error. Specifically we found two major problems: 1) it is difficult to measure at the bottom of the trap due to the weak signal, and 2) as a result of the probe beam being off-resonant for most of the atomic cloud, a spatially-dependent phase shift leads to a lensing effect on the imaging beam which can distort measurements.

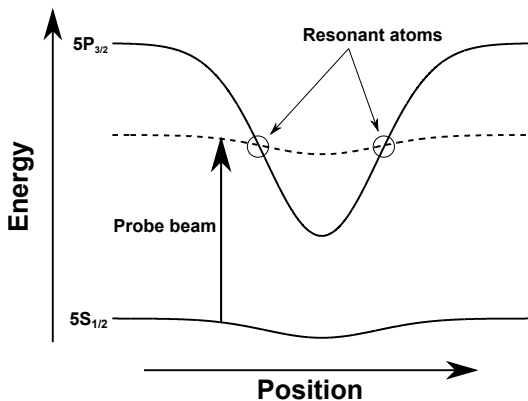


**Figure 1:** Light-shift of a <sup>87</sup>Rb atom in a 1560 nm Gaussian laser beam.

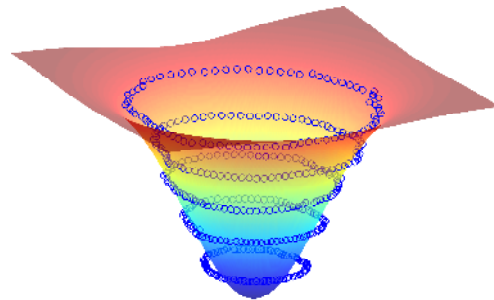


**Figure 2:** Reconstructed crossed-dipole trap from measured isopotentials.

## References

- [1] J. P. Brantut *et al.* PRA 031401 **78** (2008)

## Localization in disordered time-dependent lattices

M. Plodzien<sup>1</sup>, J. Zakrzewski<sup>1</sup>, and J. Major<sup>1</sup>

<sup>1</sup>*Atomic Optics Department, Jagiellonian University, Krakow, Poland*

Presenting Author: jan.major@uj.edu.pl

The Anderson localization is a phenomenon present in disordered systems, where particles eigenstates are exponentially localized and the transport vanishes [1]. Recently it is widely studied in systems of cold atoms in optically generated potentials [2]. Fast periodic modulation of parameters of such a system can lead to qualitatively new behaviour by creating new terms in time averaged Hamiltonian [3]. In disordered systems we can using this method get various types of off-diagonal disorder. We examine effect of such a new part of Hamiltonian on presence of localization, transition between localized and delocalized states, localization length.

### References

- [1] P. Anderson PhysRev. **109**, 1492–1505 (1958)
- [2] C.Muller, D.Delande arXiv, arXiv:1005.0915 (2012)
- [3] E. Arimondo *et al.* arXiv, arXiv:1203.1259v2 (2012)

## Studying Anderson transitions with atomic matter waves

C. Hainaut<sup>1</sup>, I. Manai<sup>1</sup>, J.F. Clément<sup>1</sup>, R. Chicireanu<sup>1</sup>, P. Szriftgiser<sup>1</sup>, and J.C. Garreau<sup>1</sup>

<sup>1</sup>Laboratoire PhLAM, CNRS and University of Lille, F-59655, Villeneuve d'Ascq

Presenting Author: isam.manai@univ-lille1.fr

In the presence of a disordered potential, the classical diffusive transport of a particle can be inhibited by quantum interference between the various paths where the particle is multiply scattered by disorder, a puzzling phenomenon known as Anderson localization [1]. The dimensionality of the system plays a major role, which can be understood qualitatively from the scaling theory of localization [2,3]. In dimension  $d = 3$ , there is delocalized-localized (or metal-insulator in solid state physics language) transition — known as the Anderson transition — with a mobility edge  $E_c$  separating localized motion at low energy (strong disorder) from diffusive motion at high energy (low disorder). On the localized side, the localization length  $\xi$  diverges algebraically  $\xi(E) \propto (E_c - E)^{-\nu}$ , with  $\nu$  the critical exponent of the transition. On the diffusive side, the diffusion constant vanishes like  $D(E) \propto (E - E_c)^s$  with, according to the scaling theory,  $s = (d - 2)\nu$  [3, 4].

A key prediction of the scaling theory is that the critical exponents are **universal**, that is do not depend on the microscopic details of the model used, such as the correlation functions of the disorder, the dispersion relation of the particles, etc. Numerical experiments on simple models [5, 6, 7] such as the tight-binding Anderson model, have confirmed this universality, with a non-trivial value of the critical exponent around  $\nu = 1.57$  for spinless time-reversal invariant 3-dimensional (3D) systems [8]. However, there is a huge lack of experimental results in this area.

We experimentally test the universality of the Anderson three dimensional metal-insulator transition, using a quasiperiodic atomic kicked rotor [9]. Nine sets of parameters controlling the microscopic details have been tested. Our observation indicates that the transition is of second order, with a critical exponent independent of the microscopic details. We thus demonstrate that the value of the critical exponent is universal. The average value  $1.63 \pm 0.05$  agrees very well with the numerically predicted value  $\nu = 1.58$  [10].

More recently, we have modified our experimental setup to increase significantly the interaction time between cold atoms and the pulsed 1D optical lattice. It allows us to apply 1000 optical pulses on the cold atomic sample (6-fold improvement on maximum pulse number). One can thus extend soon our experimental study on Anderson model to higher dimensions ( $d = 4$ ).

### References

- [1] P. W. Anderson, Phys. Rev. **109**, 1492 (1958).
- [2] E. Abrahams *et al.*, Phys. Rev. Lett. **42**, 673 (1979).
- [3] C. A. Müller and D. Delande, Ultracold Gases and Quantum Information, Les Houches Summer School session XCI, 441 (2011).
- [4] F. Wegner, Electrons in Disordered Systems. Scaling near the Mobility Edge, Z. Phys., **B25**, 327 (1976),
- [5] K. Slevin and T. Ohtsuki, Phys. Rev. Lett., **82**, 382 (1999).
- [6] F. Milde, R. A. Römer and V. Uski, Eur. Phys. J. B, **15**, 685 (2000)
- [7] G. Lemarié, B. Grémaud and D. Delande, EPL, **87**, 37007 (2009)
- [8] F. Evers and A. D. Mirlin, Rev. Mod. Phys., **80**, 1355 (2008).
- [9] J. Chabé *et al.*, Phys. Rev. Lett. **101**, 255702 (2008)
- [10] M. Lopez *et al.*, Phys. Rev. Lett. **108**, 095701 (2012)

# Tomographic reconstruction of molecular properties from interference measurements

J. Fiedler<sup>1</sup> and S. Scheel<sup>1</sup>

<sup>1</sup>*Institute of Physics, University of Rostock, D-18055 Rostock*

Presenting Author: johannes.fiedler@uni-rostock.de

Dispersion forces, such as van-der-Waals forces between atoms or molecules, Casimir-Polder forces between atoms and macroscopic bodies and Casimir forces between macroscopic objects, are all effective electromagnetic forces caused by ground-state fluctuations of the quantised electromagnetic field [1]. Because of their short interaction range, dispersion forces can play a major role in situations where two (microscopic or macroscopic) objects are brought close together. For example, in experiments with trapped ultracold atoms the Casimir-Polder interaction can exceed the magnetic trapping force [2] and lead to unwanted losses. In molecular interferometry, these Casimir-Polder interactions influence the intensity distribution in the measured interference pattern [3], as a phase shift depending on the position of the molecule inside the grating is accumulated. Such interactions have already led to estimates of bond lengths and binding energies in small van der Waals clusters [4].

We investigate the possibility of reconstructing the Casimir-Polder potential between an atom or molecule and a dielectric object tomographically from the interference data obtained from atomic or molecular interferometry. We show that information about electromagnetic response properties of the atom/molecule such as transition dipole moments or permanent dipole moments, can be reconstructed in this way. Our method is based on the observation that the interference pattern obtained from varying incidence angles traces different paths of the atom/molecule-surface interaction potential landscape.

## References

- [1] S. Scheel, S.Y. Buhmann *Acta Phys. Slov.* **58**, 675–809 (2008)
- [2] Y.J. Lin *et al.* *Phys. Rev. Lett.* **92**, 050404 (2004)
- [3] B. Brezger *et al.* *Phys. Rev. Lett.* **88**, 100404 (2002)
- [4] R.E. Grisenti *et al.* *Phys. Rev. Lett.* **85**, 2284 (2000)

## Heating-rate measurements in micro-fabricated surface traps containing $\text{Sr}^+$ ions

B. Szymanski<sup>1</sup>, J.-P. Likforman<sup>1</sup>, S. Guibal<sup>1</sup>, C. Manquest<sup>1</sup>, L. Guidoni<sup>1</sup>, and M. Woytasik<sup>2</sup>

<sup>1</sup>Univ Paris Diderot, Sorbonne Paris Cité, Laboratoire Matériaux et Phénomènes Quantiques, UMR 7162, Bat. Condorcet, 75205 Paris Cedex 13, France

<sup>2</sup>Institut d'Électronique Fondamentale, UMR CNRS 8622, Université Paris Sud, Centre Scientifique d'Orsay, France

Presenting Author: luca.guidoni@univ-paris-diderot.fr

We designed, realized and operated a micro-fabricated ion surface trap [1] with Copper electroplated electrodes on a silica substrate. We load the trap with single  $^{88}\text{Sr}^+$  ions that are Doppler cooled by addressing the  $5s\ ^2S_{1/2} \rightarrow 5p\ ^2P_{1/2}$  transition ( $\nu = 711\ \text{THz}$ ,  $\lambda = 422\ \text{nm}$ ) using two different strategies in order to avoid the accumulation of the population into the metastable  $4d\ ^2D_{3/2}$  state during the cooling process (see figure 1). In a first (quite usual) case we drive the  $4d\ ^2D_{3/2} \rightarrow 5p\ ^2P_{1/2}$  275 THz transition with a "repumping" laser. In a second case we drive both the  $4d\ ^2D_{3/2} \rightarrow 5p\ ^2P_{3/2}$  (299 THz) and  $4d\ ^2D_{5/2} \rightarrow 5p\ ^2P_{3/2}$  (290 THz) transitions in order to avoid coherent population trapping phenomena that originate in the previous  $\Lambda$  scheme [2]. We characterize the heating-rate of the trap by applying the Doppler re-cooling method that has been first developed and applied in the case of ions that do not have metastable states [3]. We analyze and compare the Doppler re-cooling experimental results obtained with the same trap and under identical conditions but using these two different "repumping" strategies.

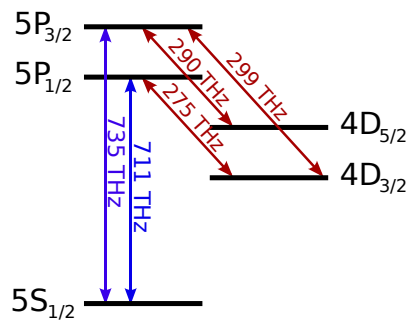


Figure 1: Low energy levels scheme for  $\text{Sr}^+$ .

### References

- [1] S. Seidelin *et al.* Phys. Rev. Lett. **96**, 253003 (2006)
- [2] D. T. C. Allcock *et al.* New J. Phys. **12**, 053026 (2010)
- [3] J. H. Wesenberg *et al.* Phys. Rev. A **76**, 053416 (2007); R. J. Epstein *et al.* Phys. Rev. A **76**, 033411 (2007)

# Focused ion beam based on laser cooling: towards sub-nm ion beam milling

G. ten Haaf<sup>1</sup>, S.H.W. Wouters<sup>1</sup>, S.B. van der Geer<sup>1,2</sup>, O.J. Luiten<sup>1</sup>, P.H.A. Mutsaers<sup>1</sup>, and E.J.D. Vredenburg<sup>1</sup>

<sup>1</sup>Coherence and Quantum Technology group, Department of Applied Physics,  
Eindhoven University of Technology, PO Box 513, 5600 MB Eindhoven, Netherlands  
<sup>2</sup>Pulsar Physics, [www.pulsar.nl](http://www.pulsar.nl)

Presenting Author: [g.t.haaf@tue.nl](mailto:g.t.haaf@tue.nl)

Focused ion beams (FIBs) are indispensable tools in the semiconductor industry and materials science, because they can create structures at the nanometer length scale without lithography. The current state of the art FIB for milling purposes is the liquid metal ion source, which can reach a spot size of 5 nm with a Ga<sup>+</sup> ion beam containing 1 pA. Recently, ideas have come up to create a FIB based on photo-ionization of a laser cooled and compressed atomic beam [1]. Here we present simulations and calculations on the formation and focusing of an ion beam created from such a laser-intensified atomic beam of rubidium which originated from a Knudsen cell.

In a FIB based on laser cooling, ions will be produced at random locations in the ionization region after the magneto optical compressor. Therefore, so-called disorder-induced heating will occur due to the mutual Coulomb interaction between the ions at random locations [2, 3]. This heating can be suppressed by a sufficiently large electric field, which lowers the ion density and creates a so called pencil beam. However, due to the photo-ionization process, the energy spread of the ions, and thus the amount of chromatic aberration of the downstream lens system, will be proportional to this electric field. Therefore an optimum value of this electric field will exist, which leads to the smallest spot size. The process of disorder-induced heating was investigated with particle tracing simulations. They were used to find a relation between the current and flux density of the ion beam and the electric field needed to suppress disorder-induced heating. This relation was used as input for analytical calculations of the minimum achievable spot size, which included the effects of the initial temperature and flux density achieved after the magneto optical compressor and chromatic and spherical aberration of a realistic electrostatic lens system. Figure shows the result of these calculations in terms of the spot size that can be reached with a 1 pA beam as a function of the initial temperature and flux density of the atomic beam.

A very important part of the source discussed here is the Knudsen cell and especially the collimation tube connected to it. From this collimation tube, a thermal atomic beam of Rubidium will effuse that is laser cooled and compressed in the next stage. The properties of this atomic beam, such as the flux, transverse velocity distribution and brightness will influence the performance of the rest of the setup. We will show laser-induced fluorescence measurements of these properties and discuss their impact.

## References

- [1] B. Knuffman, A.V. Steele and J.J. McClelland, *Journal of Applied Physics* **114**, 044303 (2013)
- [2] S.B. van der Geer *et al.*, *Journal of Applied Physics* **102**, 094312 (2007)
- [3] L. Kime *et al.*, *Physical Review A* **88**, 033424 (2013)

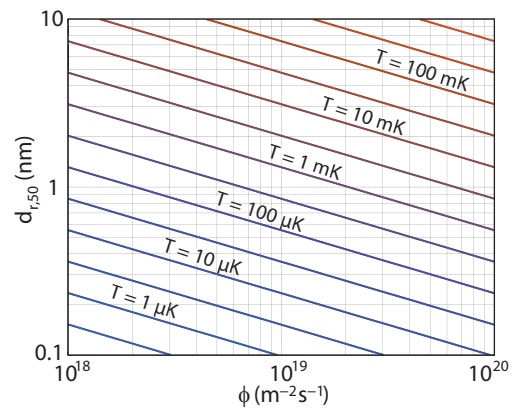


**Figure 1:** The expected spot size (50% diameter) as a function of the initial flux density  $\phi$  and temperature  $T$ , which are expected to be  $5 \times 10^{19} \text{ m}^{-2} \text{ s}^{-1}$  and 1 mK.

## Towards precision laser spectroscopy with cold highly charged ions

L. Schmöger<sup>1,2</sup>, O.O. Versolato<sup>1,2</sup>, M. Schwarz<sup>1,2</sup>, M. Kohnen<sup>1</sup>, T. Leopold<sup>1</sup>, A. Windberger<sup>2</sup>, J. Ullrich<sup>1</sup>,  
P.O. Schmidt<sup>1,3</sup>, and J.R. Crespo López-Urrutia<sup>2</sup>

<sup>1</sup>*Physikalisch-Technische Bundesanstalt, Bundesallee 100, 38116 Braunschweig, Germany*

<sup>2</sup>*Max-Planck-Institut für Kernphysik, Saupfercheckweg 1, 69117 Heidelberg, Germany*

<sup>3</sup>*Institut für Quantenoptik, Leibniz Universität Hannover, Hannover, Germany*

Presenting Author: lisa.schmoeger@mpi-hd.mpg.de

Laser spectroscopy with highly charged ions (HCI) enables studies of QED, relativistic and nuclear size effects which follow charge-dependent scaling laws. Narrow optical transitions found between fine structure levels in HCI are of great interest for investigations of possible variations of the fine structure constant  $\alpha$  [1] and for realisations of high accuracy frequency standards. Optical clocks based on such transitions will benefit from a low susceptibility to external fields which largely suppresses systematic shifts. Moreover, strong relativistic effects enhance their sensitivity to possible  $\alpha$  drifts. Electron beam ion traps (EBIT) have recently enabled optical laser spectroscopy with trapped HCI [2, 3]. However, typical translational temperatures higher than  $10^5$  K of the HCI trapped in an EBIT severely limit the achievable resolution. To overcome this, our cryogenic linear Paul trap CryPTE<sub>x</sub> [4] will enable trapping and sympathetic cooling of a wide range of EBIT-produced HCI by means of  $\text{Be}^+$  ions laser-cooled into Coulomb crystals. Achievable ion temperatures on the order of mK will give access to the natural linewidth of forbidden optical transitions in HCI on the order of tens of Hz. A recently commissioned deceleration beamline with time-focusing properties for efficient ion extraction and injection feeds CryPTE<sub>x</sub> with HCI extracted from an EBIT and  $\text{Be}^+$  Coulomb crystal studies (Fig. 1) have been performed. The slowing down and capturing of HCIs (in particular  $\text{Ar}^{13+}$ ) in  $\text{Be}^+$  Coulomb crystals is the next step. Additionally, a narrow-linewidth laser system based on a Ti:Sa laser is currently being developed, which will span most of the visible spectrum for high precision laser spectroscopy of HCIs.

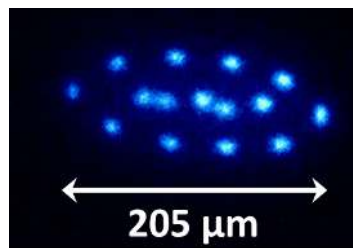


**Figure 1:** Small  $\text{Be}^+$  Coulomb crystal obtained with axial and radial trap frequencies of  $97 \times 2\pi$  kHz and  $365 \times 2\pi$  kHz, respectively.

### References

- [1] J. C. Berengut *et al.* Phys. Rev. Lett. **106**,210802 (2011)
- [2] V. Mäckel *et al.* Phys. Rev. Lett. **107**,143002 (2011)
- [3] K. Schnorr *et al.* Astrophys. J. **776**, 121 (2013)
- [4] M. Schwarz *et al.* Rev. Sci. Instrum. **83**, 083115 (2012)

# A novel cryogenic Paul Trap for Quantum Logic Spectroscopy of Highly Charged Ions

M. Schwarz<sup>1,2</sup>, O.O. Versolato<sup>1,2</sup>, L. Schmöger<sup>1,2</sup>, M. Kohnen<sup>2</sup>, T. Leopold<sup>2</sup>, P. Micke<sup>1,2</sup>, J. Ullrich<sup>2</sup>,  
P.O. Schmidt<sup>2,3</sup>, and J.R. Crespo López-Urrutia<sup>1</sup>

<sup>1</sup>Max-Planck-Institut für Kernphysik, Saupfercheckweg 1, 69117 Heidelberg, Germany

<sup>2</sup>Quest Institute for Experimental Quantum Metrology, Physikalisch-Technische Bundesanstalt, Bundesallee 100, 38116 Braunschweig, Germany

<sup>3</sup>Institut für Quantenoptik, Leibniz Universität Hannover, 30167 Hannover, Germany

Presenting Author: m.schwarz@mpi-hd.mpg.de

A linear cryogenic Paul trap experiment (CryPTE<sub>x</sub>) has been set up in-line with an electron beam ion trap (EBIT). CryPTE<sub>x</sub> will provide long storage times for highly charged ions (HCIs) due to the extremely low background pressure within a 4K enclosure [1]. First experiments on the storage of HCIs in this trap are presently under way. Since HCIs generally do not allow for direct laser cooling, as their optical transitions have low transition rates, one needs to apply sympathetic cooling. The trapped HCIs will be coupled by Coulomb-interaction to a low-temperature bath of laser-cooled ions what ultimately should allow to resolve the natural linewidth of forbidden transitions. Our final goal is the application of quantum logic spectroscopy [2], where a singly charged ion species (Be<sup>+</sup>) is responsible for the sympathetic cooling and state detection of the HCI. For the purpose of these high precision measurements, a second cryogenic Paul trap is currently being designed at MPIK in collaboration with PTB. The design of this trap is based on CryPTE<sub>x</sub>, where a cryogenic housing together with the ion injection capability have been realized. The next generation design will focus on decoupling of the vibration and magnetic field noise in order to obtain a noise-free environment as required for precision spectroscopy.

## References

- [1] M. Schwarz *et al.* Rev. Sci. Instrum. **83** 083115 (1997)
- [2] P.O.Schmidt, T. Rosenband, C. Langer, Science **309**, 749–752 (2005)

# Cold hydrogen molecular ion spectroscopy for proton to electron mass ratio measurement

J.-Ph. Karr<sup>1</sup>, A. Douillet<sup>1</sup>, N. Sillitoe<sup>1</sup>, and L. Hilico<sup>1</sup>

<sup>1</sup>*Laboratoire Kastler Brossel, UMR 8552, UEVE, UPMC, CNRS, ENS, F-75252, Paris*

Presenting Author: hilico@spectro.jussieu.fr

Cold hydrogen molecular ions  $H_2^+$  or  $HD^+$  allows for direct optical determination of the proton to electron mass ratio  $m_p/m_e$  using high resolution laser spectroscopy. The expected relative accuracy is limited by theoretical predictions at the  $6 \times 10^{-11}$  level [1], and will soon be improved by a factor of 4, challenging the present CODATA by one order of magnitude as well as the bound-electron g-factor measurement method [2]. Some selected rovibrational transitions have extremely high quality factors [3,4], making hydrogen molecular ions extremely good candidates for  $m_p/m_e$  time variation analysis.

We first discuss the best Doppler-free transitions in  $H_2^+$  and  $HD^+$  towards these metrological goals (counter propagating two-photon transitions versus dipole allowed/quadrupole transitions in the Lamb-Dicke regime), taking into account initial molecular state preparation, ion trapping and sympathetic cooling as well as transition detection.

We present the experimental set-up we are setting up in Paris, including a REMPI state selected  $H_2^+$  ion source, a linear trap for light molecular ions sympathetic cooling by laser cooled  $Be^+$  ions, as well as the laser sources.

Sympathetic cooling of light ions produced in an external source and injected in a linear trap is an experimental issue that deserves intense numerical simulations to determine optimal trapping and injection conditions. Beyond hydrogen molecular ions, they are useful for highly charged ion or antimatter ion cooling [6,7]. We report on our recent progress in implemented a highly efficient (4.5 TFlops) multi-GPU simulation code taking into account the exact N-body dynamics in time dependant RF fields of the trap, and the cooling laser interaction.

## References

- [1] V. I. Korobov, L. Hilico, J.-Ph. Karr, *Precision spectroscopy of the hydrogen molecular ions and antiprotonic helium*, Physical Review Letters **112**, 103003 (2014)
- [2] S. Sturm *et al.*, *High-precision measurement of the atomic mass of the electron* Nature **506**, 467–470 (2014)
- [4] S. Schiller, D. Bakalov, V.I. Korobov, *Simple Molecules and Clocks*, <http://arxiv.org/abs/1402.1789>
- [5] J.-Ph. Karr,  *$H_2^+$  and  $HD^+$ : candidates for a molecular clock* <http://arXiv.org/abs/1403.6925>
- [6] L. Hilico *et al.*, *Preparing single ultra-cold antihydrogen atoms for the free-fall in GBAR*, International Journal of Modern Physics, Conference Series (2014)
- [7] <https://gbar.web.cern.ch/GBAR/index.php>

# Photon BEC in a dye-microcavity system and the effects of interactions

R.A. Nyman<sup>1</sup> and J. Marelic<sup>1</sup>

<sup>1</sup>Centre for Cold Matter, Imperial College London, United Kingdom, SW7 2AZ

Presenting Author: r.nyman@imperial.ac.uk

Photons are bosons, but they don't normally make Bose-Einstein condensates because their number is not conserved in thermal equilibrium. However, light pumped into a fluorescent dye can exchange energy with the dye-solvent mixture, coming to thermal equilibrium without destroying the photons. The electronic structure of the dye sets a minimum energy, preventing the photon from being destroyed altogether. Placing this system between two curved, high-reflectivity mirrors, the light is confined for about a nanosecond, which is much faster than the picosecond it takes for thermalisation. Therefore thermal equilibrium can be achieved at room temperature with a photon number determined by the pumping intensity. At a fixed temperature, and sufficient density, a Bose-Einstein condensate (BEC) will form, as first achieved in 2010 [1].

Recently, we have demonstrated Bose-Einstein condensation in our lab: see Fig. 1. We have confirmed the thermalisation of photons at room temperature, and have achieved sufficient photon density to see the BEC phase transition. The project's aims include measuring the interaction strength, characterising the coherence properties of the condensate, and fabricating mirror shapes which would allow observation of 1D gases of photons as well as photon BECs with mesoscopic numbers.

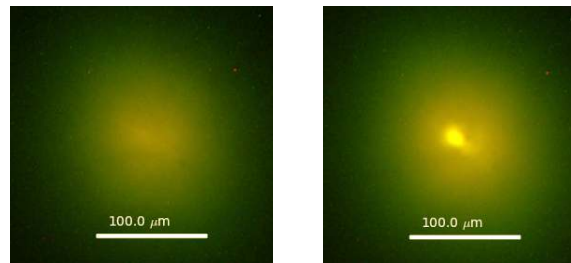


**Figure 1:** Real-colour images of thermalised photons in our dye-filled microcavity. Left: just below threshold. Right: just above threshold, showing macroscopic occupation of the lowest energy state.

The equation of motion which describes a photon BEC is very similar to the Gross-Pitaevskii equation which is familiar from atomic BEC. However, the effects of continual pumping and decay via cavity mirrors also appear, making the equation complex. The parameters of this equation, especially the interactions, are not yet known. We have analysed an experimental method for inferring the strength of interactions in photon BEC, by observing these excitations using angle-resolved spectroscopy of the light that leaks through the mirrors [2]. Even very weak interactions should be detectable this way.

## References

- [1] J. Klaers *et al.*, Nature, **468**, 545–548 (2010)
- [2] R.A. Nyman and M.H. Szymańska, Phys. Rev. A, **89** 033844 (2014)

## Investigation of the excited electronic KCs states studied by polarization labeling spectroscopy

A. Grochola<sup>1</sup>, J. Szczepkowski<sup>2</sup>, W. Jastrzebski<sup>2</sup>, and P. Kowalczyk<sup>1</sup>

<sup>1</sup>*Institute of Experimental Physics, Faculty of Physics, University of Warsaw, Hoża 69, 00-681 Warsaw, Poland*

<sup>2</sup>*Institute of Physics, Polish Academy of Sciences, Al. Lotników 32/46, 02-668 Warsaw, Poland*

Presenting Author: anna.grochola@fuw.edu.pl

The heteronuclear KCs molecule belongs to the least known alkali diatomics. Till the late 1990s the sole semi-empirical characteristics of KCs consisted in some ground state spectroscopic constants estimated by interpolation from the corresponding experimental values of K<sub>2</sub> and Cs<sub>2</sub>. Also among theoreticians, the interest in KCs was very limited. The rapid development of cold physics in the past two decades brought heteronuclear alkali diatomics, with KCs among them, into wider attention, particularly because of their permanent electric dipole moments. New trends have inspired quantum chemistry calculations first [1], followed by experiments employing modern spectroscopic methods [2,3]. To date, seven electronic states of KCs have been observed experimentally: the ground state and six excited states extending up to about 18500 cm<sup>-1</sup> above the bottom of the ground state potential energy curve.

In our work we investigate excited electronic states of KCs molecule, dissociating to the K(4S) + Cs(5D) and K(3D) + Cs(6S) asymptotes, within the excitation energy range 18000 - 21000 cm<sup>-1</sup>. The molecular states of KCs should be described rather in Hund's case (c) than Hund's case (a), what makes possible to observe transitions to nominally forbidden states and therefore increases the number of observed states. In this contribution we present first description of selected electronic states in the energy region mentioned above, using the Dunham expansion. Results are compared with theoretical calculations [4].

### References

- [1] M. Korek *et al.* Can. J. Phys. **78** 977–988 (2000)
- [2] M. Tamanis *et al.* Phys. Rev. A **82** 032506 (2010)
- [3] J. Szczepkowski *et al.* J. Mol. Spectrosc. **19** 276–277 (2012)
- [4] M. Korek, Y.A. Moghrabi, A.R. Allouche, J. Chem. Phys. **124** 094309 (2006)

## Spectroscopic study of the $4^1\Sigma^+$ state of LiCs and comparison with theory

J. Szczepkowski<sup>1</sup>, P. Jasik<sup>2</sup>, A. Grochola<sup>3</sup>, W. Jastrzebski<sup>1</sup>, J.E. Sienkiewicz<sup>2</sup>, and P. Kowalczyk<sup>3</sup>

<sup>1</sup>*Institute of Physics, Polish Academy of Sciences, Al. Lotników 32/46, 02-668 Warszawa, Poland*

<sup>2</sup>*Department of Theoretical Physics and Quantum Information, Faculty of Applied Physics and Mathematics, Gdańsk University of Technology, ul. Narutowicza 11/12, 80-233 Gdańsk, Poland*

<sup>3</sup>*Institute of Experimental Physics, Faculty of Physics, University of Warsaw, Hoża 69, 00-681 Warszawa, Poland*

Presenting Author: Pawel.Kowalczyk@fuw.edu.pl

The  $4^1\Sigma^+$  electronic state of  $^7\text{LiCs}$  molecule was investigated experimentally for the first time. Two colour polarization labelling experiment (see e.g. [1]) measuring the  $4^1\Sigma^+ \leftarrow X^1\Sigma^+$  band system under rotational resolution furnished energies of about 400 rovibronic levels in the  $4^1\Sigma^+$  state with an accuracy better than  $0.1 \text{ cm}^{-1}$ . The observed vibrational progressions exhibited irregular intervals for two reasons. First, the potential curve of the  $4^1\Sigma^+$  state was expected to be of irregular shape because of an anticrossing with the lower  $3^1\Sigma^+$  state. Second, numerous strong, local perturbations of  $4^1\Sigma^+$  by the neighbouring electronic states were evident. To aid the interpretation of the experiment, theoretical calculations of adiabatic potentials for excited states of LiCs including  $4^1\Sigma^+$  were performed with the MOLPRO program package [2]. They confirmed the assumption of unusual shape of the  $4^1\Sigma^+$  state potential and also provided a good starting point for the inverted perturbation approach (IPA) procedure [3], which allowed to construct the potential energy curve of this state from the experimental observations. A full deperturbation treatment of the  $4^1\Sigma^+$  state was not attempted, but a robust weighting scheme [4] was used to reduce the influence of levels that cannot be properly represented by a single channel model. Parameters derived in a fit of the potential curve include term energy  $T_e=18848.4 \text{ cm}^{-1}$ , well depth  $D_e=1931 \text{ cm}^{-1}$  and equilibrium distance  $R_e=4.91 \text{ \AA}$ .

### References

- [1] A. Grochola *et al.*, J. Chem. Phys. **135** art. no. 044318 (2011)
- [2] MOLPRO, version 2006.1, a package of ab initio programs, H.-J. Werner, P. J. Knowles *et al.*, see <http://www.molpro.net>
- [3] A. Pashov, W. Jastrzebski, P. Kowalczyk, Comput. Phys. Commun. **128** 622–634 (2000)
- [4] J. K. G. Watson, J. Mol. Spectrosc. **219** 326–328 (2003)

## Spectroscopic studies on binding of novel pheophorbide - phenazine conjugate to synthetic polynucleotides

O. Ryazanova<sup>1</sup>, V. Zozulya<sup>1</sup>, I. Voloshin<sup>1</sup>, V. Karachevtsev<sup>1</sup>, L. Dubey<sup>2</sup>, and I. Dubey<sup>2</sup>

<sup>1</sup>*Dept. of Molecular Biophysics, B. Verkin Institute for Low Temperature Physics and Engineering of NAS of Ukraine, Kharkov, Ukraine*

<sup>2</sup>*Dept. of Synthetic Bioregulators, Institute of Molecular Biology and Genetics of NAS of Ukraine, Kyiv, Ukraine*

Presenting Author: ryazanova@ilt.kharkov.ua

Porphyrins are macrocyclic compounds possessing by unique photophysical properties and having the great potential for application in nanotechnology, biology and medicine. Pheophorbide-*a* (Pheo-*a*) is well-known anionic porphyrin derivative which selectively accumulates in tumor cells. It has a high extinction coefficient in the red region of spectrum where the transparency of tissues to light increases considerably, that determines widespread using of Pheo-*a* as a photosensitizer for PDT of tumor. Novel conjugate formed by pheophorbide-*a* with intercalative amino-phenazinium dye (Pheo-Pzn) was synthesized. Its spectroscopic properties, as well as binding affinity to synthetic polynucleotides of different secondary structure (double-stranded poly(A)·poly(U), poly(G)·poly(C) and four-stranded poly(G)) were studied using absorption, polarized fluorescence and fluorescent titration techniques. Investigations were carried out in 2 mM Na<sup>+</sup> cacodylate and phosphate buffered solutions (pH6.9) containing 2 -10% of ethanol, 0.5 mM EDTA and 0.1 M NaCl. The measurements were performed in a wide range of molar polymer-to-dye ratios (*P/D*) by registering the changes in the intensity and polarization degree of the pheophorbide fluorescence. Spectroscopic properties of the conjugate-polynucleotide complexes were compared with those for free constituents. It was found that in aqueous solution formation of internal heterodimer with stacking of the chromophores was occurred, manifesting itself by strong fluorescence quenching (in tens of thousands times in comparison with ethanol solution). External binding of Pheo-Pzn to poly(A)·poly(U) and poly(G)·poly(C) is apparently realised without the dimer destruction: only insignificant rise of the emission was registered along with increase of fluorescence polarisation degree up to 0.15. The binding to four-stranded poly(G) differs substantially from that for double-stranded polynucleotides. Substantial blue shift of absorption bands, 10 nm red shift of fluorescence band, 50-fold rise of pheophorbide emission, and increase in its fluorescence polarization degree up to  $p = 0.3$  evidences the heterodimer disintegration and intercalation of pheophorbide moiety into the intermolecular G-quadruplex. So the conjugate studied can be used as fluorescent probe for recognition of G-quadruplex structure.

## Precise line-shape measurements of oxygen B-band transitions with absolute frequency reference

S. Wójtewicz<sup>1</sup>, A. Cygan<sup>1</sup>, P. Masłowski<sup>1</sup>, J. Domysławska<sup>1</sup>, P. Wcisło<sup>1</sup>, M. Zaborowski<sup>1</sup>, M. Piwiński<sup>1</sup>, D. Lisak<sup>1</sup>, R.S. Trawiński<sup>1</sup>, and R. Ciuryło<sup>1</sup>

<sup>1</sup>*Institute of Physics, Faculty of Physics, Astronomy and Informatics, Nicolaus Copernicus University, Grudziadzka 5/7, 87-100 Toruń, Poland*

Presenting Author: piotr.wcislo@fizyka.umk.pl

We present high-resolution and high-sensitivity line-shape measurements of self- and foreign-broadened P-branch transitions of the oxygen B band occurring near 689 nm. Data were acquired using the optical frequency comb-assisted Pound-Drever-Hall-locked frequency-stabilized cavity ring-down spectrometer (OFC-assisted PDH-locked FS-CRDS) [1, 2]. In the line-shape analysis the line narrowing described by Dicke narrowing or the speed dependence of collisional broadening were taken into account. The multispectrum fitting technique was used to minimize correlation between line-shape parameters. The relation between the parameters describing Dicke narrowing with the use of the soft- and hard-collision models is discussed and verified experimentally in the self-broadened case in the low pressure regime (below 5 kPa). We report line positions with uncertainties of about 170 kHz, intensities and the collisional broadening coefficients with subpercent uncertainties [3]. We compare these results to data available in the literature.

The research is part of the program of the National Laboratory FAMO in Toruń, Poland, and is supported by the Polish National Science Centre Projects no. DEC-2011/01/B/ST2/00491 and UMO-2012/05/N/ST2/02717. The research is also supported by the Foundation for Polish Science TEAM and HOMING PLUS Projects co-financed by the EU European Regional Development Fund. A. Cygan is partially supported by the Foundation for Polish Science START Project.

### References

- [1] J. Domysławska *et al.* *J. Chem. Phys.* **139**, 194312-1–194312-10(2013)
- [2] A. Cygan *et al.* *Eur. Phys. J.-Spec. Top.* **222**, 2119–2142 (2013)
- [3] S. Wójtewicz *et al.* *J. Quant. Spectrosc. Radiat. Transfer.* (2014) – accepted

# Towards ab initio dynamical simulations of atoms, molecules, and clusters in femtosecond XUV pulses

P.R. Kaprálová-Žánská<sup>1,2</sup> and J. Šmydke<sup>1,2</sup>

<sup>1</sup>J. Heyrovsky Institute of Physical Chemistry, Academy of Sciences of the Czech Republic, Dolejškova 3, 18223 Prague 8, Czech Republic

<sup>2</sup>Department of Radiation and Chemical Physics, Institute of Physics, Academy of Sciences of the Czech Republic, Na Slovance 2, 182 21 Prague 8, Czech Republic

Presenting Author: kapralova@jh-inst.cas.cz

In this paper, we focus on a correct representation of electronic wavefunctions of the laser-driven systems. Out of various approaches developed for atoms and diatomics, making use of B-splines, numerical lattices, and basis sets, only the latter seem to be readily portable to other molecules due to an anisotropy resulting from the properties of the Coulomb potential. With the help of the Wigner representation, we will discuss numerical implications of a complex scaling transformation, which is used in order to properly account for ionization as well as to keep a feasible size of the dressed-states basis set [1]. Then we will demonstrate that Gaussian primitives that are optimized for a high accuracy of Rydberg states, happen to be unexpectedly beneficial for a numerical precision of complex scaling calculations [2]. Our conclusions will be demonstrated for example calculations of the field-free and driven helium atom [3,4]. Finally, we will briefly discuss the intended application of the Gaussian basis sets to other atoms and molecules.

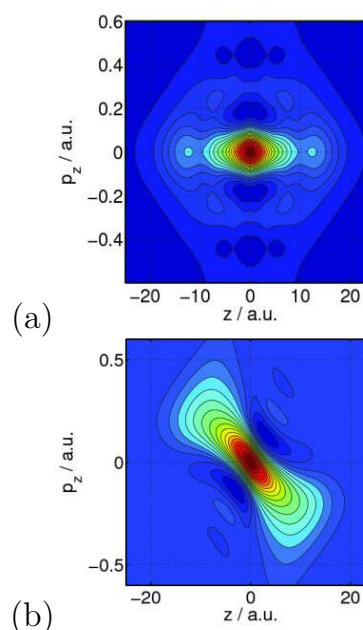


**Figure 1:** Wigner distribution of the 5s state of hydrogen: (a) unscaled, (b) complex scaled.

| $\theta$ | aug-cc-pV5Z                     | ExTG5G                          |
|----------|---------------------------------|---------------------------------|
| 0        | -2.903201                       | -2.903506                       |
| 0.2      | $-2.903230 + 10^{-4}i$          | $-2.903505 + 2 \times 10^{-6}i$ |
| 0.6      | $-2.904047 + 7 \times 10^{-3}i$ | $-2.903509 + 7 \times 10^{-6}i$ |

**Table 1:** Complex energies of the helium ground state obtain artificial non-zero imaginary parts for non-zero values of the complex scaling parameter  $\theta$  due to insufficient basis sets. The second column shows results for a standard quantum chemistry basis set, while the third column for the new optimized Gaussian basis set.

## References

- [1] P. R. Kaprálová-Žánská, J. Chem. Phys. **134**, 204101 (2011)
- [2] P. R. Kaprálová-Žánská and J. Šmydke, J. Chem. Phys. **138**, 024105 (2013)
- [3] P. R. Kaprálová-Žánská, J. Šmydke, and S. Civis, J. Chem. Phys. **139**, 104314 (2013)
- [4] P. R. Kaprálová-Žánská and N. Moiseyev, submitted to J. Chem. Phys.

## First analysis of the Herzberg ( $C^1\Sigma^+ \rightarrow A^1\Pi$ ) band system in the lesser-abundant $^{13}\text{C}^{17}\text{O}$ isotopologue

R. Hakalla<sup>1</sup>, M. Zachwieja<sup>1</sup>, W. Szajna<sup>1</sup>, I. Piotrowska<sup>1</sup>, M. Ostrowska-Kopec<sup>1</sup>, P. Kolek<sup>1</sup>, and R. Kępa<sup>1</sup>

<sup>1</sup>Materials Spectroscopy Laboratory, Department of Experimental Physics, Faculty of Mathematics and Natural Science, University of Rzeszów, ul. Prof. S. Pigońia 1, 35-959 Rzeszów, POLAND

Presenting Author: hakalla@univ.rzeszow.pl

It has been presented high-resolution emission spectra measurements of the so far non-analysed in the  $^{13}\text{C}^{17}\text{O}$  isotopologue, the Herzberg band system. The  $C \rightarrow A(0, 1)$ ,  $(0, 2)$ , and  $(0, 3)$  bands have been recorded in the 22 950 – 26 050  $\text{cm}^{-1}$  region using high-accuracy dispersive optical spectroscopy [1–3]. The  $^{13}\text{C}^{17}\text{O}$  molecules were formed and excited in a stainless steel hollow-cathode lamp with two anodes. All 224 rovibrational spectra lines, up to  $J = 30$ , were precisely measured with an estimated accuracy of about 0.0030  $\text{cm}^{-1}$ , and rotationally analysed.

We are going to present the values of molecular parameters determined for the first time in  $^{13}\text{C}^{17}\text{O}$ : the merged rotational constants of the  $C^1\Sigma^+(v = 0)$  Rydberg state and the individual rotational constants of the  $A^1\Pi(v = 3)$  state, the rotational and vibrational equilibrium constants for the  $C^1\Sigma^+$  state, the band origins of the  $C \rightarrow A$  system, the isotope shifts, and the  $\Delta G_{1/2}^C$  vibrational quantum as well as the RKR turning points, Franck - Condon factors, relative intensities, and r-centroids for the Herzberg band system as well as the main, isotopically invariant parameters of the  $C^1\Sigma^+$  state in the CO molecule within the Born-Oppenheimer approximation.

The combined analysis of now obtained Herzberg bands and earlier analyzed Ångström ( $B^1\Sigma^+ \rightarrow A^1\Pi$ ) system [4, 5] yielded a precise relative characteristic of the  $C^1\Sigma^+(v = 0)$  and  $B^1\Sigma^+(v = 0, 1)$  Rydberg states in the  $^{13}\text{C}^{17}\text{O}$  molecule, among others:  $\nu_{00}^{CB}$ ,  $\nu_{01}^{CB}$  vibrational quanta.

For the  $A^1\Pi(v = 3)$  state of  $^{13}\text{C}^{17}\text{O}$ , considerable irregularities of the rotational structure have been observed and analysed in detail. Simultaneously, the  $C^1\Sigma^+(v = 0)$  state was observed to be quite regular up to the observed  $J_{\text{max}}$  level.

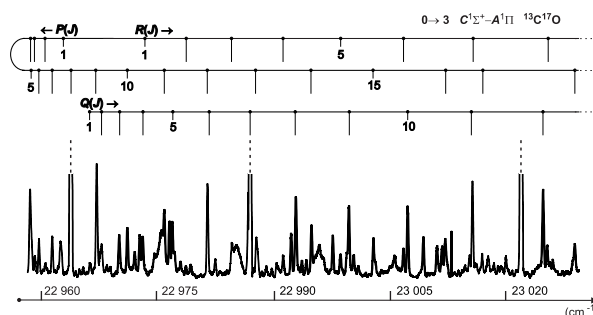


**Figure 1:** The emission spectrum of carbon monoxide showing the first observation and rotational interpretation of the  $C \rightarrow A(0, 3)$  transition in the  $^{13}\text{C}^{17}\text{O}$  isotopologue, on an expanded scale. Peaks of the atomic Th calibration lines are marked with broken lines.

### References

- [1] R. Hakalla, M. Zachwieja, W. Szajna *J. Quant. Spectrosc. Radiat. Transf.* **140**, 7–17 (2014).
- [2] R. Hakalla, W. Szajna, M. Zachwieja *J. Phys. B: At. Mol. Opt. Phys.* **45**, 215102–215111 (2012).
- [3] R. Hakalla *et al.* *Acta Phys. Pol. A* **122**, 674–683 (2012).
- [4] R. Hakalla, M. Zachwieja *J. Mol. Spectrosc.* **272**, 11–18 (2012).
- [5] R. Hakalla, W. Szajna, M. Zachwieja *J. Phys. Chem. A* **117**, 12299–12312 (2013).

# High resolution spectroscopy on alkali-alkaline earth molecules

M. Ivanova<sup>1</sup>, A. Pashov<sup>1</sup>, H. Knöckel<sup>2</sup>, A. Stein<sup>2</sup>, and E. Tiemann<sup>2</sup>

<sup>1</sup>Department of Physics, Sofia University, Sofia, Bulgaria

<sup>2</sup>QUEST and Institute of Quantum Optics, Leibniz University Hannover, Hannover, Germany

Presenting Author: knoeckel@iqo.uni-hannover.de

The mixed alkali-alkaline earth molecules have recently attracted the interest of the scientific community due to possible applications in the field of cold and ultracold molecules, in fundamental physics, quantum computing etc.. The combination of an alkali and an alkaline earth atom leads to molecules which have permanent electric and as well magnetic dipole moments and by this offer opportunities for manipulation of their states by external fields. On the theoretical side, several ab initio calculations [1-4] have been published on atomic combinations like LiCa, LiSr, SrRb by various groups, reflecting the increasing interest [5,6] by experimentalists working with cold and ultracold alkali and/or alkaline earth atoms. On the experimental side, not so much is known about molecular electronic states. Up to now the ground state and two electronically excited states of LiCa [7-9] and few states of BaLi [10] have been characterized.

After the spectroscopic work on LiCa [8,9] we have successfully recorded the near infrared spectra of SrLi and CaK. The molecules were created in a heatpipe with the locations of the alkali and alkaline earth metals kept at different temperatures, this way accounting for the different vapour pressures. The thermal emission was dispersed by a high resolution Fourier transform spectrometer. The assignment of the dense spectrum was made possible by shining a beam of a diode laser into the sample tuned to a molecular line.

This trick allowed to find and assign those transitions connected with the laser excitation. An example of the recorded spectrum for LiSr is shown in figure 1. The present report will focus on the  $2^2\Sigma^+ - X^2\Sigma^+$  transition of SrLi. The IR spectrum of CaK looks very similar in the overall appearance like LiSr, but its assignment is presently hindered by the lack of an appropriate laser. First spectral structures, which are probably attributable to SrRb were also observed.

## References

- [1] A. R. Allouche, M. Aubert-Frecon, J. Chem. Phys. 100, 938 (1994)
- [2] G. Gopakumar *et al.*, J. Chem. Phys. 138, 194307 (2013)
- [3] K.-L. Xiao *et al.*, J. Chem. Phys. 139, 074305 (2013)
- [4] P.S. Zuchowski *et al.*, <http://arxiv.org/abs/1402.0702v1>
- [5] N. Nemitz *et al.*, Phys. Rev. A 79, 061403 (2009)
- [6] H. Hara *et al.*, Phys. Rev. Lett. 106, 205304 (2011)
- [7] L. M. Russon *et al.*, J. Chem. Phys. 109, 6655 (1998)
- [8] M. Ivanova *et al.*, J. Chem. Phys. 135, 174303 (2011)
- [9] A. Stein *et al.*, J. Chem. Phys. 138, 114306 (2013)
- [10] e.g. A. Stringat *et al.*, J. Mol. Spectr. 168, 514 (1994)

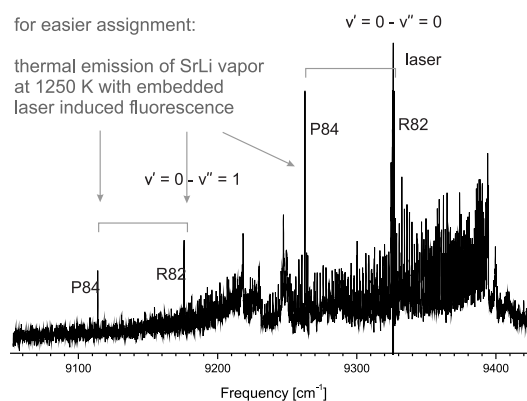


**Figure 1:** Example: part of the near infrared emission spectrum of SrLi with laser induced fluorescence for marking related transitions.

# Separation of overlapped profiles originated from different complexes excited in a supersonic expansion beam experiment

T. Urbanczyk<sup>1</sup> and J. Koperski<sup>1</sup>

<sup>1</sup>Smoluchowski Institute of Physics, Jagiellonian University, Reymonta 4, 30-057 Krakow, Poland

Presenting Author: tomek.urbanczyk@uj.edu.pl

A method of separation of overlapped spectra originating from different laser-excited complexes in a supersonic expansion beam will be presented. The method, which general idea is illustrated in Fig. 1, is used to analyze data recorded in the experiment using a high temperature pulsed supersonic beam of diatomic complexes containing cadmium i.e., Cd<sub>2</sub> and CdRg, where Rg=rare gas [1],[2]. The method is based on the observation that lifetimes of different complexes in their excited electronic states differ. Therefore, by applying the proper subtraction of spectra obtained for different time-gating windows, one can obtain the spectrum in which admixture from unwanted molecule is considerably reduced (for the time-gating window detection see [1]). As an example, the separation of overlapped profiles recorded using the  $B^31 \leftarrow X^10^+$  and  $b^30_u^+ \leftarrow X^10_g^+$  transitions in CdAr and Cd<sub>2</sub>, respectively [3] will be presented.

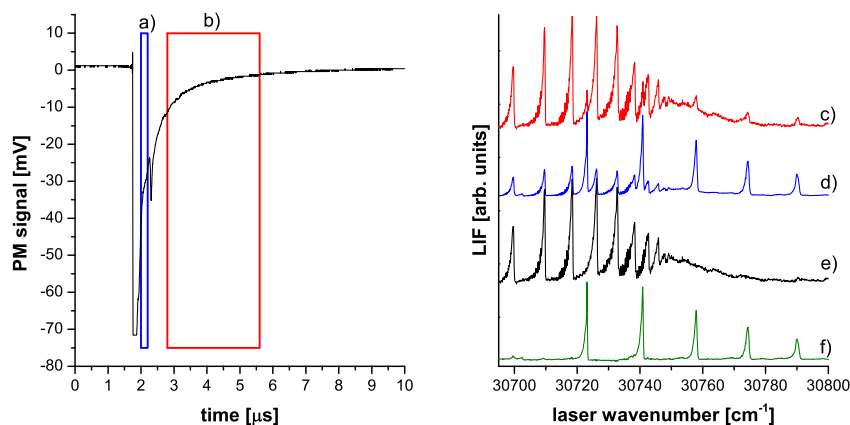


**Figure 1:** Illustration of the spectra separation method using an example of overlapped Cd<sub>2</sub> and CdAr excitation spectra. a) Blue (narrow) time-gating window employed in the detection of Cd<sub>2</sub> using the  $b^30_u^+ \leftarrow X^10_g^+$  transition with an unwanted admixture of CdAr; b) red (wide) time-gating window employed in detection of CdAr excitation spectrum using the  $B^31 \leftarrow X^10^+$  transition with an admixture of Cd<sub>2</sub>; c) excitation spectrum corresponding to the red (wide) time-gating window; d) excitation spectrum corresponding to the blue (narrow) time-gating window; e) result of subtraction of spectra presented in (c) and (d): resulting CdAr spectrum contains only small admixture of Cd<sub>2</sub>; f) as in (e) but showing restoration of the Cd<sub>2</sub> spectrum.

Presented studies are supported by the National Science Centre Poland according to contract no.

UMO-2011/01/B/ST2/00495.

## References

- [1] T. Urbanczyk, J. Koperski Rev. Sci. Instrum. **83**, 083114 (2012)
- [2] T. Urbanczyk, J. Koperski Eur. Phys. J. Special Topics **222**, 2187-2195 (2013)
- [3] T. Urbanczyk, J. Koperski Chem. Phys. Lett. **591**, 64-68 (2014)

# Direct laser cooling of the BH molecule

D.A. Holland<sup>1</sup>, R.J. Hendricks<sup>1</sup>, S. Truppe<sup>1</sup>, B.E. Sauer<sup>1</sup>, and M.R. Tarbutt<sup>1</sup>

<sup>1</sup>Centre for Cold Matter, Blackett Laboratory, Imperial College London, Prince Consort Road, London SW7 2AZ, UK

Presenting Author: darren.holland11@imperial.ac.uk

Ultracold polar molecules are of interest for a variety of applications [1], including tests of fundamental physics, ultracold chemistry, and simulation of many-body quantum systems. The laser cooling techniques that have been so successful in producing ultracold atoms are difficult to apply to molecules. The extra vibrational and rotational degrees of freedom make it difficult to find a closed system for optical cycling. Recently however, laser cooling has been applied successfully to a few molecular species [2–5], and a magneto-optical trap of SrF molecules has now been demonstrated [6]. We have investigated the BH molecule as a candidate for laser cooling [7]. We have produced a molecular beam of BH and have measured the branching ratios for the excited electronic state,  $A^1\Pi(v'=0)$ , to decay to the various vibrational states of the ground electronic state,  $X^1\Sigma$ . Our measured branching ratios are shown in figure 1. We verify that the branching ratio for the spin-forbidden transition to an intermediate triplet state is inconsequentially small. We measure the frequency of the lowest rotational transition of the X state, and the hyperfine structure in the relevant levels of both the X and A states, and determine the nuclear electric quadrupole and magnetic dipole coupling constants. Our results show that, with a relatively simple laser cooling scheme, a Zeeman slower and magneto-optical trap can be used to cool, slow and trap BH molecules.

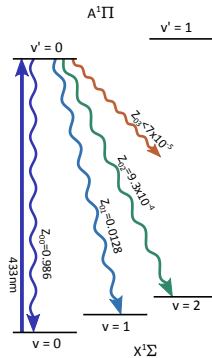


**Figure 1:** Vibrational branching ratios,  $Z_{0n}$ , for the  $A^1\Pi \rightarrow X^1\Sigma$  transition in BH.

## References

- [1] L. D. Carr, D. DeMille, R. V. Krems and J. Ye, *New J. Phys.* **11** 055049 (2009)
- [2] E. S. Shuman, J. F. Barry, and D. DeMille, *Nature* **467**, 820 (2010)
- [3] M. T. Hummon, M. Yeo, B. K. Stuhl, A. L. Collopy, Y. Xia, and J. Ye, *Phys. Rev. Lett.* **110**, 143001 (2013)
- [4] J. F. Barry, E. S. Shuman, E. B. Norrgard, and D. DeMille, *Phys. Rev. Lett.* **108**, 103002 (2012)
- [5] V. Zhelyazkova, A. Cournol, T. E. Wall, A. Matsushima, J. J. Hudson, E. A. Hinds, M. R. Tarbutt, and B. E. Sauer, *Phys. Rev. A* **89**, 053416 (2014)
- [6] J. F. Barry, D. J. McCarron, E. B. Norrgard, M. H. Steinecker, and D. DeMille, <http://arxiv.org/abs/1404.5680>
- [7] R. J. Hendricks, D. A. Holland, S. Truppe, B. E. Sauer, and M. R. Tarbutt, <http://arxiv.org/abs/1404.6174>

# Ultra-narrow-linewidth Mid-infrared Optical Parametric Oscillator

I. Ricciardi<sup>1</sup>, S. Mosca<sup>1</sup>, M. Parisi<sup>1</sup>, P. Maddaloni<sup>1</sup>, L. Santamaria<sup>1</sup>, M. De Rosa<sup>1</sup>, G. Giusfredi<sup>2</sup>, and P. De Natale<sup>2</sup>

<sup>1</sup>CNR-INO, Istituto Nazionale di Ottica, Via Campi Flegrei 34, 80078 Pozzuoli (NA), Italy

<sup>2</sup>CNR-INO, Istituto Nazionale di Ottica, and LENS, via Carrara 1, 50019 Sesto Fiorentino FI, Italy

Presenting Author: iolanda.ricciardi@ino.it

Highly stable and spectral pure laser sources are crucial for a wide range of demanding applications, including high-resolution spectroscopy, frequency metrology, and precision tests of fundamental physics. We demonstrate Hz-level narrowing of a singly resonant optical parametric oscillator (OPO), emitting in the frequency range between 2.7 and 4.2  $\mu\text{m}$  [1–2], where intense ro-vibrational transitions of many molecules with a natural linewidth as low as a few Hz are present.

In our experimental set-up a Nd:YAG laser, frequency narrowed at 1-Hz-linewidth (over 1 ms) against a stable ultra-low-expansion (ULE) Fabry–Pérot cavity, is amplified up to 10 W to pump the OPO. The OPO is based on a periodically poled MgO:LiNbO<sub>3</sub> crystal placed in a bow-tie cavity resonant for the signal. The crystal has seven different poling periods, allowing the continuous tuning of the idler frequency between 2.7 and 4.2  $\mu\text{m}$ , with about 1 Watt of emitted power. We exploit a transfer oscillator scheme [3], according to which an optical frequency comb synthesizer acts as the transfer oscillator between a highly stable pump laser mode and the resonating OPO signal mode: as a consequence, the spectral features of the pump laser are transferred to the signal mode, independently of technical fluctuations of the comb frequencies. In turn, the fluctuations of idler mode frequency will be of the same order of the pump laser ones, as in a singly-resonant OPO the idler linewidth is the sum of the two uncorrelated pump and signal linewidths. The transfer oscillator is an amplified mode-locked Er:doped fibre laser, followed by a nonlinear photonic fibre, generating an octave-spanning frequency comb, between 1–2  $\mu\text{m}$ , of equally spaced modes (repetition rate,  $f_r \simeq 250$  MHz).

For the diagnostics of the residual frequency noise of the pump mode we used a reference Fabry–Pérot cavity, made by a couple of HR mirrors glued on an invar spacer, kept under vacuum for environmental isolation. The invar cavity is loosely locked (10-Hz-bandwidth) to the pump frequency by a Pound–Drever–Hall (PDH) scheme. Thus, for spectral frequencies greater than the locking bandwidth, the power spectral density (PSD) of the PDH signal gives the free-running relative frequency noise between the pump and the invar cavity. For times shorter than 1 ms the integrated PSD gives a pump linewidth around 1 Hz.

The signal residual frequency noise has been estimated in a similar way, using a second reference invar cavity. In this case, for times shorter than 1 ms we estimated a signal linewidth around 1 Hz, which summed to the 1 Hz pump linewidth, results in an idler linewidth at the Hz-level.

## References

- [1] I. Ricciardi, E. De Tommasi, P. Maddaloni, S. Mosca, A. Rocco, J.-J. Zondy, M. De Rosa, and P. De Natale, *Opt. Express* **20**, 9178–9186 (2012)
- [2] I. Ricciardi, E. De Tommasi, P. Maddaloni, S. Mosca, A. Rocco, J.-J. Zondy, M. De Rosa, and P. De Natale, *Mol. Phys.* **110**, 2103–2109 (2012)
- [3] H. R. Telle, B. Lipphardt, and J. Stenger, *Appl. Phys. B* **74**, 1–6 (2002)

# Rotational state manipulation of trapped polyatomic molecules

R. Glöckner<sup>1</sup>, A. Prehn<sup>1</sup>, M. Krottenmüller<sup>1</sup>, M. Zeppenfeld<sup>1</sup>, and G. Rempe<sup>1</sup>

<sup>1</sup>Max-Planck-Institut für Quantenoptik, Hans-Kopfermann-Str. 1, 85748 Garching, Germany

Presenting Author: rosa.gloeckner@mpq.mpg.de

Due to their anisotropic long range interaction and many internal states, cold or ultracold molecular ensembles offer manifold possibilities for studying many-body physics and quantum information or quantum controlled collisions and chemistry. Therefore during the past years a fast growing scientific community has focused on the development of techniques for cooling molecular ensembles. However, especially for polyatomic molecules a major issue is the control over the internal states, meaning the vibrational and rotational states. A first step towards this end is to obtain the possibility for detecting the rotational state. Up to now, many detection schemes like REMPI involve the excitation of electronic states, which can lead to rapid fragmentation and predissociation. This results in an enormous line broadening and thus a loss of state selectivity.

Here we present the current status of our experiment focusing on the addressing and manipulation of rotational states for the sake of internal state detection. Our detection method is based on the removal of selected states from a trapped ensemble. The trapping time inside our microstructured electric trap on the order of 10 s [1] allows us to rely on rather slow processes such as a spontaneous vibrational decay for state manipulation. Vibrational and rotational transitions are driven with a single infrared laser and microwave source. We show results for the polyatomic molecule CH<sub>3</sub>F, which we already used to demonstrate Sisyphus cooling of the ensemble by more than one order of magnitude in temperature with an increase of phase space density by a factor of 30 [2,3]. We have developed methods for detecting the total angular momentum  $J$  and show possibilities for the detection of  $K$ , the projection of  $J$  on the symmetry axis of the molecule, and  $M$ , the projection on the electric field axis. The experimental limitations such as the spectral resolution inside our electric trap are discussed as well as effects on the measurements due to black body radiation. Our detection scheme is expected to work for a large variety of molecular species.

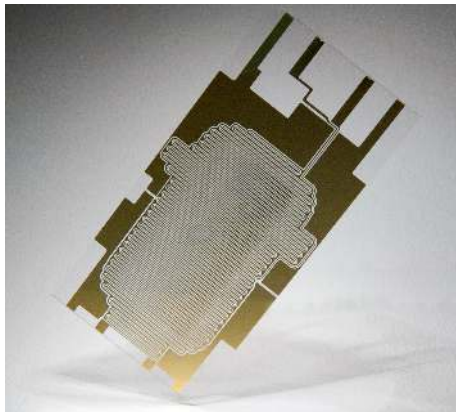


Figure 1: A picture of our microstructured trap plates

## References

- [1] B.G.U. Englert *et al.*, *Phys. Rev. Lett.* **107**, 263003 (2011).
- [2] M. Zeppenfeld *et al.*, *Phys. Rev. A* **80**, 041401 (2009).
- [3] M. Zeppenfeld *et al.*, *Nature* **491**, 570-573 (2012).

## Fine Structure Analysis of the Configuration System of V II

S Bouazza<sup>1</sup>, R.A. Holt<sup>2</sup>, D.S. Rosner<sup>2</sup>, and N.M.R. Armstrong<sup>3</sup>

<sup>1</sup>*LISM, Université de Champagne-Ardenne, Reims, France*

<sup>2</sup>*Department of Physics and Astronomy, University of Western Ontario, London, Canada*

<sup>3</sup>*Department of Physics and Astronomy, Mc Master University, Hamilton, Canada*

Presenting Author: safa.bouazza@univ-reims.fr

Using a linked-parameter technique of level-fitting calculations in a multiconfiguration basis, a parametric analysis of fine structure (fs) for even-parity levels of V II, involving six configurations, has been performed. This led us to exchange the assignments of two triplets,  $3d^3(2F)4s$  c  $3F$  and  $3d^4$  d  $3F$ , reported in earlier analyses as being located at  $30300 \text{ cm}^{-1}$  and  $30600 \text{ cm}^{-1}$ , respectively. This is confirmed by experimental hyperfine structure A constants, used as fingerprints. Moreover, the current singlet  $3d^24s^2$   $1D_2$  position is likely too high. The  $3d^34p$ ,  $3d^35p$  and  $3d^24s4p$  odd configurations of the V II spectrum have been also reanalysed and three  $3d^24s4p$  triplets are assigned higher energies than previously proposed. We have determined the fine structure parameters, the largest and next largest eigenvector percentages of levels, their calculated Landé  $g_J$ -factors and predicted positions for missing experimental levels up to  $100000 \text{ cm}^{-1}$ . Furthermore for the first time hyperfine structure (HFS) parametric treatment, involving levels has been carried out. The deduced single-electron HFS parameter values are successfully checked with those obtained by means of ab initio calculations.

| Config.       | $3d^24s^2$ |           | $3d^34s$   |           | $3d^35s$    |           |
|---------------|------------|-----------|------------|-----------|-------------|-----------|
|               | Fit        | ab-initio | Fit        | ab-initio | Fit         | ab-initio |
| $E_{av}$      | 43799(94)  | 43799     | 19730(30)  | 18489     | 84820(42)   | 78881     |
| $F^2(3d, 3d)$ | 62037(199) | 60288     | 54057(66)  | 54104     | 57330(90)   | 55519     |
| $F^4(3d, 3d)$ | 38140(271) | 37703     | 31693(236) | 33596     | 34978(92)   | 34544     |
| $G^2(3d, ns)$ |            |           | 8144 (43)  | 8207      | 1339(35)    | 1523      |
| $\zeta_{3d}$  | 200(17)    | 184       | 156(10)    | 157       | 171(10)     | 161       |
| $\alpha$      | 50(1)      |           | 50(1)      |           |             |           |
| $\beta$       | -130(19)   |           | -130(19)   |           |             |           |
| $T_s$         |            |           | 4 (11)     |           |             |           |
| $T_2$         |            |           | -45 (11)   |           |             |           |
| $T_3$         |            |           | -239(13)   |           |             |           |
| Config.       | $3d^4$     |           | $3d^34d$   |           | $3d^35d$    |           |
|               | Fit        | ab-initio | Fit        | ab-initio | Fit         | ab-initio |
| $E_{av}$      | 18687(13)  | 17691     | 89766(32)  | 83105     | 103174(351) | 100986    |
| $F^2(3d, 3d)$ | 48480(56)  | 47503     | 56710(118) | 55559     | 57837 (360) | 55725     |
| $F^4(3d, 3d)$ | 28317(72)  | 29249     | 33302(178) | 34573     | 32727(330)  | 34682     |
| $\zeta_{3d}$  | 138(9)     | 131       | 166(9)     | 161       | 166(9)      | 161       |
| $\zeta_{nd}$  |            |           | 11(6)      | 9         | 5(3)        | 4         |
| $\alpha$      | 50(1)      |           | 7 (1)      |           |             |           |
| $\beta$       | -130(19)   |           | -83(16)    |           |             |           |
| $T_2$         | -45(11)    |           |            |           |             |           |
| $F^2(3d, 4d)$ |            |           | 4484(98)   | 5238      | 1910 (82)   | 1847      |
| $F^4(3d, 4d)$ |            |           | 2196(99)   | 2230      | 864(39)     | 826       |
| $G^0(3d, 4d)$ |            |           | 1923(26)   | 2155      | 717 (10)    | 1247      |
| $G^2(3d, 4d)$ |            |           | 1551(124)  | 1927      | 610(50)     | 922       |
| $G^4(3d, 4d)$ |            |           | 1900(86)   | 1449      | 758(34)     | 637       |

**Table 1:** *Fine structure parameters for even-parity levels*

## Molecular dynamics simulations of palmitic acid adsorbed on NaCl surface.

J. Lovric<sup>1</sup>, S. Briquez<sup>1</sup>, D. Duflot<sup>1</sup>, M. Monnerville<sup>1</sup>, B. Pouilly<sup>1</sup>, and C. Toubin<sup>1</sup>

<sup>1</sup>PhLAM institute, UMR CNRS 8523, University of Lille, F-59655, Villeneuve d'Ascq

Presenting Author: josip.lovric@univ-lille1.fr

The aerosol and gases effects in the atmosphere play an important role on health, air quality and climate, affecting both political decisions and economic activities around the world [1]. Among the several approaches of studying the origin of these effects, computational modeling is of fundamental importance in providing insights on the elementary chemical processes. Sea salts are the most important aerosol particles in the troposphere ( $10^9$ T/year) [2]. Our theoretical work consists in modeling a (100) NaCl surface coated with palmitic acid (PA) molecules at different PA coverages. Molecular dynamics simulations were carried out with the GROMACS package[5], in the NPT ensemble at  $T= 235$ K. We have tested several force fields [3–4] to describe the molecular interactions in the fatty acid/salt crystal system. In this study, we focused on transition in molecular orientation of the adsorbate as a function of PA coverage, on the effect of humidity, by adding water molecules, on organization of the fatty acid at the salt surface, and especially on the occurrence of PA isolated islands.

**Acknowledgments:** this research has been supported by the CaPPA project (Chemical and Physical Properties of the Atmosphere), funded by the French National Research Agency (ANR) through the PIA (Programme d'Investissement d'Avenir) under contract ANR-10-LABX-005.

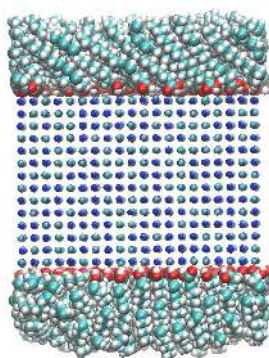


**Figure 1:** Monolayer of palmitic acid adsorbed on (100) NaCl.

### References

- [1] O. Boucher et al, *5th Assessment Report IPCC*, (2013)
- [2] B. J. Finlayson-Pitts, *Chem. Rev.***103**, 4801–4822 (2003)
- [3] G. A. Kaminski, et al *J. Phys. Chem. B* **103**, 6474–6487 (2001)
- [4] M. Patra, M. Karttunen *J. Comput. Chem.* **25**, 678–6879 (2004)
- [5] <http://www.gromacs.org/>

## WFT-in-DFT Embedding with Coupled-Cluster Wavefunctions

A.S.P. Gomes<sup>1</sup>, F. Réal<sup>1</sup>, V. Vallet<sup>1</sup>, Ch.R. Jacob<sup>2</sup>, S. Höfener<sup>3,4</sup>, and L. Visscher<sup>4</sup>

<sup>1</sup>Laboratoire de Physique des Lasers, Atomes et Molécules (PhLAM), CNRS UMR 8523, Université de Lille 1, Bâtiment P5, 59655 Villeneuve d'Ascq, France

<sup>2</sup>Karlsruhe Institute of Technology (KIT), Center for Functional Nanostructures and Institute of Physical Chemistry, Wolfgang-Gaede-Str. 1a, 76131 Karlsruhe, Germany

<sup>3</sup>Karlsruhe Institute of Technology (KIT), Theoretical Chemistry Department and Institute of Physical Chemistry, Wolfgang-Gaede-Str. 1a, 76131 Karlsruhe, Germany

<sup>4</sup>Amsterdam Center for Multiscale Modeling, Section Theoretical Chemistry, Faculty of Sciences, VU University Amsterdam, De Boelelaan 1083, 1081 HV Amsterdam, The Netherlands

Presenting Author: andre.gomes@univ-lille1.fr

Coupled-cluster (CC) methods are perhaps the most reliable wavefunction theory (WFT)-based approach currently available for investigating the properties of molecules such as (but not restricted to) electronic spectra. However, unlike density functional theory (DFT)-based approaches such as TDDFT, their steep computational scaling poses rather severe constraints on their application to relatively large systems, such as those one would wish to investigate in most chemically interesting cases (e.g. species in solution, at interfaces or trapped in solid matrices).

Since spectral properties of interest often arise from rather localized phenomena (e.g. electronic transitions predominantly involving orbitals centered on one of a few chromophores), the use of embedding approaches [1] such as frozen density embedding (FDE) [2] is particularly appealing, as it provides an efficient way to incorporate the effect of the surroundings in the WFT calculation.

In this contribution we discuss the formulation and implementation of CC-in-DFT approaches within a framework based on response theory [3], which is general enough as to allow any desired combination of methods (e.g. CC-in-CC [4]) and offers a (formal) path to couple electronic excitations from different subsystems [5] akin to a purely DFT formulation [6]. Furthermore, we discuss computational approximations that allow for efficient CC-in-DFT calculations, and their connection to formulations which do not rely on CC response theory [7].

### References

- [1] A.S.P. Gomes, Ch.R. Jacob, *Annu. Rep. Prog. Chem., Sect. C: Phys. Chem.*, **108**, 222 (2012)
- [2] T.A. Wesolowski, A. Warshel *J. Phys. Chem.* **97** (1993) 8050
- [3] S. Höfener, A.S.P. Gomes, L. Visscher, *J. Chem. Phys.* **136**, 044104 (2012); S. Höfener, A.S.P. Gomes, L. Visscher, *J. Chem. Phys.* **139**, 104106 (2013)
- [4] S. Höfener, L. Visscher, *J. Chem. Phys.* **137**, 204120 (2012)
- [5] S. Höfener, L. Visscher, in preparation
- [6] J. Neugebauer *J. Chem. Phys.* **126**, 134116 (2007); J. Neugebauer *J. Chem. Phys.* **131**, 084104 (2009)
- [7] A.S.P. Gomes, Ch.R. Jacob, L. Visscher, *Phys. Chem. Chem. Phys.*, **10**, 5353 (2008); P. Tecmer *et al.* *J. Chem. Phys.* **137**, 084308 (2012); A.S.P. Gomes *et al.*, *Phys. Chem. Chem. Phys.*, **15**, 15153, (2013)

## Theoretical modeling of thermodynamical properties of actinide complexes

M. Olejniczak<sup>1</sup>, F. Réal<sup>1</sup>, A.S.P. Gomes<sup>1</sup>, F. Virot<sup>2</sup>, and V. Vallet<sup>1</sup>

<sup>1</sup>PhLAM, UMR 8523 CNRS/Lille 1, Université Lille 1 Sciences et Technologies, 59655 Villeneuve d'Ascq, France

<sup>2</sup>IRSN, PSN-RES, SAG, LETR, BP3, 13115 Saint-Paul-les-Durance Cedex, France

Presenting Author: gosia.olejniczak@univ-lille1.fr

The aim of presented work is to establish a new set of thermodynamic constants for plutonium oxides and hydroxydes in gas phase by accurate ab-initio methods. Theoretical studies are driven by the importance of Pu compounds in nuclear science and industry and by large discrepancies in experimental values of these constants [1]. Chemistry of Pu is very complex [2] and its theoretical description requires the use of methods which account for electron correlation and relativistic effects. This poster will show preliminary values of enthalpies of reactions involving oxides and hydroxides of Pu, obtained with relativistic Hamiltonians: Zeroth Order Regular Approximation (ZORA) and Douglas-Kroll-Hess (DKH); various methods: based on density functional theory (DFT) and wave function theories (WFT) which use the concept of complete active space (CAS); various basis sets: all-electron (AE) and pseudopotentials (PP). In modelling of compounds in condensed phase, additional difficulty arises from the need to describe its environment and the compound-environment interactions. One possibility to deal with this problem is to use the Frozen Density Embedding (FDE) scheme [3–4], in which the compound of interest (e.g. Pu oxide) is described by accurate methods (WFT), while environment is modelled by cheaper techniques (such as DFT). This poster will present basic concepts behind FDE.

### References

[1] R. J. M. Konings *et al.* J. Phys. Chem. Rev. Data 43, 013101 (2014)

[2] D. L. Clark, Los Alamos Science, 26 (2000)

<https://www.fas.org/sgp/othergov/doe/lanl/pubs/00818038.pdf>

[3] A. S. P. Gomes *et al.* PCCP 15 (36), 15153-62 (2013)

[4] A. S. P. Gomes, C. R. Jacob Annual Reports Section C (Physical Chemistry) 108, 222 (2012)

# Spectropolarimetry of the FeH molecule in the near-IR

G. Dobrev<sup>1,2</sup>, A. Pashov<sup>1</sup>, P. Crozet<sup>2</sup>, and A. Ross<sup>2</sup>

<sup>1</sup>*Faculty of Physics, Sofia University, 5 J. Bourchier Blvd, 1164 Sofia, Bulgaria*

<sup>2</sup>*Institut Lumière Matière, UMR5306 Université Lyon 1 – CNRS, Université de Lyon, 69622 Villeurbanne CEDEX, France*

Presenting Author: g\_dobrev@phys.uni-sofia.bg

We present experimental data for the  $F^4\Delta-X^4\Delta$  transition frequencies and effective Landé factors of the FeH molecule in the near-infrared, prompted by the interest in transition metal monohydrides arising from the identification of such molecules in the spectra of cool stars and sunspots[1–4]. Iron hydride is good remote magnetic field probe due to its strong Zeeman response[5] and its relatively high abundance in the cold stellar atmosphere layers. The complex electronic structure resulting from mixing between sextet and quartet states makes theoretical work very difficult, so that accurate predictions of spectral signatures is impossible. Whence the need for laboratory measurements. FeH molecules are produced in a hollow cathode sputtering source in a  $H_2 + Ar$  gas mixture discharge. A tunable cw Ti:sapphire laser is used to excite the 0-0 band near 989 nm and 1-0 band near 890 nm of the  $F^4\Delta-X^4\Delta$  system in FeH and the laser-induced fluorescence signal is recorded. A permanent magnet introduced into the source provides a homogenous magnetic field where the laser and molecules interact. The magnetic field is calibrated to 0.5% accuracy from the Zeeman response of metastable Ar atomic lines. The measurements without magnetic field allow us to refine wavenumbers for low  $J$  transitions predicted in the FeH atlas[2]. We have also recorded Zeeman patterns extending the previous laboratory investigations [6,7].

## References

- [1] D.Shulyak *et al.* *Astronomy & Astrophysics* **523**, A37 (2010)
- [2] L. Wallace *et al.* N.S.O. Technical Report 1998-002 (1998), Available online : <ftp://nsokp.nso.edu/pub/atlas/spot3alt>
- [3] C. M. Johns-Krull, J. A. Valenti *Proceedings of the 13th Cambridge Workshop on Cool Stars, Stellar Systems and the Sun - Proceedings* **560** 261 (2005)
- [4] A. Reiners, G. Basri. *Astrophys. J.* **656** 1121–1135 (2007)
- [5] N.Afram *et al.* *Astronomy & Astrophysics* **482**, 387 (2008)
- [6] M. Dulick *et al.* *Astrophys. J.* **594** (1), 651 (2003)
- [7] J. J. Harrison *et al.* *Astrophys. J.* **679** (1), 854 (2008)

## Low Temperature Plasma Jet for Application in Dental Bleaching

C.H. Chang<sup>1</sup>, C.H. Liu<sup>1</sup>, K.F. Lee<sup>1</sup>, K.Y. Lin<sup>1</sup>, R.S. Chen<sup>2</sup>, and M.H. Chen<sup>2</sup>

<sup>1</sup>*Mechanical and Systems Research Laboratories, Industrial Technology Research Institute, 195, Sec. 4, Chung Hsing Rd., Chutung, Hsinchu 31040, Taiwan*

<sup>2</sup>*School of Dentistry, National Taiwan University, No.1, Changde St., Zhongjheng District, Taipei 100, Taiwan*

Presenting Author: changch@itri.org.tw

We demonstrated a time modulated rf driven low temperature atmospheric pressure plasma jet used for dental bleaching. Conventionally, hydrogen peroxide ( $H_2O_2$ ) is most commonly used for dental bleaching and has proven its efficiency over the years. However, there exist some dangerous side-effect risks while the concentration of hydrogen peroxide increases for the better bleaching efficiency. Otherwise, some other enhance methods using thermal treatment to accelerate the bleaching process, without critical control of emitting thermal energy and power, which might cause damage of tissues. In recently, the potential of low temperature atmospheric pressure plasma has been valued for applications in bio-medicine, includes the dental bleaching [1, 2], which greatly enhances safety and minimizes risk of treatments. In this article, a time modulated rf driven low temperature atmospheric pressure plasma jet was constructed for investigation of dental bleaching without hydrogen peroxide. The dental bleaching results as well as the dental tissue damage were compared with different plasma operating conditions and the characterization of plasma was carried out by using a home-made impedance meter and a commercial OES system. Some other critical experiment parameters such as treatment time and the gap between tooth and plasma jet were also adjusted and analyzed according to experiment design. After plasma treatment, the shade of teeth that stained by food coloring was change from B4 to B1 by using the Vitapan Classical shade guides and the dental pulp tissue was not damaged.

### References

- [1] H. W. Lee *et al.* Journal of Endodontics **35** 587–591 (2009)
- [2] J. Pan *et al.* IEEE Trans. Plasma Sci. **38** 3143–3151 (2010)

## Transport properties drawn from ion-atom collisions. Case of ${}^6\text{Li}-{}^6\text{Li}^+$ and ${}^6\text{Li}-{}^7\text{Li}^+$

F. Bouchelaghem<sup>1</sup> and M. Bouledroua<sup>2</sup>

<sup>1</sup>*Physics Department, Badji Mokhtar University, Annaba 23000, Algeria*

<sup>2</sup>*Faculté de Médecine and Laboratoire de Physique des Rayonnements, Badji Mokhtar University, Annaba 23000, Algeria*

Presenting Author: boulmoncef@netscape.net

This investigation treats quantum mechanically the ion-atom collisions and computes the transport coefficients, such as the coefficients of mobility and diffusion. For the case of lithium, the calculations start by determining the *gerade* and *ungerade* potential curves through which ionic lithium approaches ground lithium. Then, by considering the isotopic effects and nuclear spins, the elastic and charge-transfer cross sections are calculated for the case of  ${}^6\text{Li}^+$  and  ${}^7\text{Li}^+$  colliding with  ${}^6\text{Li}$ . Finally, the temperature-dependent diffusion and mobility coefficients are analyzed, and the results are contrasted with those obtained from literature.

# Laboratory astrophysics: EBIT spectra around the EUV bands of the SDO/AIA instrument

E. Träbert<sup>1,2</sup> and P. Beiersdorfer<sup>2</sup>

<sup>1</sup>*Astronomisches Institut, Ruhr-Universität Bochum, 44780 Bochum, Germany*

<sup>2</sup>*Physics Division, Lawrence Livermore National Laboratory, Livermore CA 94550, USA*

Presenting Author: traebert@astro.rub.de

Solar observations in the Extreme Ultraviolet (EUV) strive for high cadences (high exposure frequency) in order to capture the temporal variability of the conditions in the solar environment. The AIA experiment onboard the Solar Dynamics Observatory (SDO) spacecraft [1] achieves this by observations in seven channels, each of which based on a multilayer mirror for light gathering and wavelength selection. The seven observation channels target 6 bands (94, 131, 171, 193, 211, 355 Å) with prominent iron lines and the bright He II line at 304 Å. In combination and supported by extensive modeling, the observations permit the observer to establish the temperature in the solar coronal field of view. The seven data channels have spectral band passes from 1 Å to about 20 Å. In parallel, and in a 10 s cadence, a grating spectrograph monitors the EUV spectrum with a band width of 1 Å.

Our laboratory approach is complementary to this. An electron beam ion trap (EBIT) offers the laboratory environment closest in density and working conditions to the solar corona. Various elements of coronal interest (He, C, N, O, F, Ne, Mg, Si, S, Ar, Ca, Fe, Ni) are introduced into EBIT and ionized and excited by an energetic electron beam. The EUV spectra in the vicinity of the SDO/AIA observation channels are studied with spectrographs of resolving powers 1100 to 3000 and at various electron beam energies. We thus check the consistency and completeness of the spectral data that are used in the collisional-radiative modeling necessary for the interpretation of the SDO/AIA raw data.

We mainly compare our observations with the NIST on-line data base [2] and with the CHIANTI data base (v. 7.1) [3]; the latter compiles wavelength data and models the relative line intensities. We note that the CHIANTI wavelengths are more consistent with our observations. However, we also find a number of spectral lines that may have been underappreciated in the spectral models. Of our work in progress, the results for the vicinities of the 131 and 211 Å AIA channels have been submitted for publication [4,5].

This work was performed under the auspices of the U.S. Department of Energy by Lawrence Livermore National Laboratory under Contract DE-AC52-07NA27344 and was supported by the Solar and Heliospherical Physics Program of the National Aeronautics and Space Administration under award NNH10AN31I. E.T. acknowledges support from the German Research Association (DFG) (grants Tr171/18 and Tr171/19).

## References

- [1] W. D. Pesnell, B. J. Thompson, P. C. Chamberlin *Sol. Phys.* **275**, 3 (2012) (special issue)
- [2] A. Kramida *et al.* <http://physics.nist.gov/asd>
- [3] E. Landi *et al.* <http://www.chiantidatabase.org/database>
- [4] E. Träbert *et al.* *Astrophys. J. Suppl. Ser.* **211**, 14 (2014)
- [5] P. Beiersdorfer *et al.* *Astrophys. J. Suppl. Ser.* (to be published)

## Absorption line shape analysis beyond the bandwidth detection limit: application to the Boltzmann constant determination

F. Rohart<sup>1</sup>, S. Mejri<sup>2</sup>, P.L.T. Sow<sup>2</sup>, S.K. Tokunaga<sup>2</sup>, B. Darquié<sup>2</sup>, C. Daussy<sup>2</sup>, A. Castrillo<sup>3</sup>, H. Dinesan<sup>3</sup>, E. Fasci<sup>3</sup>, and L. Gianfrani<sup>3</sup>

<sup>1</sup>Laboratoire de Physique des Lasers, Atomes et Molécules, Université Lille 1, F-59655 Villeneuve d'Ascq cedex, France

<sup>2</sup>Université Paris 13, Sorbonne Paris Cité, Laboratoire de Physique des Lasers, F-93430 Villetaneuse, France

<sup>3</sup>Dipartimento di Matematica e Fisica, Seconda Università di Napoli, Viale Lincoln 5, I-81100 Caserta, Italy

Presenting Author: Francois.Rohart@univ-lille1.fr

In recent years, there has been a growing interest toward precise and accurate observations of spectral line shapes, for the purpose of either applications (atmospheric sounding, isotope research, chemical analysis in the gas phase) or fundamental studies (molecular collisions, fundamental metrology, tests of quantum mechanical calculations). An interesting example is the recent implementations of Doppler broadening thermometry for the aims of an optical determination of the Boltzmann constant. In this latter field, accuracies in the  $10^{-5}$  range have been demonstrated [1, 2]. To this purpose, a careful error budget analysis is required, but the bandwidth detection limit has not been considered in details, so far [3].

A theoretical model of the influence of the detection bandwidth properties on observed line shapes will be described [4]. In case of a continuous evolution of the laser frequency, the line shape can be set in a quasi-analytical form that easily highlights consequences on the retrieval of the line center frequency and broadening parameter or on line asymmetry. For the sake of completeness, these results have been extended via numerical simulations to the case of a step-by-step frequency evolution.

This model has been accurately validated thanks to experiments performed with laser spectrometers in Paris 13 and Naples 2 laboratories [4]. In order to get robust tests, quite unusual bandwidth misadjustments were used. Resulting frequency shifts, extra broadenings and line asymmetries were perfectly taken into account by the model, leading to line parameters in very good agreement with those resulting from well-designed experiments.

Finally, the influence of detection bandwidth properties on frequency and Doppler width measurements will be discussed in details, including a comparison of several filter designs ( $1^{st}$  and  $2^{nd}$  orders). A particular emphasis will be given to the detection bandwidth adjustments required for the  $10^{-6}$  precision that is targeted by the Boltzmann constant experiments.

### References

- [1] C. Daussy *et al.*, Phys. Rev. Lett. **98**, 250801 (2007); C. Lemarchand *et al.*, New J. Phys. **13**, 073028 (2011)
- [2] L. Moretti *et al.*, Phys. Rev. Lett. **111**, 060803 (2013); A. Castrillo *et al.*, J. Mol. Spectroscopy <http://dx.doi.org/10.1016/j.jms.2014.04.001> (2014)
- [3] C.H. Townes, A.L. Schawlow, *Microwave Spectroscopy* (McGraw-Hill, New York, 1955)
- [4] F. Rohart *et al.*, Phys. Rev. A, submitted (2014)

## Frequency conversion with a photomixer for high-resolution broadband spectroscopy

F.L. Constantin<sup>1</sup>

<sup>1</sup>*Laboratoire PhLAM, CNRS UMR 8523, F-59655 Villeneuve d'Ascq*

Presenting Author: FL.Constantin@univ-lille1.fr

Optical heterodyne conversion with two near-infrared lasers and a biased photomixer has been used to generate broadband tunable THz-waves with high spectral performances. Device design relies on a low-temperature-grown GaAs photoconductor with sub-picosecond electron recombination time, high mobility and large breakdown field that is coupled with interdigitated electrodes to a planar antenna. Electrical transport mechanisms lead to a nonlinear current-voltage response of the device that is exploited here for broadband frequency conversion. The device is electrically addressed with a bias-t and THz-waves are focused to the antenna with a silicon lens. Rectification in the THz regime allows direct detection with the photomixer. Spectral components of a THz-wave pulse-modulated at a radiofrequency rate are detected by phase-coherent frequency conversion to dc by coupling radiofrequency to the photomixer. Alternatively, heterodyne detection of a THz field is performed by using the optical beat between the lasers as local oscillator. Spectral components of a THz-wave pulse-modulated at a radiofrequency rate are detected individually by down-conversion to the microwave domain with the heterodyne detection scheme. Thermal noise of the photomixer operated at room temperature limits the detection sensitivity at  $\sim 0.3$  nW/Hz<sup>1/2</sup> for a device with 1.2 ps electron lifetime and 20 mW laser power. Precision spectroscopy is an important application of this approach where a THz-wave with a great number of coherent modes addresses molecular energy levels. Detection with the photomixer allows spectral resolution, identification and measurement of the amplitude or probing the relative phase of the modes. A Doppler-limited spectroscopy setup is presented as an example with scanning over  $\sim 150$  MHz at video rate and a spectral resolution of  $\sim 1$  MHz determined by optical beat linewidth.

# Close-coupling CI-approach of atomic and molecular collisions: new perspectives on inner-shell processes in $H^+ - Li$

G. Labaigt<sup>1,2</sup> and A. Dubois<sup>1,2</sup>

<sup>1</sup>Sorbonne Universités, UPMC Univ Paris 06, UMR 7614, Laboratoire de Chimie Physique-Matière et Rayonnement, F-75231 Paris Cedex 05, France

<sup>2</sup>CNRS, UMR 7614, LCPMR, 75005 Paris, France

Presenting Author: gabriel.labaigt@upmc.fr

We present a novel approach to describe multi-electronic processes (electron transfer, excitation and ionization) occurring in ion-atom and ion-molecule collisions in the intermediate keV energy range. The treatment is based on the so called impact parameter semiclassical approximation [1,2] in which the electronic time-dependent Schrödinger equation is solved non perturbatively, taking into account all the electrons of the system with static and dynamic correlations.

The equation is solved using a CI approach where the scattering wave function carries all information about spatial symmetry and spin multiplicity for the total system and for the isolated partners of the collision. For that purpose we use the permutation group theory together with Young diagram formalism instead of a Slater determinant approach [3].

We apply this model to a genuine, benchmark, three-electron system,  $H^+ - Li$ , for which we present results for exchange processes from valence and inner-shell compared with experimental results [4] when available. In the conference we shall give a peculiar insight on new features brought by this full multi-electronic treatment compared to the quasi one-electron model commonly used. We shall focus our attention on the couplings between valence and inner shell processes that can lead to two types of inner-shell capture mechanisms : direct or two-steps. Differences will be highlighted by the analysis of the inner-electron density temporal profile, as shown in the figure below.

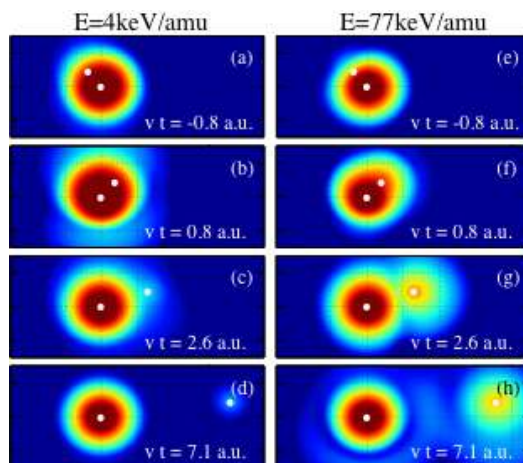


**Figure 1:** Inner-electron density in the  $x,z$  plane calculated for two different collision energies at four different times. The spatial grid interval is 2 a.u. The color palette extends over 4 orders of magnitude.

## References

- [1] W. Fritsch and C. Lin, Phys. Rep. **202**, 1 (1991)
- [2] J. Caillat *et al.* Phys. Rev. A **70** 032715 (2004)
- [3] F. A. Matsen, J. Phys. Chem. **68** 3282 (1964)
- [4] D. Wutte *et al.* Atom. Data and Nucl. Data **65** 155 (1997) and references therein.

# Collisions dynamics of electrons, photons, and highly-charged ions with clusters to probe the aggregation in a pulsed supersonic jet

C. Prigent<sup>1</sup>, M. Trassinelli<sup>1</sup>, E. Lamour<sup>1</sup>, A. Lévy<sup>1</sup>, S. Macé<sup>1</sup>, J.-P. Rozet<sup>1</sup>, S. Steydli<sup>1</sup>, and D. Vernhet<sup>1</sup>

<sup>1</sup>Sorbonne Universités, CNRS, UPMC Univ Paris 06, UMR 7588, Institut des NanoSciences de Paris, F-75005, Paris, France

Presenting Author: martino.trassinelli@insp.jussieu.fr

Collimated intense supersonic beams of atoms, molecules, and clusters constitute an ideal target for many collision investigations in which the kinematics have to be well defined. Reliable predictions of cluster size distribution [1, 2], clustering rate and absolute atomic densities [3] remain still debated and require to be quantitatively determined. Combining three different experimental approaches, we achieve a good understanding of the temporal evolution of a pulsed rare gas supersonic jet. More precisely we discriminate between the temporal contribution of the atomic density and the cluster one within the same bunch. Looking at the X-ray emission resulting from inner-shell vacancy production [4], we exploit the fact that those experiments with the supersonic jet are: i) sensitive to all atoms, aggregated or not when interacting with a well collimated beam of electrons, ii) only sensitive to clusters with intense ultra-short laser pulses [5] and iii) mainly sensitive to unclustered atoms with Highly Charged Ions [6]. Those three measurements, performed under well-controlled conditions, are fully consistent with each other and give access, for the first time, to the clustering rate in a rare gas supersonic jet. Further experiments, currently under progress, should provide a full characterization of the aggregation depending upon different parameters of the cluster jet.

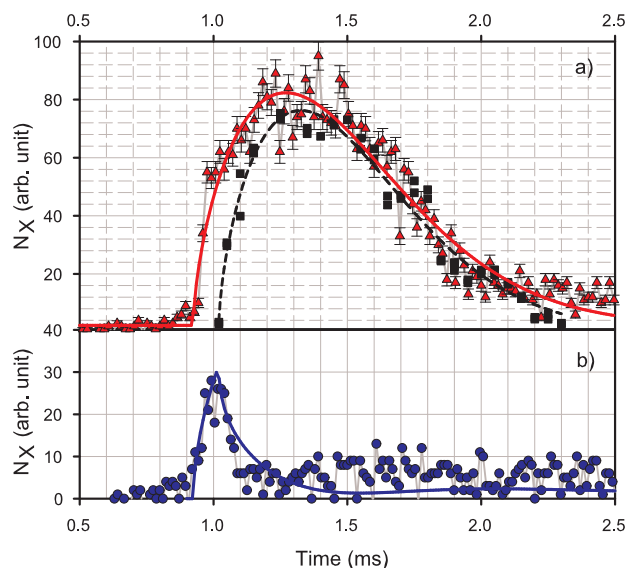


**Figure 1:** Time dependant X-ray signal for the interaction of argon cluster bunches with electron (a - triangle), fs laser pulses (a - square), with Highly Charged Ions (b).

## References

- [1] O. F. Hagen, *Rev. Sci. Instrum* **63** 2374 (1992)
- [2] S. Schütte *et al.* *Int. J. Mass Spec.* **220** 183 (2002)
- [3] F. Dorchies *et al.* *Phys. Rev. A* **68** 023201 (2003)
- [4] C. Prigent *et al.* *J. Phys. Conf. Series ICPEAC 2013*, in press
- [5] C. Prigent *et al.* *Phys. Rev. A* **78** 053201 (2008)
- [6] M. Trassinelli *et al.* *J. Phys. B* **45** 085202 (2012p)

# Multipole expansions in the theory of light radiation by atomic systems

M.Ya. Agre<sup>1</sup>

<sup>1</sup>*Department of Physical and Mathematical Sciences, National University of "Kyiv-Monyla Academy", 04655 Kyiv, Ukraine*

Presenting Author: magrik@ukr.net

The probability of spontaneous radiation of a photon with the unit polarization vector  $\mathbf{e}$  and the momentum  $\mathbf{k}$  is written down through the so-called radiation amplitude

$$V_{fi} = \mathbf{e}^* \int e^{-i\mathbf{k}\mathbf{r}} \mathbf{j}_{fi}(\mathbf{r}) d\mathbf{r}, \quad (1)$$

where  $\mathbf{j}_{fi}$  is the current density vector for the transition of a radiating system from the initial to final state [1]. The cross section of photoeffect and the composite matrix elements for multiphoton transitions are also expressed through  $V_{fi}$  (1). In the first nonvanishing order of long-wave approximation ( $ka \ll 1$ , where  $a$  is the radius of the atomic system)  $V_{fi}$  proves to be proportional to the electric dipole moment of transition that corresponds to dipole approximation. In general case multipole expansion of the radiation amplitude (1) is very useful, but the structure of the known expansion makes it difficult for applications.

In the present paper we derive the compact multipole expansion for the amplitude of spontaneous radiation (1) using the mathematical technique of irreducible tensors [2]. The found multipole series gives to the total amplitude  $V_{fi}$  the form of the sum of amplitudes

$$V_{fi} = \sum_{l=1}^{\infty} (V_l^{(E)} + V_l^{(M)}), \quad (2)$$

where  $V_l^{(E)}$  is the radiation amplitude of electric  $2^l$ -pole ( $El$ ) photon and  $V_l^{(M)}$  is the radiation amplitude of magnetic  $2^l$ -pole ( $Ml$ ) photon. Here

$$V_l^{(E)} = (D_l \cdot \{\mathbf{e}^* \otimes Y_{l-1}(\mathbf{k}_0)\}_l), \quad V_l^{(M)} = (A_l^{(l)} \cdot \{\mathbf{e}^* \otimes Y_l(\mathbf{k}_0)\}_l), \quad (3)$$

where  $Y_{lm}(\mathbf{k}_0)$  is the spherical function, the unit vector  $\mathbf{k}_0 = \mathbf{k}/k$ , and all information about the radiating system is contained in the coefficients of the series (2), which are the irreducible tensors determined by the current density of transition,

$$A_{Lm}^{(l)} = 4\pi(-i)^l \int \{g_l(kr)Y_l(\mathbf{n}) \otimes \mathbf{j}_{fi}(\mathbf{r})\}_{Lm} d\mathbf{r}, \quad D_{lm} = A_{lm}^{(l-1)} + \sqrt{\frac{l}{l+1}} A_{lm}^{(l+1)}, \quad (4)$$

where  $g_l(x) = \sqrt{\pi/(2x)} J_{l+1/2}(x)$  is the spherical Bessel function,  $\mathbf{n} = \mathbf{r}/r$ . The standard designations [2] for the tensor and scalar products of two irreducible tensors are used in equations (3) and (4).

The angular momentum and parity selection rules keep only few terms in the series (2). In the long-wave approximation  $A_{Lm}^{(l)}$  (4) has the order  $(ka)^l$ ,  $A_{lm}^{(l)}$  proving to be proportional to magnetic  $2^l$ -pole moment of transition and  $A_{lm}^{(l-1)}$ ,  $D_{lm}$  – to electric one. Correspondingly,  $V_1^{(E)}$  in the series (2) becomes the amplitude of dipole radiation,  $V_2^{(E)}$  becomes the amplitude of quadrupole radiation,  $V_1^{(M)}$  becomes the amplitude of magnetic dipole radiation and so on.

The derived multipole expansion can be used in theoretical studies of electromagnetic field – atomic system interaction both in long-wave approximation and outside its framework.

## References

- [1] V. B. Berestetskii, E. M. Lifshitz and L. P. Pitaevskii, *Quantum Electrodynamics* (Pergamon Press, Oxford, 1982)  
 [2] D. A. Varshalovich, A. N. Moskalev, V. K. Khersonskii, *Quantum Theory of Angular Momentum* (World Sci. Publ., Singapore, 1988)

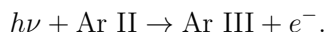
# Photoionization cross sections of Ar<sup>+</sup> ions

N.B. Tyndall<sup>1</sup> and C.A. Ramsbottom<sup>1</sup>

<sup>1</sup>Queens University Belfast, BT7 1NN, Northern Ireland

Presenting Author: ntyndall01@qub.ac.uk

The ground state photoionization of an initial Ar II ion containing 17 electrons can be described by the following process (A benchmark for comparison can be obtained in the literature [1]);



The ground state of Ar II has electronic configuration  $1s^2 2s^2 2p^6 3s^2 3p^5 (^2P^o)$  and the ion Ar III is left in a possible excited final target state with an ejected electron in the continuum. To compute any relevant atomic data, we implemented a fully relativistic Breit-Pauli R-matrix calculation [2, 3]. The R-matrix method [4, 5] deals with the division of configuration space into an internal and external region by a sphere of fixed radius  $r_a = 16.6$  a.u. centered upon the nucleus of point mass. The photoionization cross sections  $\sigma$ , are obtained by matching the solutions at open and closed channel boundary conditions via the R-matrix at  $r_a$  and are defined in the following way,

$$\sigma = \frac{4}{3} \pi^2 a_o^2 \alpha^2 \frac{\omega}{g_i} S.$$

Where  $a_o$  is the bohr radius,  $\alpha$  the fine structure constant,  $\omega$  the photon energy and  $g_i$  the statistical weight of the initial bound state. S is given as the generalized line-strength describing a transition between an initial bound state to a final free state comprised of either the dipole length or velocity approximations. These dipole approximations arise from the truncation of the wave function which results in minor discrepancies. The final scattering state is represented by the wavefunction of the residual ion plus the ejected continuum electron.

The present model has been established by implementing Hartree-Fock orbitals of 1s, 2s, 3s, 2p, 3p from the tables of Clementi and Roetti [6]. In order to extend the model, the orbitals 3d, 4s, 4p, 4d were optimized on the lowest lying energy levels observed by NIST <sup>1</sup> with the aid of CIV3 [7], whilst maintaining a closed  $1s^2 2s^2 2p^6$  core. The addition of these optimized orbitals resulted in a total of 7 possible configurations and 64 LS $\pi$  target states. The possible 17-electron configurations are thus constructed from this orbital set. The partial wave contribution included L=0 to L=10 for both even and odd parities and in the external region a mesh of 80,000 energy points was chosen for the continuum electron to obtain convergence of the resonant structures.

In consideration with the  $^2P^o$  initial ground state, we are primarily concerned with the dipole matrices describing the transitions of  $^2P^o \rightarrow ^2S^e, ^2P^e, ^2D^e$  in compliance with the selection rules. With this information we are able to obtain partial and total cross sections. Results will be presented at the conference for both LS $\pi$  transitions and J $\pi$  fine-structure transitions. Also presented along with ground state photoionization will be excited state photoionization cross-section results.

## References

- [1] Covington et al. , arXiv:1203.4292v1 [astro-ph.EP]
- [2] Berrington et al. , Comput. Phys. Commun. **8** (1974) 149
- [3] Berrington et al. , Comput. Phys. Commun. **14** (1978) 367
- [4] Burke and Seaton, Methods Comput. Phys. **10** (1971) 1
- [5] Burke and Robb, Adv. At. Mol. Phys. **11** (1975) 143
- [6] Clementi and Roetti, ADNDT **14** (1974) 177-478
- [7] Hibbert, Comput. Phys. Commun. , **9** (1975) 141

<sup>1</sup>[http://physics.nist.gov/PhysRefData/ASD/levels\\_form.html](http://physics.nist.gov/PhysRefData/ASD/levels_form.html)

## Determination of Radiative Parameters for the V I and V II Spectra: TR-LIF Measurements and HFR+CPOL Calculations

P. Palmeri<sup>1</sup>, P. Quinet<sup>1,2</sup>, Z.W. Dai<sup>3,4</sup>, Q. Wang<sup>3,4</sup>, L.Y. Jiang<sup>3,4</sup>, X. Shang<sup>3,4</sup>, Y.S. Tian<sup>3,4</sup>, and W. Zhang<sup>1</sup>

<sup>1</sup>*Astrophysique et Spectroscopie, Université de Mons – UMONS, B-7000 Mons, Belgium*

<sup>2</sup>*IPNAS, Université de Liège, B-4000 Liège, Belgium*

<sup>3</sup>*College of Physics, Jilin University, Changchun 130012, China*

<sup>4</sup>*Key Lab of Coherent Light, Atomic and Molecular Spectroscopy, Ministry of Education, Changchun 130012, China*

Presenting Author: Patrick.Palmeri@umons.ac.be

The determination of elemental abundances and their patterns in stellar atmospheres has recently challenged the accuracy of the oscillator strengths used in the stellar spectrum modelling. Actually, recent studies [1–2] showed that an accuracy of the order of  $\sim 0.05$  dex in differential abundances (and therefore also in  $\log gf$ ) is needed to detect the effect of planet formation in the stellar atmospheres. These effects are marked by a  $\sim 20\%$  depletion of refractory elements with respect to the volatile elements. Vanadium ( $Z = 23$ ) is a refractory element that belongs to the iron group. Due to its complex electronic structure related to an open 3d subshell and a relatively high cosmic abundance, many lines of V I and V II are observed in solar and stellar spectra. The experimental oscillator strengths are essential to achieve the level of accuracy currently needed in elemental abundance determination. A reliable method for obtaining experimental oscillator strengths is through the combination of measured radiative lifetimes with accurate branching fractions.

In this work, radiative lifetimes of 79 levels of V I and of 27 levels of V II have been measured using time-resolved laser-induced fluorescence (TR-LIF) spectroscopy (see, e.g. Ref. [3]) in laser-produced plasma. The lifetime values range between 3.2 ns and 494 ns and their uncertainties are within  $\pm 10\%$ . A good agreement was obtained with previous data. In order to obtain the branching fractions, the Hartree-Fock atomic structure package of R.D. Cowan [4] have been used in which a core-polarization potential and a correction to the dipole transition operator have been incorporated giving rise to the HFR+CPOL method [5]. The calculated branching fractions were then combined with the available experimental lifetimes to determine semi-empirical oscillator strengths for E1 transitions in V I and V II.

### References

- [1] J. Meléndez *et al.* *Astrophys. J.* **704**, L66 (2009)
- [2] I. Ramírez, J. Meléndez, M. Asplund *Astron. Astrophys.* **181**, A7 (2014)
- [3] W. Zhang *et al.* *J. Phys. B* **46**, 045003 (2010)
- [4] R. D. Cowan, *The Theory of Atomic Structure and Spectra* (University of California Press, Berkeley, 1981)
- [5] P. Quinet *et al.* *Mon. Not. R. Astron. Soc.* **307**, 934 (1999)

# Similarity between Ps-atom and electron-atom scattering

I.I. Fabrikant<sup>1</sup> and G.F. Gribakin<sup>2</sup>

<sup>1</sup>Department of Physics and Astronomy, University of Nebraska, Lincoln, Nebraska 68588-0299, USA

<sup>2</sup>School of Mathematics and Physics, Queen's University Belfast, Belfast BT7 1NN, Northern Ireland, UK

Presenting Author: g.gribakin@qub.ac.uk

Recently observed similarities between the positronium (Ps) scattering and the electron scattering from a number of atoms and molecules [1,2] suggest that both processes are largely controlled by the same interactions. Plotted as a function of the projectile velocity, the total electron and Ps cross sections are close and even show similar resonance-like features. In this work we calculate Ps scattering from Ar and Kr using the *impulse approximation* (IA), which is applicable above the Ps ionization threshold because Ps is diffuse and weakly-bound compared with noble-gas atoms. Our results lend theoretical support to the similarity of electron-atom and Ps-atom scattering.

The main assumption of IA is that during the scattering event only one of the constituent particles in Ps interacts with the target. The Ps-atom scattering amplitude is hence the sum of two terms [3],

$$f_{ba}(\mathbf{p}_f, \mathbf{p}_i) = 2 \int g_b^*(\mathbf{q}) f^-(\mathbf{v}_f^-, \mathbf{v}_i^-) g_a(\mathbf{q} + \Delta\mathbf{p}/2) d^3\mathbf{q} + 2 \int g_b^*(\mathbf{q}) f^+(\mathbf{v}_f^+, \mathbf{v}_i^+) g_a(\mathbf{q} - \Delta\mathbf{p}/2) d^3\mathbf{q}, \quad (1)$$

where  $\Delta\mathbf{p} = \mathbf{p}_f - \mathbf{p}_i$  is the change in the Ps momentum,  $a$  and  $b$  are the initial and final internal states of Ps,  $g_a(\mathbf{q})$  is the Ps internal wave function in momentum space, and  $f^\pm(\mathbf{v}', \mathbf{v})$  are the positron-atom and electron-atom scattering amplitudes for the velocities  $\mathbf{v}_i^\pm = \mathbf{p}_i/2 - \Delta\mathbf{p}/2 \pm \mathbf{q}$ ,  $\mathbf{v}_f^\pm = \mathbf{p}_i/2 + \Delta\mathbf{p}/2 \pm \mathbf{q}$ . The electron and positron scattering amplitudes are derived from polarized-orbital calculations [4,5]. Our total Ps-Kr scattering cross sections agree well with the measurements [1] above  $v = 0.5$  a.u., although, in contrast to observations, the calculated peak is very weak. Similar results have also been obtained for Ar.

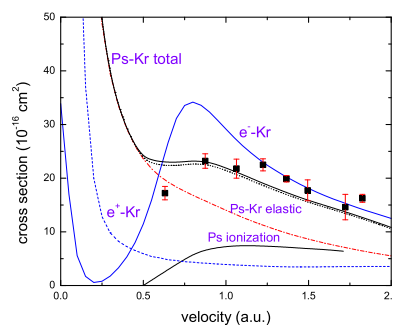


**Figure 1:**  $e^-$ -Kr,  $e^+$ -Kr and Ps-Kr scattering cross sections. Dotted black line is the sum of elastic and ionization [3] cross section; the line “Ps-Kr total” also contains contribution from excitation of the  $n = 2$  levels of Ps. Experimental data (squares) are from Ref. [1]. Data for  $e^-$ -Kr and  $e^+$ -Kr scattering are from [4,5]. Cross sections for  $e^+$  at  $v > 1.3$  a.u. were obtained by extrapolation from [4].

## References

- [1] S. J. Brawley, S. Armitage, J. Beale, D. E. Leslie, A. I. Williams, G. Laricchia, *Science* **330**, 789 (2010)
- [2] S. J. Brawley, A. I. Williams, M. Shipman, G. Laricchia, *Phys. Rev. Lett.* **105**, 263401 (2010)
- [3] C. Starrett, M. T. McAlinden, and H. R. J. Walters, *Phys. Rev. A* **72**, 012508 (2005)
- [4] R. P. McEachran, A. D. Stauffer, and L. E. M. Campbell, *J. Phys. B* **13**, 1281 (1980)
- [5] R. P. McEachran and A. D. Stauffer, *J. Phys. B* **17**, 2507 (1984)

# Energetics of intermediate velocity proton collision with naphthalene

P.M. Mishra<sup>1</sup>, J. Rajput<sup>2</sup>, C.P. Safvan<sup>3</sup>, S. Vig<sup>1</sup>, and U. Kadhane<sup>1</sup>

<sup>1</sup>Indian Institute of Space Science and Technology, Trivandrum-695547, India

<sup>2</sup>University of Delhi, Delhi-110 007, India

<sup>3</sup>Inter-University Accelerator Centre, Aruna Asaf Ali Marg, New Delhi-110 067, India

Presenting Author: mishra.preetimanjari@gmail.com

The proton collision with polycyclic aromatic hydrocarbons is important from astrophysical as well as biological point of view [1]. Due to broader energy deposition in ion-molecule collision, plasmon excitations are difficult to isolate from other physical processes. The proton (50 keV to 240 keV) collision with gaseous naphthalene at Low Energy Ion Beam Facility, IUAC, New Delhi using an electron cyclotron resonance ion source was performed in both electron emission (EE) and capture (EC) mode of detection. This study explores isolation of EE and EC mode of collision dynamics on the basis of energetics involved in respective modes by comparing the yields with photo dissociation curves. The independent nature of ionization as well as evaporation cross sections in EE mode and fragmentation yield in EC mode for all impact energy are attributed to the collective excitation and resonant capture phenomenon respectively [2]. However the decreasing trend of fragmentation yield as a function of impact energy in EE mode was reproduced (Fig. 1) with the help of theoretical cross section obtained by our *Monte Carlo* simulation for electronic stopping within Local density approximation [3].

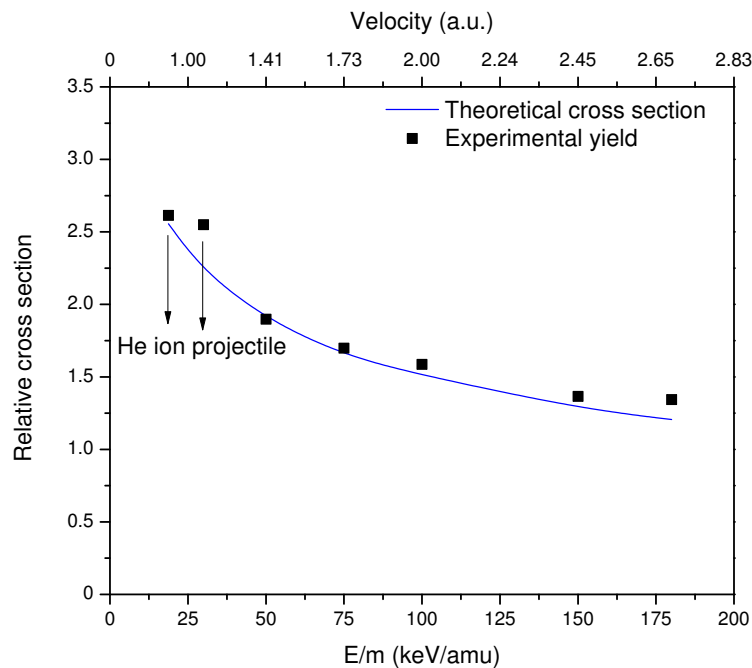


**Figure 1:** Fragmentation yield (obtained in EE mode) comparison with theoretical cross section (obtained from Monte Carlo simulation) as a function of impact energy.

## References

- [1] A. G. G. M. Tielens *Annu. Rev. Astro. Astrophys.* **46**, 289–337 (2008)
- [2] P. M. Mishra *et al.* *Phys. Rev. A* **88** 052707 (2013)
- [3] P. M. Mishra *et al.* *J Phys. B: At. Mol. Opt. Phys.* **47** 085202 (2014)

## Valence shell photoelectron spectroscopy for PAHs and its significance

P.M. Mishra<sup>1</sup>, L. Avaldi<sup>2</sup>, P. Bolognesi<sup>2</sup>, K.C. Prince<sup>3</sup>, R. Richter<sup>3</sup>, and U. Kadhane<sup>1</sup>

<sup>1</sup>Indian Institute of Space Science and Technology, Trivandrum-695547, India

<sup>2</sup>CNR-Istituto di Metodologie Inorganiche e dei Plasmi, Area della Ricerca di Roma 1, CP10-00016 Monterotondo, Italy

<sup>3</sup>Elettra-Sincrotrone Trieste, Strada Statale 14, km 163.5, Area Science Park, I-34149 Basovizza, Italy

Presenting Author: mishra.preetimanjari@gmail.com

Polycyclic aromatic hydrocarbons (PAHs) are efficient absorber of UV and fluoresce in IR giving rise to unidentified interstellar bands (UIB) observed in stellar medium [1]. Hence to study the stability/energy dissipation mechanism of PAHs under harsh interstellar environment and relate various excitation modes to the UIBs, the state selective photoelectron spectrum (PES) measurements were done on pyrene and fluorene using synchrotron radiation source facility at Elettra for 15 to 40 eV photon beam. The PES of a molecule is typically associated with a broadening due to Franck-Condon (FC) overlap of vibrational states. Using Hartree-Fock (HF) and Density functional technique (DFT), the FC factor for vibrational progression in  $D_0 \leftarrow S_0$  transition are calculated within harmonic approximation which compares well with our experimental results. The C-C trans-annular stretching in plane mode with  $a_g$  symmetry is found to be the dominant mode of vibration corresponding to  $\sim 1400 \text{ cm}^{-1}$  band for all PAHs and is attributed to one of the prominent feature observed in UIR bands of ISM [2]. Such calculations would be very useful in determining the IR fluorescence processes in ISM where UV photo ionization is a very common process. The PES as a function of photon energy showed a sharp increase in inner valence photoelectron cross section (binding energy 10-12 eV) for around 16-25eV photon energy due to plasmon excitation (Fig. 1). Outer valence Green's function technique is used to assign the symmetry and binding energy to molecular orbital [3].

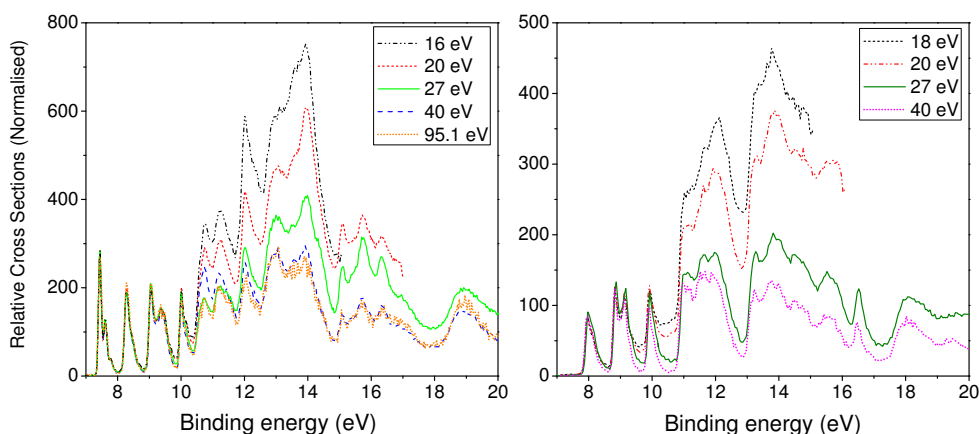


Figure 1: Pyrene (left) and fluorene (right) photoelectron spectra for different photon energy.

### References

- [1] A. G. G. M. Tielens *Annu. Rev. Astro. Astrophys.* **46**, 289–337 (2008)
- [2] P. M. Mishra *et al.* (to be published)
- [3] P. M. Mishra *et al.* *J Chem. Phys. A* (2014) (accepted for publication)

# Two-photon sequential double ionization of noble gases by circular polarized XUV radiation

E.V. Gryzlova<sup>1</sup>, A.N. Grum-Grzhimailo<sup>1</sup>, S.I. Strakhova<sup>1</sup>, and E.I. Kuzmina<sup>2</sup>

<sup>1</sup>Skobeltsyn Institute of Nuclear Physics, Lomonosov Moscow State University, 119991, Moscow, Russia

<sup>2</sup>Physical Department of Lomonosov Moscow State University, 119991 Moscow, Russia

Presenting Author: algrgr1492@yahoo.com

With the advent of free electron lasers (FELs) generating intense short pulses of XUV radiation, studies of sequential multiple ionization with analysis of the photoelectron angular distributions (PADs) and angular correlations became feasible. Experimental results as well as the corresponding theoretical predictions are limited so far to the case of linearly polarized radiation. The present theoretical work, where the PADs and correlations are considered for the sequential two-photon double ionization (2PDI) by circular polarized radiation, is motivated by the recent start-up of FERMI in Trieste (Italy) providing intense XUV pulses of variable polarization. The general statistical tensor approach within the stepwise model of the process developed and applied in [1,2] to the linearly polarized FEL is suitable for arbitrary polarization of the radiation. Similar to the previous studies we concentrate on the double ionization of the outer  $np^6$  shell of the noble gases, Ne, Ar, Kr. In contrast to the case of linearly polarized radiation, the intermediate ionic  $np^5\ ^2P_{1/2,3/2}$  states are oriented, not only aligned. The PAD for both, first- and second-step photoelectrons ( $i = 1$  and  $i = 2$ , respectively) are presented as the sum of the Legendre polynomials

$$\frac{d\sigma_i}{d\Omega_i} = \frac{\sigma_i}{4\pi} \left( 1 + \sum_{n=1,5} \beta_n^{(i)} P_n(\cos\vartheta_i) \right), \quad (1)$$

where  $\beta_n^{(i)}$  are the asymmetry parameters,  $\sigma_i$  is the angle-integrated cross section and the angle of the photoemission  $\vartheta_i$  is counted from the direction of the FEL beam. Eq. (1) takes into account the first-order nondipole corrections due to the interference between electric dipole (E1) and electric quadrupole (E2) photoionization amplitudes. The influence of the nondipole corrections, represented by terms with  $n=\text{odd}$  in Eq. (1), was found less important than in the case of linearly polarized radiation [3].

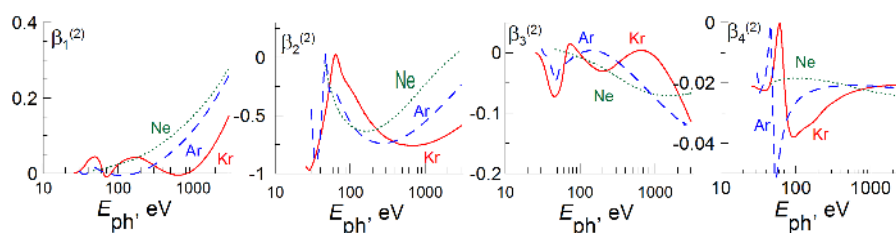


Figure 1: Asymmetry parameters in 2PDI of Ne, Ar and Kr for the  $np^4\ ^3P$  term of the residual ion.

Figure 1 shows, as example, the asymmetry parameters  $\beta_n^{(2)}$  in sequential 2PDI into the  $np^4\ ^3P$  term of the residual ion ( $\beta_5^{(2)}$  is small and not shown). Results for other terms of the residual ion, the angular correlation functions between the two photoelectrons and the general discussion will be presented at the conference.

The work is supported by the Russian Foundation for Basic Research under Grant No. 12-02-01123.

## References

- [1] S. Fritzsche *et al.* J. Phys. B **41**, 165601 (12pp) (2008)
- [2] A.N. Grum-Grzhimailo, E.V. Gryzlova, M. Meyer J. Phys. B **45**, 215602 (9pp) (2012)
- [3] E.V. Gryzlova *et al.* J. Phys. B **46**, 164014 (6pp) (2013)

## Cavity cooling of silicon nanoparticles

P. Asenbaum<sup>1</sup>, S. Kuhn<sup>1</sup>, U. Sezer<sup>1</sup>, S. Nimmrichter<sup>1</sup>, and M. Arndt<sup>1</sup>

<sup>1</sup>*Faculty of Physics, VCQ, University of Vienna, A-1090, Boltzmannngasse 5*

Presenting Author: peter.asenbaum@univie.ac.at

Cavity assisted laser cooling has been successfully applied to single atoms[1], ions[2] and atomic ensembles[3,4]. It is however, most indispensable for nanoparticles, where direct laser cooling techniques are not applicable. We demonstrate far off-resonant cavity cooling of a silicon particle with a reduction of the transverse kinetic energy by a factor of over 30 [5]. Laser induced acoustic desorption launches the nanoparticles beneath a high finesse cavity in high vacuum environment. While the particles transit through the intense cavity field the transverse velocity is reduced. By detecting the scattered light from the particle we can trace its movement in real time. Advancing this technique is crucial to enable quantum coherence experiments with nanoparticles.

### References

- [1] P. Maunz *et al.* Nature **428**, 50-52 (2004)
- [2] D. R. Leibbrandt *et al.* PRL **103**, 103001 (2009)
- [3] H. W. Chan, A. T. Black, V. Vuletic **90**, 063003 (2003)
- [4] M. Wolke *et al.* Science **337**, 75–78 (2012)
- [5] P. Asenbaum *et al.* Nat. Commun. **4**:2743 (2013)

# Screening effect on multiple ionization of Ar<sub>2</sub> by highly charged ions

T. Ohyama-Yamaguchi<sup>1</sup> and A. Ichimura<sup>2</sup>

<sup>1</sup>*Tokyo Metropolitan College of Industrial Technology, Tokyo 140-0011, Japan*  
<sup>2</sup>*Institute of Space and Astronautical Science, JAXA, Sagami-hara 252-5210, Japan*

Presenting Author: yamaguti@s.metro-cit.ac.jp

Much attention has been called to the Coulomb explosion of molecules in collisions with slow (velocities of  $v \ll 1$  atomic unit) highly charged ions. Recent progress of multiple coincidence techniques permits us to measure the dissociating ion pair distribution produced in the collisions. Such findings are of great interest from the viewpoint of multi-center multi-electron dynamics. In contrast with covalent molecules, however, little effort has been devoted to rare gas dimers.

About ten years ago, we proposed a three-center Coulombic over-barrier model to describe sequential multiple ionization of rare gas dimers [1]. In a recent work [2] we modified the model so as to incorporate the effect of partial screening for non-active target atomic site (B or C) in respective steps of electron removal during a collision. The measured result [3] of ion pair distribution up to four electron removal in Ar<sup>9+</sup> + Ar<sub>2</sub> collisions was best reproduced with the model by taking a screening parameter of  $s = 0.4$  (see figure 1).

In the present work, we further consider the screening effect for the projectile ion A<sup>q+</sup> so as to make a consistent framework. The three charges in the three center Coulomb potential

$$U(\mathbf{r}) = -\frac{q_A}{|\mathbf{r} - \mathbf{R}_A|} - \frac{q_B}{|\mathbf{r} - \mathbf{R}_B|} - \frac{q_C}{|\mathbf{r} - \mathbf{R}_C|}$$

are effectively taken as

$$\begin{aligned} q_A &= q - (Q_B + Q_C)(1 - s) \\ q_B &= Q_B + 1, \\ q_C &= (1 - s)Q_C \end{aligned}$$

for the active electron at site B, and

$$\begin{aligned} q_A &= q - (Q_B + Q_C)(1 - s) \\ q_B &= (1 - s)Q_B, \\ q_C &= Q_C + 1 \end{aligned}$$

for the active electron at site C.

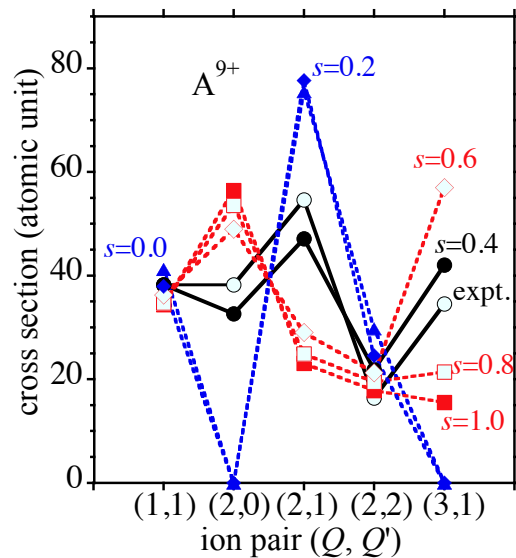


**Figure 1:** Dependence of the ion pair  $(Q, Q')$  formation cross sections on the parameter  $s$  for the collisions of  $A^{9+} + Ar_2$ , where the screening effect is introduced only in the target.

It was found that the projectile screening effect is noticeable in the population of highly charge-asymmetric pairs such as  $(Q, Q') = (2, 0)$  and  $(3, 1)$ . We have also analyzed the collisions of  $Xe^{20+} + Ar_2$  and found that the measured ion-pair distribution [4] could be reasonably reproduced with  $s \simeq 0.6$ . The physical meaning of this result is discussed.

## References

- [1] T. Ohyama-Yamaguchi and A. Ichimura, Nucl. Instrum. Methods **205**, 620 (2003).
- [2] T. Ohyama-Yamaguchi and A. Ichimura, Physica Scripta T**144**, 014028 (2011); *ibid.* T**156**, 014043 (2013).
- [3] J. Matsumoto *et al.*, Phys. Rev. Lett. **105**, 263202 (2010); *ibid.* Physica Scripta T**144**, 014016 (2011).
- [4] A. Cassimi *et al.*, XXVIII ICPEAC, Lanzhou, China (2013).





## List of Authors (cross-referenced to abstract page)

### A

Ackemann, T., 33  
Agababaev, V.A., 94  
Agre, M.Ya., 180  
Agueny, H., 71  
Ahokas, J., 145  
Alì-Khan, M., 30  
Alexander, J.D., 121  
Al-Labady, N., 82  
Almond, J.A., 122  
Amand, L., 50  
Amaro, P., 42  
Amy-Klein, A., 96, 117  
Andreev, O.Yu., 58, 67  
Antognini, A., 13  
Argence, A., 117  
Argence, B., 96  
Arimondo, E., 110, 128  
Armstrong, N.M.R., 168  
Arndt, M., 48, 187  
Arnold, A.S., 33, 138, 139  
Arnold, C.L., 25  
Asenbaum, P., 187  
Atalay, B., 83  
Auzinsh, M., 104–106  
Avaldi, L., 185

### B

Babilotte, Ph., 41  
Bäckström, E., 115, 121  
Baker, M., 35  
Ballin, P., 27

Baluja, K.L., 87  
Barredo, D., 31  
Barrow, J.D., 73  
Barstow, M.A., 73  
Başar, Gö., 74, 81–83  
Başar, Gü., 74  
Baszanowska, E., 119  
Battesti, R., 110  
Bautista, M., 99  
Baye, D., 103  
Beguín, L., 31  
Behbood, N., 32  
Beiersdorfer, P., 175  
Berengut, J.C., 72, 73  
Bernitt, S., 42, 100  
Bertoldi, A., 50  
Berzins, A., 104, 105  
Bethlem, H.L., 54  
Bilicki, S., 137  
Billard, F., 23  
Binder, T., 79  
Biraben, F., 24  
Björkhage, M., 121  
Bjerlin, J., 20  
Blaum, K., 38, 107  
Bloch, D., 27, 86  
Blom, M., 121  
Blondel, C., 41  
Böll, O., 97  
Bolognesi, P., 185  
Bolpasi, V., 35

Bonert, A.E., 66  
Bordas, C., 47  
Bouazza, S., 168  
Bouchelaghem, F., 174  
Bouledroua, M., 174  
Bourgain, R., 40  
Bouyer, P., 50  
Brännholmä, L., 121  
Brazhnikov, D.V., 66  
Bressanini, D., 14  
Briant, T., 123  
Briquez, S., 169  
Brouri, M., 43  
Browaeyns, A., 31, 40  
Bruce, G., 102  
Bruner, B., 8  
Büchner, M., 75, 76  
Bumby, J.S., 122  
Busaite, L., 106

## C

Cabrera-Gutiérrez, C., 29  
Cacciapuoti, L., 46  
Caer, C., 123  
Canuel, B., 50  
Carette, T., 112  
Carlström, S., 118  
Carrat, V., 29  
Carson, C.H., 139  
Caruso, F., 30  
Cassidy, D.B., 16, 44  
Cassinerio, M., 92  
Castrillo, A., 92, 176  
Cataliotti, F.S., 30  
Cavalieri, S., 88  
Cederbaum, L.S., 26  
Cederquist, H., 121  
Cederwall, B., 77  
Çelik, G., 83

Cerchiari, G., 57  
Chaibi, W., 50  
Champenois, C., 55  
Chang, C.H., 173  
Chardonnet, C., 96, 117  
Cheinet, P., 128  
Chen, M.H., 173  
Chen, R.S., 173  
Cherukattil, S., 30  
Chicireanu, R., 149  
Cho, S.U., 15  
Chotia, A., 36  
Christensen, B.T.R., 135  
Chwirot, S., 113  
Ciampini, D., 110  
Ciuryło, R., 137  
Ciuryło, R., 53, 65, 160  
Clément, J.F., 149  
Clark, T.W., 12  
Cohadon, P-F, 123  
Cohen, S., 47  
Colangelo, G., 32  
Collucelli, N., 92  
Condylis, P.C., 35  
Constantin, F.L., 177  
Coop, S., 131, 142, 143, 147  
Cormier, E., 50  
Cotta, D., 102  
Creffield, C.E., 134  
Crespo López-Urrutia, J.R., 18, 42, 100, 153, 154  
Crozet, P., 172  
Cybulski, H., 65  
Cygan, A., 53, 160

## D

Dagan, M., 8  
Dahlström, J.M., 25  
Dai, Z.W., 182

Dalibard, J., 19  
Darquié, B., 96, 117, 176  
Daussy, C., 96, 117, 176  
Daxner, M., 52  
De Natale, P., 166  
de Paz, A., 36  
De Rosa, M., 166  
Decamps, B., 75  
Delande, D., 37  
Deleglise, S., 123  
Deli, M., 89  
Dembczynski, J., 79  
Demekhin, Ph.V., 26, 60  
Denifl, S., 52  
Diermaier, M., 111  
Dijck, E.A., 97  
Dinesan, H., 176  
Dobrev, G., 172  
Domysławska, J., 160  
Dörner, R., 14, 26  
Dörre, N., 48  
Douillet, A., 155  
Drag, C., 41  
Drewsen, M., 18  
Drozdowski, R., 116, 119  
Dubey, I., 159  
Dubey, L., 159  
Dubois, A., 71, 178  
Dubrovich, V., 63  
Ducloy, M., 86  
Dudovich, N., 8  
Duflot, D., 169  
Dulieu, O., 126  
Dulitz, K., 49  
Dunseath, K., 43  
Dziczek, D., 113  
Dzuba, V.A., 59, 72

## E

Efremidis, N.K., 35  
Efremova, E., 85  
Ehresmann, A., 26, 68–70  
Eismann, U., 133  
Engström, L., 115  
Engström, L., 114  
Epp, S.W., 100  
Er, A., 74, 81–83  
Es-sebbar, Et., 89

## F

Fabrikant, I.I., 183  
Faoro, R., 128  
Farooq, A., 89  
Fasci, E., 92, 176  
Faucher, O., 23  
Federmann, S., 111  
Ferber, R., 81, 82, 104, 105  
Ferri, F., 140  
Fiedler, J., 150  
Filippin, L., 103  
Fini, L., 88  
Firth, W.J., 33  
Fitch, N., 122  
Fivet, V., 99  
Flambaum, V.V., 59, 72, 73  
Fleig, T., 21  
Fletcher, R.J., 132  
Fleurbaey, H., 24  
Flores, A.S., 28  
Förstel, M., 26  
Fouché, M., 110  
Franke-Arnold, S., 12  
Fritzsche, S., 42

## G

Gaffet, S., 50  
Gahbauer, F., 104, 105  
Galtier, S., 24

Galzerano, G., 92  
Gambetta, A., 92  
Gamper, B., 79  
Garcia, S., 140  
Garreau, J.C., 146, 149  
Gatchell, M., 121  
Gauguet, A., 75, 76  
Gaul, A., 70  
Geiger, R., 50  
Génévriez, M., 43  
Geyer, P., 48  
Giacobino, E., 6  
Gianfrani, L., 92, 176  
Gillot, J., 75, 76  
Giner, L., 6  
Gingell, A., 18  
Gisselbrecht, M., 25  
Giusfredi, G., 166  
Glöckner, R., 167  
Glazov, D.A., 94  
Godefroid, M., 103  
Godefroid, M.R., 112  
Gomes, A.S.P., 170, 171  
Gomes, P., 33  
Goncharov, A., 96, 117  
Goncharov, A.N., 66  
González Férez, Rosario, 17  
Googlev, K.A., 70  
Gorceix, O., 36  
Gordeev, M., 85  
Gori-Giorgi, P., 20  
Gribakin, G.F., 91, 183  
Grier, A.T., 97  
Griffin, P.F., 138, 139  
Grisenti, R., 14  
Grochola, A., 157, 158  
Grum-Grzhimailo, A.N., 186  
Gryzlova, E.V., 186  
Guénot, D., 25

Guibal, S., 151  
Guidoni, L., 151  
Guthöhrlein, G.H., 80  
Guyomarc'h, D., 55  
Güzelçimen, F., 74, 81–83

## H

Hadzibabic, Z., 132  
Hainaut, C., 149  
Hakalla, R., 162  
Hakhumyan, H., 84  
Hakonen, P.J., 15  
Halldén, P., 121  
Haller, E., 102  
Hans, A., 26  
Hansen, A.K., 18  
Hanstorp, D., 121  
Harman, Z., 42  
Haroche, S., 4  
Hartman, H., 114, 115  
Haslinger, P., 48  
Heidmann, A., 123  
Heikkilä, T.T., 15  
Hellberg, F., 121  
Hendricks, R.J., 165  
Hennequin, D., 141  
Henriksen, M.R., 135  
Hergenhahn, U., 26  
Hertz, E., 23  
Higaki, H., 111  
Hilico, L., 155  
Hinds, E.A., 122  
Hinney, J., 102  
Hoekstra, S., 54, 97  
Höfener, S., 170  
Hogan, S.D., 44, 120  
Holberg, J.B., 73  
Hole, O.M., 121  
Holland, D.A., 165

Holt, R.A., 168  
Holzinger, D., 70  
Hou, J., 107  
Houssin, M., 55  
Huber, S.E., 52  
Huckfeldt, H., 70  
Hudson, J., 102  
Hühnermann, H., 78

## I

Ichimura, A., 188  
Ignesti, E., 88  
Ivanov, M., 8  
Ivanova, M., 163

## J

Jacob, Ch.R., 170  
Jacquey, M., 29  
Jahnke, T., 14, 26  
Järvinen, J., 145  
Jasik, P., 158  
Jastrzebski, W., 157, 158  
Jenkins, S.D., 40  
Jennewein, S., 40  
Jiang, L.Y., 182  
Jilani, S., 80  
Jordan, E., 57  
Julien, L., 24  
Jungmann, K., 97

## K

Kadhane, U., 184, 185  
Kaiser, R., 33  
Källberg, A., 121  
Källersjö, G., 121  
Kalninsh, U., 105  
Kalvans, L., 104–106  
Kamiński, P., 119  
Kaminska, M., 121  
Kamsap, M.R., 55

Kanai, Y., 111  
Kanda, S., 90  
Kaprálová-Žánská, P.R., 95, 161  
Karachevtsev, V., 159  
Karr, J.-Ph., 155  
Karras, G., 23  
Kaushal, J., 101  
Kędziera, D., 28  
Kellerbauer, A., 57  
Kelly, A., 102  
Keřpa, R., 162  
Khaykovich, L., 51, 125  
Kheifets, A.S., 25  
Kim, H., 14  
Kinnunen, J.J., 136  
Kirchner, T., 45  
Kłosowski, Ł., 18, 113  
Knöckel, H., 61, 163  
Knie, A., 26  
Knoop, M., 55  
Knoop, S., 28  
Köhler, F., 38, 107  
Kohnen, M., 153, 154  
Kokkermans, S., 51, 125  
Kolek, P., 162  
Kolganova, E.A., 129  
Koperski, J., 164  
Korobitsin, A.A., 129  
Kosior, A., 34  
Koval, E.A., 127, 130  
Koval, O.A., 127, 130  
Kovtun, O., 77  
Kowalczyk, P., 157, 158  
Kozakov, A.T., 70  
Kozlov, A., 59  
Kröger, S., 82  
Krasnokutska, I., 123  
Kristensen, S.B., 18  
Kröger, S., 74, 81, 83

Kroon, D., 25  
Krottenmüller, M., 167  
Kuhn, S., 187  
Kuhr, S., 102  
Kuleff, A.I., 26  
Kunitzki, M., 14  
Kuroda, N., 111  
Kuzmina, E.I., 186  
Kwela, J., 78, 116  
Kwong, C.C., 37

## L

Labaigt, G., 178  
Labeyrie, G., 33  
Labuhn, H., 31  
Laburthe-Tolra, B., 36  
Labzowsky, L., 63  
Lagutin, B.M., 68–70  
Lahaye, T., 31  
Laliotis, A., 27, 86  
Lamour, E., 45, 179  
Lancuba, P., 120  
Landragin, A., 50  
Laporta, P., 92  
Laurat, J., 6  
Lavorel, B., 23  
Law, S.M.K., 64  
Lazda, R., 106  
Le Targat, R., 133  
Leali, M., 111  
Lebouteiller, C., 140  
Lee, K.F., 173  
Lehtonen, L., 145  
Leontein, S., 121  
Leopold, T., 153, 154  
Lepers, M., 126  
Lépine, F., 47  
Lepoutre, S., 76  
Leroy, C., 84

Lévy, A., 179  
L’Huillier, A., 25  
Likforman, J.-P., 151  
Liljeby, L., 121  
Lin, K.Y., 173  
Lisak, D., 53, 160  
Liu, C.H., 173  
Lodewyck, J., 133  
Lodi Rizzini, E., 111  
Löfgren, P., 121  
Long, R., 140  
Lopez, O., 96, 117  
Lovecchio, C., 30  
Lovric, J., 169  
Luiten, O.J., 56, 152  
Lundberg, H., 114, 115  
Lyaschenko, K.N., 67

## M

Macé, S., 179  
Machtey, O., 51, 125  
Maddaloni, P., 166  
Major, J., 148  
Makhoute, A., 71  
Makles, K., 123  
Makles, M., 123  
Malbrunot, C., 111  
Malet Giralt, F., 20  
Man, J., 132  
Manai, I., 149  
Mannervik, S., 121  
Manquest, C., 151  
Mansson, E.P., 25  
Maréchal, E., 36  
Marangoni, M., 92  
Marelic, J., 156  
Martin Ciurana, F., 32  
Martinez de Escobar, Y.N., 143  
Martinez, N., 131, 142, 147

Mascagna, V., 111  
Masłowski, P., 160  
Masłowski, P., 53  
Massel, F., 15  
Massiczek, O., 111  
Mathavan, S.C., 54  
Matsuda, Y., 111  
Mauracher, A., 52  
Maurin, I., 27, 86  
Mauritsson, J., 118  
Maxein, D., 6  
McGilligan, J.P., 138  
Meinema, C., 54  
Mejri, S., 96, 117, 176  
Melezhik, V.S., 124, 127  
Mendl, C., 20  
Mentel, Ł., 28  
Meshkov, V.V., 93  
Michishio, K., 111  
Micke, P., 154  
Mirtschink, A., 20  
Mishra, H.P., 28  
Mishra, P.M., 184, 185  
Mistonova, E.A., 58  
Mitchell, M.W., 32, 131, 142, 143, 147  
Mizutani, T., 111  
Mohanty, A., 97  
Mohri, A., 111  
Monnerville, M., 169  
Morigi, G., 11  
Morrissey, M.J., 35  
Mosca, S., 166  
Motsch, M., 49  
Moufarej, E., 27  
Mozers, A., 104  
Munoz-Rodriguez, R., 137  
Murtagh, D.J., 111  
Mutsaers, P.H.A., 56, 152

## N

Nagórny, B., 137  
Nagahama, H., 111  
Nagashima, Y., 111  
Nagata, Y., 111  
Napolitano, M., 32  
Nascimento, R., 121  
Navon, N., 132  
Ndong, M., 23  
Nemouchi, M., 112  
Nez, F., 24  
Nicolas, A., 6  
Nikolsky, A.V., 70  
Nilsson, H., 114, 115  
Nimmrichter, S., 48, 187  
Nogrette, F., 31  
Notermans, R.P.M.J.W., 98  
Nuñez Portela, M., 97  
Nyman, R.A., 156

## O

Ohtsuka, M., 111  
Ohyama-Yamaguchi, T., 188  
Olejniczak, M., 171  
Onderwater, C.J.G., 97  
Ong, A., 72, 73  
Oppen, G. von, 119  
Oppo, G.-L., 33  
Orenstein, G., 8  
Ostrowska-Kopec, M., 162  
O'Sullivan, G., 5  
Öztürk, I.K., 74, 81–83

## P

Paál, A., 121  
Palacios, S., 131, 142, 143, 147  
Palmeri, P., 182  
Papoyan, A., 105  
Parisi, M., 166  
Pashayan-Leroy, Y., 84

Pashov, A., 61, 163, 172  
Passerat de Silans, T., 86  
Patkóš, V., 108  
Pedatzur, O., 8  
Pedregosa-Gutierrez, J., 55  
Pedri, P., 36  
Pelle, B., 128  
Pellegrino, J., 40  
Petrov, I.D., 68–70  
Pierrat, R., 37  
Pillet, P., 128  
Piotrowska, I., 162  
Pirkkalainen, J.-M., 15  
Piwiński, M., 113, 160  
Plodzien, M., 148  
Plunien, G., 63, 94  
Postler, J., 52  
Pouilly, B., 169  
Prehn, A., 167  
Preval, S.P., 73  
Prevedelli, M., 46  
Prigent, C., 45, 179  
Prince, K.C., 185  
Pruvost, L., 29  
Przewięźlikowski, B., 137  
Puchalski, M., 28

## Q

Quinet, P., 99, 182  
Quint, W., 38, 107

## R

Radics, B., 111  
Radwell, N., 12  
Rajput, J., 184  
Ramsbottom, C.A., 181  
Ravets, S., 31  
Réal, F., 170, 171  
Reichel, J., 140  
Reimann, S., 20

Reinhard, P., 121  
Rempe, G., 7, 167  
Rengelink, R.J., 98  
Rey, H., 101  
Ricciardi, I., 166  
Richter, R., 185  
Riis, E., 138, 139  
Rizzo, C., 110  
Robb, G.R.M., 33  
Robert-de-Saint-Vincent, M., 132  
Roby, J.-L., 133  
Rodewald, J., 48  
Rohart, F., 176  
Romain, R., 141  
Rosén, S., 121  
Rosi, G., 46  
Rosner, D.S., 168  
Ross, A., 172  
Rozet, J.-P., 45, 179  
Rozhdestvensky, Yu., 85  
Rudolph, J.K., 100  
Rundans, R., 105  
Ruostekoski, J., 40  
Ryazanova, O., 159

## S

Sacha, K., 34  
Safvan, C.P., 184  
Sahagun, D., 35  
Sakurai, S., 111  
Salehzadeh, A., 45  
Sansone, G., 9  
Santamaria, L., 166  
Sargsyan, A., 84  
Sarkisyan, D., 84, 105  
Sauer, B.E., 122, 165  
Sauerzopf, C., 111  
Schäffer, S.A., 135  
Schöllkopf, W., 14

- Schafer, K.J., 118  
Schartner, K.-H., 68  
Scheel, S., 150  
Scheier, P., 52  
Schmöger, L., 153, 154  
Schmidt, H.T., 121  
Schmidt, L., 14  
Schmidt, P.O., 153, 154  
Schmoranzner, H., 68, 69  
Schöffler, M., 14  
Schwarz, M., 18, 153, 154  
Scotto, S., 110  
Serbinenko, V., 8  
Sewell, R.J., 32  
Sezer, U., 187  
Shabaev, V.M., 94  
Shafir, D., 8  
Shah, C., 42  
Shang, X., 182  
Sharma, A., 36  
Shchepetnov, A.A., 94  
Shearer, S.F.C., 64  
Shelkovnikov, A., 96  
Sheludyakov, S., 145  
Shi, C., 133  
Shilov, A.M., 66  
Shotan, Z., 51, 125  
Sienkiewicz, J.E., 158  
Sillanpää, M.A., 15  
Sillitoe, N., 155  
Simonsson, A., 121  
Singh, J., 87  
Skoff, S., 122  
Smirnova, O., 8, 101  
Smith, R.P., 132  
Smits, J., 106  
Šmydke, J., 95, 161  
Softley, T.P., 49  
Soifer, H., 8  
Sokolov, M.M., 94  
Solovyev, D., 63  
Sols, F., 134  
Song, X., 15  
Sorensen, S.L., 25  
Sorrentino, F., 46  
Sortais, Y.R.P., 40  
Sow, P.L.T., 117  
Sow, P.L.T., 96, 176  
Spiss, A., 104  
Stefańska, P., 62  
Stein, A., 163  
Steinbrügge, R., 42, 100  
Steydli, S., 45, 179  
Stolyarov, A.V., 93  
Strakhova, S.I., 186  
Sturm, S., 38, 107  
Sugny, D., 23  
Sukhorukov, V.L., 68–70  
Suominen, K.-A., 145  
Surzhykov, A., 42, 77  
Suzuki, K., 111  
Swann, A.R., 91  
Szajna, W., 162  
Szczepkowski, J., 157, 158  
Szmytkowski, R., 62  
Szriftgiser, P., 149  
Szymanski, B., 151
- T**  
Tabosa, J.W., 29  
Taichenachev, A.V., 66  
Tajima, M., 111  
Tamanis, M., 81, 82  
Tarbutt, M.R., 122, 165  
Tashenov, S., 42, 77  
Tauschinsky, A., 49  
Temelkov, I., 61  
ten Haaf, G., 56, 152

- Terao-Dunseath, M., 43  
Tesio, E., 33  
Thibault, F., 65  
Thomas, R.D., 121  
Thomsen, J.W., 135  
Tian, Y.S., 182  
Tiemann, E., 61, 163  
Timmermans, R.G.E., 97  
Tino, G.M., 46  
Tioukine, V., 77  
Toennies, J.P., 52  
Tokunaga, S.K., 117  
Tokunaga, S.K., 96, 176  
Tommasi, F., 88  
Tonoyan, A., 84  
Torii, H.A., 111  
Tóth, G., 32  
Touat, A., 112  
Toubin, C., 169  
Träbert, E., 175  
Trassinelli, M., 45, 179  
Trawiński, R.S., 53, 160  
Trinter, F., 14  
Truppe, S., 165  
Tuorila, J., 15  
Tupitsyn, I.I., 94  
Tyndall, N.B., 181
- U**  
Ubachs, Wim, 1  
Uddin, Z., 80  
Ulbricht, H., 39  
Ullrich, J., 18, 100, 153, 154  
Ulmer, S., 111  
Urbain, X., 43  
Urbanczyk, T., 164  
Uzan, A.J., 8
- V**  
Vainio, O., 145  
Valappol, A., 97  
Vallet, V., 170, 171  
van den Berg, J.E., 54  
van der Geer, S.B., 56, 152  
van der Hart, H., 101  
van der Zande, W., 2  
Van Gorp, S., 111  
van Rens, J.F.M., 56  
Vanderbruggen, T., 131, 142, 147  
Vanderburggen, T., 143  
Vandevraye, M., 41  
Vanhaecke, N., 49  
Vasiliev, S., 145  
Vassen, W., 28, 98  
Veissier, L., 6  
Vemersch, B., 146  
Venturelli, L., 111  
Verkerk, P., 141  
Vernac, L., 36  
Vernhet, D., 45, 179  
Vernier, A., 31  
Versolato, O.O., 18, 153, 154  
Viaris de Lesegno, B., 29  
Vig, S., 184  
Vigué, J., 75, 76  
Virot, F., 171  
Visscher, L., 170  
Voigtsberger, J., 14  
Voitkiv, A.B., 58  
Voloshin, I., 159  
Volotka, A.V., 94  
von Klitzing, W., 35  
Vrakking, M.J.J., 47  
Vredenbregt, E.J.D., 56, 152
- W**  
Wagner, A., 38, 107  
Wall, T.E., 44  
Wang, Q., 182

Wcisło, P., 53, 65

Wcisło, P., 160

Webb, J.K., 73

Weidemüller, M., 10

Wenz, A. N., 22

Werbowy, S., 78

Werth, G., 38, 107

Westergaard, P.G., 135

Widmann, E., 111

Wilkowski, D., 37

Willmann, L., 97

Wilschut, H.W., 97

Windberger, A., 18, 153

Windholz, L., 74, 78–80, 116

Wineland, D.J., 3

Witkowski, M., 137

Wójtewicz, S., 53, 160

Wouters, S.H.W., 56, 152

Woytasik, M., 151

Wünschek, B., 111

Wyart, J.-F., 126

## Y

Yamazaki, Y., 111

Yang, T., 37

Ye, J., 135

Yerokhin, V.A., 77

Yousif Al-Mulla, S.Y., 109

Yuce, C., 144

Yudin, V.I., 66

## Z

Zaborowski, M., 160

Zachwieja, M., 162

Zakrzewski, J., 148

Zamastil, J., 108

Zawada, M., 137

Zehra, S., 80

Zeller, S., 14

Zeppenfeld, M., 167

Zhai, Yueyang, 139

Zhang, W., 182

Zmeskal, J., 111

Zozulya, V., 159

Żuchowski, P.S., 28, 137

Zurlo, N., 111

Zvezdov, D., 145



## List of Participants

(cross-referenced to the contribution numbers)

|                               |                            |  |
|-------------------------------|----------------------------|--|
| Agre, Mark                    | P-122                      | <a href="mailto:magrik@ukr.net">magrik@ukr.net</a>   |
| Agueny, Hicham                | P-013                      | <a href="mailto:h.agueny@gmail.com">h.agueny@gmail.com</a>                                     |
| Allabady, Nadia               |                            | <a href="mailto:ikanat@istanbul.edu.tr">ikanat@istanbul.edu.tr</a>                             |
| Andreev, Oleg Yu.             | CT-36, P-009               | <a href="mailto:olyuan@gmail.com">olyuan@gmail.com</a>   |
| Antognini, Aldo               | IT-5                       | <a href="mailto:aldo@phys.ethz.ch">aldo@phys.ethz.ch</a>                                       |
| Asenbaum, Peter               | P-129                      | <a href="mailto:peter.asenbaum@univie.ac.at">peter.asenbaum@univie.ac.at</a>                   |
| Auzinsh, Marcis               | P-046, P-047, P-048        | <a href="mailto:Marcis.Auzins@lu.lv">Marcis.Auzins@lu.lv</a>                                   |
| Bachau, Henri                 |                            | <a href="mailto:bachau@celia.u-bordeaux1.fr">bachau@celia.u-bordeaux1.fr</a>                   |
| Barker, Peter                 |                            | <a href="mailto:p.barker@ucl.ac.uk">p.barker@ucl.ac.uk</a>                                     |
| Başar, Gönül                  | P-016, P-023, P-024, P-025 | <a href="mailto:gbasar2004@yahoo.com">gbasar2004@yahoo.com</a>                                 |
| Behbood, Naeimeh              | CT-10                      | <a href="mailto:naeimeh.behbood@icfo.es">naeimeh.behbood@icfo.es</a>                           |
| Berengut, Julian              | P-014, P-015               | <a href="mailto:jcb@phys.unsw.edu.au">jcb@phys.unsw.edu.au</a>                                 |
| Blondel, Christophe           | CT-19                      | <a href="mailto:christophe.blondel@u-psud.fr">christophe.blondel@u-psud.fr</a>                 |
| Bordas, Christian             | CT-25                      | <a href="mailto:christian.bordas@univ-lyon1.fr">christian.bordas@univ-lyon1.fr</a>             |
| Bouazza, Safa                 | P-110                      | <a href="mailto:safa.bouazza@univ-reims.fr">safa.bouazza@univ-reims.fr</a>                     |
| Bouledroua, Moncef            | P-116                      | <a href="mailto:boulmoncef@netscape.net">boulmoncef@netscape.net</a>                           |
| Briquez, Stéphane             | P-111                      | <a href="mailto:stephane.briquez@univ-lille1.fr">stephane.briquez@univ-lille1.fr</a>           |
| Büchner, Matthias             | P-017, P018                | <a href="mailto:matthias.buchner@irsamc.ups-tlse.fr">matthias.buchner@irsamc.ups-tlse.fr</a>   |
| Bumby, James                  | P-064                      | <a href="mailto:james.bumby08@imperial.ac.uk">james.bumby08@imperial.ac.uk</a>                 |
| Cacciani, Patrice             |                            | <a href="mailto:Patrice.Cacciani@univ-lille1.fr">Patrice.Cacciani@univ-lille1.fr</a>           |
| Carson, Christopher           | P-081                      | <a href="mailto:christopher.carson@strath.ac.uk">christopher.carson@strath.ac.uk</a>           |
| Cassidy, David B.             | IT-08, CT-22               | <a href="mailto:d.cassidy@ucl.ac.uk">d.cassidy@ucl.ac.uk</a>                                   |
| Castrillo, Antonio            | P-034, P-118               | <a href="mailto:antonio.castrillo@unina2.it">antonio.castrillo@unina2.it</a>                   |
| Cataliotti, Francesco         | CT-08                      | <a href="mailto:fsc@lens.unifi.it">fsc@lens.unifi.it</a>                                       |
| Cavaliere, Stefano            | P-030                      | <a href="mailto:stefano.cavaliere@unifi.it">stefano.cavaliere@unifi.it</a>                     |
| Cheinet, Patrick              | P-070                      | <a href="mailto:patrick.cheinet@u-psud.fr">patrick.cheinet@u-psud.fr</a>                       |
| Chia-hao, Chang               | P-115                      | <a href="mailto:changch@itri.org.tw">changch@itri.org.tw</a>                                   |
| Chicireanu, Radu              | P-091                      | <a href="mailto:radu.chicireanu@univ-lille1.fr">radu.chicireanu@univ-lille1.fr</a>             |
| Clément, Jean-François        | P-091                      | <a href="mailto:jean-francois.clement@univ-lille1.fr">jean-francois.clement@univ-lille1.fr</a> |
| Constantin, Florin Lucian     | P-119                      | <a href="mailto:FL.Constantin@univ-lille1.fr">FL.Constantin@univ-lille1.fr</a>                 |
| Coop, Simon                   | P-073, P-084, P-085, P-089 | <a href="mailto:simon.coop@icfo.es">simon.coop@icfo.es</a>                                     |
| Cosléou, Jean                 |                            | <a href="mailto:Jean.Cosleou@univ-lille1.fr">Jean.Cosleou@univ-lille1.fr</a>                   |
| Creffield, Charles            | P-076                      | <a href="mailto:c.creffield@fis.ucm.es">c.creffield@fis.ucm.es</a>                             |
| Crespo López-Urrutia, José R. | CT-20, P-042               | <a href="mailto:crespojr@mpi-hd.mpg.de">crespojr@mpi-hd.mpg.de</a>                             |
| Crozet, Patrick               | P-114                      | <a href="mailto:patrick.crozet@univ-lyon1.fr">patrick.crozet@univ-lyon1.fr</a>                 |
| Dalibard, Jean                | PL-09                      | <a href="mailto:jean.dalibard@lkb.ens.fr">jean.dalibard@lkb.ens.fr</a>                         |
| De Bièvre, Stéphane           |                            | <a href="mailto:stephan.de-bievre@univ-lille1.fr">stephan.de-bievre@univ-lille1.fr</a>         |
| Decamps, Boris                | P-017                      | <a href="mailto:decamps@irsamc.ups-tlse.fr">decamps@irsamc.ups-tlse.fr</a>                     |
| Demekhin, Philipp             | CT-04, P-002               | <a href="mailto:demekhin@physik.uni-kassel.de">demekhin@physik.uni-kassel.de</a>               |
| Dobrev, Georgi                | P-114                      | <a href="mailto:g_dobrev@phys.uni-sofia.bg">g_dobrev@phys.uni-sofia.bg</a>                     |
| Drewsen, Michael              | IT-10                      | <a href="mailto:drewsen@phys.au.dk">drewsen@phys.au.dk</a>                                     |
| Drozdowski, Ryszard           | P-058, P-061               | <a href="mailto:fizrd@ug.edu.pl">fizrd@ug.edu.pl</a>   |
| Dudovich, Nirit               | PL-08                      | <a href="mailto:Nirit.Dudovich@weizmann.ac.il">Nirit.Dudovich@weizmann.ac.il</a>               |
| Dulitz, Katrin                | CT-27                      | <a href="mailto:katrin.dulitz@chem.ox.ac.uk">katrin.dulitz@chem.ox.ac.uk</a>                   |
| Dörner, Reinhard              | IT-06                      | <a href="mailto:doerner@atom.uni-frankfurt.de">doerner@atom.uni-frankfurt.de</a>               |
| Engström, Lars                | P-056, P-057               | <a href="mailto:lars.engstrom@fysik.lth.se">lars.engstrom@fysik.lth.se</a>                     |
| Er, Alev                      | P-016, P-023, P-024, P-025 | <a href="mailto:alever@istanbul.edu.tr">alever@istanbul.edu.tr</a>                             |
| Es-Sebbar, Et-Touhami         | P-031                      | <a href="mailto:Ettouhami.Essebbar@kaust.edu.sa">Ettouhami.Essebbar@kaust.edu.sa</a>           |

|                         |                            |  |
|-------------------------|----------------------------|--|
| Fabre, Nathalie         |                            | <a href="mailto:nathalie.fabre@univ-paris13.fr">nathalie.fabre@univ-paris13.fr</a>         |
| Fiedler, Johannes       | P-092                      | <a href="mailto:johannes.fiedler@uni-rostock.de">johannes.fiedler@uni-rostock.de</a>       |
| Filippin, Livio         | P-045                      | <a href="mailto:lifilipp@ulb.ac.be">lifilipp@ulb.ac.be</a>                                 |
| Fleig, Timo             | PL-10                      | <a href="mailto:timo.fleig@irsamc.ups-tlse.fr">timo.fleig@irsamc.ups-tlse.fr</a>           |
| Franke-Arnold, Sonja    | IT-04                      | <a href="mailto:sonja.franke-arnold@glasgow.ac.uk">sonja.franke-arnold@glasgow.ac.uk</a>   |
| Galtier, Sandrine       | CT-02                      | <a href="mailto:galtier@lkb.upmc.fr">galtier@lkb.upmc.fr</a>                               |
| Garreau, Jean-Claude    | P-088, P-091               | <a href="mailto:jean-claude.garreau@univ-lille1.fr">jean-claude.garreau@univ-lille1.fr</a> |
| Geiger, Remi            | CT-28                      | <a href="mailto:remi.geiger@obspm.fr">remi.geiger@obspm.fr</a>                             |
| Génévriez, Matthieu     | CT-21                      | <a href="mailto:matthieu.genevriez@uclouvain.be">matthieu.genevriez@uclouvain.be</a>       |
| Geyer, Philipp          | CT-26                      | <a href="mailto:philipp.geyer@univie.ac.at">philipp.geyer@univie.ac.at</a>                 |
| Giacobino, Elisabeth    | PL-06                      | <a href="mailto:elisabeth.giacobino@lkb.upmc.fr">elisabeth.giacobino@lkb.upmc.fr</a>       |
| Glazov, Dmitry          | P-036                      | <a href="mailto:glazov.d.a@gmail.com">glazov.d.a@gmail.com</a>                             |
| Glöckner, Rosa          | P-109                      | <a href="mailto:rosa.gloeckner@mpq.mpg.de">rosa.gloeckner@mpq.mpg.de</a>                   |
| Gomes, Pedro            | CT-11, P-112, P-113        | <a href="mailto:pedro.gomes@strath.ac.uk">pedro.gomes@strath.ac.uk</a>                     |
| González-Férez, Rosario | IT-09                      | <a href="mailto:rogonzal@ugr.es">rogonzal@ugr.es</a>                                       |
| Gorceix, Olivier        | CT-14                      | <a href="mailto:olivier.gorceix@univ-paris13.fr">olivier.gorceix@univ-paris13.fr</a>       |
| Gordeev, Maksim         | P-027                      | <a href="mailto:mxmgordeev@gmail.com">mxmgordeev@gmail.com</a>                             |
| Gribakin, Gleb          | P-033, P-125               | <a href="mailto:g.gribakin@qub.ac.uk">g.gribakin@qub.ac.uk</a>                             |
| Grochola, Anna          | P-099, P-100               | <a href="mailto:Anna.Grochola@fuw.edu.pl">Anna.Grochola@fuw.edu.pl</a>                     |
| Grum-Grzhimailo, Alexei | P-128                      | <a href="mailto:algrgr1492@yahoo.com">algrgr1492@yahoo.com</a>                             |
| Guenot, Diego           | CT-3                       | <a href="mailto:diego.guenot@fysik.lth.se">diego.guenot@fysik.lth.se</a>                   |
| Guidoni, Luca           | P-093                      | <a href="mailto:luca.guidoni@univ-paris-diderot.fr">luca.guidoni@univ-paris-diderot.fr</a> |
| Güzelçimen, Feyza       | P-016, P-023, P-024, P-025 | <a href="mailto:feyzag@istanbul.edu.tr">feyzag@istanbul.edu.tr</a>                         |
| Hakalla, Rafal          | P-104                      | <a href="mailto:hakalla@ur.edu.pl">hakalla@ur.edu.pl</a>                                   |
| Haroche, Serge          | PL-04                      | <a href="mailto:Serge.Haroche@lkb.ens.fr">Serge.Haroche@lkb.ens.fr</a>                     |
| Heber, Oded             |                            | <a href="mailto:oded.heber@weizmann.ac.il">oded.heber@weizmann.ac.il</a>                   |
| Hennequin, Daniel       | P-083                      | <a href="mailto:daniel.hennequin@univ-lille1.fr">daniel.hennequin@univ-lille1.fr</a>       |
| Henriksen, Martin Romme | P-077                      | <a href="mailto:spk144@nbi.ku.dk">spk144@nbi.ku.dk</a>                                     |
| Hilico, Laurent         | P-097                      | <a href="mailto:hilico@spectro.jussieu.fr">hilico@spectro.jussieu.fr</a>                   |
| Hinney, Jakob           | P-044                      | <a href="mailto:jakob.hinney@gmx.de">jakob.hinney@gmx.de</a>                               |
| Hole, Odd Magnar        | P-063                      | <a href="mailto:Odd.hole@fysik.su.se">Odd.hole@fysik.su.se</a>                             |
| Holland, Darren         | P-107                      | <a href="mailto:darren.holland11@imperial.ac.uk">darren.holland11@imperial.ac.uk</a>       |
| Ichimura, Atsushi       | P-130                      | <a href="mailto:ichimura_atsushi@nifty.com">ichimura_atsushi@nifty.com</a>                 |
| Jacquey, Marion         | CT-07                      | <a href="mailto:marion.jacquey@u-psud.fr">marion.jacquey@u-psud.fr</a>                     |
| Jordan, Elena           | CT-35                      | <a href="mailto:ejordan@mpi-hd.mpg.de">ejordan@mpi-hd.mpg.de</a>                           |
| Järvinen, Jarno         | P-087                      | <a href="mailto:jaanja@utu.fi">jaanja@utu.fi</a>   |
| Kanat Öztürk, Ipek      | P-025                      | <a href="mailto:ikanat@istanbul.edu.tr">ikanat@istanbul.edu.tr</a>                         |
| Kanda, Sohtaro          | P-032                      | <a href="mailto:kanda@post.kek.jp">kanda@post.kek.jp</a>                                   |
| Kapralova, Petra Ruth   | P-103                      | <a href="mailto:kapralova@jh-inst.cas.cz">kapralova@jh-inst.cas.cz</a>                     |
| Karras, Gabriel         | CT-01                      | <a href="mailto:gabriel.karras@u-bourgogne.fr">gabriel.karras@u-bourgogne.fr</a>           |
| Khalal, Mehdi           |                            | <a href="mailto:khalalm@yahoo.fr">khalalm@yahoo.fr</a>                                     |
| Khaykovich, Lev         | CT-29, P-067               | <a href="mailto:lev.khaykovich@biu.ac.il">lev.khaykovich@biu.ac.il</a>                     |
| Kinnunen, Jami          | P-078                      | <a href="mailto:jami.kinnunen@aalto.fi">jami.kinnunen@aalto.fi</a>                         |
| Knie, André             | CT-04                      | <a href="mailto:knie@physik.uni-kassel.de">knie@physik.uni-kassel.de</a>                   |
| Knoop, Martina          | CT-33                      | <a href="mailto:martina.knoop@univ-amu.fr">martina.knoop@univ-amu.fr</a>                   |
| Knoop, Steven           | CT-06                      | <a href="mailto:s.knoop@vu.nl">s.knoop@vu.nl</a>   |
| Knöckel, Horst          | P-003, P-105               | <a href="mailto:knockel@iqo.uni-hannover.de">knockel@iqo.uni-hannover.de</a>               |
| Kokkelmans, Servaas     | CT-29, P-067               | <a href="mailto:s.kokkelmans@tue.nl">s.kokkelmans@tue.nl</a>                               |
| Korobitsin, Artem       | P-071                      | <a href="mailto:koroaa@mail.ru">koroaa@mail.ru</a>   |
| Kortyna, Andrew         |                            | <a href="mailto:kortynaa@lafayette.edu">kortynaa@lafayette.edu</a>                         |
| Koval, Eugene           | P-069, P-072               | <a href="mailto:e-cov@yandex.ru">e-cov@yandex.ru</a>                                       |

|                                |                            |  |
|--------------------------------|----------------------------|--|
| Koval, Oksana                  | P-069, P-072               | <a href="mailto:kov.oksana20@gmail.com">kov.oksana20@gmail.com</a>                                 |
| Kovtun, Oleksiy                | P-019                      | <a href="mailto:kovtun@physi.uni-heidelberg.de">kovtun@physi.uni-heidelberg.de</a>                 |
| Kowalczyk, Pawel               | P-099, P-100               | <a href="mailto:Pawel.Kowalczyk@fuw.edu.pl">Pawel.Kowalczyk@fuw.edu.pl</a>                         |
| Kozlov, Alexander              | P-001                      | <a href="mailto:alex.kozloff@gmail.com">alex.kozloff@gmail.com</a>                                 |
| Kröger, Sophie                 | P-016, P-023, P-024, P-025 | <a href="mailto:sophie.kroeger@htw-berlin.de">sophie.kroeger@htw-berlin.de</a>                     |
| Kwela, Jerzy                   | P-020, P-058               | <a href="mailto:fizjk@ug.edu.pl">fizjk@ug.edu.pl</a>   |
| Köhler, Florian                | CR-16, P-049               | <a href="mailto:florian.koehler.email@googlemail.com">florian.koehler.email@googlemail.com</a>     |
| Labaigt, Gabriel               | P-120                      | <a href="mailto:gabriel.labaigt@upmc.fr">gabriel.labaigt@upmc.fr</a>                               |
| Laliotis, Athanasios           | CT-05, P-028               | <a href="mailto:laliotis@univ-paris13.fr">laliotis@univ-paris13.fr</a>                             |
| Lancuba, Patrick               | P-062                      | <a href="mailto:patrick.lancuba.12@ucl.ac.uk">patrick.lancuba.12@ucl.ac.uk</a>                     |
| Law, Sam                       | P-006                      | <a href="mailto:slaw08@qub.ac.uk">slaw08@qub.ac.uk</a>   |
| Le Targat, Rodolphe            | P-075                      | <a href="mailto:rodolphe.letargat@obspm.fr">rodolphe.letargat@obspm.fr</a>                         |
| Lebouteiller, Claire           | P-082                      | <a href="mailto:claire.lebouteiller@lkb.ens.fr">claire.lebouteiller@lkb.ens.fr</a>                 |
| Lehtonen, Lauri                | P-087                      | <a href="mailto:lauri.lehtonen@utu.fi">lauri.lehtonen@utu.fi</a>                                   |
| Lepers, Maxence                | P-068                      | <a href="mailto:maxence.lepers@u-psud.fr">maxence.lepers@u-psud.fr</a>                             |
| Leroy, Claude                  | P-026                      | <a href="mailto:claud.leroy@u-bourgogne.fr">claud.leroy@u-bourgogne.fr</a>                         |
| Leroy-Pashayan, Yevgenya       |                            | <a href="mailto:yevgenya.pashayan-leroy@u-bourgogne.fr">yevgenya.pashayan-leroy@u-bourgogne.fr</a> |
| Lovric, Josip                  | P-111                      | <a href="mailto:josip.lovric@univ-lille1.fr">josip.lovric@univ-lille1.fr</a>                       |
| Lundberg, Hans                 | P-056, P-057               | <a href="mailto:hans.lundberg@fysik.lth.se">hans.lundberg@fysik.lth.se</a>                         |
| Lyashchenko, Konstantin        | P-009                      | <a href="mailto:Laywer92@mail.ru">Laywer92@mail.ru</a>   |
| Major, Jan                     | P-090                      | <a href="mailto:jan.major@uj.edu.pl">jan.major@uj.edu.pl</a>                                       |
| Makles, Kevin                  | P-065                      | <a href="mailto:makles@spectro.jussieu.fr">makles@spectro.jussieu.fr</a>                           |
| Malet Giralt, Francesc         | IT-11                      | <a href="mailto:f.maletgiralt@vu.nl">f.maletgiralt@vu.nl</a>                                       |
| Manai, Isam                    | P-091                      | <a href="mailto:isam.manai@univ-lille1.fr">isam.manai@univ-lille1.fr</a>                           |
| Mannervik, Sven                | P-063                      | <a href="mailto:mannervik@fysik.su.se">mannervik@fysik.su.se</a>                                   |
| Martinez de Escobar, Y. Natali | P-085                      | <a href="mailto:natali.martinez@icfo.es">natali.martinez@icfo.es</a>                               |
| Mathavan, Sreekanth            | CT-32                      | <a href="mailto:s.chirayath.mathavan@rug.nl">s.chirayath.mathavan@rug.nl</a>                       |
| McGilligan, James Patrick      | P-080                      | <a href="mailto:james.mcgilligan.2013@uni.strath.ac.uk">james.mcgilligan.2013@uni.strath.ac.uk</a> |
| Melezhik, Vladimir             | P-066, P-069               | <a href="mailto:melezhik@theor.jinr.ru">melezhik@theor.jinr.ru</a>                                 |
| Meshkov, Vladimir              | P-035                      | <a href="mailto:volodya.meshkov@gmail.com">volodya.meshkov@gmail.com</a>                           |
| Mishra, Preeti Manjari         | CT-06, P-126, P-127        | <a href="mailto:preeti.10@iist.ac.in">preeti.10@iist.ac.in</a>                                     |
| Mohanty, Amita                 | P-039                      | <a href="mailto:a.mohanty@rug.nl">a.mohanty@rug.nl</a>   |
| Morigi, Giovanna               | IT-03                      | <a href="mailto:giovanna.morigi@physik.uni-saarland.de">giovanna.morigi@physik.uni-saarland.de</a> |
| Nemouchi, Messaoud             | P-054                      | <a href="mailto:mnemouchi@usthb.dz">mnemouchi@usthb.dz</a>   |
| Nyman, Robert                  | P-098                      | <a href="mailto:r.nyman@imperial.ac.uk">r.nyman@imperial.ac.uk</a>                                 |
| O'Sullivan, Gerry              | PL-05                      | <a href="mailto:gerry.osullivan@ucd.ie">gerry.osullivan@ucd.ie</a>                                 |
| Ohyama-Yamaguchi, Tomoko       | P-130                      | <a href="mailto:rsp19371@nifty.com">rsp19371@nifty.com</a>   |
| Olejniczak, Malgorzata         | P-113                      | <a href="mailto:gosia.olejniczak@univ-lille1.fr">gosia.olejniczak@univ-lille1.fr</a>               |
| Pachucki, Krzysztof            |                            | <a href="mailto:krp@fuw.edu.pl">krp@fuw.edu.pl</a>   |
| Palacios, Silvana              | P-073, P-084, P-085, P-089 | <a href="mailto:silvana.palacios@icfo.es">silvana.palacios@icfo.es</a>                             |
| Palmeri, Patrick               | P-124                      | <a href="mailto:patrick.palmeri@umons.ac.be">patrick.palmeri@umons.ac.be</a>                       |
| Parzyński, Ryszard             |                            | <a href="mailto:parzynsk@amu.edu.pl">parzynsk@amu.edu.pl</a>                                       |
| Patkos, Vojtech                | P-050                      | <a href="mailto:patkosv@email.cz">patkosv@email.cz</a>   |
| Pedregosa, Jofre               | CT-33                      | <a href="mailto:jofre.pedregosa@univ-amu.fr">jofre.pedregosa@univ-amu.fr</a>                       |
| Piwiniski, Mariusz             | P-055, P-102               | <a href="mailto:piwek@fizyka.umk.pl">piwek@fizyka.umk.pl</a>                                       |
| Postler, Johannes              | CT-30                      | <a href="mailto:johannes.postler@uibk.ac.at">johannes.postler@uibk.ac.at</a>                       |
| Pruvost, Laurence              | CT-07                      | <a href="mailto:laurence.pruvost@u-psud.fr">laurence.pruvost@u-psud.fr</a>                         |
| Quinet, Pascal                 | P-041, P-124               | <a href="mailto:quinet@umons.ac.be">quinet@umons.ac.be</a>   |
| Ravets, Sylvain                | CT-09                      | <a href="mailto:sylvain.ravets@gmail.com">sylvain.ravets@gmail.com</a>                             |
| Réal, Florent                  | P-112, P-113               | <a href="mailto:florent.real@univ-lille1.fr">florent.real@univ-lille1.fr</a>                       |
| Rempe, Gerhard                 | PL-07, P-109               | <a href="mailto:gerhard.rempe@mpq.mpg.de">gerhard.rempe@mpq.mpg.de</a>                             |

|                                 |                     |  |
|---------------------------------|---------------------|--|
| Ricciardi, Iolanda              | P-108               | <a href="mailto:iolanda.ricciardi@ino.it">iolanda.ricciardi@ino.it</a>                       |
| Robert de Saint vincent, Martin | P074                | <a href="mailto:mrds2@cam.ac.uk">mrds2@cam.ac.uk</a>   |
| Rohart, François                | P-118               | <a href="mailto:Francois.Rohart@univ-lille1.fr">Francois.Rohart@univ-lille1.fr</a>           |
| Romain, Rudy                    | P-083               | <a href="mailto:rudy.romain@gmail.com">rudy.romain@gmail.com</a>                             |
| Ross, Amanda                    | P-114               | <a href="mailto:amanda.ross@univ-lyon1.fr">amanda.ross@univ-lyon1.fr</a>                     |
| Sacha, Krzysztof                | CT-12               | <a href="mailto:krzysztof.sacha@uj.edu.pl">krzysztof.sacha@uj.edu.pl</a>                     |
| Sansone, Giuseppe               | IT-01               | <a href="mailto:giuseppe.sansone@polimi.it">giuseppe.sansone@polimi.it</a>                   |
| Schmöger, Lisa                  | P-095, P-096        | <a href="mailto:lisa.schmoeger@mpi-hd.mpg.de">lisa.schmoeger@mpi-hd.mpg.de</a>               |
| Schwarz, Maria                  | IT-10, P-095, P-096 | <a href="mailto:m.schwarz@mpi-hd.mpg.de">m.schwarz@mpi-hd.mpg.de</a>                         |
| Schäffer, Stefan Alaric         | P-077               | <a href="mailto:shaffer@nbi.dk">shaffer@nbi.dk</a>   |
| Scotto, Stefano                 | P-052               | <a href="mailto:stefano.scotto@lncmi.cnrs.fr">stefano.scotto@lncmi.cnrs.fr</a>               |
| Severo Pereira Gomes, Andre     | P-112               | <a href="mailto:andre.gomes@univ-lille1.fr">andre.gomes@univ-lille1.fr</a>                   |
| Shah, Chintan                   | CT-20               | <a href="mailto:chintan@physi.uni-heidelberg.de">chintan@physi.uni-heidelberg.de</a>         |
| Shearer, Francesca              | P-006               | <a href="mailto:f.shearer@qub.ac.uk">f.shearer@qub.ac.uk</a>                                 |
| Sillanpää, Mika                 | IT-07               | <a href="mailto:Mika.Sillanpaa@aalto.fi">Mika.Sillanpaa@aalto.fi</a>                         |
| Singh, Jasmeet                  | P-029               | <a href="mailto:rajvanshi_jasmeet@yahoo.co.in">rajvanshi_jasmeet@yahoo.co.in</a>             |
| Solovyev, Dmitry                | P-005               | <a href="mailto:solovyev.d@gmail.com">solovyev.d@gmail.com</a>                               |
| Sorrentino, Fiodor              | CT-24               | <a href="mailto:sorrentino@fi.infn.it">sorrentino@fi.infn.it</a>                             |
| Sortais, Yvan                   | CT-18               | <a href="mailto:yvan.sortais@institutoptique.fr">yvan.sortais@institutoptique.fr</a>         |
| Sow, Lat                        | P-038, P-059, P-118 | <a href="mailto:papalattabara.sow@univ-paris13.fr">papalattabara.sow@univ-paris13.fr</a>     |
| Stefańska, Patrycja             | P-004               | <a href="mailto:pstefanska@mif.pg.gda.pl">pstefanska@mif.pg.gda.pl</a>                       |
| Stefanos, Carlström             | P-060               | <a href="mailto:stefanos.carlstrom@fysik.lth.se">stefanos.carlstrom@fysik.lth.se</a>         |
| Sukhorukov, Victor              | P-010, P-011, P-012 | <a href="mailto:sukhorukov_v@mail.ru">sukhorukov_v@mail.ru</a>                               |
| Szriftgiser, Pascal             | P-091               | <a href="mailto:pascal.szriftgiser@univ-lille1.fr">pascal.szriftgiser@univ-lille1.fr</a>     |
| Šmydke, Jan                     | P-037, P-103        | <a href="mailto:jan.smydke@jh-inst.cas.cz">jan.smydke@jh-inst.cas.cz</a>                     |
| Tajima, Minoru                  | P-053               | <a href="mailto:tajima@radphys4.c.u-tokyo.ac.jp">tajima@radphys4.c.u-tokyo.ac.jp</a>         |
| Temelkov, Ivo                   | P-003               | <a href="mailto:temelkov.ivo@gmail.com">temelkov.ivo@gmail.com</a>                           |
| ten Haaf, Gijs                  | CT-34, P-094        | <a href="mailto:g.t.haaf@tue.nl">g.t.haaf@tue.nl</a>   |
| Tino, Guglielmo M.              | CT-24               | <a href="mailto:tino@fi.infn.it">tino@fi.infn.it</a>   |
| Tokunaga, Sean K.               | P-038, P-059, P-118 | <a href="mailto:sean.tokunaga@univ-paris13.fr">sean.tokunaga@univ-paris13.fr</a>             |
| Tonoyan, Ara                    | P-026               | <a href="mailto:aratonoyan@gmail.com">aratonoyan@gmail.com</a>                               |
| Touat, Amirouche                | P-054               | <a href="mailto:atouat@usthb.dz">atouat@usthb.dz</a>   |
| Trassinelli, Martino            | CT-23, P-121        | <a href="mailto:martino.trassinelli@insp.jussieu.fr">martino.trassinelli@insp.jussieu.fr</a> |
| Tricot, François                |                     | <a href="mailto:fjmtricot@gmail.com">fjmtricot@gmail.com</a>                                 |
| Träbert, Elmar                  | P-117               | <a href="mailto:traebert@astro.rub.de">traebert@astro.rub.de</a>                             |
| Tyndall, Niall                  | P-123               | <a href="mailto:ntyndall01@qub.ac.uk">ntyndall01@qub.ac.uk</a>                               |
| Ubachs, Wim                     | PL-01               | <a href="mailto:w.m.g.ubachs@vu.nl">w.m.g.ubachs@vu.nl</a>                                   |
| Ulbricht, Hendrik               | CT-17               | <a href="mailto:h.ulbricht@soton.ac.uk">h.ulbricht@soton.ac.uk</a>                           |
| Urbain, Xavier                  | CT-21               | <a href="mailto:xavier.urbain@uclouvain.be">xavier.urbain@uclouvain.be</a>                   |
| Urbanczyk, Tomasz               | P-106               | <a href="mailto:tomek.urbanczyk@uj.edu.pl">tomek.urbanczyk@uj.edu.pl</a>                     |
| Vainio, Otto                    | P-087               | <a href="mailto:otarva@utu.fi">otarva@utu.fi</a>   |
| Vallet, Valérie                 | P-112, P-113        | <a href="mailto:valerie.vallet@univ-lille1.fr">valerie.vallet@univ-lille1.fr</a>             |
| van der Zande, Wim              | PL-02               | <a href="mailto:W.vanderZande@fnwi.ru.nl">W.vanderZande@fnwi.ru.nl</a>                       |
| Vanderbruggen, Thomas           | P-073, P-084, P-089 | <a href="mailto:thomas.vanderbruggen@icfo.es">thomas.vanderbruggen@icfo.es</a>               |
| Vassen, Wim                     | CT-06, P-040        | <a href="mailto:w.vassen@vu.nl">w.vassen@vu.nl</a>   |
| Vedel, Fernande                 |                     | <a href="mailto:fernande.vedel@univ-amu.fr">fernande.vedel@univ-amu.fr</a>                   |
| Verkerk, Philippe               | P-083               | <a href="mailto:Philippe.Verkerk@univ-lille1.fr">Philippe.Verkerk@univ-lille1.fr</a>         |
| von Klitzing, Wolf              | CT-13               | <a href="mailto:wvk@iesl.forth.gr">wvk@iesl.forth.gr</a>                                     |
| Vredenburg, Edgar               | CT-34, P-094        | <a href="mailto:e.j.d.vredenburg@tue.nl">e.j.d.vredenburg@tue.nl</a>                         |
| Wall, Thomas                    | CT-22               | <a href="mailto:t.wall@ucl.ac.uk">t.wall@ucl.ac.uk</a>                                       |
| Weislo, Piotr                   | CT-31, P-007, P-102 | <a href="mailto:piotr.wcislo@fizyka.umk.pl">piotr.wcislo@fizyka.umk.pl</a>                   |

|                        |                              |  |
|------------------------|------------------------------|--|
| Weidemüller, Matthias  | IT-02                        | <a href="mailto:weidemueller@uni-heidelberg.de">weidemueller@uni-heidelberg.de</a>       |
| Wenz, Andre            | IT-12                        | <a href="mailto:wenz@physi.uni-heidelberg.de">wenz@physi.uni-heidelberg.de</a>           |
| Wester, Roland         |                              | <a href="mailto:roland.wester@uibk.ac.at">roland.wester@uibk.ac.at</a>                   |
| Wilkowski, David       | CT-15                        | <a href="mailto:david.wilkowski@ntu.edu.sg">david.wilkowski@ntu.edu.sg</a>               |
| Windholz, Laurentius   | P-16, P-20, P-21, P-22, P-58 | <a href="mailto:windholz@tugraz.at">windholz@tugraz.at</a>                               |
| Wineland, David        | PL-03                        | <a href="mailto:david.wineland@nist.gov">david.wineland@nist.gov</a>                     |
| Witkowski, Marcin      | P-079                        | <a href="mailto:marcin@skyhost.pl">marcin@skyhost.pl</a>                                 |
| Wlodarczak, Georges    |                              | <a href="mailto:georges.wlodarczak@univ-lille1.fr">georges.wlodarczak@univ-lille1.fr</a> |
| Wouters, Steinar       | CT-34, P-094                 | <a href="mailto:s.h.w.wouters@tue.nl">s.h.w.wouters@tue.nl</a>                           |
| Yousif Al-Mulla, Samir | P-051                        | <a href="mailto:samir.al-mulla@hb.se">samir.al-mulla@hb.se</a>                           |
| Yuce, Cem              | P-086                        | <a href="mailto:cyuce@anadolu.edu.tr">cyuce@anadolu.edu.tr</a>                           |





